VOLUME 3

Head and Neck, Eye, Central Nervous System

Atlas of the Newborn

Rudolph

VOLUME 3

Head and Neck, Eye, Central Nervous System

Atlas of the Newborn

Arnold J. Rudolph, M.D.
1918-1995

Arnold J. Rudolph, M.D.
1918–1995
Professor of Pediatrics,
Obstetrics, and Gynecology
Baylor College of Medicine
Houston, Texas

VOLUME 3

Head and Neck, Eye, Central Nervous System

Atlas of the Newborn

Arnold J. Rudolph, M.D.
1918-1995

with a chapter on neonatal ophthalamology by
Helen A. Mintz-Hittner, M.D.

1997

B.C. Decker Inc.
Hamilton • London

B.C. Decker Inc.
4 Hughson Street South
P.O. Box 620, L.C.D. 1
Hamilton, Ontario L8N 3K7
Tel: 905 522-7017
Fax: 905 522-7839
e-mail: info@bcdecker.com

Printed in Canada

97 98 99 00/BP/9 8 7 6 5 4 3 2 1

ISBN 1-55009-033-X

Sales and distribution

United States
Blackwell Science Inc.
Commerce Place
350 Main Street
Malden, MA 02148
U.S.A.
Tel: 1-800-215-1000

Canada
Copp Clark Ltd.
200 Adelaide Street West
3rd Floor
Toronto, Ontario
Canada M5H 1W7
Tel: 416-597-1616
Fax: 416-597-1617

Japan
Igaku-Shoin Ltd.
Tokyo International P.O. Box 5063
1-28-36 Hongo, Bunkyo-ku
Tokyo 113, Japan
Tel: 3 3817 5680
Fax: 3 3815 7805

U.K., Europe, Scandinavia, Middle East
Blackwell Science Ltd.
c/o Marston Book Services Ltd.
P.O. Box 87
Oxford OX2 0DT
England
Tel: 44-1865-79115

Australia
Blackwell Science Pty, Ltd.
54 University Street
Carleton, Victoria 3053
Australia
Tel: 03 9347 0300
Fax: 03 9349 3016

Foreword

Sir William Osler stated, "There is no more difficult task in medicine than the art of observation." The late Arnold Jack Rudolph was an internationally renowned neonatologist, a teacher's teacher, and, above all, one who constantly reminded us about how much could be learned by simply observing, in his case, the newborn infant.

This color atlas of neonatology represents a distillation of more than 50 years of observing normal and abnormal newborn infants. The *Atlas* begins with a section on the placenta, its membranes, and the umbilical cord. Jack Rudolph delighted in giving a lecture entitled "Don't Make Mirth of the Afterbirth," in which he captivated audiences by showing them how much you could learn about the newborn infant from simply observing the placenta, its membranes, and the umbilical cord.

In a few more than 60 photomicrographs, we learn to read the placenta and gain insight into such disorders as intrauterine growth retardation, omphalitis, cytomegalic inclusion disease, congenital syphilis, and congenital neuroblastoma. Congenital abnormalities of every organ system are depicted along with the appearance of newborn infants who have been subjected in utero to a variety of different drugs, toxins, or chemicals. We also learn to appreciate the manifestations of birth trauma and abnormalities caused by abnormal intrauterine positioning.

More than 250 photographs are used to illustrate the field of neonatal dermatology. The collection of photographs used in this section is superior to that which I have seen in any other textbook or atlas of neonatology or dermatology; this section alone makes this reference a required addition to the library of any clinician interested in the care of infants and children. Photographs of the Kasabach-Merritt syndrome (cavernous hemangioma with thrombocytopenia), Klippel-Trénaunay syndrome, Turner's syndrome, Waardenburg's syndrome, neurocutaneous melanosis, mastocytosis (urticaria pigmentosa), and incontinentia pigmenti (Bloch-Sulzberger syndrome) are among the best that I have seen.

Cutaneous manifestations are associated with many perinatal infections. The varied manifestations of staphylococcal infection of the newborn are depicted vividly in photomicrographs of furunculosis, pyoderma, bullous impetigo, abscesses, parotitis, dacryocystitis, inastitis, cellulitis, omphalitis, and funisitis. Streptococcal cellulitis, *Haemophilus influenzae* cellulitis, and cutaneous manifestations of listeriosis all are depicted. There are numerous photomicrographs of congenital syphilis, showing the typical peripheral desquamative rash on the palms and soles, as well as other potential skin manifestations of congenital syphilis which may produce either vesicular, bullous, or ulcerative lesions. The various radiologic manifestations of congenital syphilis, including pneumonia alba, ascites, growth arrest lines, Wegner's sign, periostitis, and syphilitic osteochondritis, are depicted. Periostitis of the clavicle (Higouménaki's sign) is shown in a photograph that also depicts periostitis of the ribs. A beautiful photomicrograph of Wimberger's sign also has been included; this sign, which may appear in an infant with congenital syphilis, reveals radiolucency due to erosion of the medial aspect of the proximal tibial metaphysis.

The *Atlas* also includes a beautiful set of photographs which delineate the ophthalmologic examination of the newborn. Lesions which may result from trauma, infection, or congenital abnormalities are included. There are numerous photographs of the ocular manifestations of a variety of systemic diseases, such as Tay-Sachs disease, tuberous sclerosis, tyrosinase deficiency, and many more. Photographs of disturbances of each of the various organ systems, or disorders affecting such organ systems, also are included along with numerous photographs of different forms of dwarfism, nonchromosomal syndromes and associations, and chromosomal disorders. In short, this *Atlas* is the complete visual textbook of neonatology and will provide any

physician, nurse, or student with a distillation of 50 years of neonatal experience as viewed through the eyes of a master clinician.

Arnold Jack Rudolph was born in 1918, grew up in South Africa, and graduated from the Witwatersrand Medical School in 1940. Following residency training in pediatrics at the Transvaal Memorial Hospital for Children, he entered private pediatric practice in Johannesburg, South Africa. After almost a decade, he left South Africa and moved to Boston, where he served as a Senior Assistant Resident in Medicine at the Children's Medical Center in Boston, Massachusetts, and subsequently pursued fellowship training in neonatology at the same institution and at the Boston Lying-In Hospital, Children's Medical Center and Harvard Medical School under Dr. Clement A. Smith.

In 1961, Dr. Rudolph came to Baylor College of Medicine in Houston, Texas, the school at which he spent the remainder of his career. He was a master teacher, who received the outstanding teacher award from pediatric medical students on so many occasions that he was elected to the Outstanding Faculty Hall of Fame in 1982. Dr. Rudolph also received numerous awards over the years from the pediatric house staffs for his superb teaching skills.

He was the Director of the Newborn Section in the Department of Pediatrics at Baylor College of Medicine for many years, until he voluntarily relinquished that position in 1986 for reasons related to his health. Nevertheless, Jack Rudolph continued to work extraordinarily long hours in the care of the newborn infant, and was at the bedside teaching both students and house staff, as well as his colleagues, on a daily basis until just a few months before his death in July 1995.

Although Dr. Rudolph was the author or co-author of more than 100 published papers that appeared in the peer-reviewed medical literature, his most lasting contribution to neonatology and to pediatrics is in the legacy of the numerous medical students, house staff, fellows, and other colleagues whom he taught incessantly about how much one could learn from simply observing the newborn infant. This *Atlas* is a tour de force; it is a spectacular teaching tool that has been developed, collated, and presented by one of the finest clinical neonatologists in the history of medicine. It is an intensely personal volume that, as Dr. Rudolph himself states, "is not intended to rival standard neonatology texts," but rather to supplement them. This statement reveals Dr. Rudolph's innate modesty, since with the exception of some discussion on pathogenesis and treatment, it surpasses most neonatology texts in the wealth of clinical information that one can derive from viewing and imbibing its contents. We owe Dr. Rudolph and those who aided him in this work a debt of gratitude for making available to the medical community an unparalleled visual reference on the normal and abnormal newborn infant.

Ralph D. Feigin, M.D.
June 13, 1996

Preface

I first became attracted to the idea of producing a color atlas of neonatology many years ago. However, the impetus to synthesize my experience and compile this current collection was inspired by the frequent requests from medical students, pediatric house staff, nurses and others to provide them with a color atlas of the clinical material provided in my "slide shows." For the past few decades I have used the medium of color slides and radiographs as a teaching tool. In these weekly "slide shows" the normal and abnormal, as words never can, are illustrated.

"I cannot define an elephant but I know one when I see one."[1]

The collection of material used has been added to constantly with the support of the pediatric house staff who inform me to "bring your camera" whenever they see an unusual clinical finding or syndrome in the nurseries.

A thorough routine neonatal examination is the inalienable right of every infant. Most newborn babies are healthy and only a relatively small number may require special care. It is important to have the ability to distinguish normal variations and minor findings from the subtle early signs of problems. The theme that recurs most often is that careful clinical assessment, in the traditional sense, is the prerequisite and the essential foundation for understanding the disorders of the newborn. It requires familiarity with the wide range of normal, as well as dermatologic, cardiac, pulmonary, gastrointestinal, genitourinary, neurologic, and musculoskeletal disorders, genetics and syndromes. A background in general pediatrics and a working knowledge of obstetrics are essential. The general layout of the atlas is based on the above. Diseases are assigned to each section on the basis of the most frequent and obvious presenting sign. It seems probable that the findings depicted will change significantly in the decades to come. In this way duplication has been kept to a minimum. Additional space has been devoted to those areas of neonatal pathology (e.g., examination of the placenta, multiple births and iatrogenesis) which pose particular problems or cause clinical concern.

Obviously, because of limitations of space, it is impossible to be comprehensive and include every rare disorder or syndrome. I have tried to select both typical findings and variations in normal infants and those found in uncommon conditions. Some relevant conditions where individual variations need to be demonstrated are shown in more than one case.

As the present volume is essentially one of my personal experience, it is not intended to rival standard neonatology texts, but is presented as a supplement to them. It seems logical that references should be to standard texts or reviews where discussion on pathogenesis, treatment, and references to original works may be found.

Helen Mintz Hittner, M.D., has been kind enough to contribute the outstanding section on neonatal ophthalmology.

I have done my best to make the necessary acknowledgements to the various sources for the clinical material. If I have inadvertently omitted any of those, I apologize. My most sincere appreciation and thanks to Donna Hamburg, M.D., Kru Ferry, M.D., Michael Gomez, M.D., Virginia Schneider, PA, and Jeff Murray, M.D., who have spent innumerable hours in organizing and culling the material from my large collection. We wish to thank Abraham M. Rudolph, M.D., for his assistance in reviewing the material. We also wish to thank the following people for their photo contributions to this work: Claire Langston, Helen Mintz–Hittner, Rose Wolfson.

It is hoped that this atlas will provide neonatologists, pediatricians, family physicians, medical students and nurses with a basis for recognizing a broad spectrum of normal variations and clinical problems as well as provide them with an overall perspective of neonatology, a field in which there continues to be a rapid acceleration of knowledge and technology. One must bear in mind the caveat that pictures cannot supplant clinical experience in mastering the skill of visual recall.

1. Senile dementia of Alzheimer's type — normal aging or disease? (Editorial) *Lancet* 1989; i:476-477.

Arnold J. Rudolph, M.D.

CONTENTS

Volume III
Head and Neck, Eye, Central Nervous System

Introduction

Although several texts provide extensive written descriptions of the newborn infant, the senses of touch, hearing, and especially sight, create the most lasting impressions. Over a period of almost five decades, my brother Jack Rudolph diligently recorded, in pictorial form, his vast experiences in physical examination of the newborn infant. *Atlas of the Newborn* reflects his selection from the thousands of color slides in his collection, and truly represents the "art of medicine" as applied to neonatology. A number of unusual or rare conditions are included in this atlas. I consider this fully justified, because if one has not seen or heard of a condition, one will never be able to diagnose it.

This third volume of the five-volume series encompasses three main topics: the head and neck, the eyes, and the central nervous system.

Chapter 1 of this volume focuses on the head and neck, and includes a singular collection depicting various abnormalities of skull shape and size, demonstrating how external forces during the birth process may mold the cranial vault. Facial cleft syndromes, including midline facial defects, cleft lip, cleft palate, and other facial clefts, are graphically shown. In addition, abnormalities of the mouth, tongue, and ears are represented in outstanding photographs.

Chapter 2 concentrates on disorders of the eye, and is unique in its graphic representation of ophthalmalogic problems in the newborn. The importance of careful and systematic examination of the various components of the eye in the neonate is stressed, as often it is neglected.

Chapter 3 is dedicated to disorders of the central nervous system. In addition to pictorially representating many of the abnormalities that are noted to result from neonatal neurologic abnormalities, this chapter provides an extensive graphic description of the various forms of meningocele.

Volume III of *Atlas of the Newborn* will be extremely valuable to obstetricians, neonatologists, pediatricians and nurses involved in perinatal care, and also to clinical geneticists, surgeons, ophthalmologists and neurologists involved in the care of the newborn infant.

Abraham M. Rudolph, M.D.

Chapter 1
Head and Neck

Examination of the head should include visual inspection, palpation, auscultation (for bruits over the temporal arteries and anterior fontanelle), assessment of the shape and size relative to the rest of the body and face, distribution and character of the hair and underlying scalp, and measurement of head circumference. The hair is inspected for color, texture, distribution and directional patterns. The shape of the cranial vault reflects interaction of internal (anatomy, volume, pressure) and external (intra- and extrauterine molding, suture mobility) forces. The mode of delivery will affect the shape of the head (e.g., vaginal delivery with vertex presentation leads to a narrowed biparietal diameter and a maximal occipitomental dimension; breech presentation may accentuate the occipitofrontal dimension with parietal flattening and frontal prominence). Normal molding resolves within a few weeks, but other aberrations progress.

Normal variations in contour, size, relationships, and range of motion of the newborn neck must be distinguished from congenital anomalies and traumatic lesions. The neck should be examined passively for rotation, lateral flexion, anterior flexion, and extension. Rotation of 80° and lateral flexion of 40° should be present and symmetric to both sides. Extension and flexion are difficult to measure, but in flexion the chin should touch or nearly touch the chest wall and extension should be 45° from neutral. When rotation or lateral flexion is asymmetrical or when motion is limited, radiographs of the neck should be obtained. The neck should be extended to look for clefts and cysts. The isthmus of a normal thyroid is just palpable in the sternal notch on neck extension. Other congenital neck masses include cystic hygroma, lymphangioma, and cervical teratoma. The earlier that appropriate treatment is started, the more likely that correction can occur.

1.1

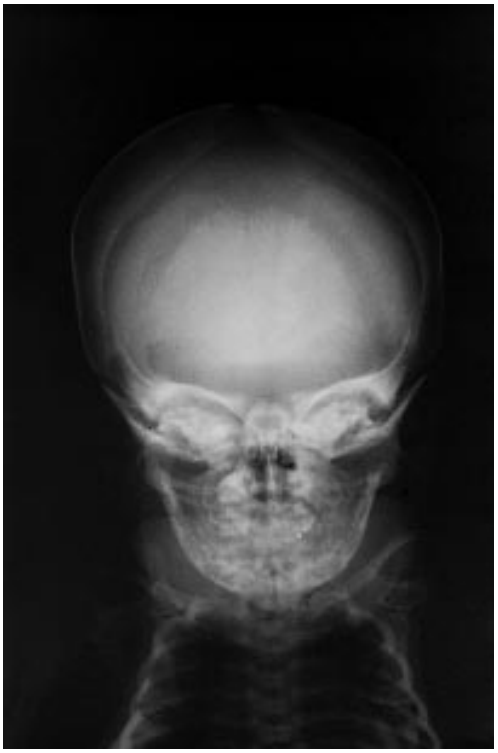

Figure 1.1. Anteroposterior radiograph of the normal newborn skull. Note the fontanelle and suture lines.

1.2

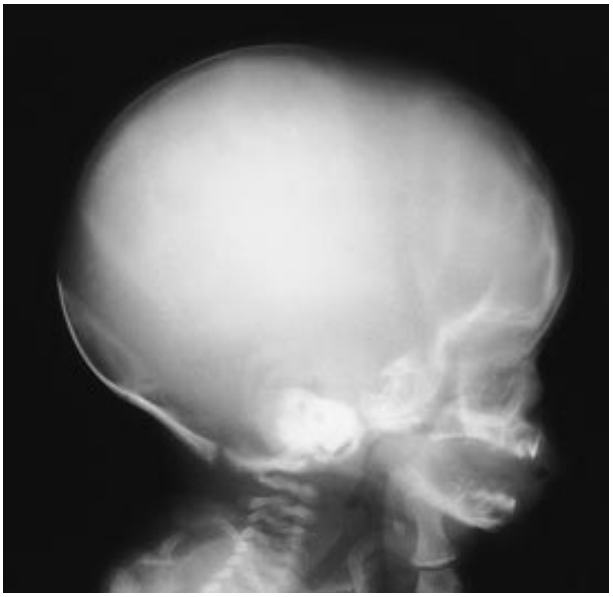

Figure 1.2. Lateral radiograph of a normal term newborn skull. Note the poor mineralization of the bones with separation of sutures. In the lateral view, mineralization of the lower teeth correlates well with gestational age. Mineralization of only the incisors indicates a gestational age of less than 33 weeks. Mineralization of the incisors and the first molars correlates with a gestational age of 33 to 37 weeks. Mineralization of the second molar in addition to the above correlates with less than 37 weeks gestation.

1.3

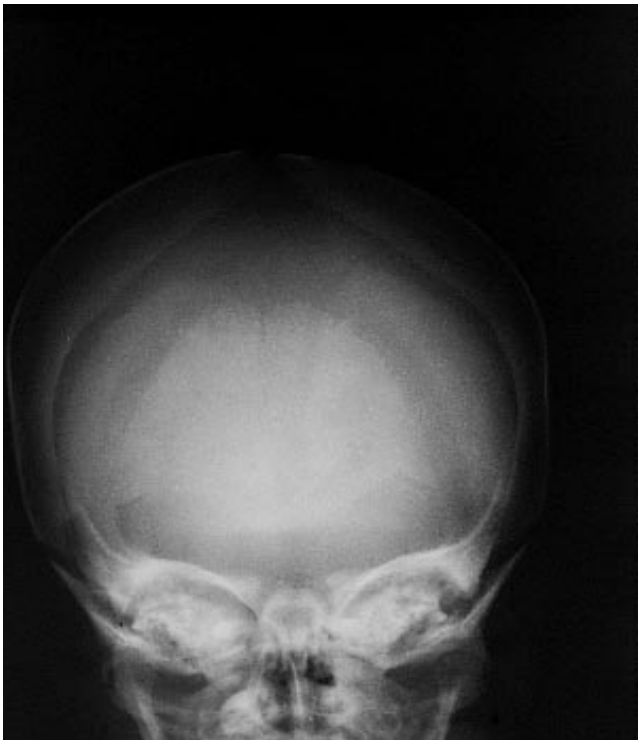

Figure 1.3. Lateral radiograph of the skull showing the presence of an anterior fontanelle bone. This infant's head is somewhat elongated. Fontanelle bones are more common over the posterior fontanelle. There are no clinical signs and as the skull mineralizes these bones become confluent with the rest of the skull. The bone may be palpable in the fontanelle.

1.4

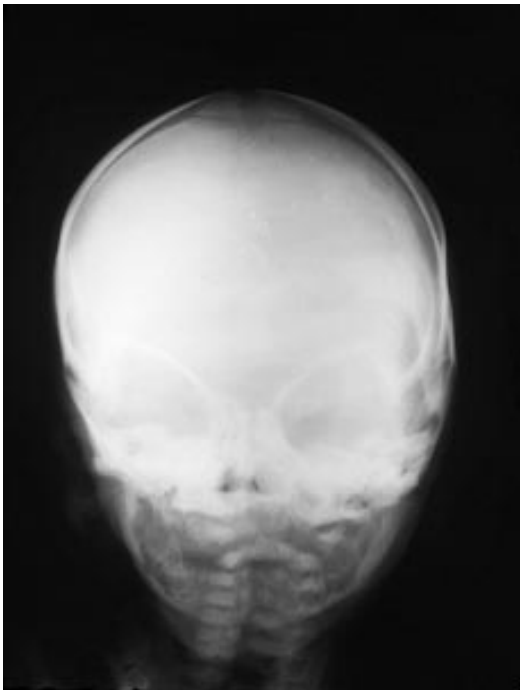

Figure 1.4. Anteroposterior radiograph of the same infant as in Figure 1.3, showing the anterior fontanelle bone. The third fontanelle is a widening of the sagittal suture near the junction of its middle and posterior thirds. It represents slowed growth of the plates of the parietal bone and may be distinguished from the posterior fontanelle by its position and round or oval appearance.

1.5

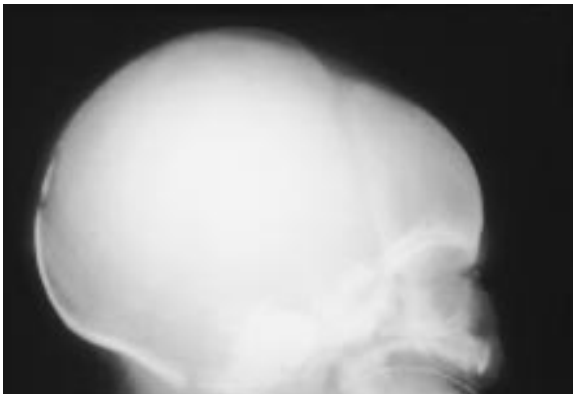

Figure 1.5. A lateral radiograph of the skull showing a posterior fontanelle bone. Note the poor mineralization of the skull in an otherwise normal infant. Mineralization of the skull may be minimal at birth in normal infants.

1.6

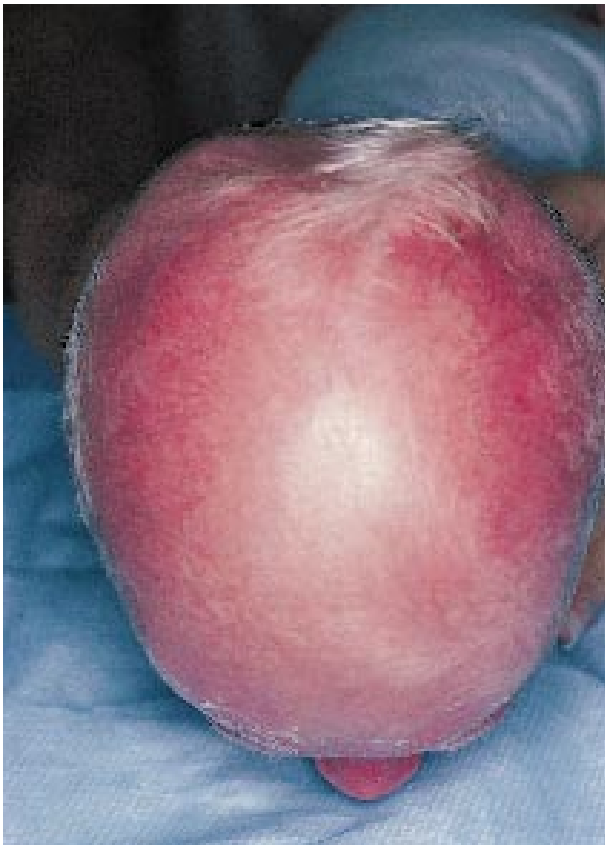

Figure 1.6. The clinical appearance of congenital parietal foramina in an otherwise normal neonate. Note that the infant is lying on his face and the depressions over the parietal area reflect the defects. These are rounded defects in the parietal bone. They are usually bilateral and vary in size from 1 mm to 3 cm. They are usually asymptomatic but may cause concern because of bulging or pulsation of the overlying scalp.

1.7

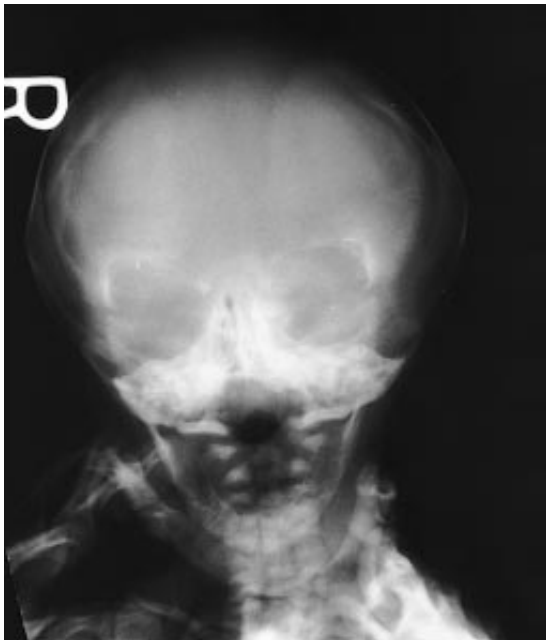

Figure 1.7. Radiograph of the skull of the same infant as in Figure 1.6. Note the posterior parietal foramina and poor mineralization of the skull with a large metopic suture.

1.8

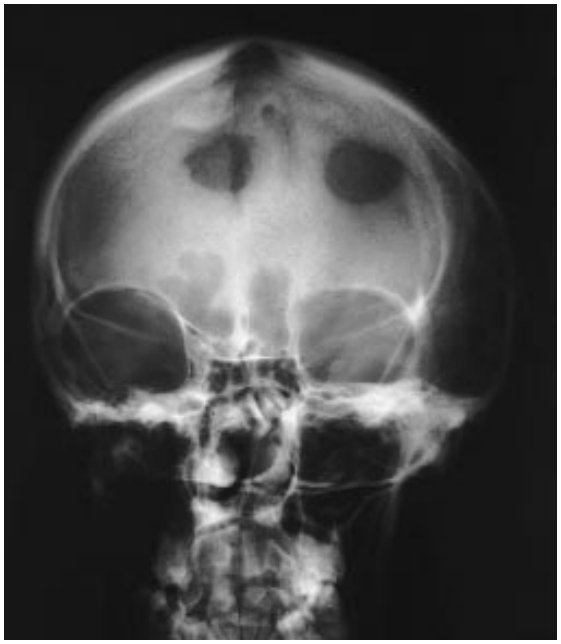

Figure 1.8. Congenital parietal foramina are often familial, as noted in this radiograph of the skull of the mother of the same infant.

1.9

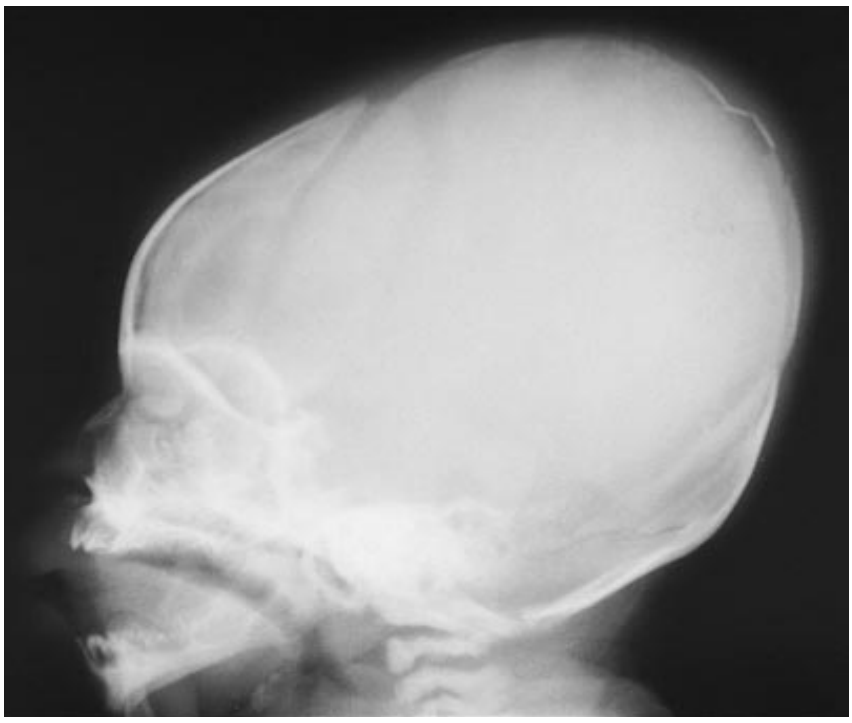

Figure 1.9. A radiograph of a linear skull fracture over the parietal bone. This is not common in the neonate but may occasionally be associated with a cephalohematoma. It can also occur as a result of trauma.

1.10

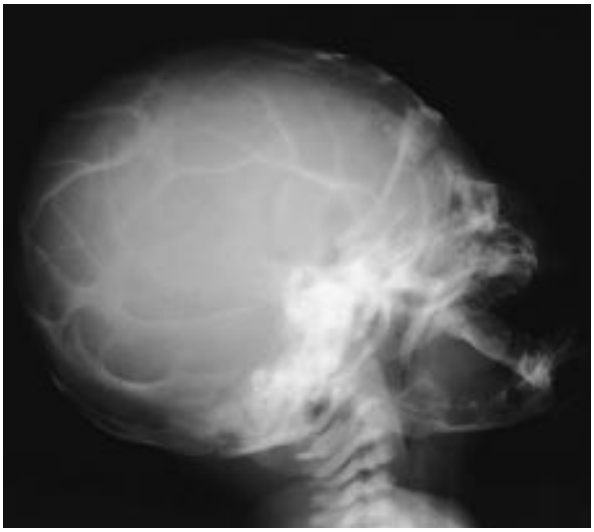

Figure 1.10. Lateral radiograph of the skull of an infant with lacunar skull (lückenschädel), which is a result of defective calcification of the skull bones. Note the characteristic honeycomb skull appearance. This malformation is commonly associated with neural tube defects (encephalocele and meningocele) and is characterized by sharply defined depressions which are usually readily palpable and situated in the frontal and parietal areas.

1.11

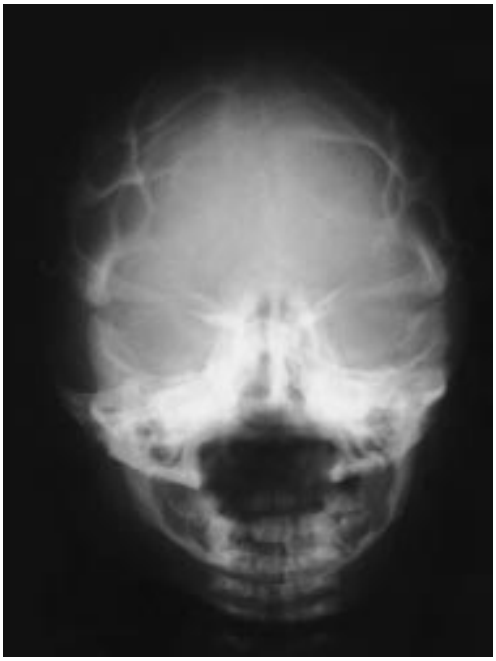

Figure 1.11. Frontal radiograph of the skull of the same infant with lückenschädel.

Compare lückenschädel with craniotabes which consists of localized areas of softening in one or several bones of the vault of the skull. The involved bones feel like parchment and are easily indented when pressed with the fingertip. When the pressure is removed, the soft bone resumes its former contour in much the same way as an indented ping pong ball recovers its shape. Craniotabes is more common in term infants than in premature infants. It is commonly found in normal infants, hydrocephalic infants, and in infants with osteogenesis imperfecta.

1.12

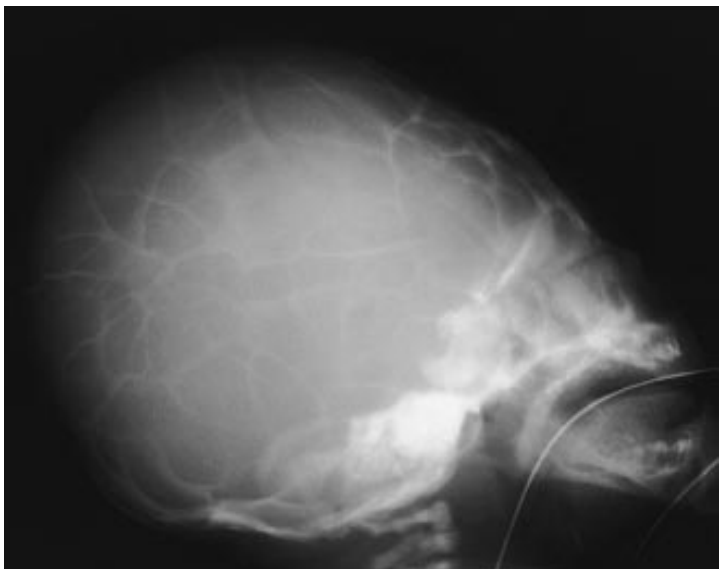

Figure 1.12. Lateral skull radiograph of lückenschädel in another infant with a lumbar meningocele, imperforate anus, and rectovaginal fistula.

1.13

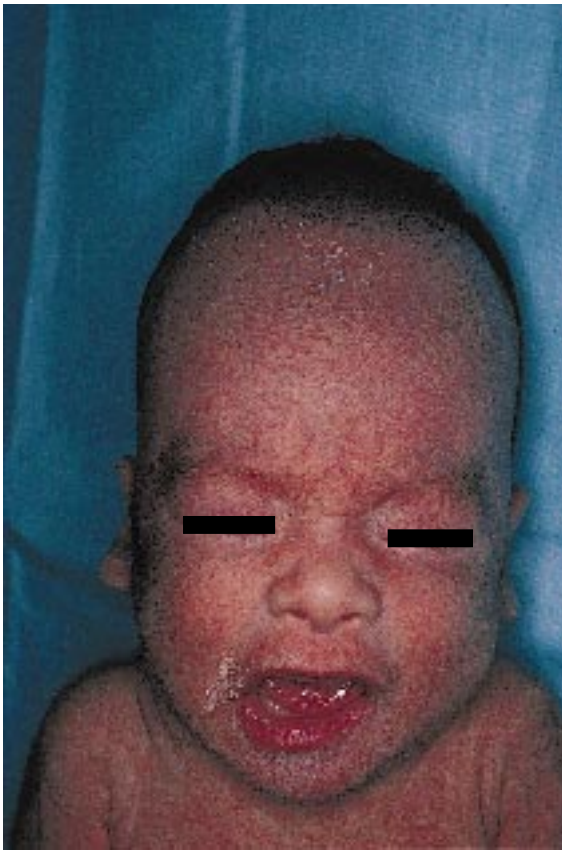

Figure 1.13. Note the typical long narrow skull of a premature infant with hypsicephaly. Hypsicephaly is a term used by anthropologists for "high heads" that are not pathologic or due to craniosynostosis. This term is used interchangeably with that of dolichocephaly when associated with prematurity.

1.14

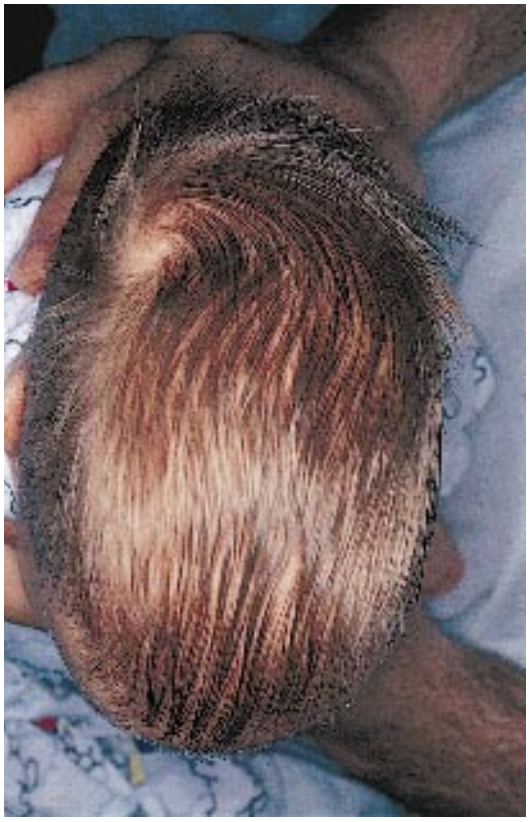

Figure 1.14. The typical appearance of dolichocephaly associated with prematurity. In these infants the sagittal suture remains open. The long, narrow head of dolichocephaly is not present at birth but results from transient molding of the skull as a result of the infant lying on its side. The large head of the small premature infant restricts frequent movement of the head, and hence this appearance is a postural deformity. Craniosynostosis with premature fusion of the sagittal suture is different from this normal postural deformity of premature infants.

1.15

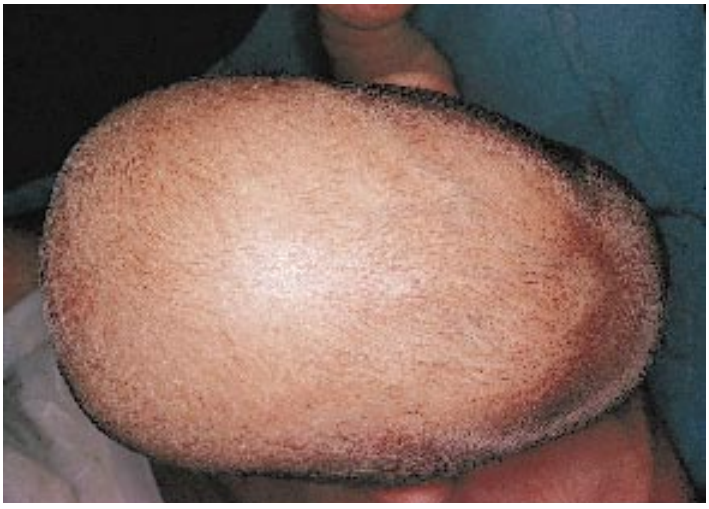

Figure 1.15. Premature fusion of the sagittal suture in this infant has resulted in scaphocephaly. Note the long, narrow head and the fused sagittal suture which presents as a ridge. This condition is more common in male infants.

1.16

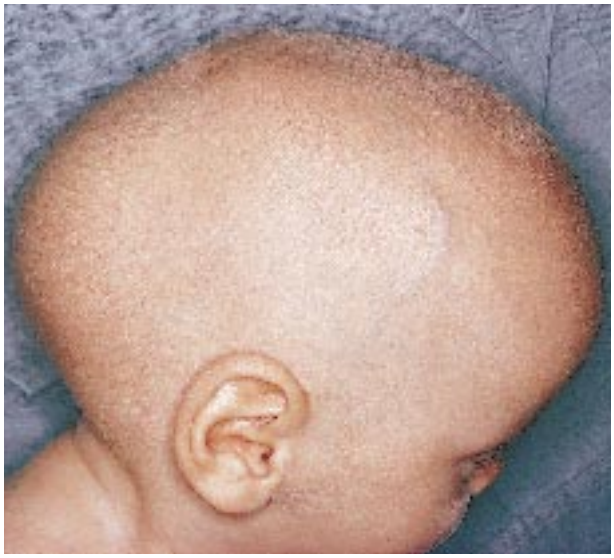

Figure 1.16. Lateral view of the head of another infant with scaphocephaly. Note the frontal and posterior bossing of the head.

1.17

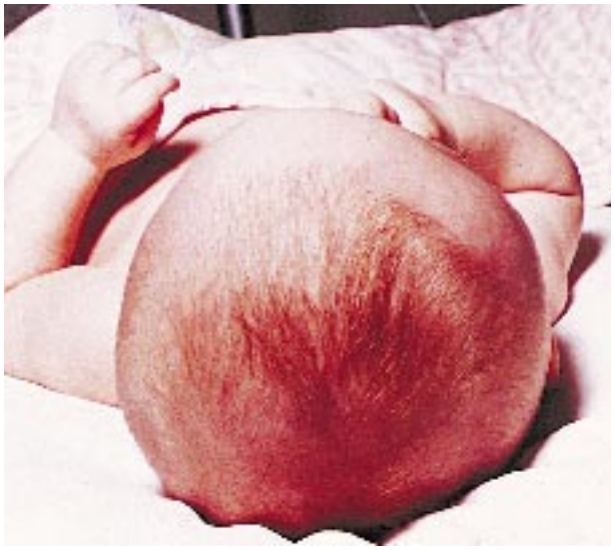

Figure 1.17. Craniosynostosis due to premature fusion of the coronal sutures has resulted in brachycephaly. Note the short, round appearance of the head with reduction of the anteroposterior diameter. This also occurs in Apert's syndrome and Carpenter's syndrome. Brachycephaly is also seen in infants with Down syndrome, Brachmann-de Lange syndrome, and cleidocranial dysostosis due to flattening of the occiput.

1.18

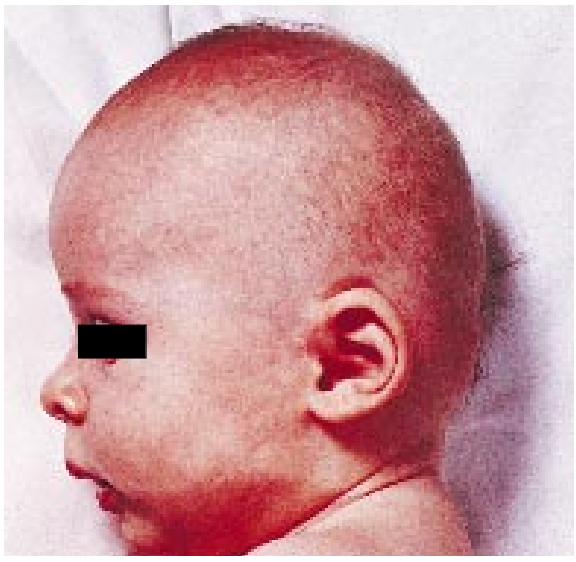

Figure 1.18. Lateral view of the head of the same infant with craniosynostosis of the coronal sutures. Note the short, round appearance of the head and the flat occiput.

1.19

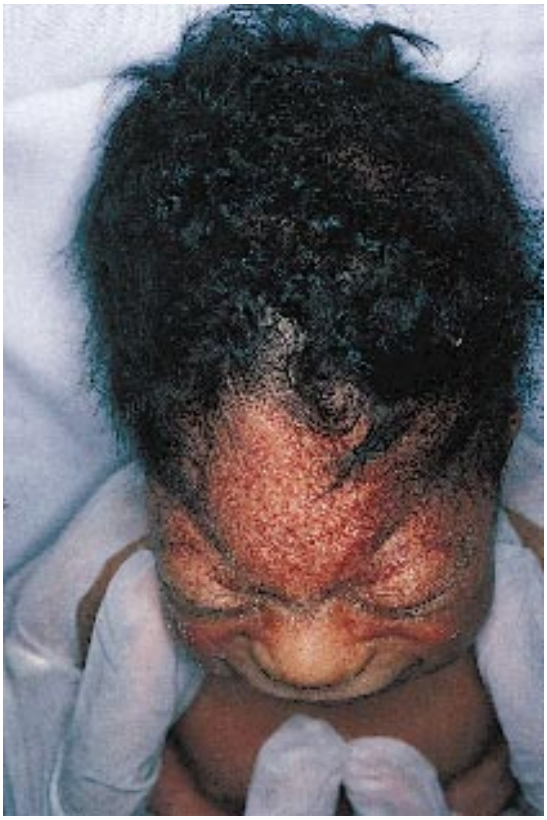

Figure 1.19. Trigonocephaly is due to premature fusion of the metopic suture and is represented clinically by a triangular-shaped head. This condition may occur in utero or in the first months of life. It may occur in otherwise normal infants, but is also seen in infants with chromosomal anomalies or the median cleft syndrome.

1.20

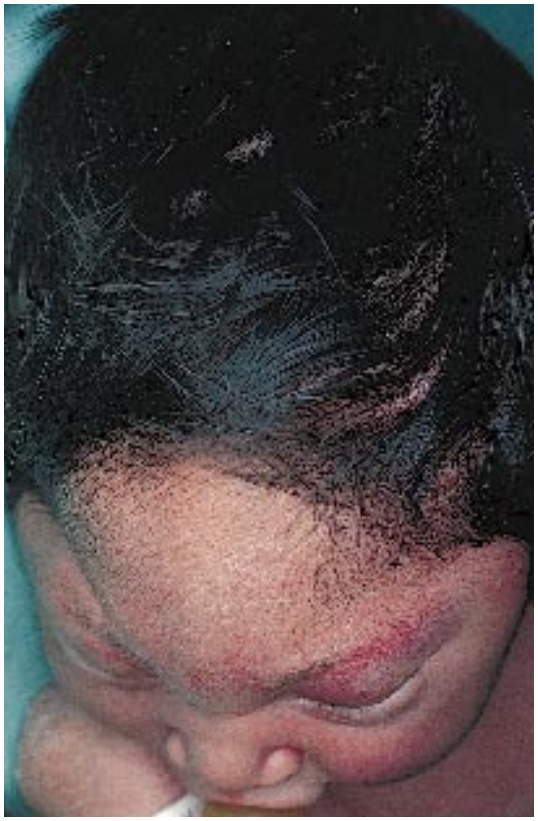

Figure 1.20. Another example of less severe trigonocephaly.

1.21

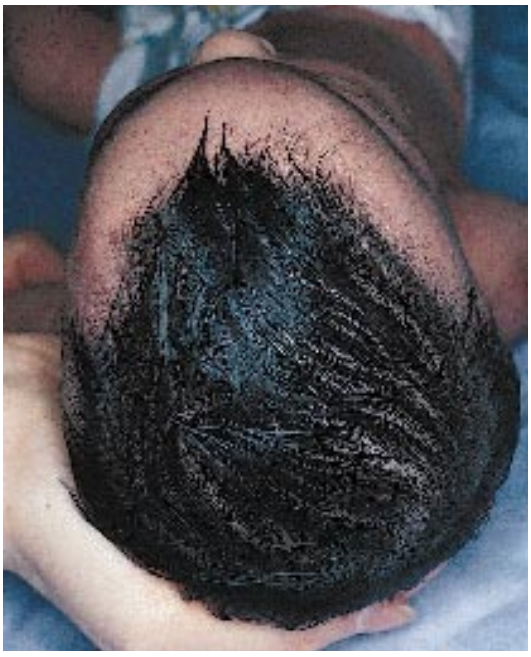

Figure 1.21. Note the asynclitism of the skull (plagiocephaly) associated with premature fusion of a single coronal suture. Plagiocephaly (oblique-shaped skull) occurs with premature fusion of a single suture (such as the coronal or lambdoidal) or with a congenital postural deformity. There is flattening of the diagonally opposite corners of the head (e.g., the right frontal and left occipital areas). In more severe cases, asymmetry of the facial features may also be seen. If plagiocephaly occurs as a result of a deformation, it is transient and corrects spontaneously. The combination of plagiocephaly and torticollis is well recognized.

1.22

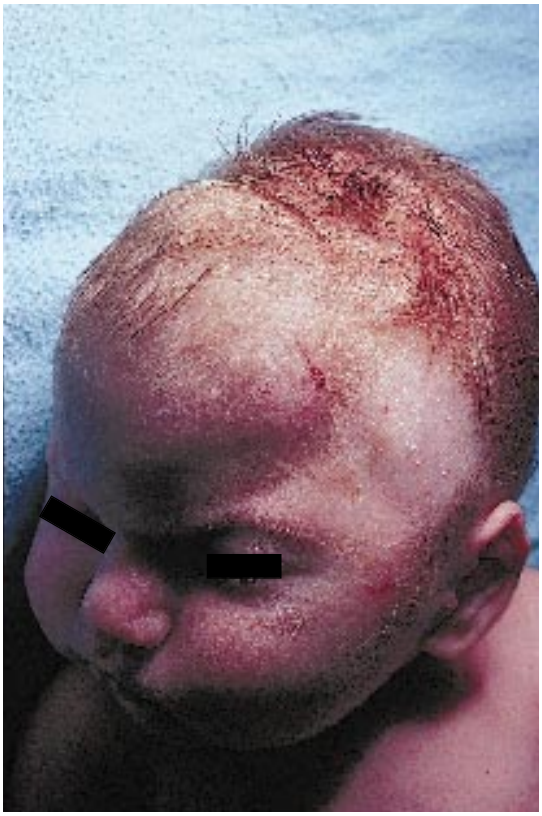

Figure 1.22. Kleeblattschädel ("cloverleaf" skull) is the result of premature fusion of the sagittal and coronal sutures. There is a trilobed appearance of the skull with indentations in the center and in the temporal regions. The ears are low set and the nasal bridge is depressed. This condition may occur in otherwise normal infants but is also noted in skeletal dysplastic conditions such as thanatophoric dwarfism.

1.23

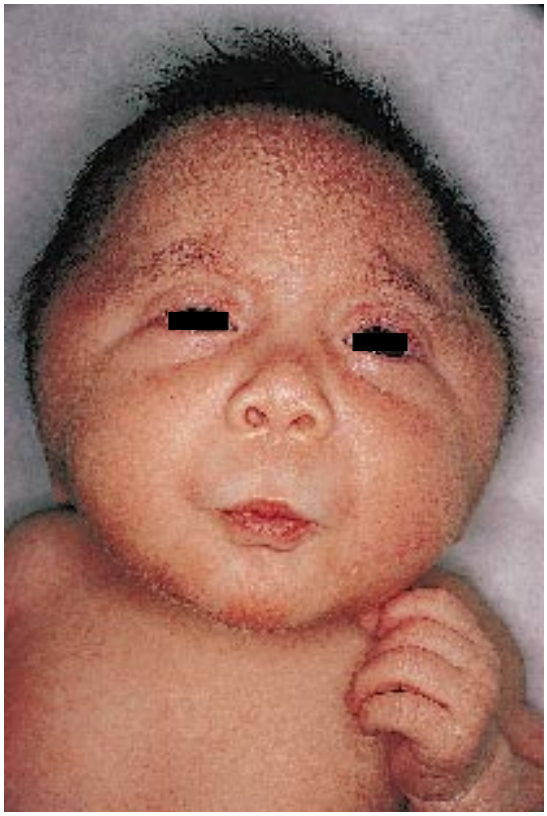

Figure 1.23. Another example of a "cloverleaf" skull. The brain is forced to grow through the anterior and temporal fontanelles resulting in upward and lateral growth.

1.24

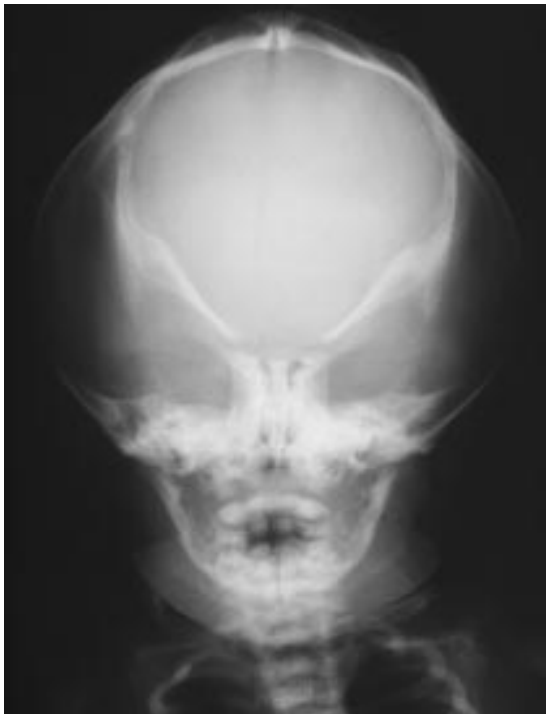

Figure 1.24. A frontal radiograph of "cloverleaf" skull in an infant exhibiting thanatophoric dwarfism.

1.25

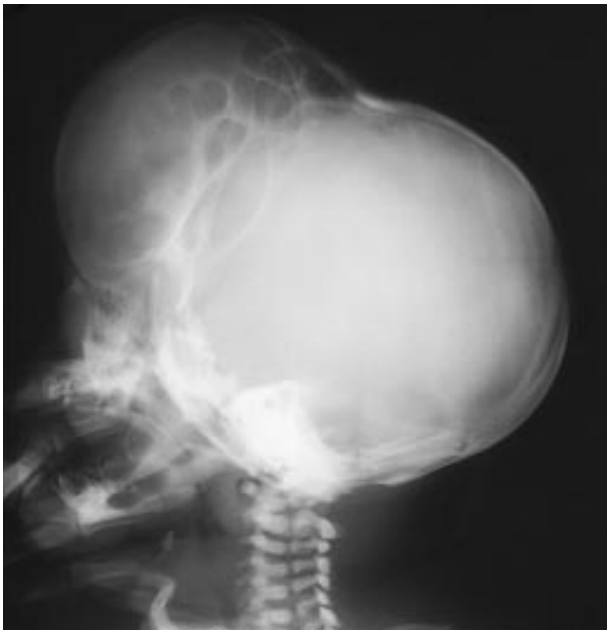

Figure 1.25. Lateral radiograph of the skull of the same infant as in Figure 1.24 with "cloverleaf" skull and thanatophoric dwarfism.

1.26

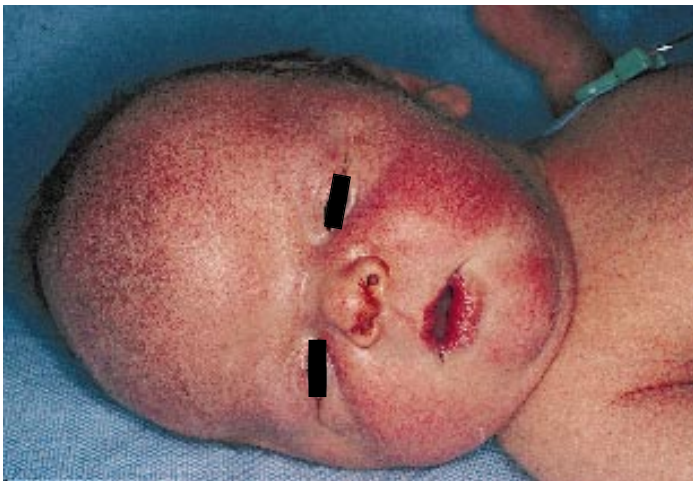

Figure 1.26. In this infant with Apert's syndrome (acrocephalosyndactyly), note the high steep frontal bone, protruding forehead, flat midface, small pinched nose, and the downward slanting of the palpebral fissures. The acrocephaly is due to premature fusion of the coronal sutures, resulting in bilateral coronal craniosynostosis. This infant also had the typical finding of a high arched palate.

1.27

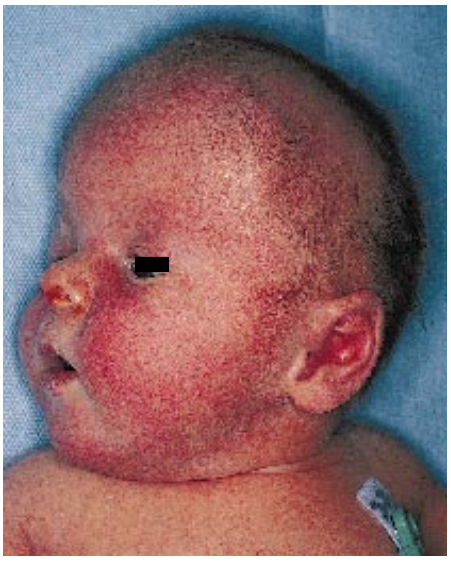

Figure 1.27. A lateral view of the head of the same infant. Again note the high steep frontal bone, protruding forehead, flat midface, small pinched nose, and the downward slanting of the palpebral fissures.

1.28

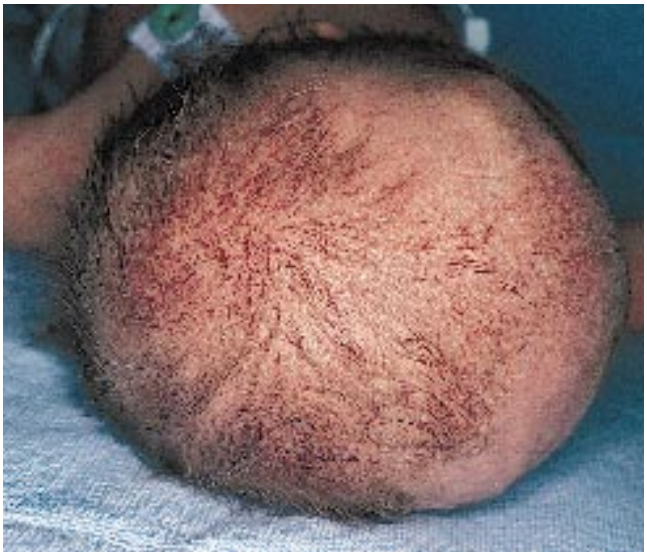

Figure 1.28. Superior view of the head of the same infant demonstrates turribrachycephaly ("tower" skull) which has occurred as a result of craniosynostosis of the coronal sutures. Note the ridges resulting from the fused sutures. The malformation of the skull occurs as a flattening of the frontal and occipital bones.

1.29

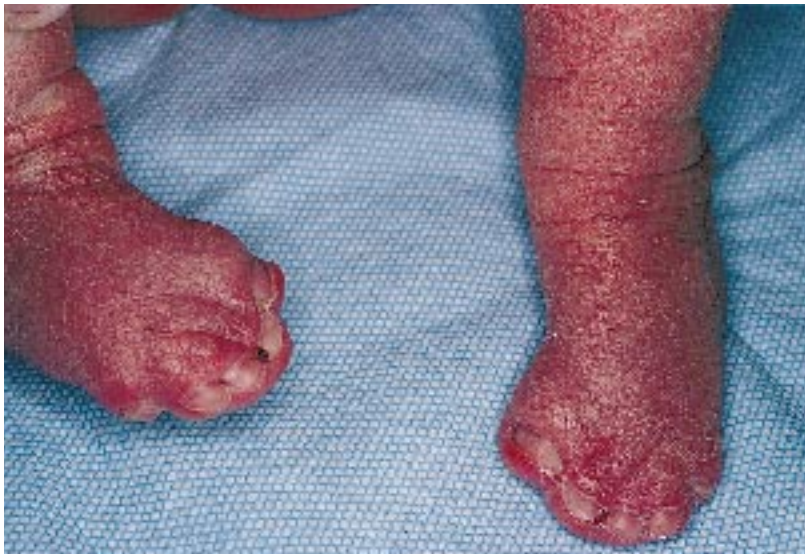

Figure 1.29. The same infant shows the characteristic symmetrical syndactyly which involves the toes. The fingers were similarly affected.

1.30

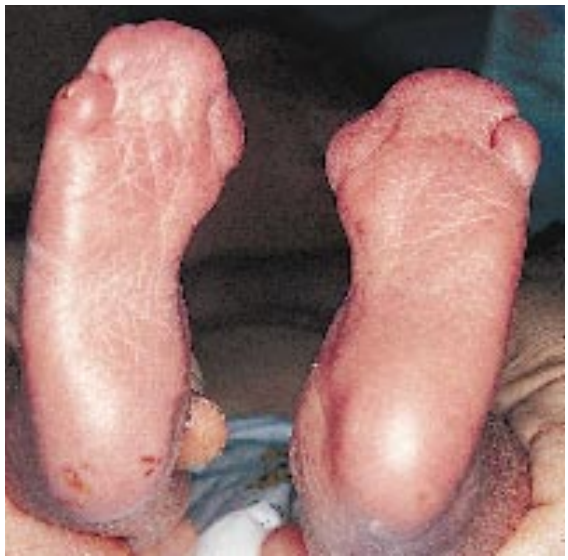

Figure 1.30. Another view of the symmetrical syndactyly of the toes in the same infant.

1.31

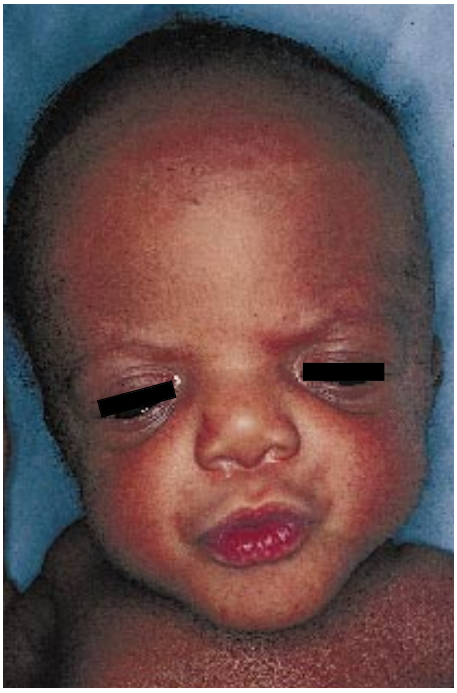

Figure 1.31. Another example of acrocephalosyndactyly in an infant whose mother had the same condition. Note the turribrachycephaly, high steep frontal bones, protruding forehead, flat midface, small pinched nose, and the downward slant of the palpebral fissures.

1.32

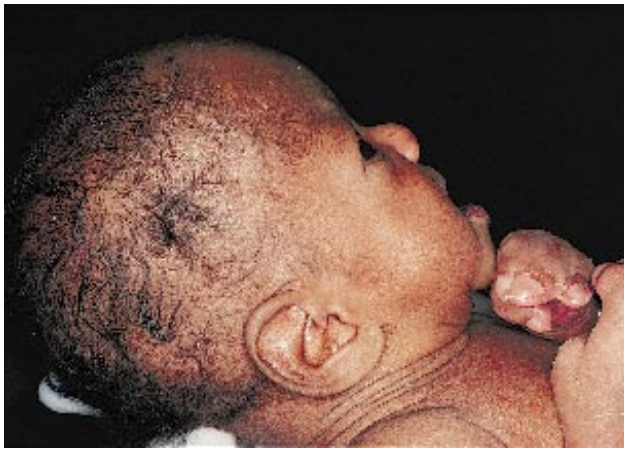

Figure 1.32. Lateral view of the same infant. Note the turribrachycephaly with the high steep forehead and note the syndactyly of the fingers of the left hand.

1.33

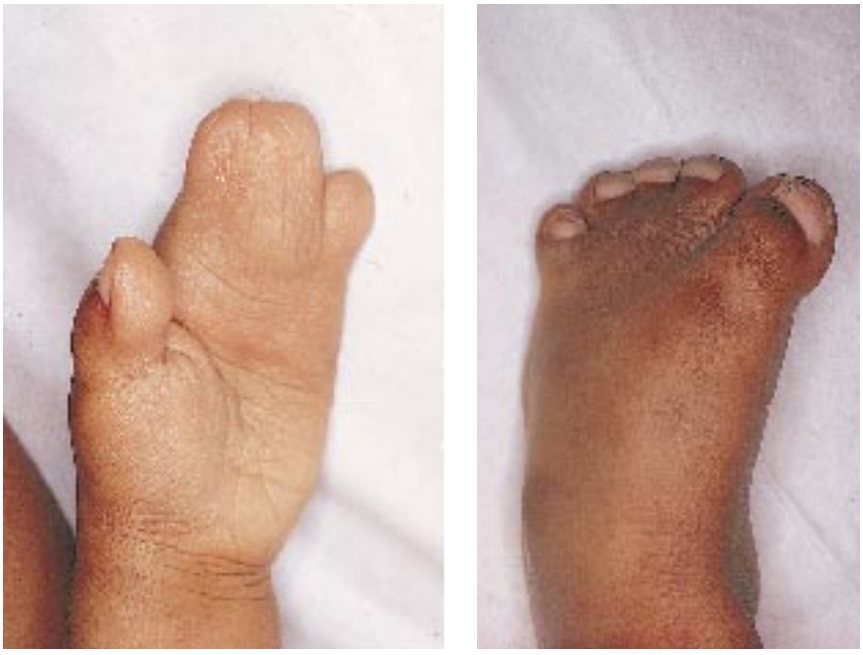

Figure 1.33. In this figure of the same infant, note on the left the syndactyly of the hand and on the right the syndactyly of the foot. These infants have symmetrical syndactyly.

1.34

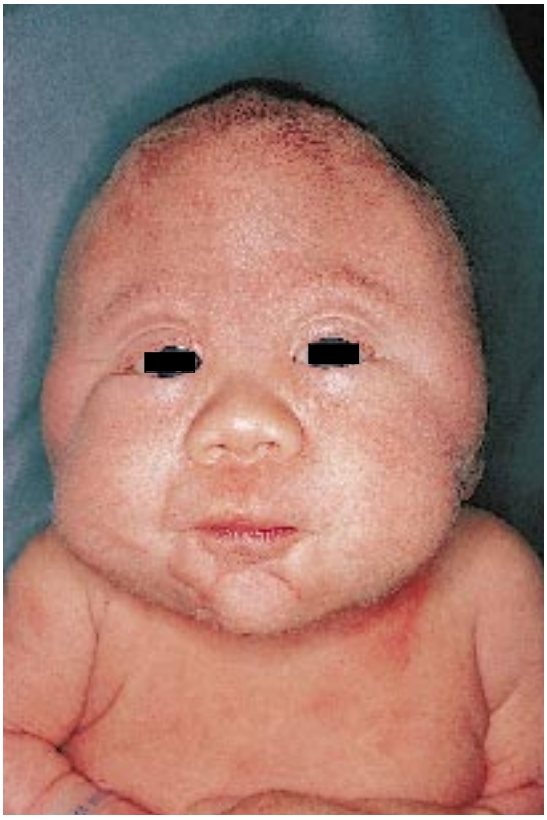

Figure 1.34. In infants with Carpenter's syndrome (acrocephalopolysyndactyly), the facial appearance is similar to that of infants with Apert's syndrome; in addition, there is polysyndactyly. This infant with Carpenter's syndrome shows the high steep protruding forehead, the flat midface, the small pinched nose, and the downward slanting of the palpebral fissures.

1.35

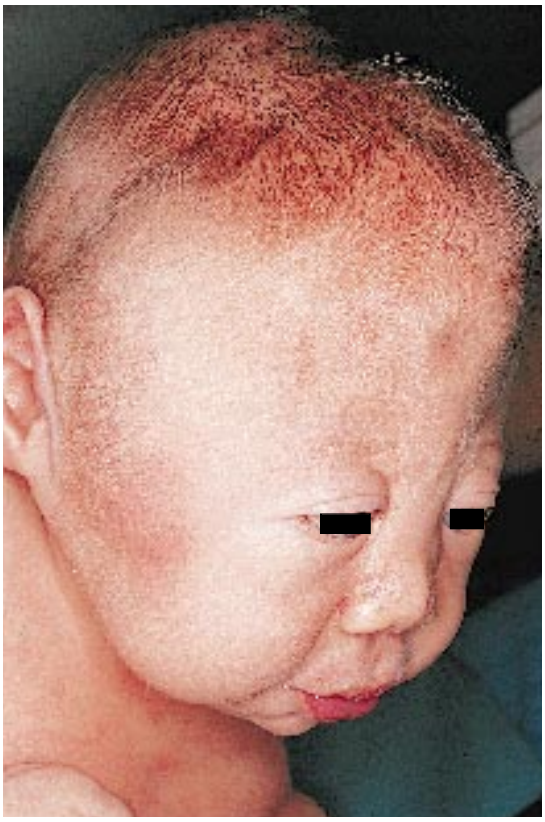

Figure 1.35. Oblique view of the same infant with Carpenter's syndrome shows the high steep forehead and turribrachycephaly. Note the ridges of the fused coronal sutures.

1.36

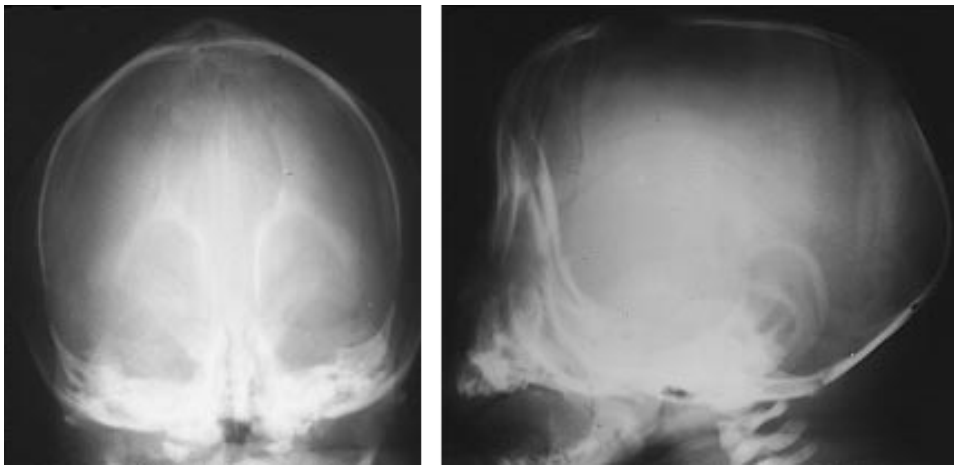

Figure 1.36. Frontal and lateral radiographs of the skull in the same infant show the premature fusion of the coronal sutures and the turribrachycephaly.

1.37

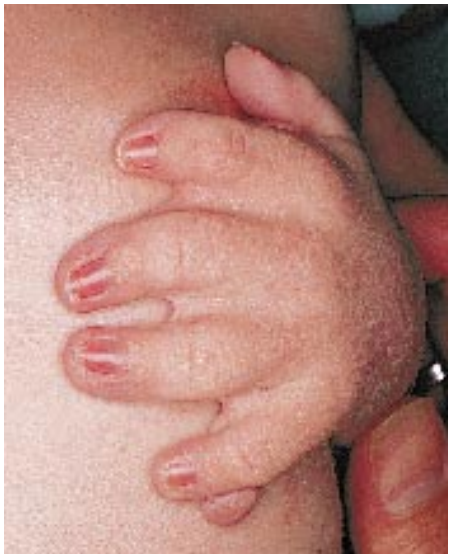

Figure 1.37. The left hand of the same infant as in Figures 1.34-1.36 with Carpenter's syndrome shows the polysyndactyly. Note the extra digit and the syndactyly which presents in the form of webbing.

1.38

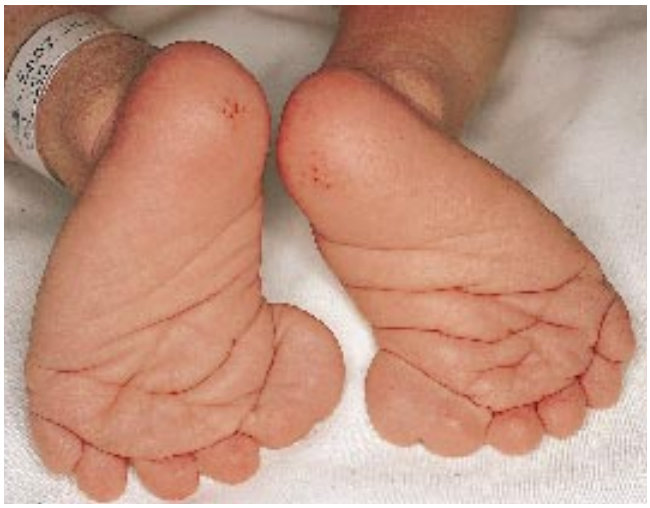

Figure 1.38. Symmetrical polysyndactyly of the feet in the same infant with Carpenter's syndrome.

1.39

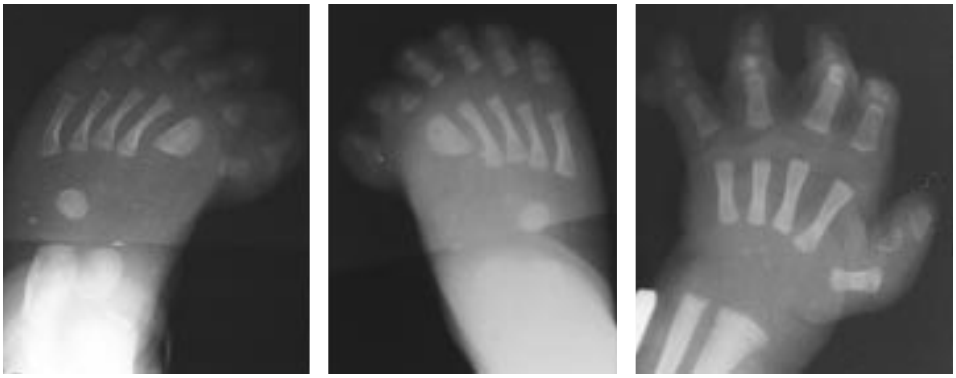

Figure 1.39. Radiographs of the feet and the right hand in the same infant with Carpenter's syndrome.

1.40

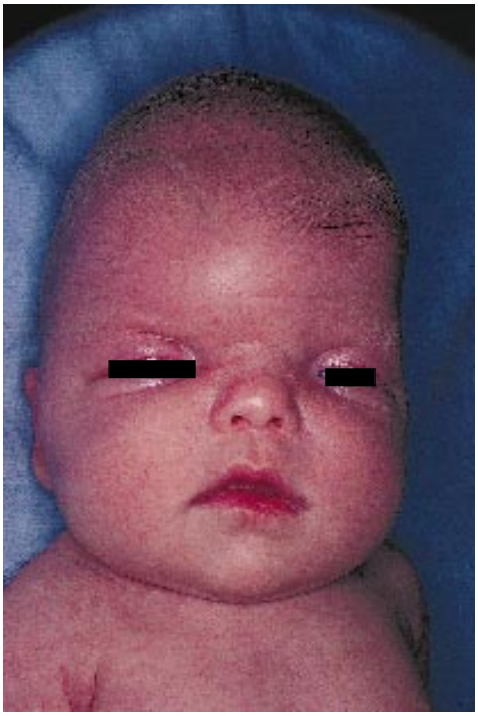

Figure 1.40. This neonate presented with the typical features of Crouzon's disease (craniofacial dysostosis). Note the deformed skull due to craniosynostosis of the coronal, sagittal, and metopic sutures. There is an antimongoloid slant to the eyes, shallow orbits with hypertelorism and hypoplasia of the facial bones. The nose is short with a low bridge. There is a short upper lip with a protruding lower lip. These infants may later develop exophthalmos.

1.41

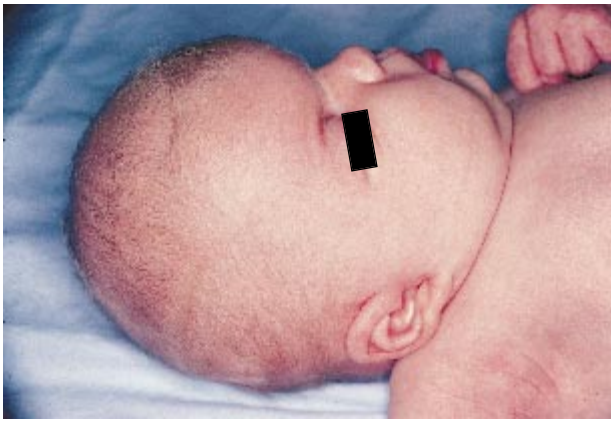

Figure 1.41. Lateral view of the same infant. Note the brachycephaly, high forehead, shallow orbits, and hypoplastic maxilla. This gives the appearance of a "dished-in" facies. The mandible may appear to be prognathic in contrast. Radiographs of the skull of these infants show premature synostosis with shortening of the base of the skull and narrowed optic foramina. Surgical treatment is essential.

1.42

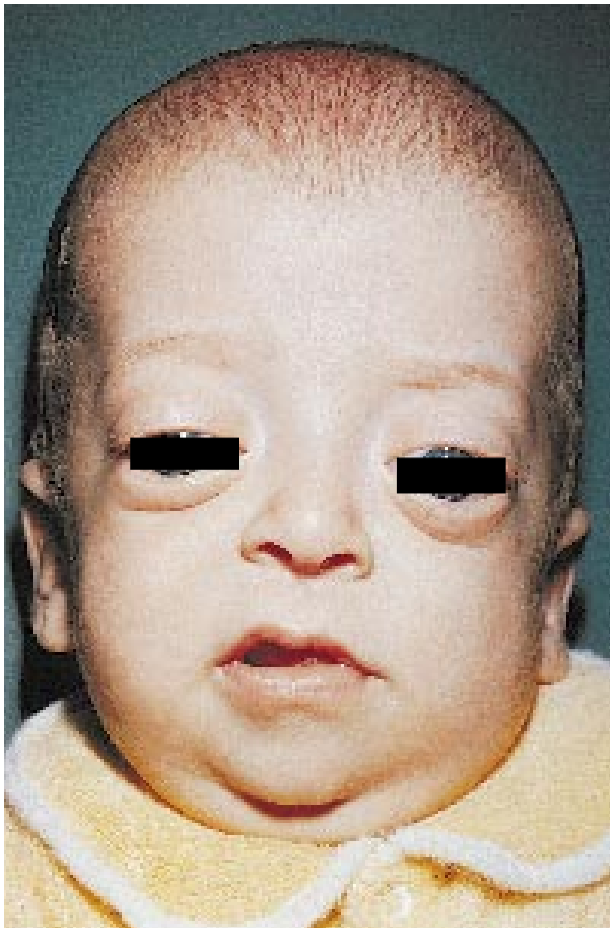

Figure 1.42. A 3-month-old infant with Crouzon's disease. Note the previous findings but in addition there is exophthalmos. Exophthalmos is not usually present at birth but develops later.

1.43

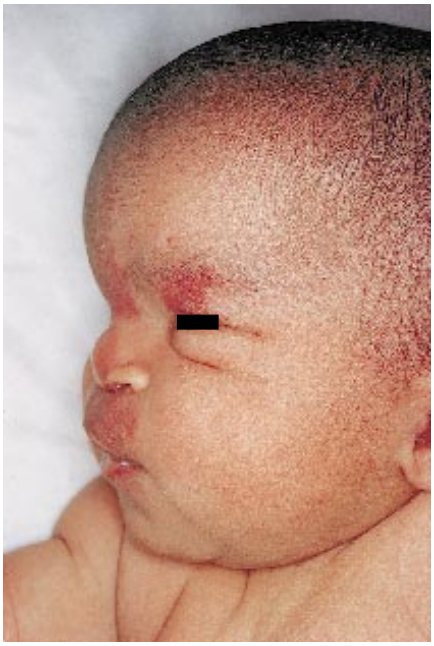

Figure 1.43. A flat facies is seen in many syndromes. It should be recognized that normal infants, such as this neonate, may present with the same appearance. Note the prominent forehead, flat nose and mild micrognathia which results in the flat facies.

1.44

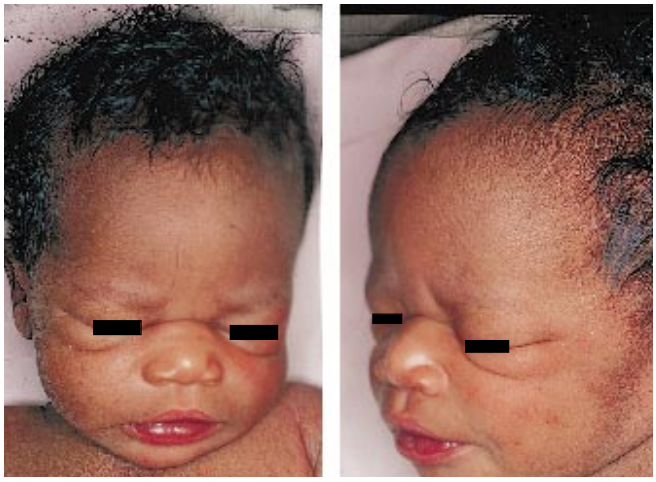

Figure 1.44. This normal infant has what appears to be a depressed nasal bridge. The mother had the same facies. Bulging over the nasal bridge, which appears when the infant cries may indicate the presence of an anterior encephalocele.

1.45

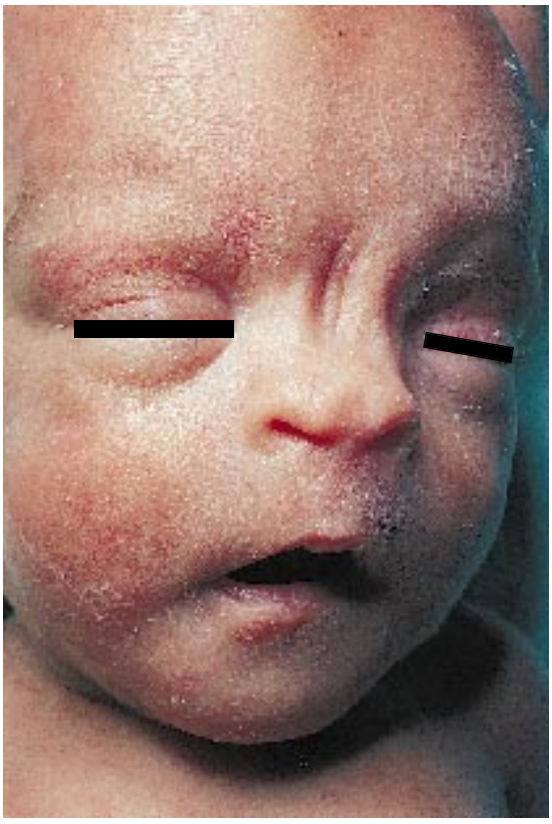

Figure 1.45. When too much tissue develops in (or migrates into) the upper midfacial zone it causes varying degrees of frontonasal dysplasia. The nasal bridge is broad, and extreme hypertelorism is always present. In severe cases there may be several centimeters of separation, with aberrant formation of the philtrum and upper lip (such as an extremely short philtrum and a tented upper lip). This infant is an example of a median cleft nose (frontonasal dysplasia). Note the prominent epicanthic folds. Although nasal clefting may be a normal variant, prominent midline clefting may be associated with holoprosencephaly, as part of the median cleft syndrome, and thus requires a diagnostic evaluation. CT scan in this infant confirmed the presence of holoprosencephaly.

1.46

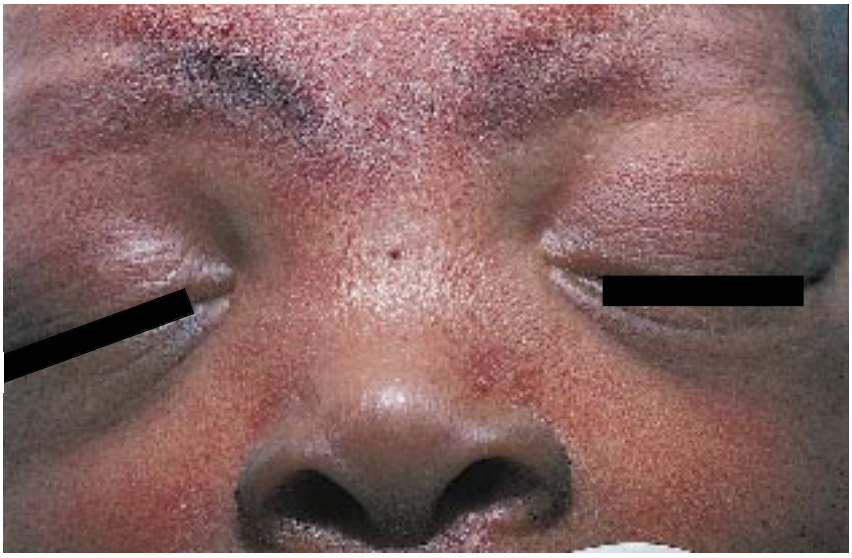

Figure 1.46. Note the median nasal pit in this infant. As with any midline lesion on the head or back, one should check to be sure this does not represent the end of a tract that communicates with the central nervous system. Danger signs include hairs implanted in the pit, fluid emerging from its depths or any underlying bony defect or cystic mass.

1.47

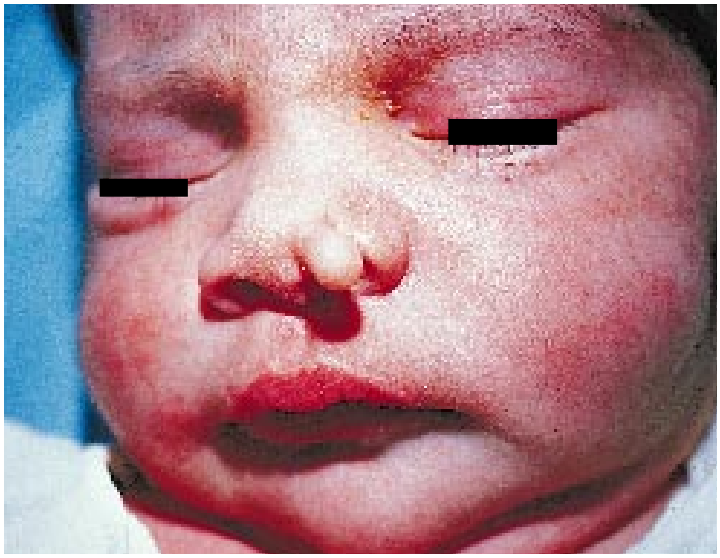

Figure 1.47. Lateral nasal clefts may occur in otherwise normal infants.

1.48

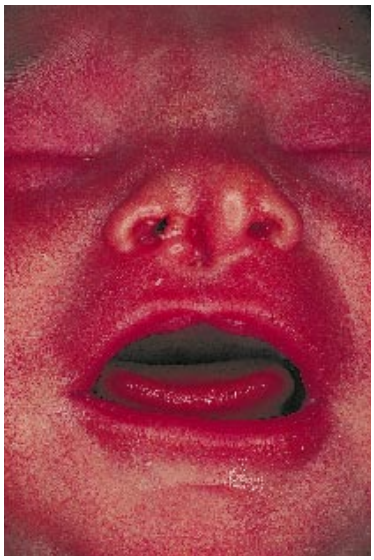

Figure 1.48. A more severe example of a lateral nasal cleft in an otherwise normal infant.

1.49

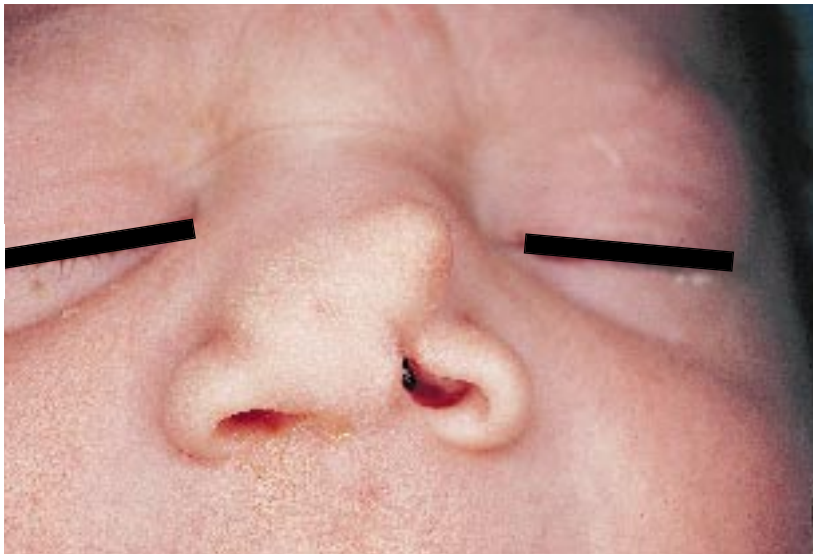

Figure 1.49. Although lateral nasal clefts, in general, are isolated findings, this infant in addition to the cleft had Holt-Oram syndrome (heart disease, in this case coarctation of the aorta, and absence of left radius and thumb).

1.50

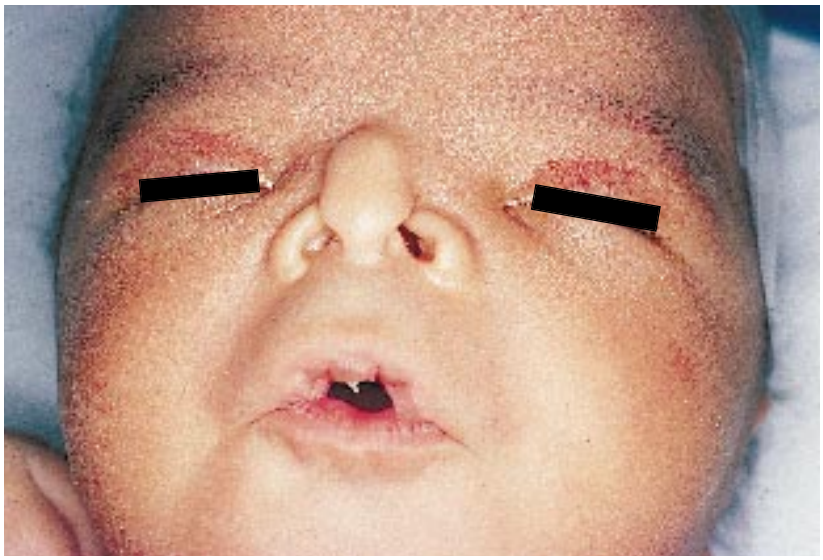

Figure 1.50. In this infant with bilateral clefting of the alae nasi, the philtrum is long and smooth because of the short nose. Note the downslanting palpebral fissures. There were bilateral cloudy corneas and congenital cataracts, a large anterior fontanelle and large metopic sutures. Karyotype was normal and MRI of the head was normal.

1.51

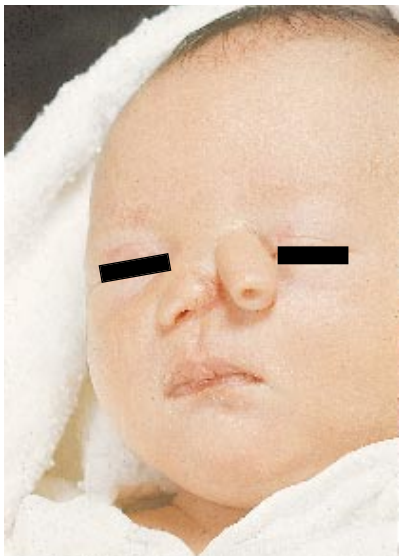

Figure 1.51. Proboscis lateralis is a congenital abnormality in which the nose fails to develop normally.

1.52

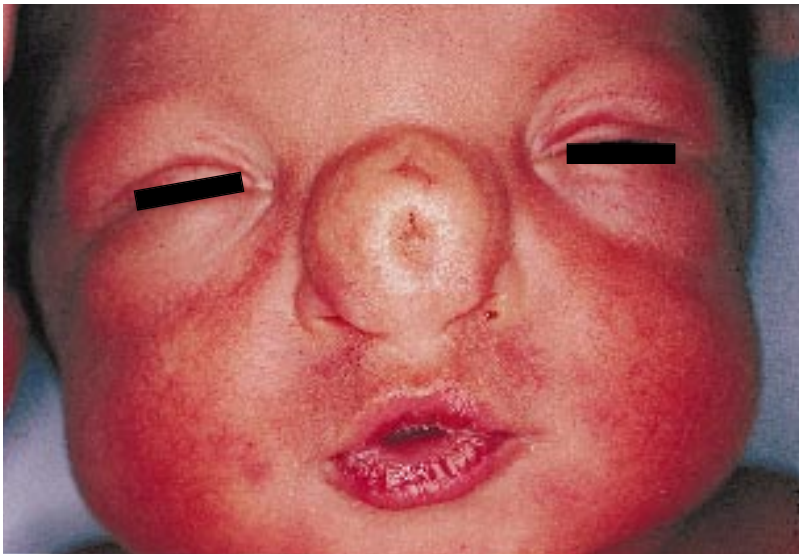

Figure 1.52. Severe midline nasal schistasis. This was confirmed to be a communicating encephalocele on CT scan.

1.53

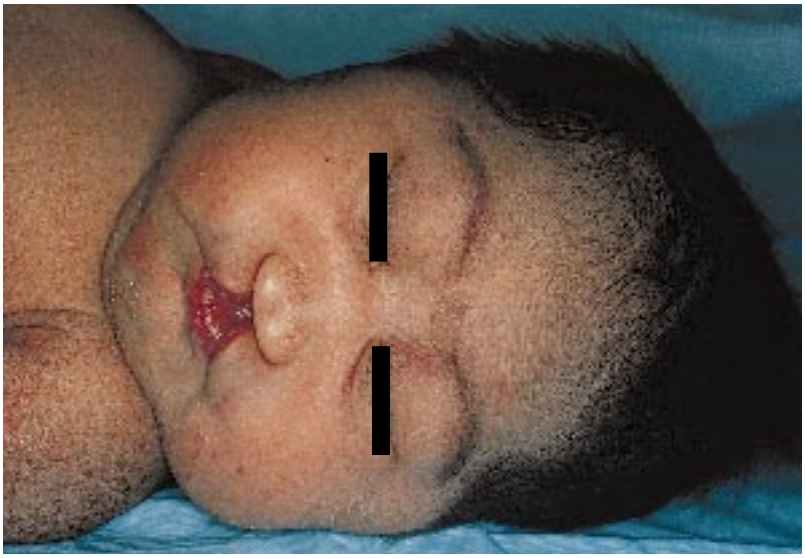

Figure 1.53. This infant has the median cleft syndrome. Note the facial features which include median cleft lip, nasal depression, hypotelorism, receding forehead, and microcephaly. A median cleft palate was also present. These findings commonly occur with alobar holoprosencephaly as a result of underdevelopment of the brain. The majority of cases of holoprosencephaly are sporadic and may occur as an isolated anomaly, in association with chromosomal abnormalities (13, 13q–, 18p–), all in syndromes associated with arhinencephaly or holoprosencephaly.

1.54

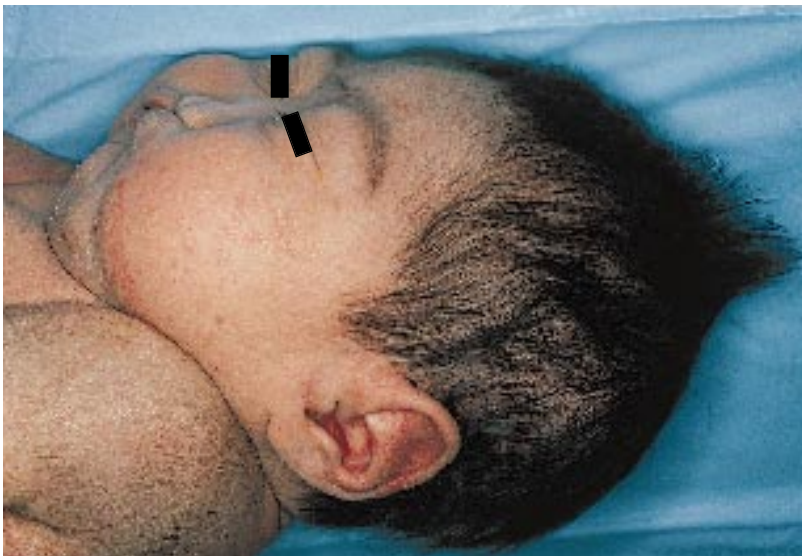

Figure 1.54. Lateral view of the same infant shows the microcephaly, receding forehead and chin, marked hypotelorism, and median cleft.

1.55

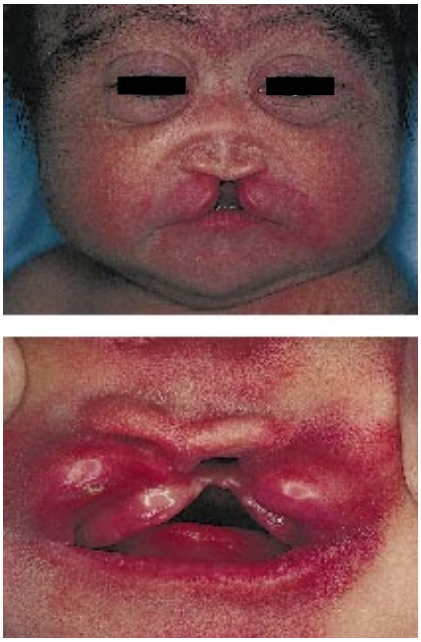

Figure 1.55. Another example of the median cleft syndrome with a normal karyotype and a head ultrasound showing holoprosencephaly. The close-up view shows clefting of the alveolar ridge which is also seen in this syndrome.
Holoprosencephaly results from maldevelopment of the forebrain (prosencephalon). It may occur as an alobar type in which there is a horseshoe-shaped single ventricle; a semilobar type in which there is partial differentiation of the ventricles, especially at the temporo-occipital horns; or a lobar type in which there is partial fusion of the frontal lobes and a narrow body of the lateral ventricles.

1.56

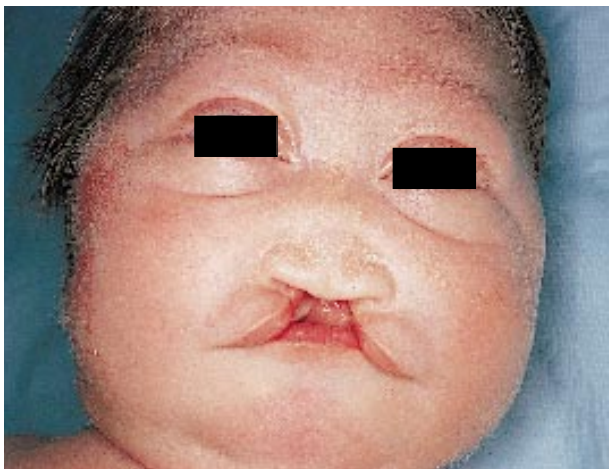

Figure 1.56. Another example of the median cleft syndrome in an infant with trisomy 13. Note the hypotelorism and midline position of the cleft lip. Embryologically this differs from the more common unilateral or bilateral cleft lip.

1.57

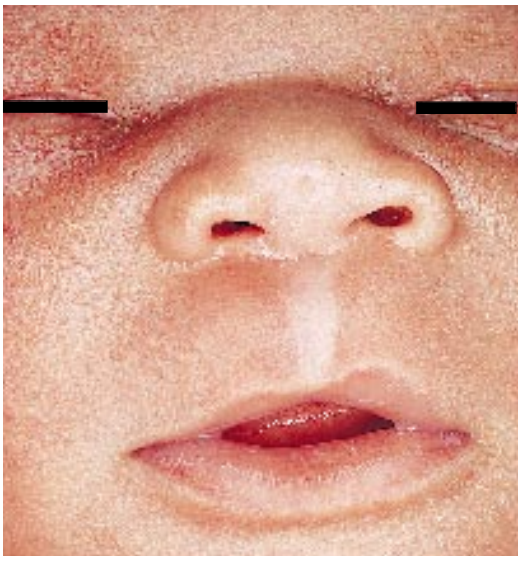

Figure 1.57. Note the midline hypopigmentation of the philtrum with lack of true clefting of the lip. This finding suggests that further evaluation should be done. Central nervous system evaluation revealed holoprosencephaly.

1.58

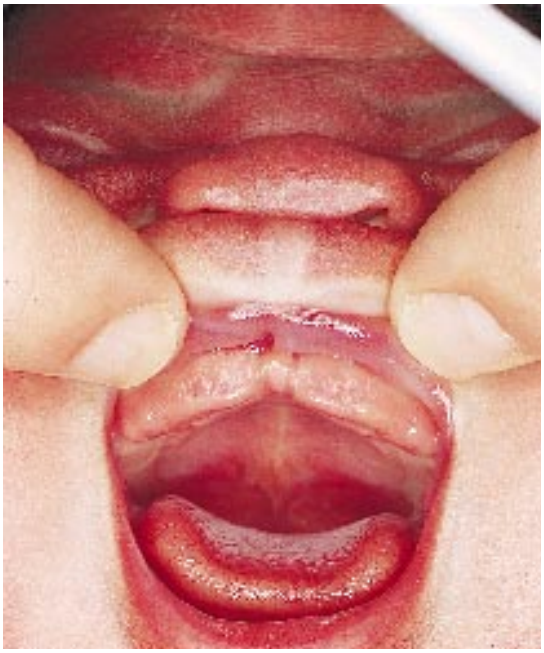

Figure 1.58. Notching of the alveolar ridge in the same infant as in Figure 1.57 with median cleft syndrome.

1.59

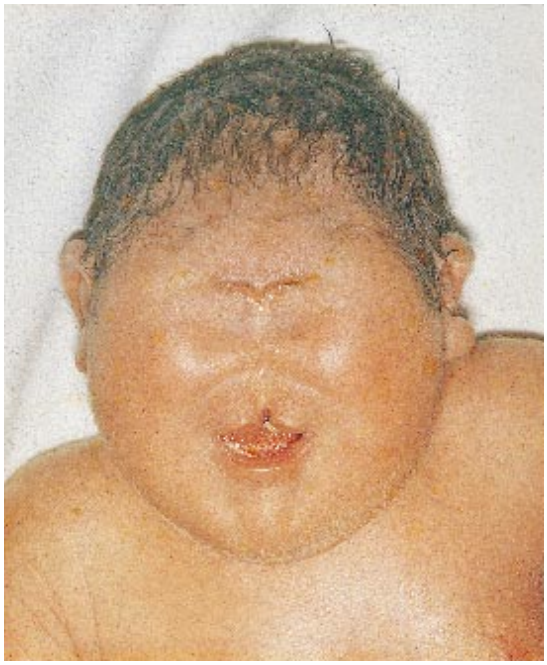

Figure 1.59. Holoprosencephaly may have other clinical manifestions. This infant is an example of cyclopia without a nose or proboscis. In cyclopia there may be a single, double or absent proboscis above or below the fused orbits. Note the marked hypotelorism resulting in fused eyes (cyclopia), lack of nose, and small median cleft of the upper lip. There is also severe microcephaly.

1.60

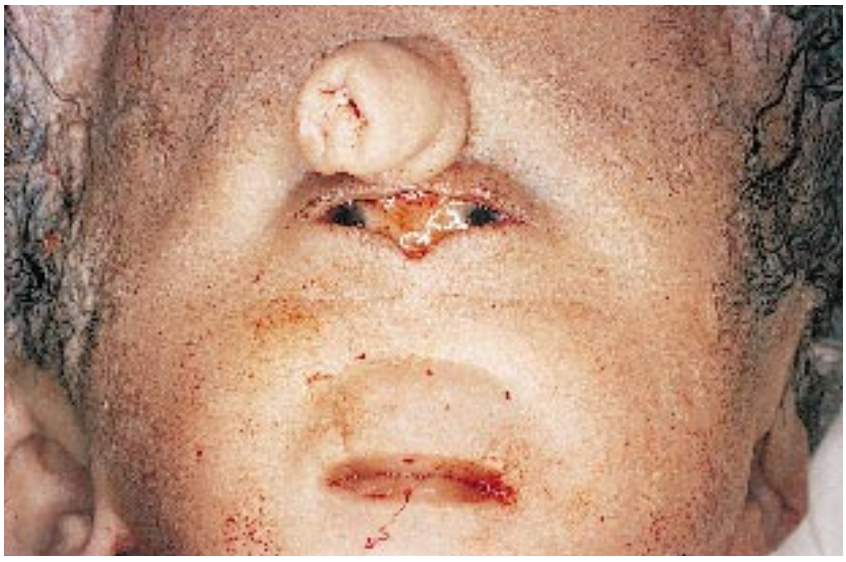

Figure 1.60. This is an example of cyclopia with a superior proboscis. Note the median cleft in the single fused lower eyelids, the fused orbits, and the hypoplasia of the facial bones. This is another example of median cleft syndrome with holoprosencephaly.

1.61

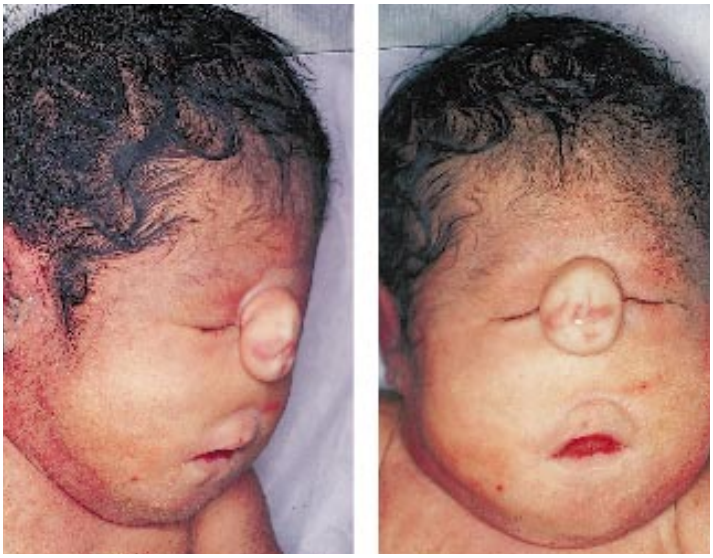

Figure 1.61. In holoprosencephaly when there are separate orbits with a proboscis above the eyes and a lack of nostril with a single or double proboscis above or below the eyes, the condition is called ethmocephaly. Note also the small mouth.

1.62

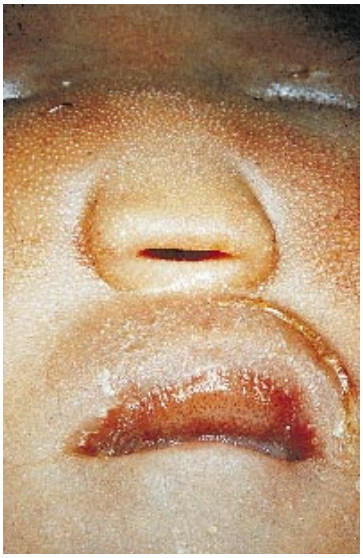

Figure 1.62. Another variant of the median cleft syndrome (holoprosencephaly) is cebocephaly in which there is a small nose with a single nostril above or below the eyes. Note the single orifice and aplasia of the nasal septum and philtrum.

1.63

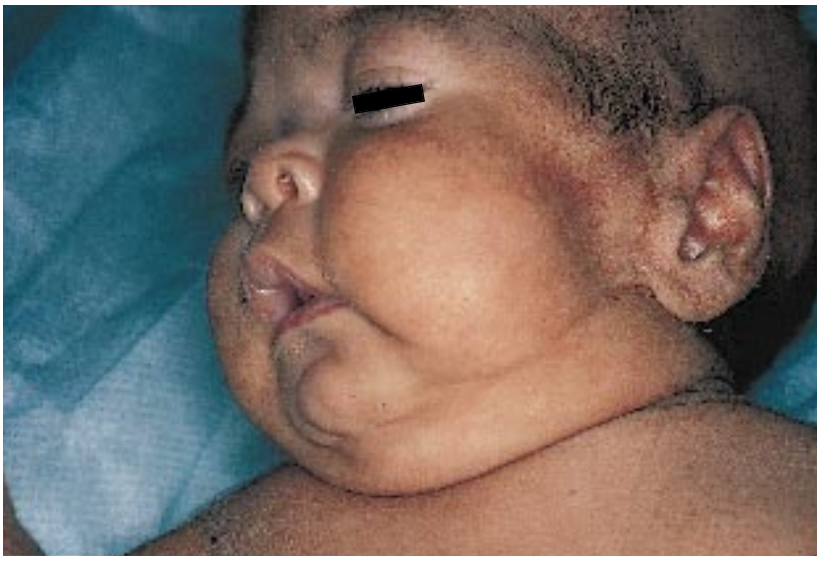

Figure 1.63. Buccal fat pads (sucking cushions) are pads of fat tissue between the fibers of the masseter muscle. When the infant is sucking they prevent collapsing of the cheeks during indrawing. These fat pads remain unaltered despite loss of adipose tissue in other body areas.

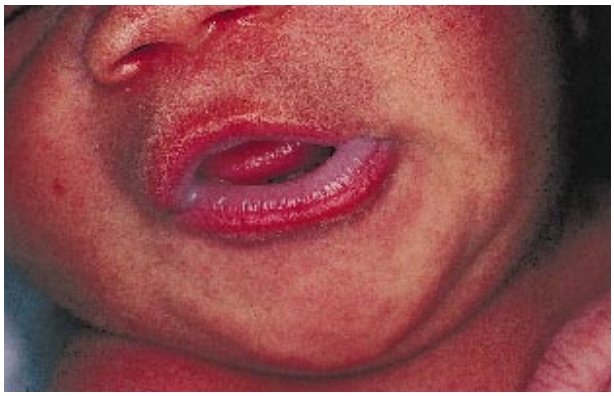

1.64

Figure 1.64. Sucking blisters (sucking calluses) on the lips are present in the newborn infant. From birth, the lips show a sharp line of demarcation where the skin meets the mucosa. The mucosa is slightly elevated, moist, glistening deep red or purple and ends abruptly with the skin which forms one-third of the visible lip. The term "sucking calluses" is a misnomer because they are not callosities due to pressure or friction. They have been seen at their most florid in infants who have never sucked (for example those with congenital heart disease). Efficient sucking requires a complete seal of the lips around the nipple, hence the development of these calluses.

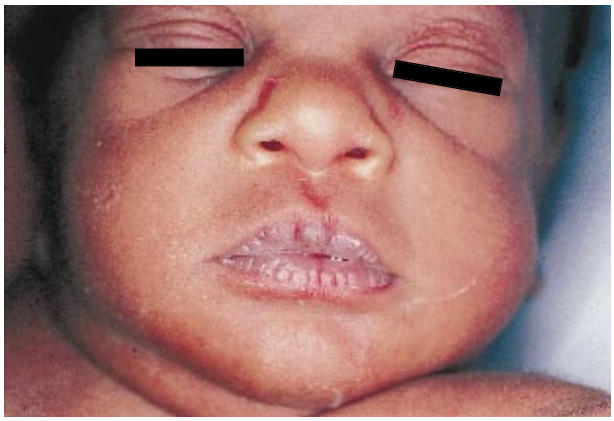

1.65

Figure 1.65. Another example of sucking blisters in an infant at 6 days of age. Note that the mucous membrane portion of the lip has a superficial furrowed appearance. With time, the outer layer dries with lifting and shedding of the cornified epithelium and new blisters may develop for a few weeks. They occur most commonly in breast-fed infants or babies who feed vigorously. Pathologically, this can also occur from overheated formula, or as an allergic reaction to the components of the nipple or the formula.

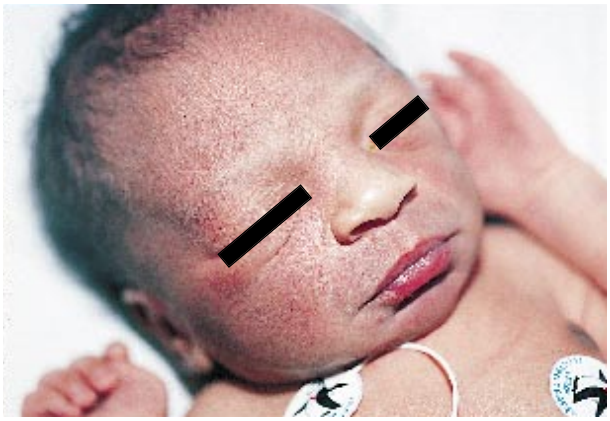

1.66

Figure 1.66. A thin vermilion border of the upper lip in a normal infant. This may also be seen in many syndromes such as the fetal alcohol syndrome.
A long philtrum may indicate a short nose and a short philtrum may indicate a long nose. Downturned corners of the mouth may reflect overgrowth in the width of the upper lip, which when combined with a short philtrum or thick lower lip results in a carp-like mouth.

1.67

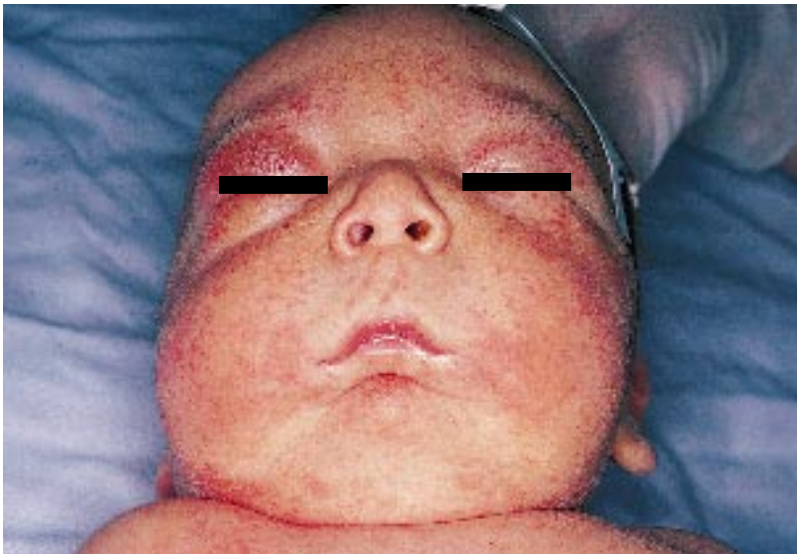

Figure 1.67. This infant is an example of microstomia occurring as a result of excessive merging of the maxillary and mandibular processes of the mandibular arch. This may occur in normal infants or is associated with many syndromes such as Hallermann-Streiff syndrome and Freeman-Sheldon syndrome. The diagnosis in this infant was mosaic trisomy 8.

1.68

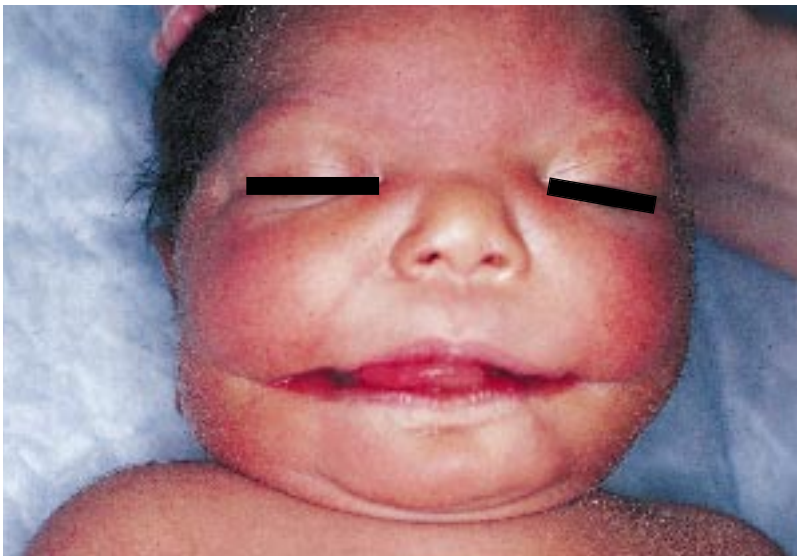

Figure 1.68. This infant with severe bilateral macrostomia is an example of a congenital lateral or transverse facial cleft which results from malformation of the mandibular arch (failure of the lateral maxillary and mandibular processes to merge). The defect may be unilateral or bilateral and is associated with deformities of the outer ear, hypoplasia of the mandible or maxilla, and cleft palate. It is also seen in Goldenhar's syndrome.

1.69

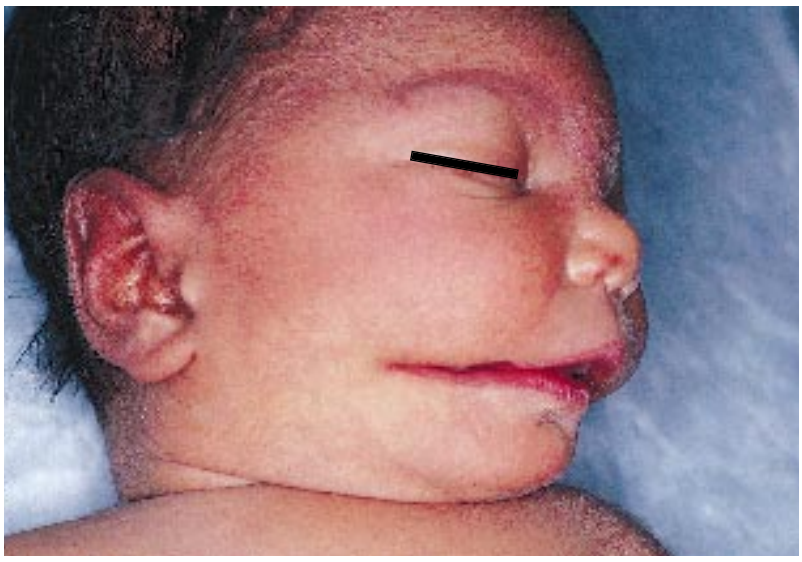

Figure 1.69. A lateral view of the severe macrostomia in the same infant. Note the micrognathia. There were no other abnormalities.
An oblique facial cleft (orbitofacial fissure) extends from the upper lip to the medial aspect of the orbit. It is often bilateral and may involve the orbit, nose, lacrimal ducts, or central nervous system. This may occur from facial clefting that results from swallowed amniotic bands and represents a disruption in that it does not follow the normal planes of fusion of the face.

1.70

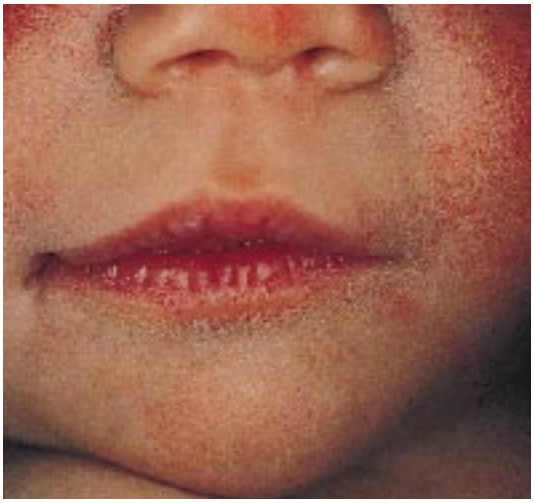

Figure 1.70. Right-sided unilateral macrostomia in an otherwise normal infant.

1.71

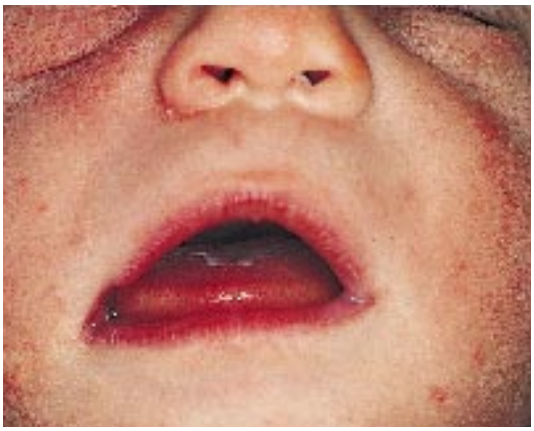

Figure 1.71. This infant with Goldenhar's syndrome has unilateral macrostomia. There was an antimongoloid slant to the eyes, preauricular skin tags, and deafness.

1.72

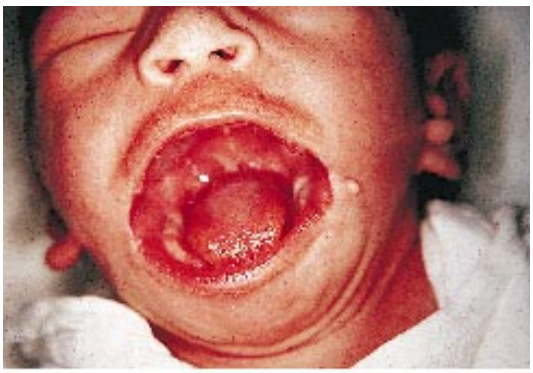

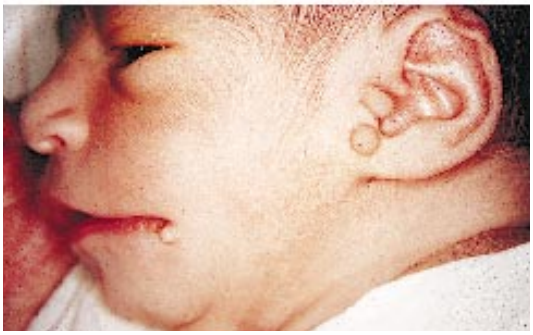

Figure 1.72. Macrostomia with cutaneous tags and preauricular skin tags. Cutaneous pits and tags may be found along a line connecting the oral commissure and the external auditory canal in Goldenhar's syndrome.

1.73

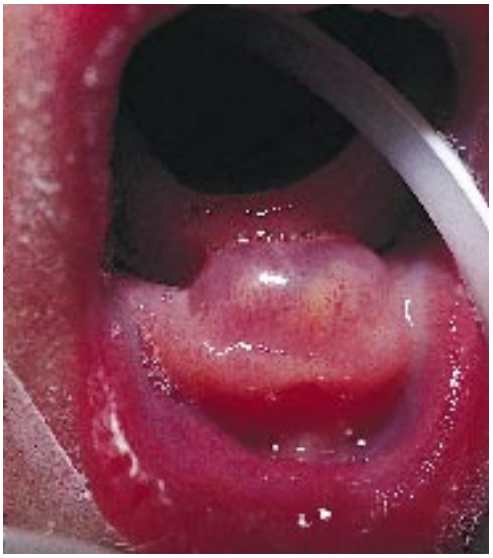

Figure 1.73. Eruption cysts in an infant at birth. Note the central lower incisors which are visible. The teeth erupted at the age of 4 days.

1.74

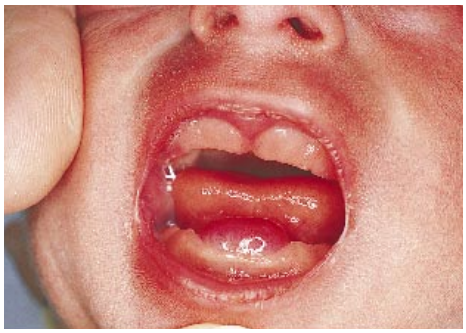

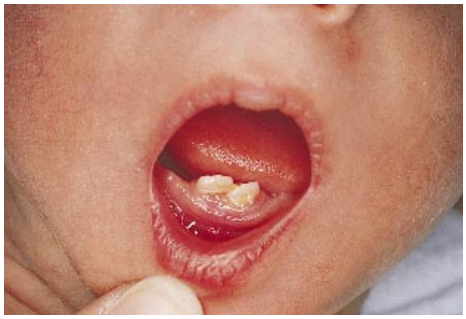

Figure 1.74. In the upper figure, note the eruption cysts which were present at birth. At the age of 7 days, both lower central incisors had erupted (lower figure). Nearly all neonatal teeth arise from the normal deciduous complement and are usually only immature caps of enamel and dentine with poor root formation. Often the eruption cyst is present on the gum at birth and the neonatal tooth appears shortly afterwards. The lower central incisors are the most common site for neonatal teeth.

1.75

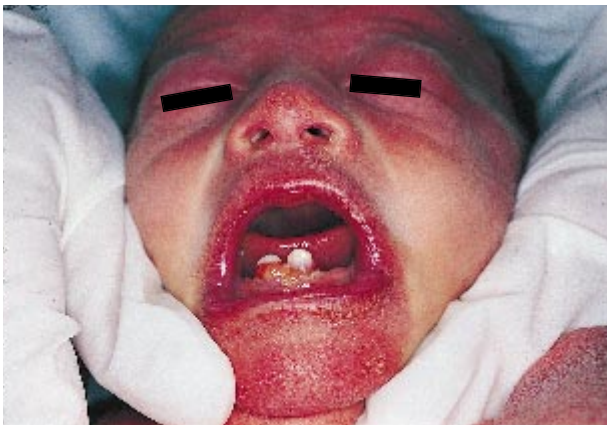

Figure 1.75. Natal teeth present at birth. Teeth that erupt after birth are neonatal teeth. These teeth have a familial pattern of occurrence and are more common in certain races such as American Indians and Eskimos. Neonatal teeth may occur in association with syndromes.

1.76

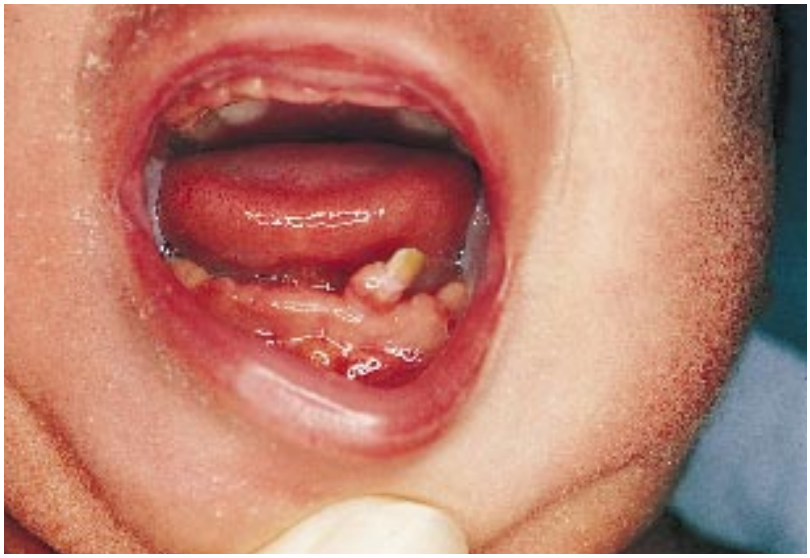

Figure 1.76. Note the poor development of this natal tooth. This should be extracted, as this may fall out spontaneously and be aspirated.

1.77

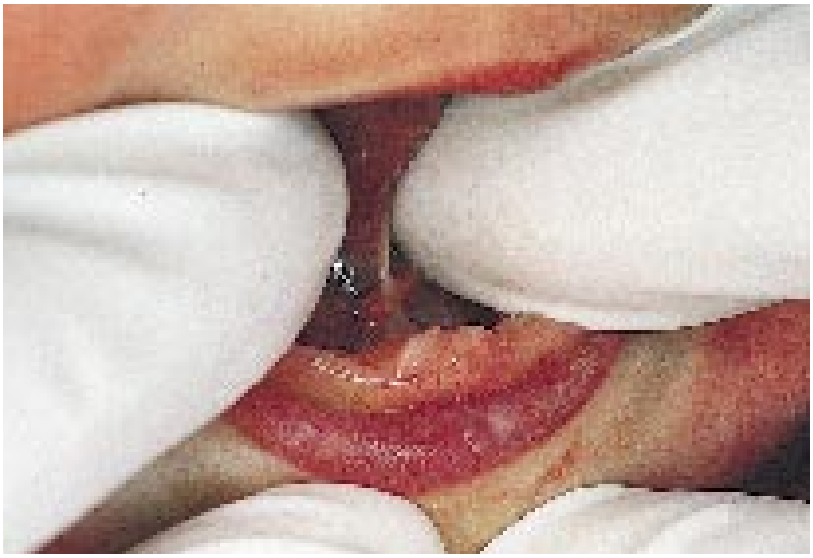

Figure 1.77. Natal teeth present at birth in a very low birthweight infant (weight 700 g).

1.78

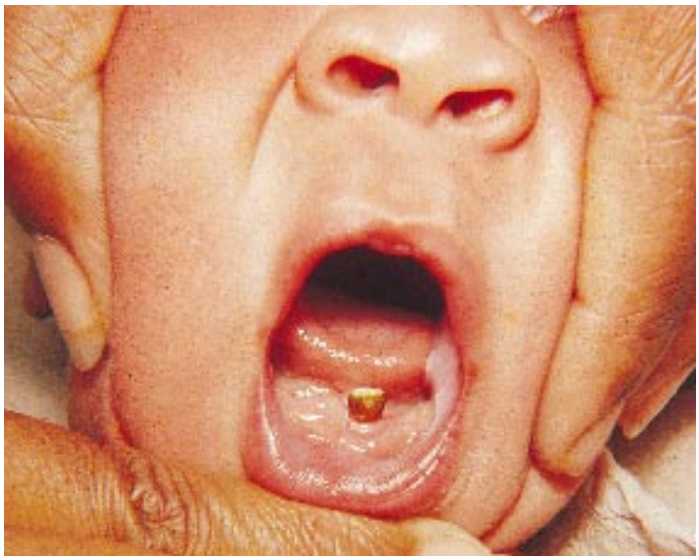

Figure 1.78. Discoloration of a natal tooth secondary to maternal treatment with tetracycline during pregnancy.

1.79

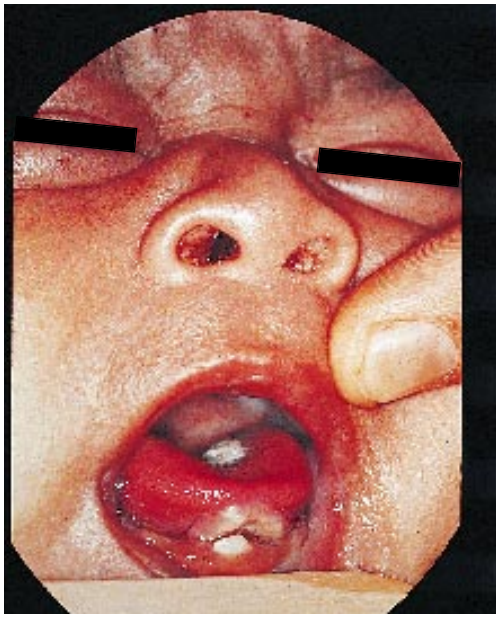

Figure 1.79. Neonatal teeth causing ulceration of the undersurface of the tongue by vigorous sucking (Riga-Fede disease). Neonatal teeth are more likely to cause this because the mucous membranes are still very delicate. These teeth require extraction to permit healing of the ulceration.

1.80

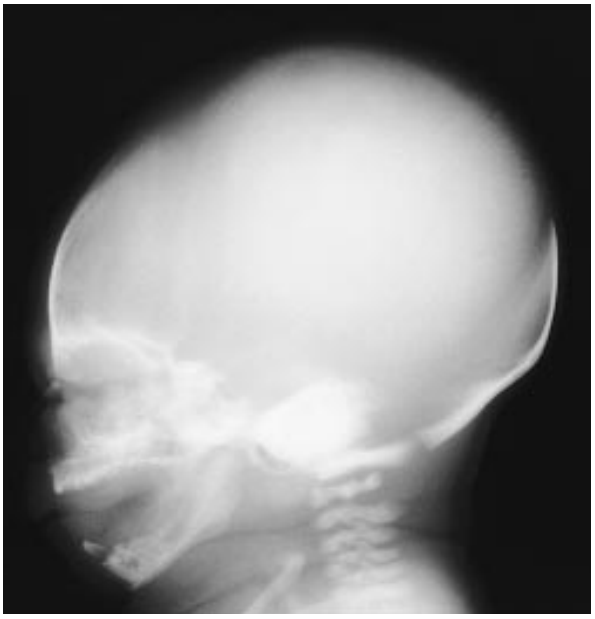

Figure 1.80. Lateral radiograph of the skull. Note the neonatal teeth.

1.81

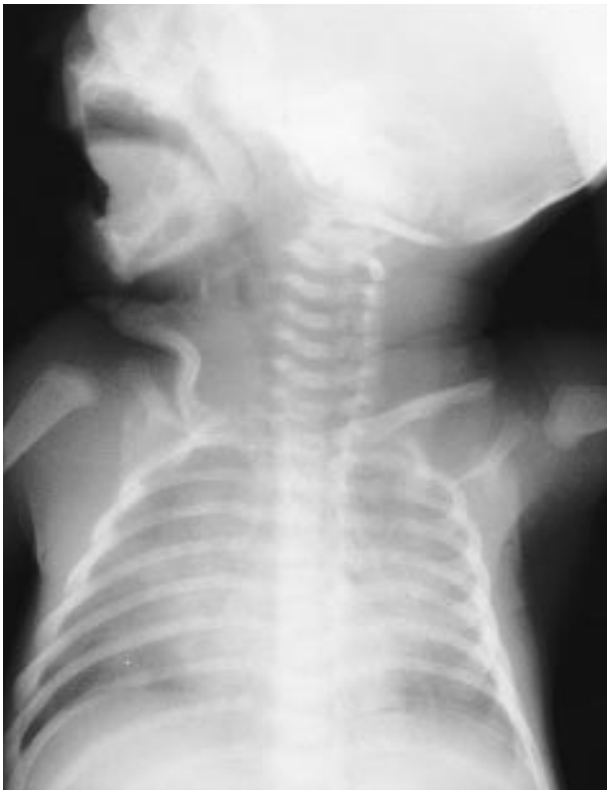

Figure 1.81. Radiograph of the face and chest showing the lack of dentition in a term infant with ectodermal dysplasia. Normally, at term there should be mineralization of the incisors and of the first and second molars.

1.82

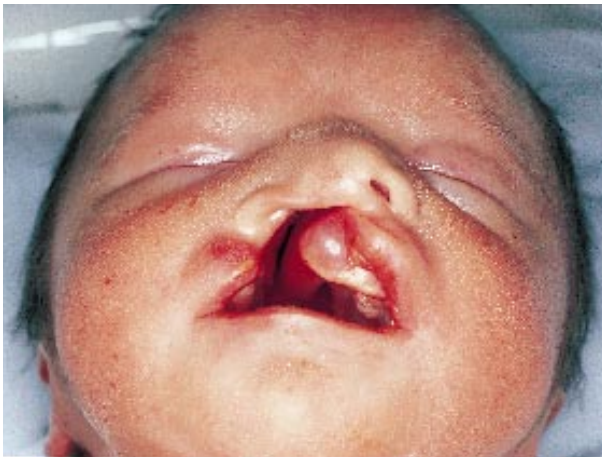

Figure 1.82. A baby with a right unilateral cleft lip and a cleft palate. Note the eruption cyst in the upper jaw. In general, neonatal teeth are more common in the lower jaw, but in the presence of a cleft lip and/or cleft palate, neonatal teeth are often present in the upper jaw.

1.83

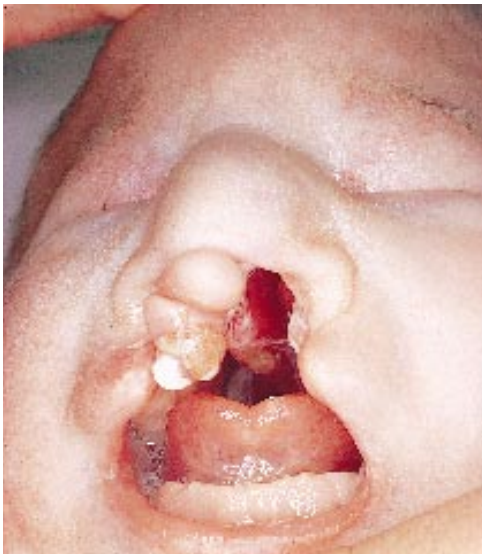

Figure 1.83. This infant with a left cleft lip and cleft palate has a neonatal tooth in the upper jaw.

1.84

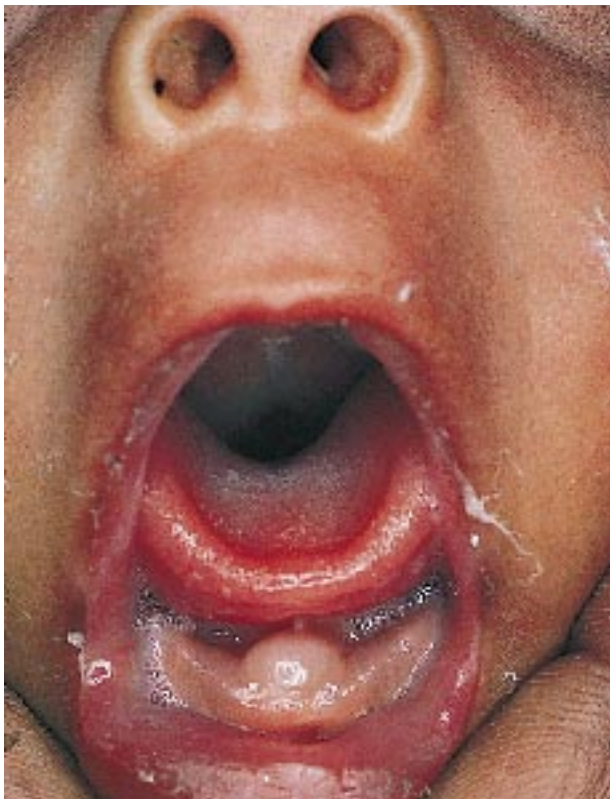

Figure 1.84. If a central eruption cyst or central mandibular incisor is present in the lower jaw, the diagnosis of median cleft syndrome must be excluded. This infant had median cleft syndrome. A single central maxillary incisor also may be seen in growth hormone deficiency.

1.85

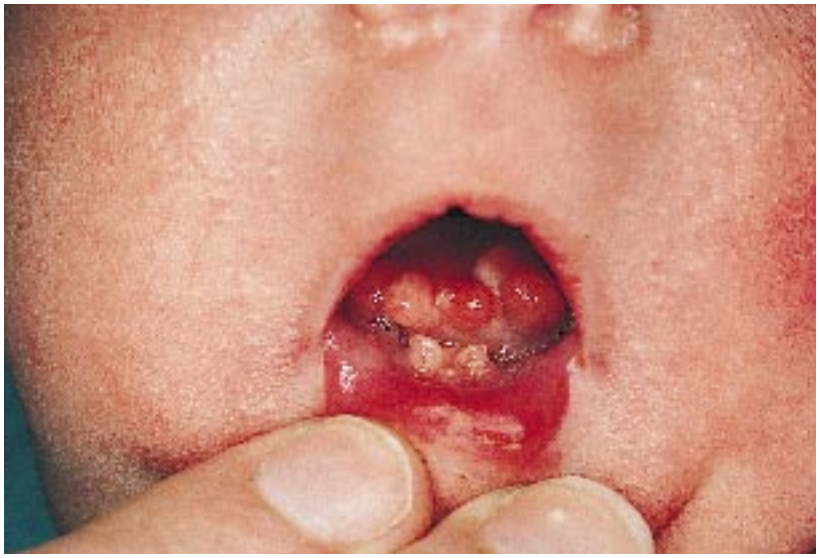

Figure 1.85. In this infant with neonatal teeth, note the small white hamartomatous masses on the ventral and dorsal surfaces of the tongue and the ankyloglossia. These findings are typical of the orofaciodigital syndrome, Type I.

1.86

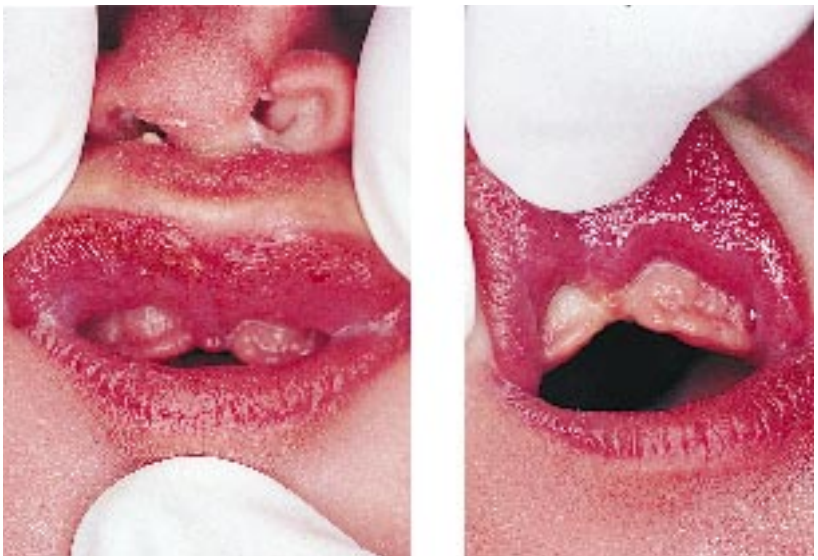

Figure 1.86. Frenulum (frenum) labialis superior. The frenulum is a continuation of the fibrous median raphe of the maxilla. It may be prominent and unusually thick and is often associated with deep notching of the alveolar ridge of the maxilla.

1.87

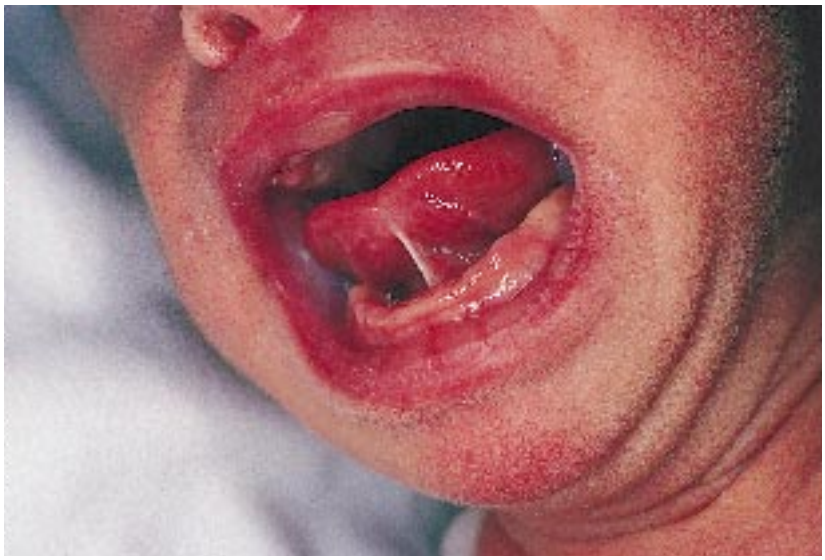

Figure 1.87. Lingual ankyloglossia ("tongue tie") in a premature infant (birthweight 1700 g). Note the indentation of the tip of the tongue. The lingual frenulum limits the movement of the tip of the tongue. True tongue tie is rare. If the tongue can be protruded beyond the lips, no intervention is necessary as the tongue grows more rapidly than the frenulum and soon becomes freely mobile.

1.88

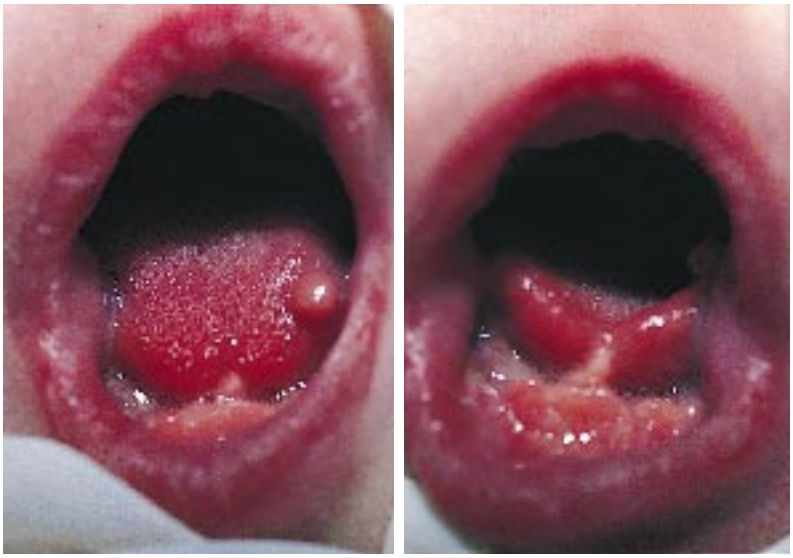

Figure 1.88. The lingual frenulum may be thick and short, and may be continuous through an alveolar notch to produce a dimpled or bifid tongue. Usually this is of no consequence. In this infant with orofaciodigital syndrome, in addition to the short frenulum, there is gum hypertrophy and a hamartoma. There was syndactyly of the second and third toes.
A thickened lingual/labial frenulum may result in a wide space (diastema) between the central incisors. As the canines begin to erupt at 9 to 11 years of age, division of the thickened frenulum allows the gap to close.

1.89

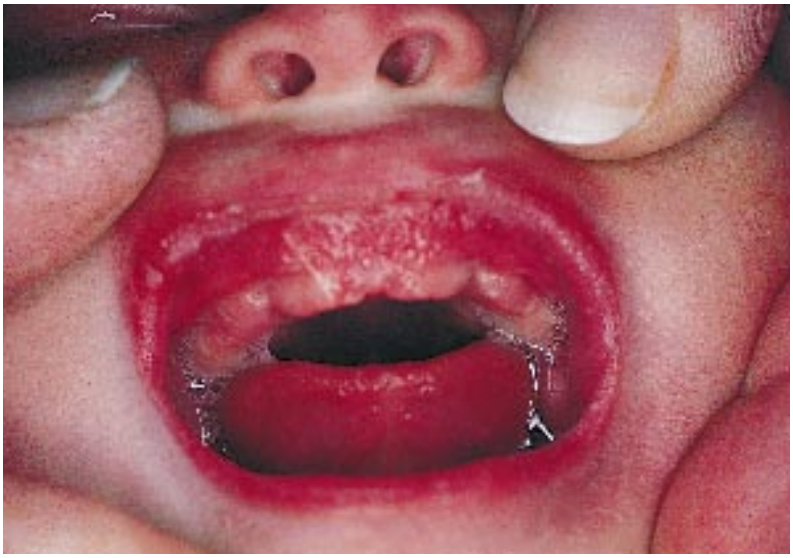

Figure 1.89. In Ellis-van Creveld syndrome (chondroectodermal dysplasia) one of the typical findings is present in the mouth. There is a defect in the upper lip due to fusion of the labiogingival margins of the upper lip so that there is no mucobuccal sulcus. Note the compartments for the individual tooth buds can be seen on the alveolar ridges.

1.90

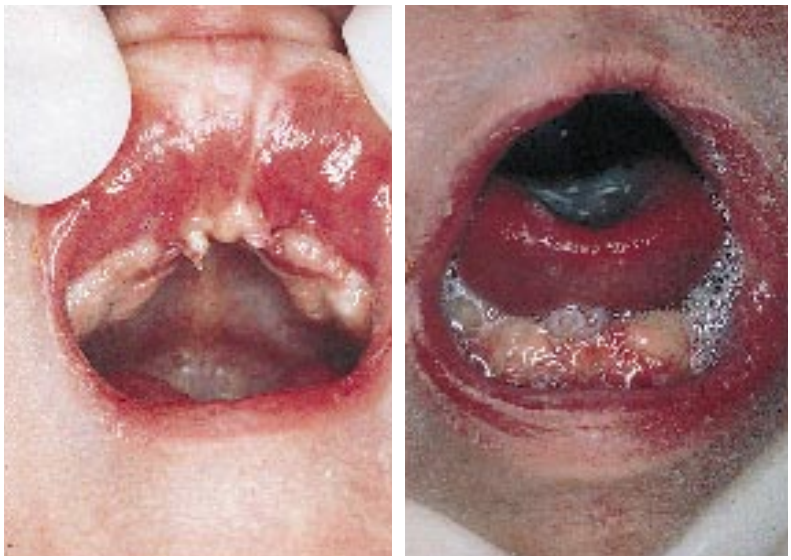

Figure 1.90. Another infant with Ellis-van Creveld syndrome showing the typical changes in the mouth. On the left, note the defect particularly in the middle of the upper lip in which there is fusion at the maxillogingival margin to the upper lip so that there is no mucobuccal sulcus. Also note the hypoplastic neonatal teeth in the upper jaw in the figure on the left and in the lower jaw in the figure on the right.

1.91

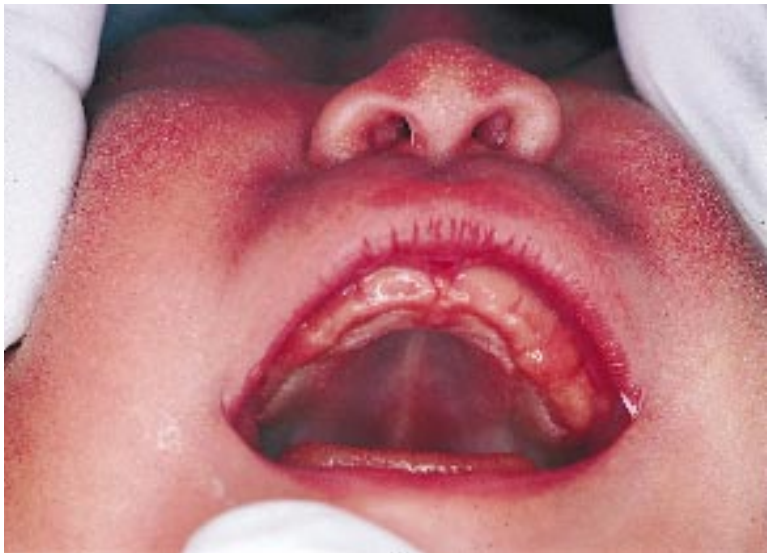

Figure 1.91. The components for each individual tooth bud can often be seen on the alveolar ridges of the maxilla and mandible in normal infants. Note the milia on the nose and the demarcation on the lip where the skin meets the mucous membrane. The sucking calluses occur on the mucous membrane part of the lip and are most prominent on the central portion.

1.92

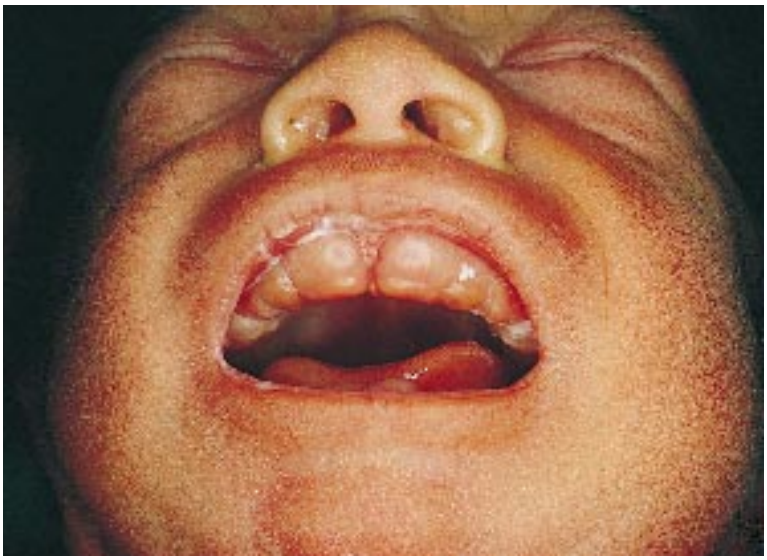

Figure 1.92. Gum hypertrophy in an infant born to a mother treated with phenytoin during pregnancy.

1.93

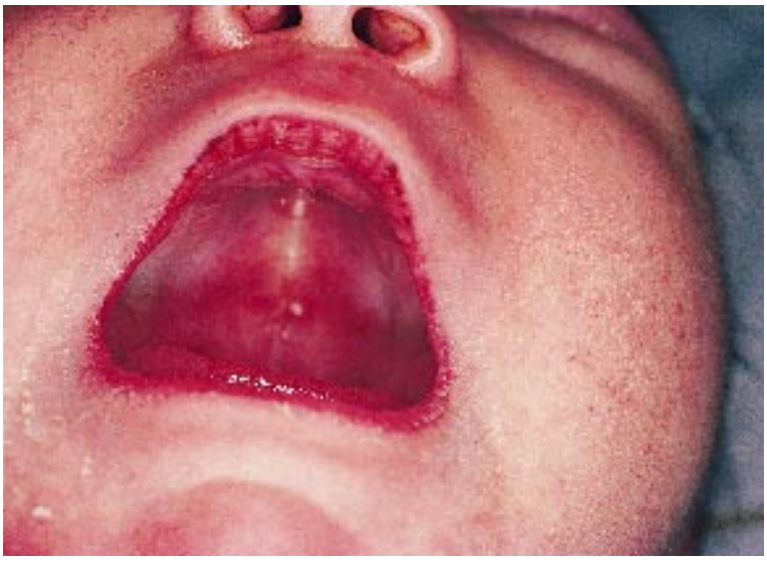

Figure 1.93. Epithelial pearls are areas where the cells are condensed in whorls or small cysts. These are most often seen in the mouth. The most common are called Epstein's pearls which consist of a small cluster of whitish-yellow swellings at the junction of the soft and hard palate in the midline.

1.94

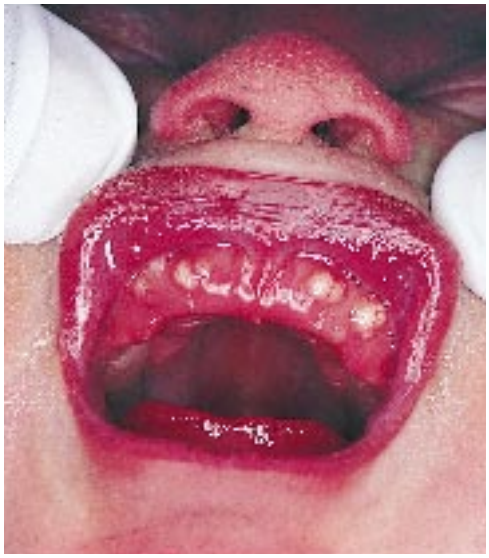

Figure 1.94. Note the Bohn's nodules (inclusion cysts) on the alveolar margin in this infant. Epithelial pearls are also seen on the areola or on the foreskin.

1.95

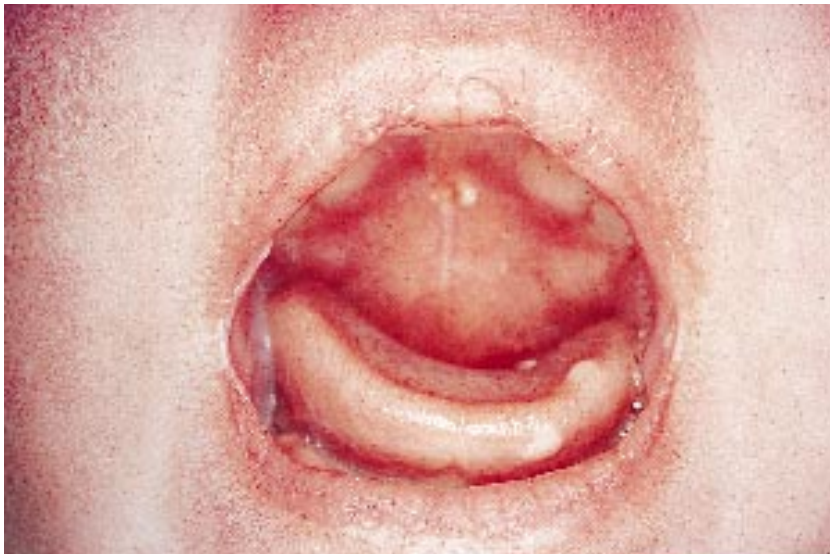

Figure 1.95. Note the inclusion cysts on the tongue and the Epstein's pearls.

1.96

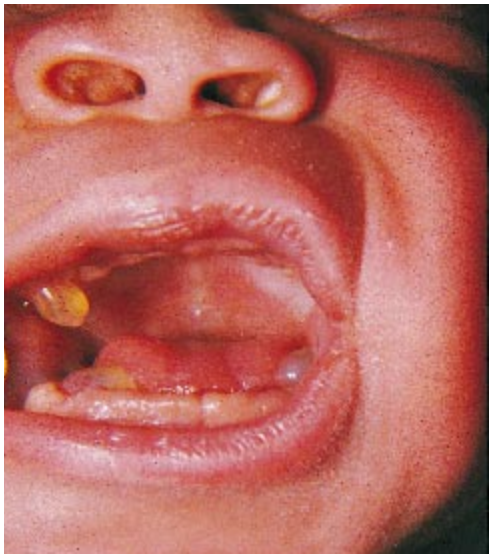

Figure 1.96. Another example of inclusion cysts which are larger. Epstein's pearls, Bohn's nodules, and inclusion cysts all improve spontanteously.

1.97

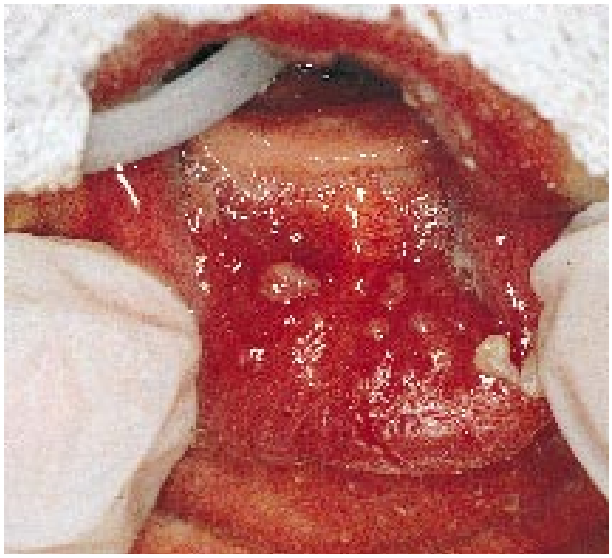

Figure 1.97. Note the mucoceles on the lower lip of this premature infant (birthweight 1200 g). Mucoceles are not true cysts but rather collections of mucus surrounded by connective tissue. They usually occur on the lower lip, are not common, and require no treatment. Differential diagnosis includes herpetic lesions.

1.98

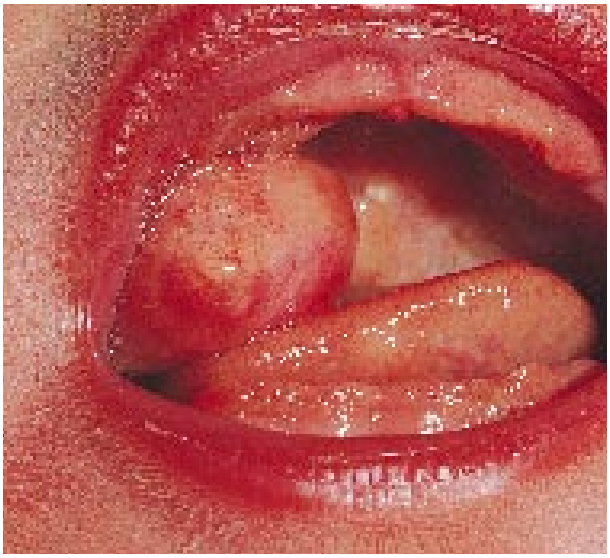

Figure 1.98. Congenital epulis may occur as a small or very large mass that protrudes from the mouth as a large tumor. They may be pedunculated and are of firm consistency. They usually occur in the region of the maxillary alveolar mucosa and are a form of embryonal hamartoma. A large epulis needs excision and rarely occurs.

1.99

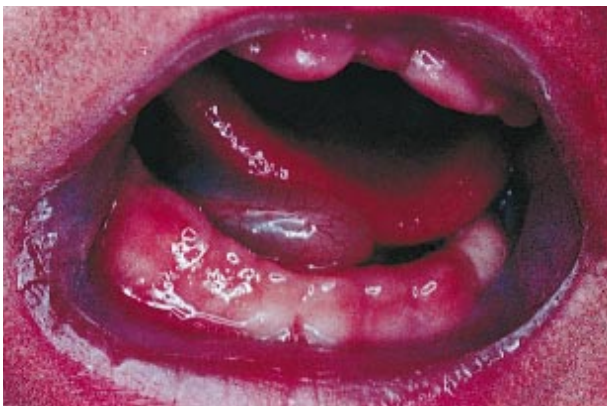

Figure 1.99. This bluish fluctuant transparent swelling in the anterior part of the floor of the mouth is a ranula which is a retention cyst arising from the sublingual gland. The term ranula originates from its similarity to the inflated bladder of a frog's throat. Ranula is a diminutive of *Rana* species of frog. Large ranulas need excision but the smaller lesions resolve spontaneously. Note the diastema in the upper jaw.

1.100

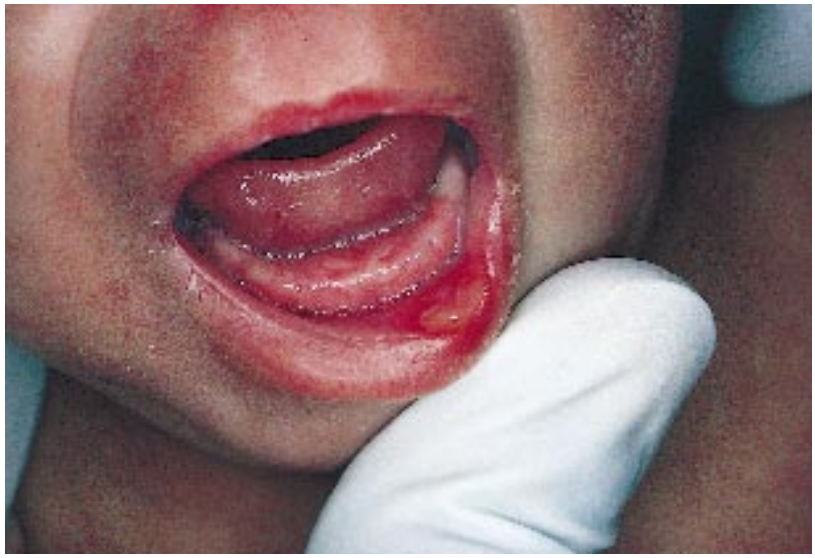

Figure 1.100. Traumatic ulcer on the lower lip of a neonate as a result of orotracheal intubation for resuscitation.

1.101

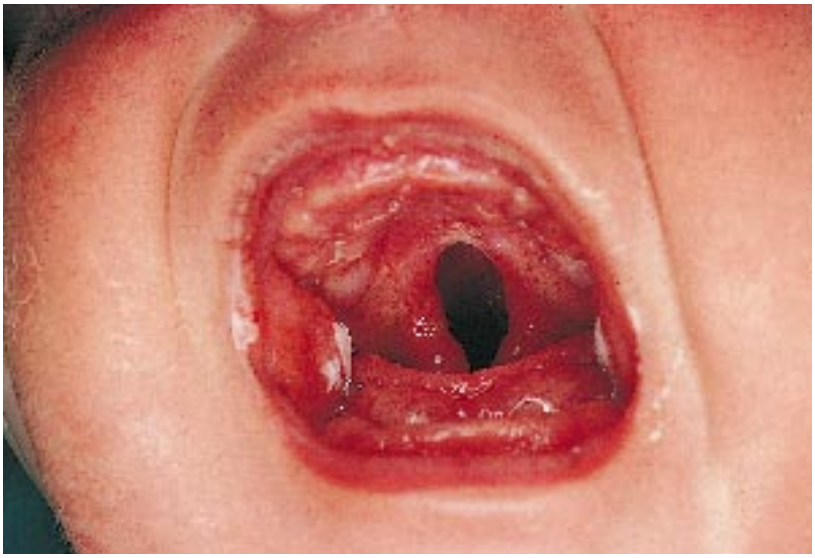

Figure 1.101. Aglossia and cleft palate in an otherwise normal infant. Aglossia occurs more frequently in the aglossia/hypoglossia adactylia syndrome. Due to the absence of a normal tongue, note how easily the cleft palate is seen. On the buccal mucosa note the oral candidiasis (thrush).

1.102

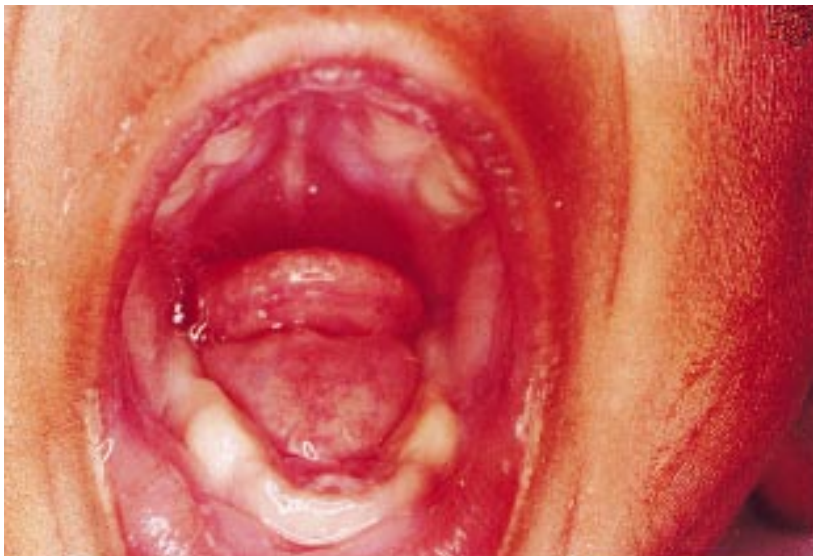

Figure 1.102. Note the small hypoplastic tongue (hypoglossia) posteriorly in this otherwise normal infant. This condition is more commonly associated with digital anomalies in the aglossia/hypoglossia adactylia syndrome.

1.103

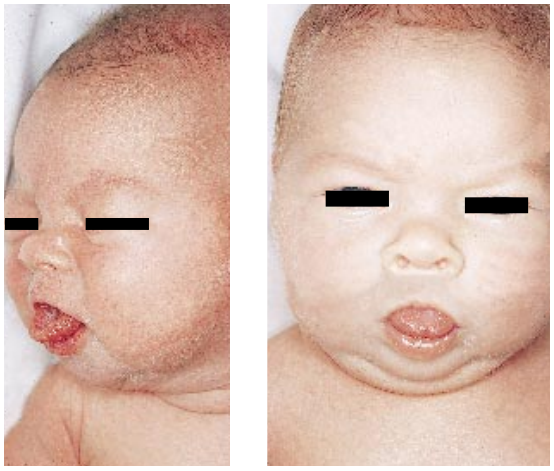

Figure 1.103. Macroglossia in an otherwise normal infant. The most common cause of macroglossia is idiopathic hypertrophy of the muscles of the tongue.

1.104

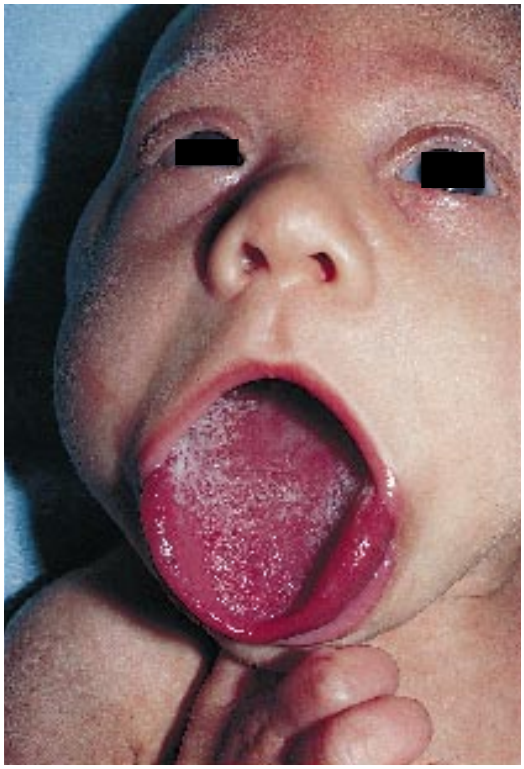

Figure 1.104. Macroglossia associated with Beckwith-Wiedemann syndrome. These infants have *e*xomphalos (omphalocele or large umbilical hernia), *m*acroglossia, and *g*igantism (EMG syndrome).

1.105

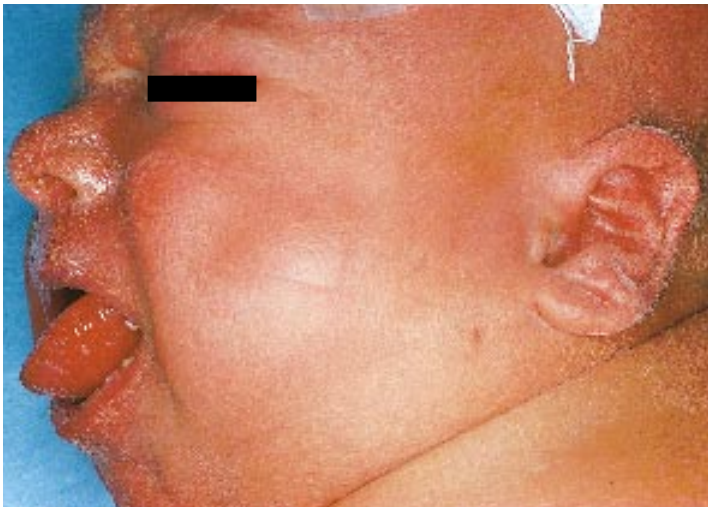

Figure 1.105. Another infant with Beckwith-Wiedemann syndrome showing the protrusion of the tongue with macroglossia. Note the other characteristic finding of a transverse crease of the earlobe.

1.106

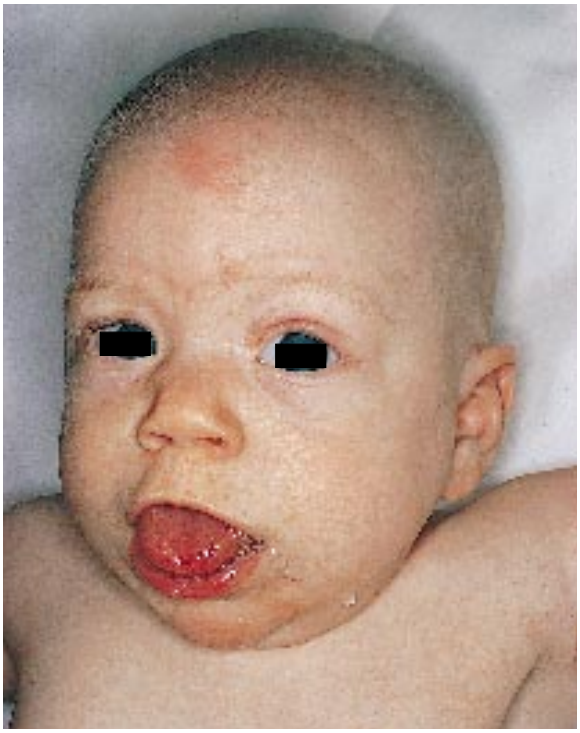

Figure 1.106. Macroglossia in a 2-month-old infant with Type II glycogen storage disease (Pompe's disease). Macroglossia is also seen in infants with congenital hypothyroidism and hemangioma or lymphangioma of the tongue.

1.107

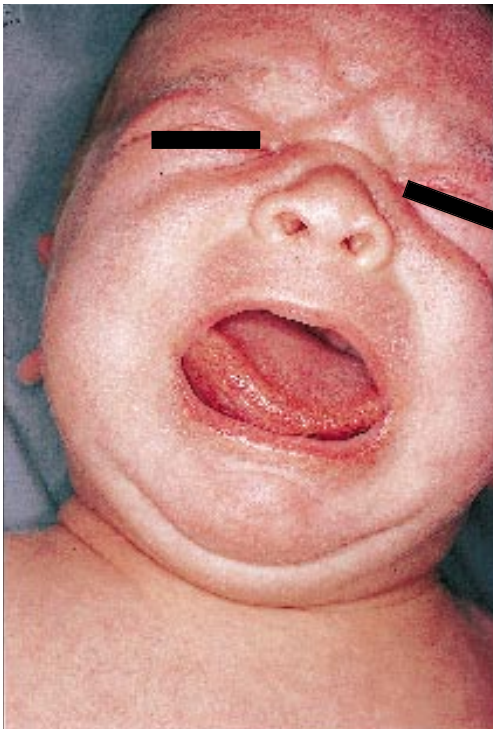

Figure 1.107. Macroglossia associated with unilateral hypertrophy of the right side of the tongue. This may be idiopathic or due to a hemangioma or lymphangioma of the tongue.

1.108

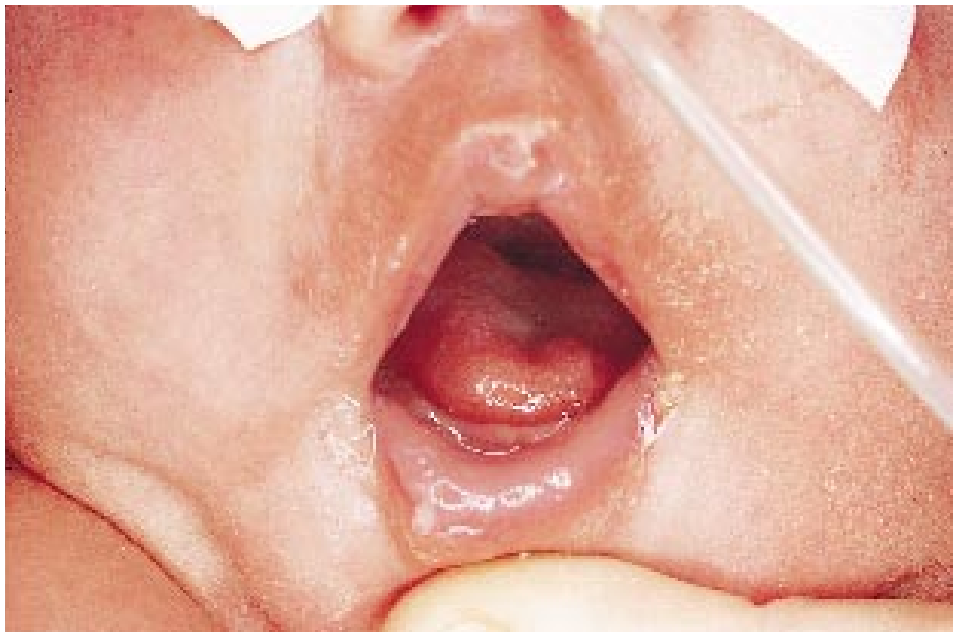

Figure 1.108. Atrophy of the left side of the tongue in an infant with Poland's anomaly and Möbius' syndrome. The association of these two conditions is not uncommon.

1.109

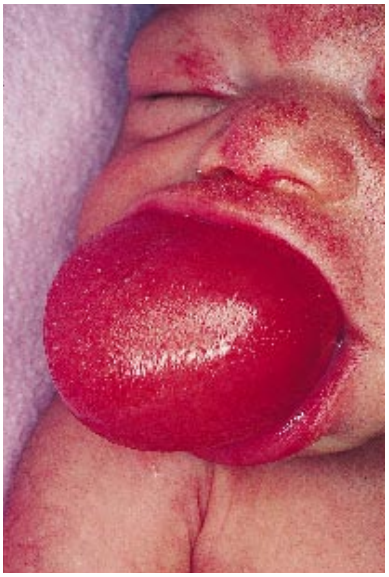

Figure 1.109. This infant with a large cystic mass of the tongue presented with severe respiratory distress. A preoperative thyroid scan was normal. The mass was resected and a diagnosis of an enterocystoma of the tongue (gastric duplication cyst) was made. The infant did well following removal of the cyst.

1.110

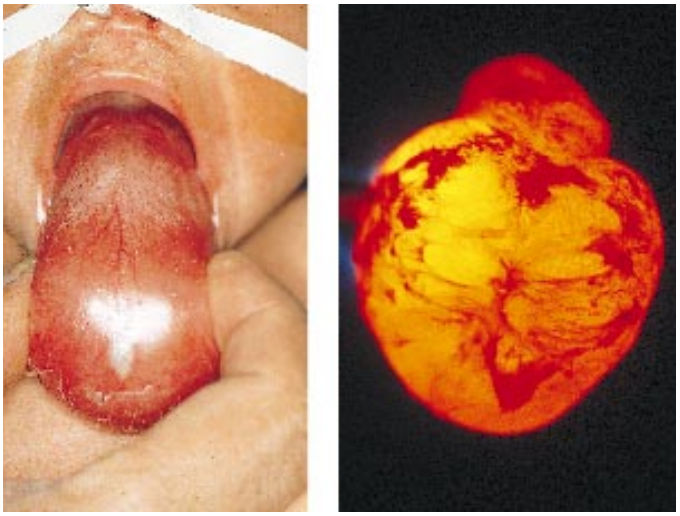

Figure 1.110. In the same infant, on the left note the large cystic swelling of the enterocystoma of the tongue. The figure on the right shows the transillumination of the cyst postoperatively.

1.111

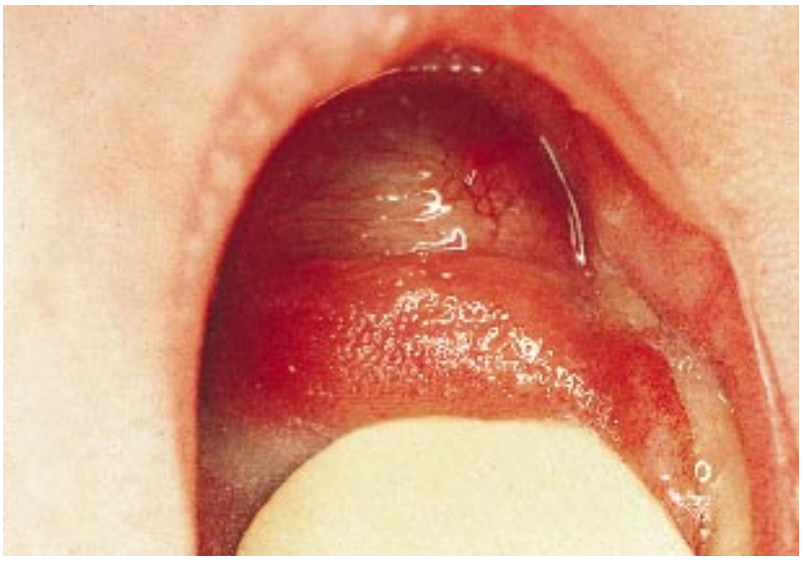

Figure 1.111. This infant presented with moderate respiratory distress and was noted to have a large cyst, especially on the left side at the base of the tongue. The cyst which was removed was diagnosed as an epithelial cyst in that it was lined by squamous epithelial cells.

1.112

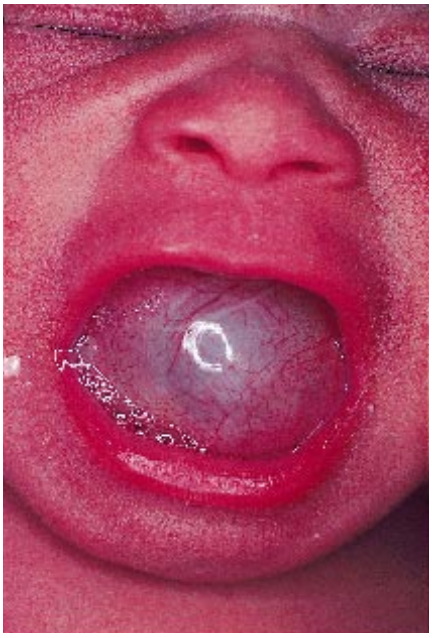

Figure 1.112. The large cystic midline swelling of the tongue in this infant was histologically diagnosed as a large thyroglossal cyst which was benign and lined by columnar epithelial cells.

1.113

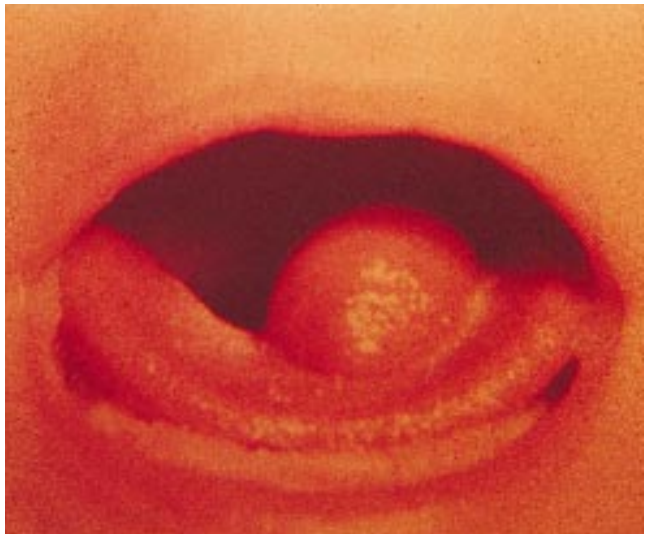

Figure 1.113. This well-circumscribed mass on the tongue was surgically removed and a diagnosis of hemangioma was made.

1.114

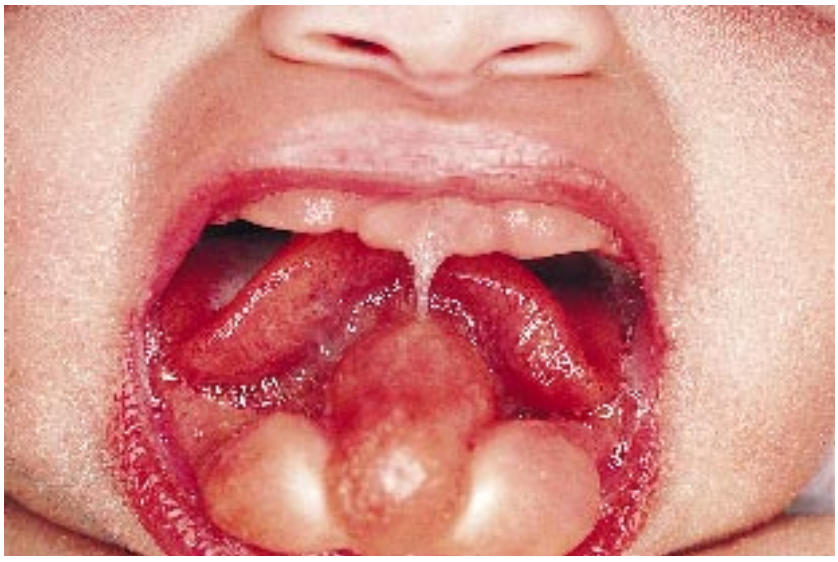

Figure 1.114. This infant at birth presented with a tumor involving the midmandible and floor of the mouth. The mass divided the tongue which was thickened and foreshortened. There was an associated midfacial cleft with a dermoid of the upper palate. With this type of defect a median cleft should be excluded. Tests for this were normal.

1.115

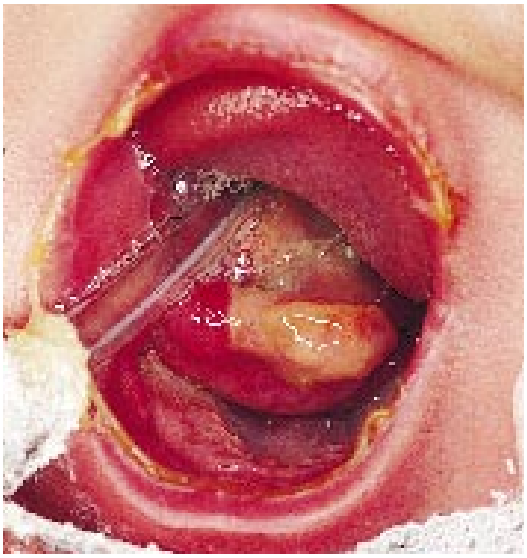

Figure 1.115. A mass involving the tongue was noted at birth in this term infant. Upon surgical removal, the diagnosis of teratoma of the tongue was confirmed. This was a benign teratoma and the infant did well.

1.116

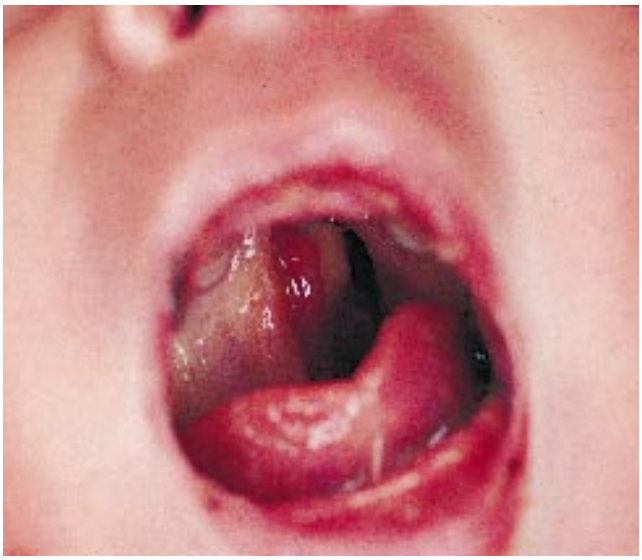

Figure 1.116. The large mass in the posterior mouth and nasopharynx in this term infant, with a cleft palate, was friable and bled easily. At surgery it was found to be a benign teratoma of the nasopharynx.

1.117

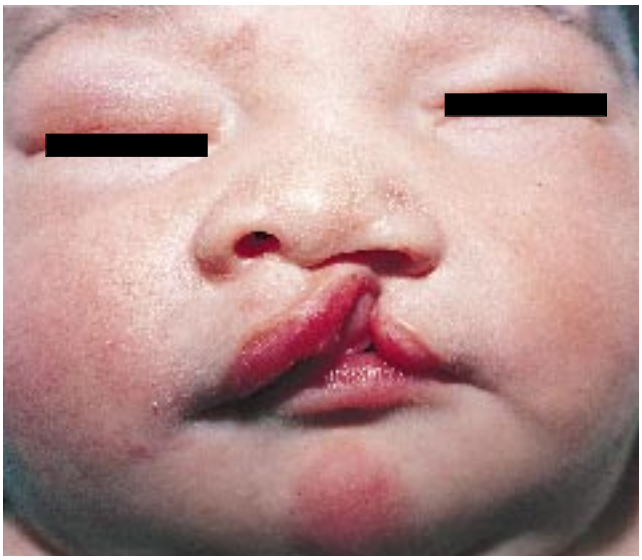

Figure 1.117. Cleft lip may be unilateral or bilateral and is often associated with a cleft palate. This normal infant has a mild unilateral cleft lip with a normal palate. The nose is flattened on the affected side. Cleft lips and palates may be seen in otherwise normal infants or in infants with syndromes or chromosomal abnormalities.

1.118

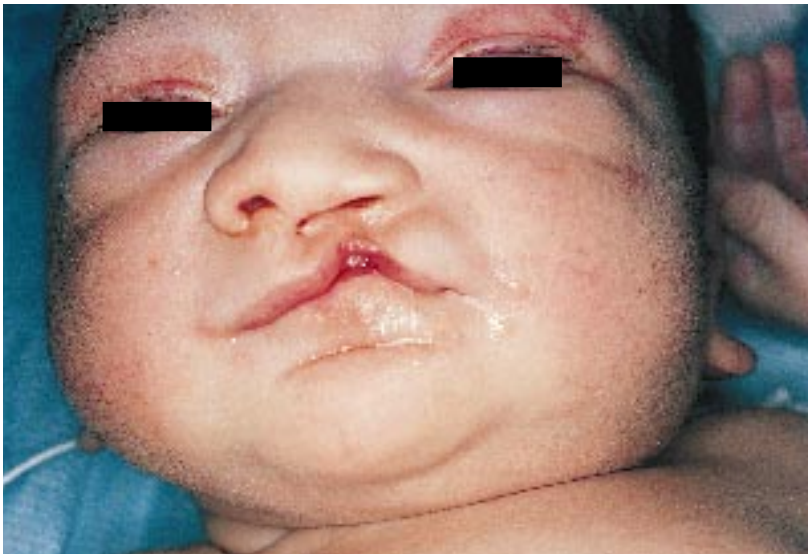

Figure 1.118. An example of a unilateral cleft lip with a normal palate in an infant with the popliteal pterygium syndrome. Note that the upper lip is indented to the left of the philtrum and the nose is flattened, but the defect does not extend into the alveolar process.

1.119

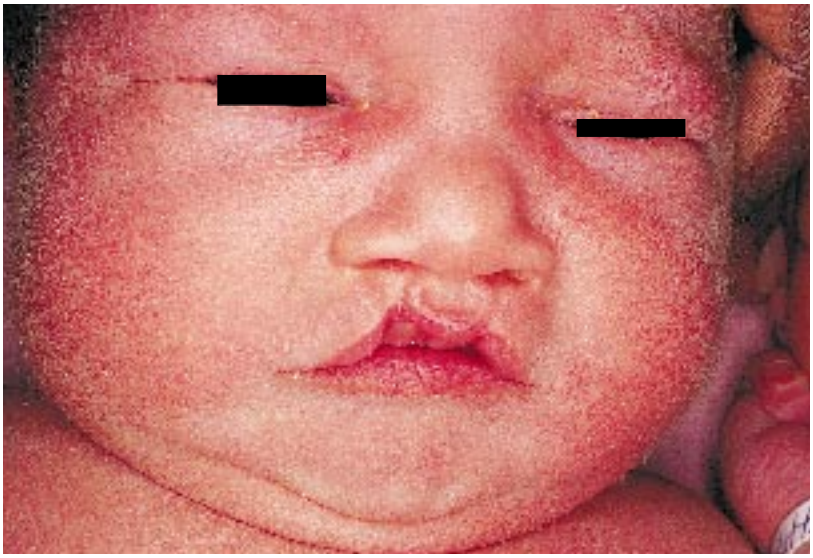

Figure 1.119. A mild bilateral cleft lip in an otherwise normal infant. In partial or complete unilateral or bilateral cleft lip, the line of clefting is paramedian and follows the ridge at either side of the philtrum.

1.120

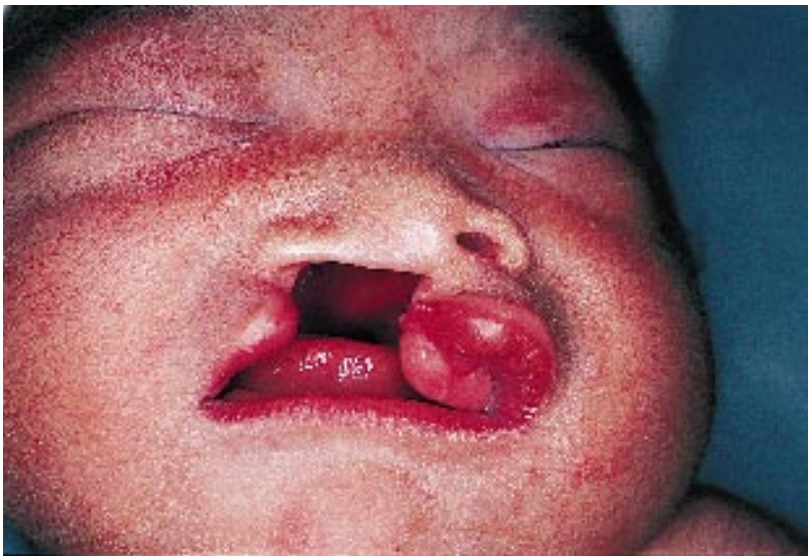

Figure 1.120. A unilateral cleft lip and cleft palate in an otherwise normal infant. The unilateral cleft lip has extended to the nostril, which is flattened and deflected. Cleft lip and palate occur in many syndromes such as trisomy 13 and the ectrodactyly-ectodermal dysplasia-clefting syndrome (EEC syndrome).

1.121

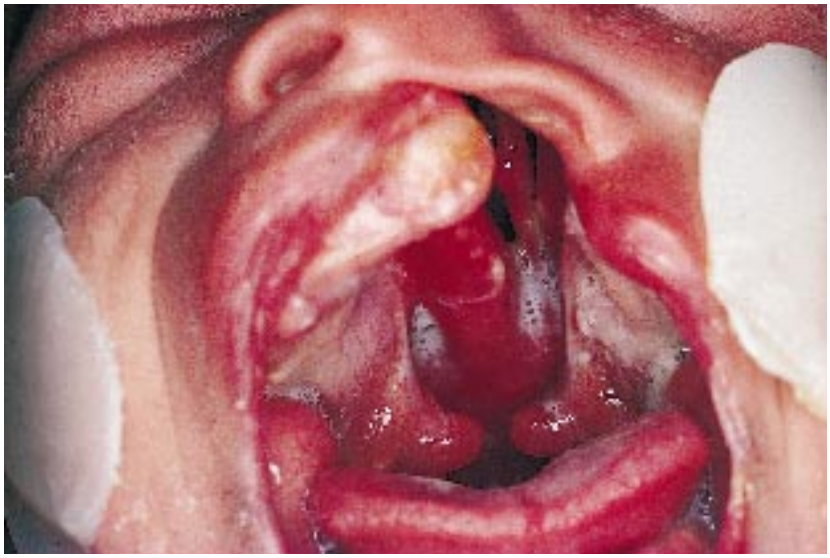

Figure 1.121. Cleft palate in an infant with a unilateral cleft lip. Note the splitting of the uvula.

1.122

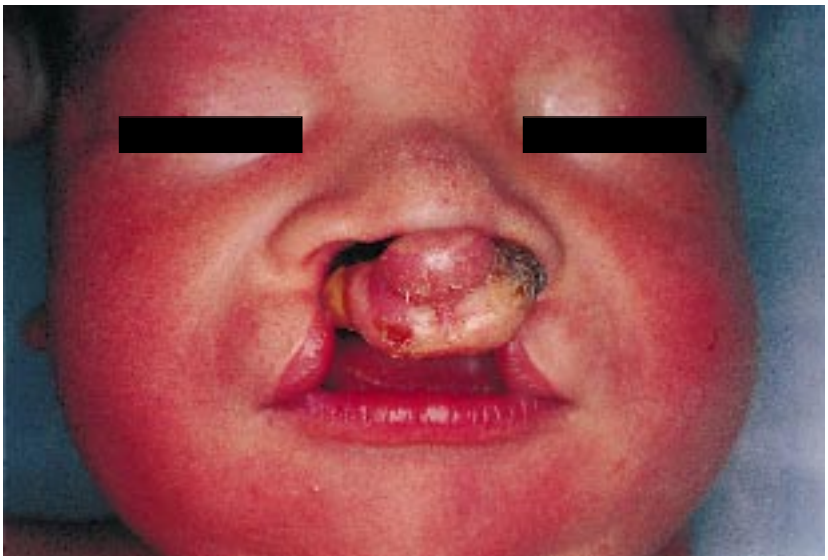

Figure 1.122. Bilateral cleft lip and cleft palate with a severe total cleft palate and incomplete bilateral cleft lip. A midline nubbin of tissue is seen attached to the columella of the nose. This represents the remnant of the intermaxillary segment, the unpaired median structure that normally would have formed the floor of the philtral groove, the center of the upper alveolar ridge, and the primary palate.

1.123

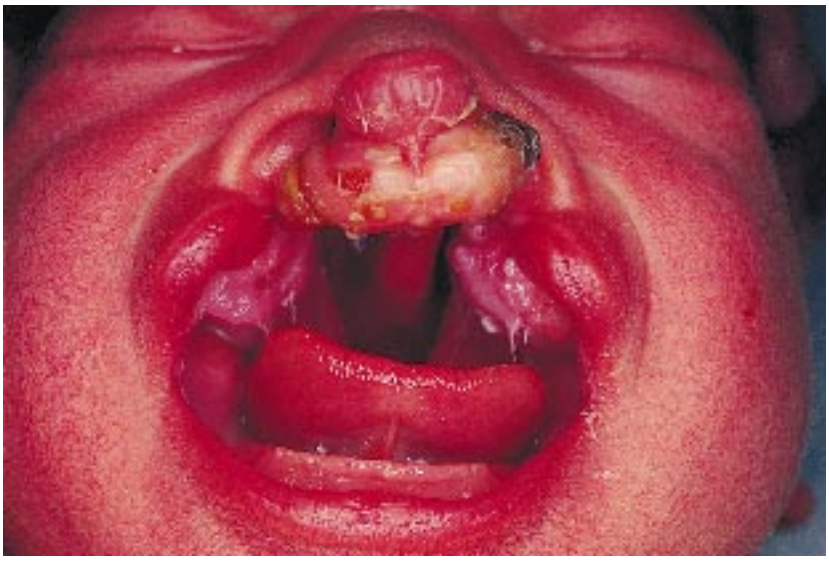

Figure 1.123. In the same infant the cleft palate is clearly demonstrated. Note the protruding vomer.

1.124

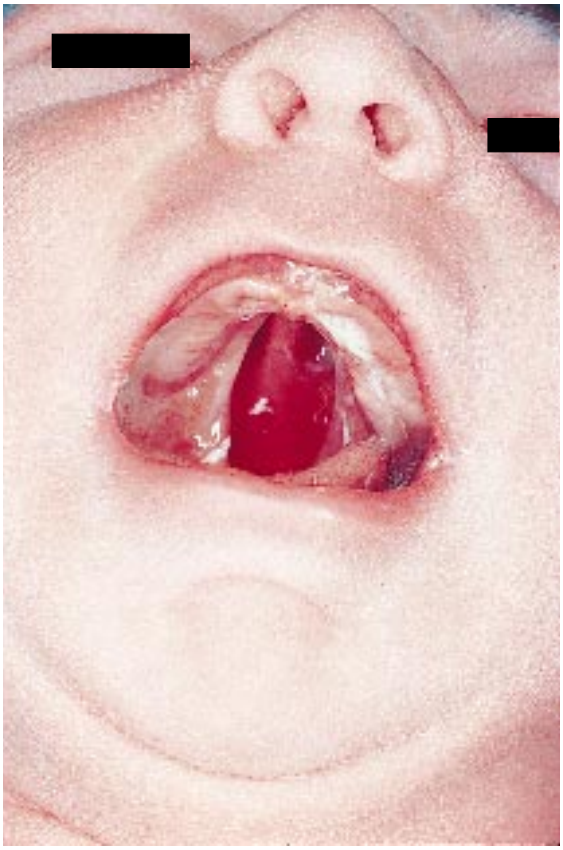

Figure 1.124. Cleft palate in an otherwise normal infant. An isolated cleft palate (either the soft palate, hard palate, or both) occurs more frequently in females and is commonly associated with other abnormalities (such as Robin's anomalad).

1.125

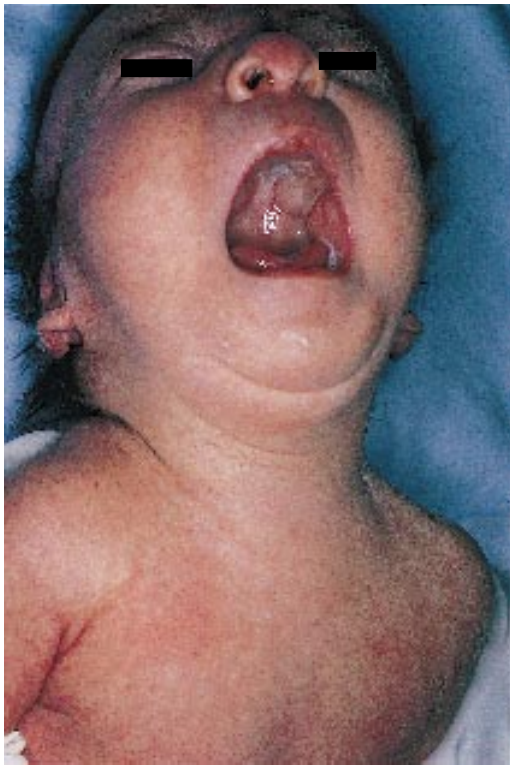

Figure 1.125. A high arched palate in a normal infant. This may occur in association with other congenital anomalies or may occur iatrogenically, secondary to prolonged orotracheal intubation.

1.126

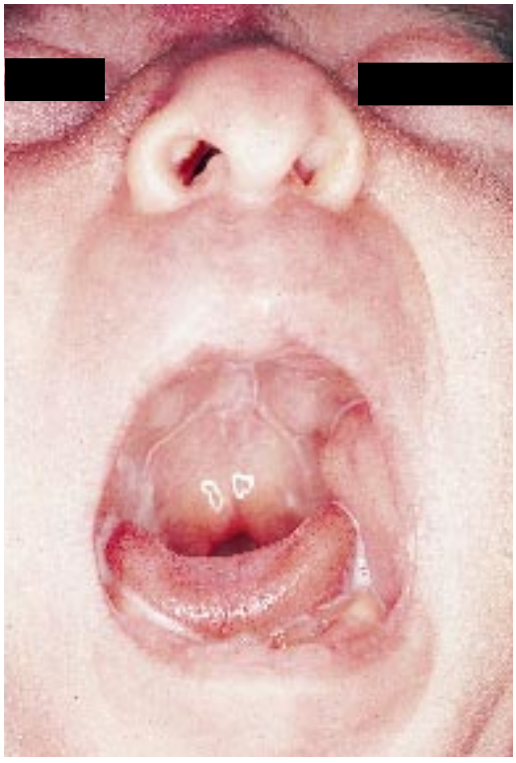

Figure 1.126. A high arched palate in an infant with a cleft of the soft palate.

1.127

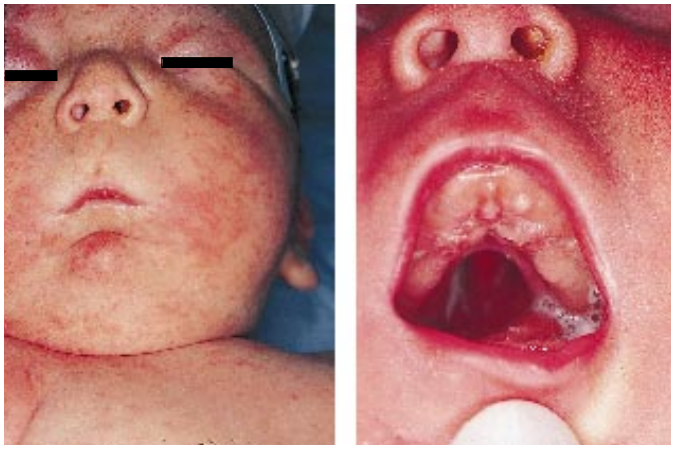

Figure 1.127. On the left, note the marked microstomia and on the right note the cleft palate, in an infant with a mosaic trisomy 8.

1.128

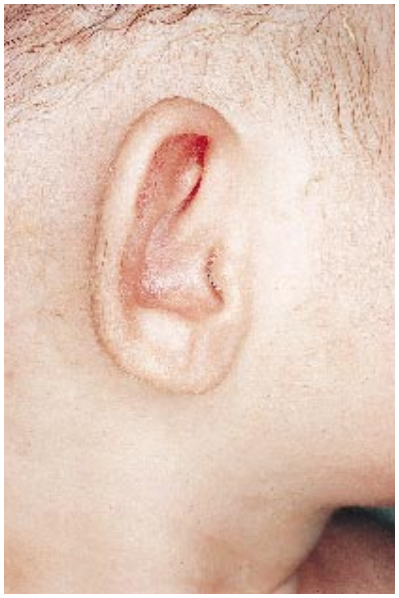

Figure 1.128. The normal ear shows many variations in the folds in relation to the cartilage. For example, in this infant poor development and deformations caused transient abnormalities in the appearance of the ears.

1.129

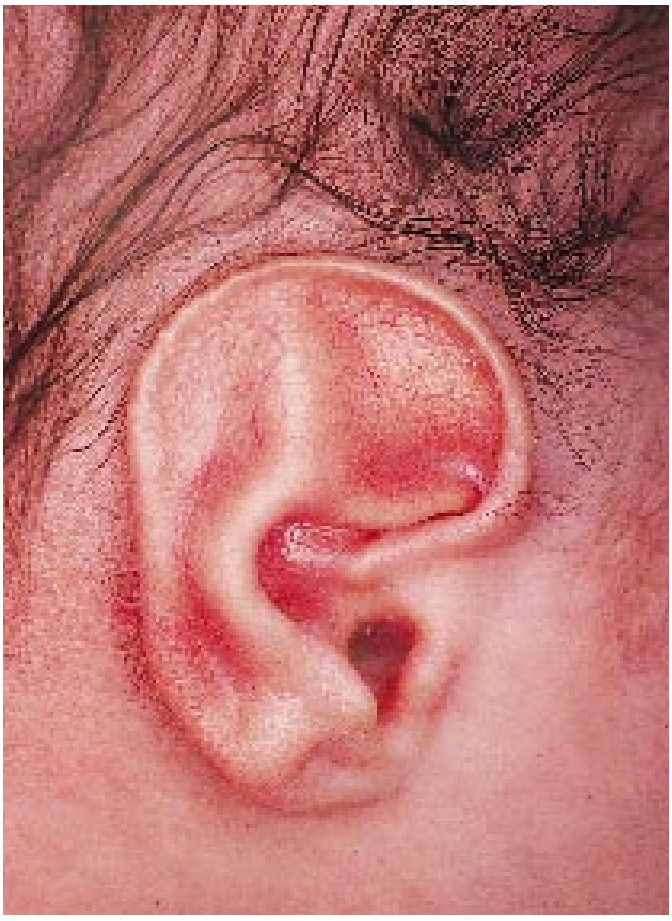

Figure 1.129. Normal ears with lack of good cartilage development may appear as large flattened ears bilaterally. These are often caused by prolonged intrauterine compression as a result of oligohydramnios.

1.130

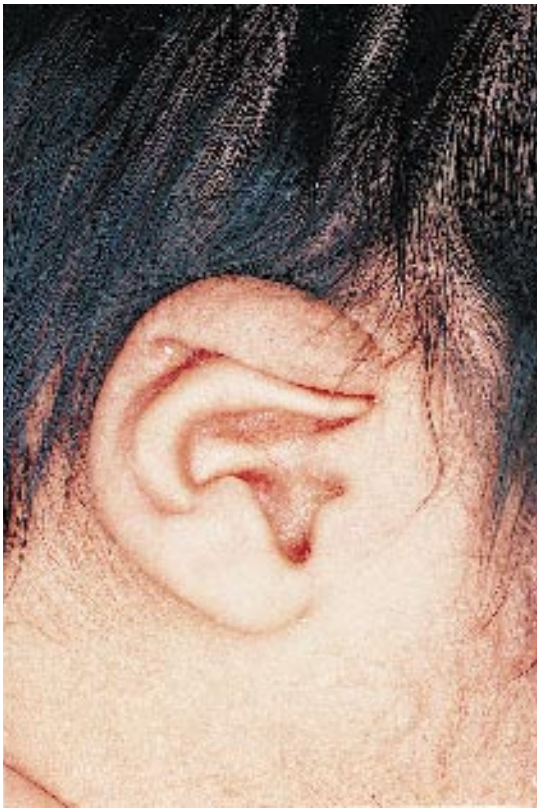

Figure 1.130. An overturned helix (a folded ear) is usually a temporary deformation secondary to in utero position.

1.131

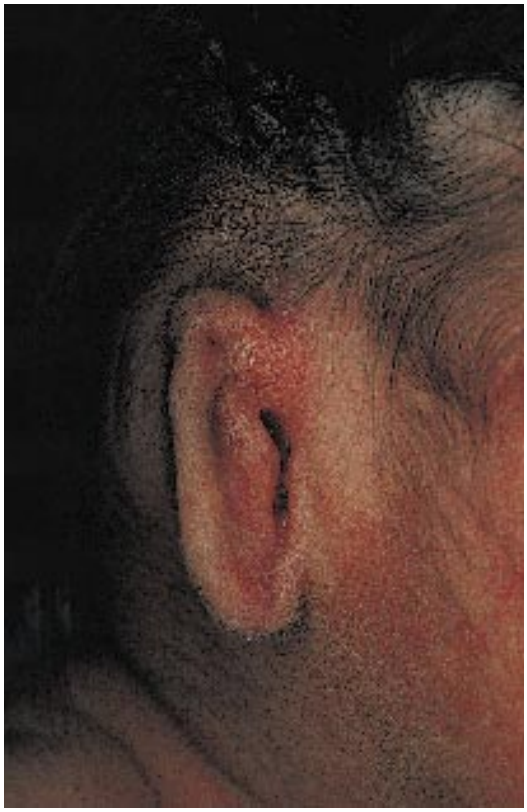

Figure 1.131. Another example of a folded helix due to in utero position.

1.132

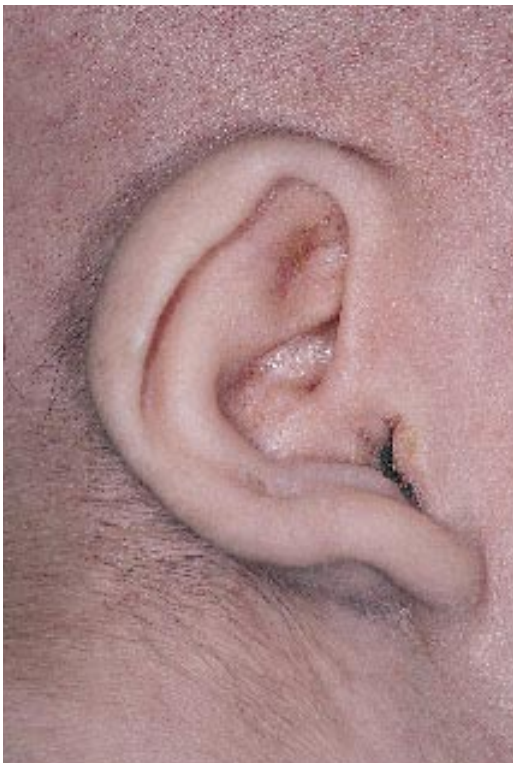

Figure 1.132. Positional deformation of a normal ear secondary to the presence of pressure of the infant's shoulder on the lobe of the ear in utero. Note that the pinna is crumpled upward and forward.

1.133

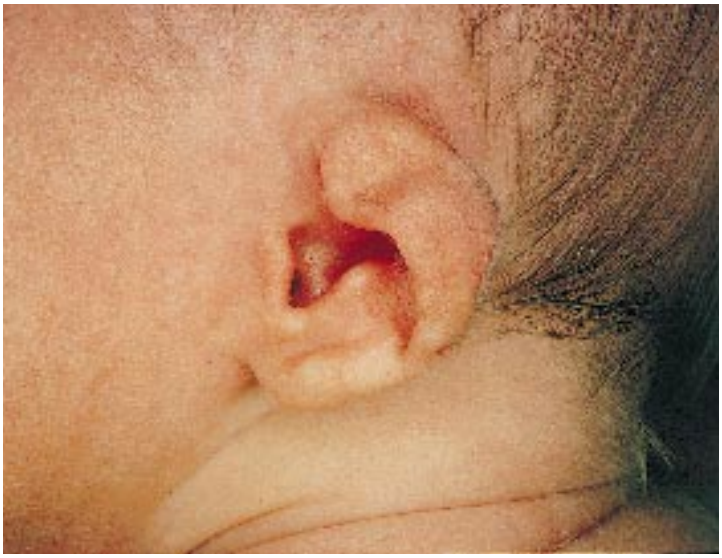

Figure 1.133. This is an example of an infant with a lop ear. Weakness or absence of the auricular muscles result in various deformities of the auricle. When the superior muscle band is absent, a lop ear occurs. If only the posterior slip is missing, a protruding ear is seen. If both muscle bands are absent, a cupped ear is formed. These characteristic abnormalities of the auricle are more commonly seen in infants with severe hypotonia.

1.134

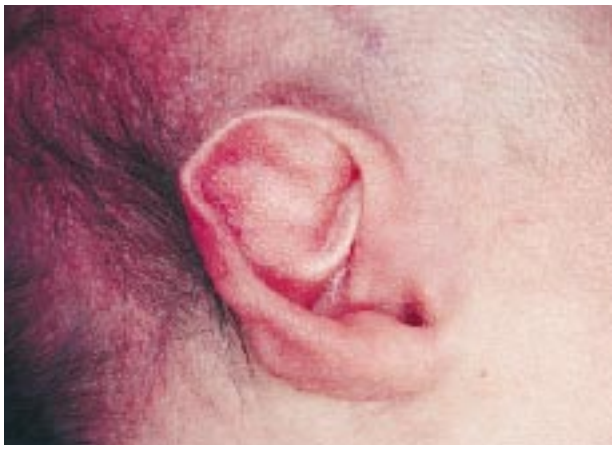

Figure 1.134. Poor development of the ear can be seen in association with a lack of or decreased fetal movement.

1.135

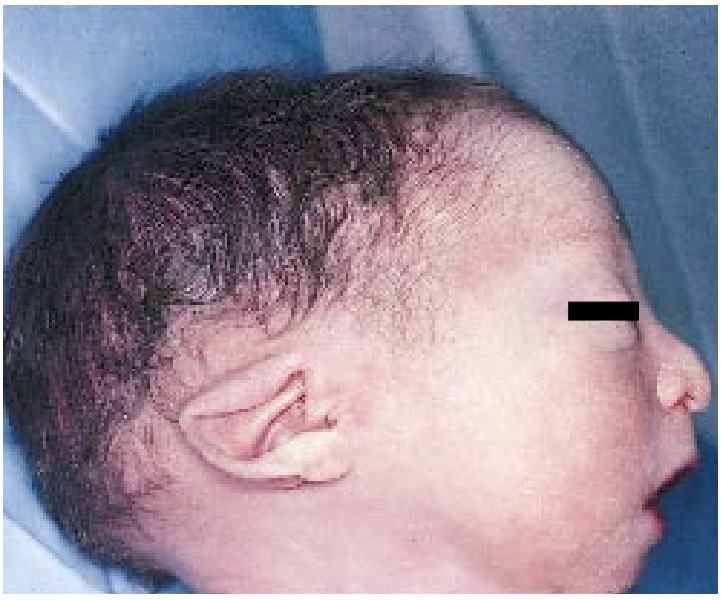

Figure 1.135. In this infant with Potter's syndrome note the slanted and low-set ear. Ears are considered slanted when the angle of slope of the auricle exceeds fifteen degrees from the perpendicular. Low placement and slanted auricles often go together and usually present a lag in morphogenesis.
Low-set ears are defined as those where the helix meets the cranium at a level below that of a horizontal plane with the corners of the orbit. The presence of low-set ears can be determined by extending a line joining both inner canthi. This accounts for any upward or downward slanting of the eyes. The illusion of low ear placement can be created by an unusually large head as is seen in hydrocephalus or by a small external ear. The pseudohydrocephalus (catch-up growth of the head) in very low birthweight infants may create the impression of low-set ears in an otherwise normal infant.

1.136

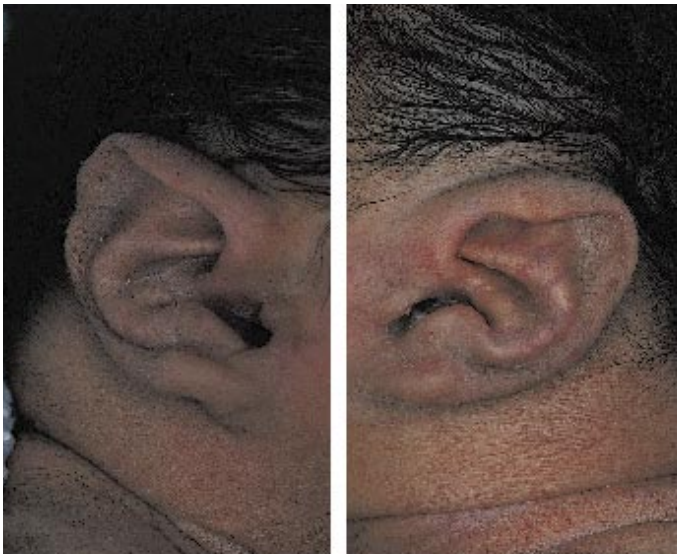

Figure 1.136. Poorly folded small and posteriorly angulated ears occurred with decreased fetal movement in this infant with the fetal akinesia syndrome.

1.137

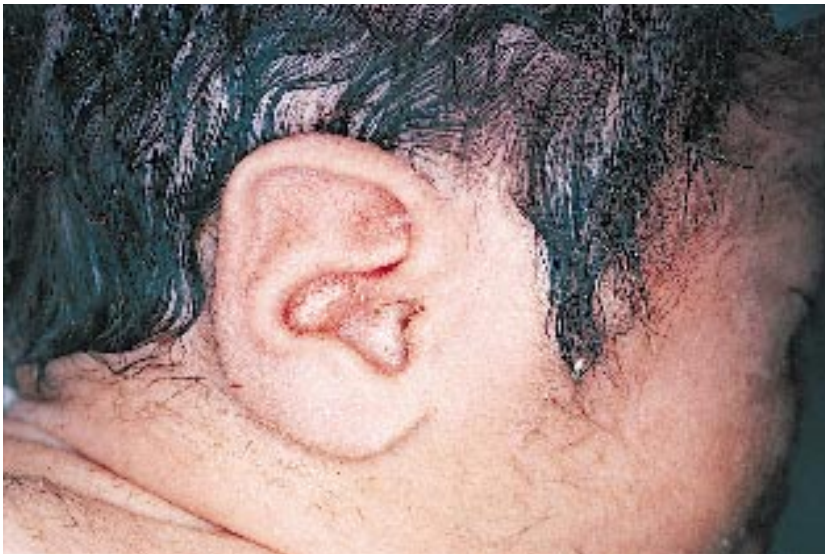

Figure 1.137. Note the attenuation and backward sweep of the upper helix in the ears of this infant. This is called the Mozart ear as it is said to have been present in Mozart and his family.

1.138

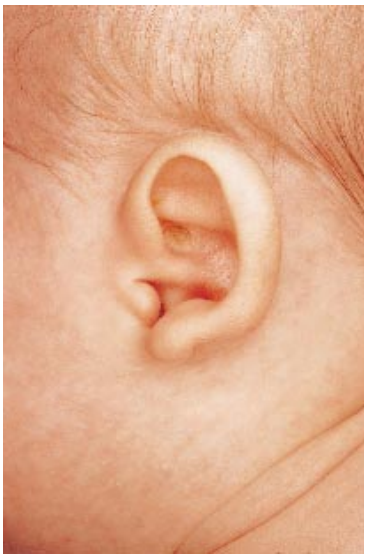

Figure 1.138. Lack of normal development of the lobule of the ear.

1.139

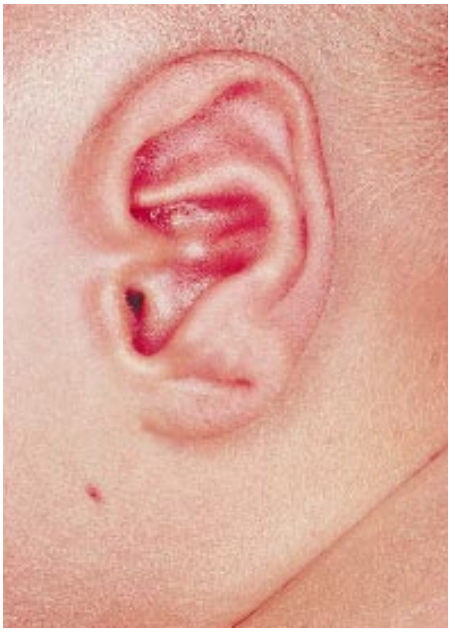

Figure 1.139. Transverse earlobe creases are a feature of some syndromes as in this infant with Beckwith-Wiedemann syndrome.

1.140

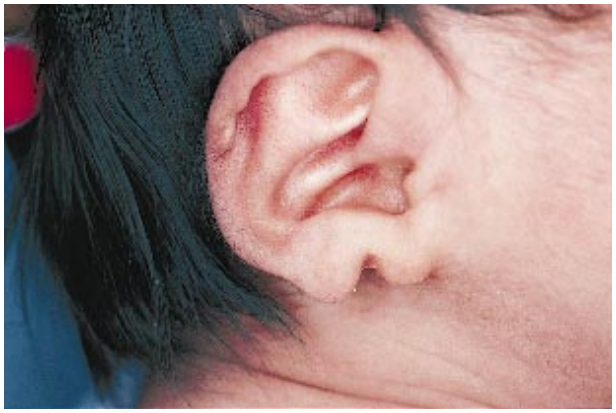

Figure 1.140. This otherwise normal infant had bilateral cleft ear lobes. This occurs as a result of incomplete fusion between the most medial embryonic hillocks.

1.141

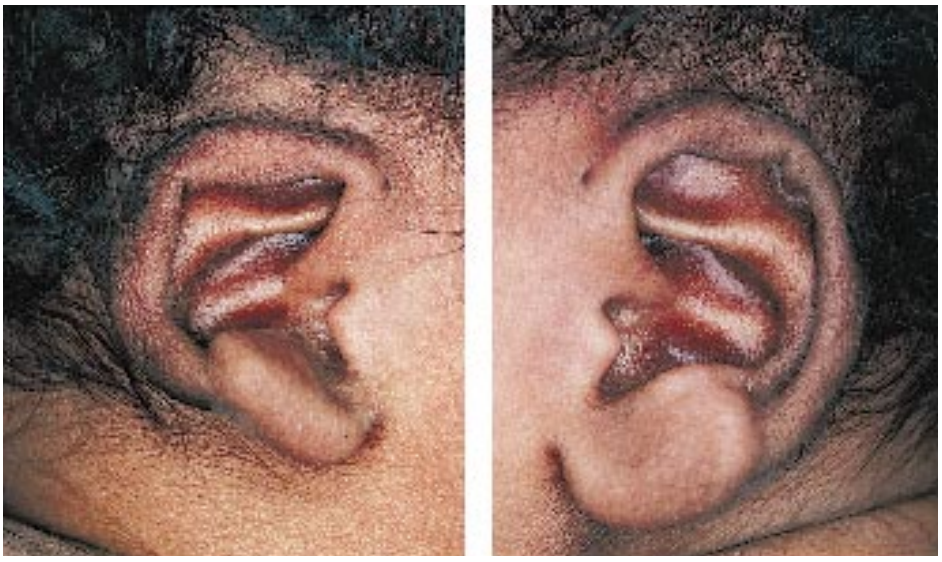

Figure 1.141. Preauricular pits in an otherwise normal infant. The mother had the same findings. Preauricular pits and preauricular tags occur in about 1% of individuals and are twice as common in females and more common in black infants. They are believed to represent remnants of early embryonic branchial cleft or arch structures.

1.142

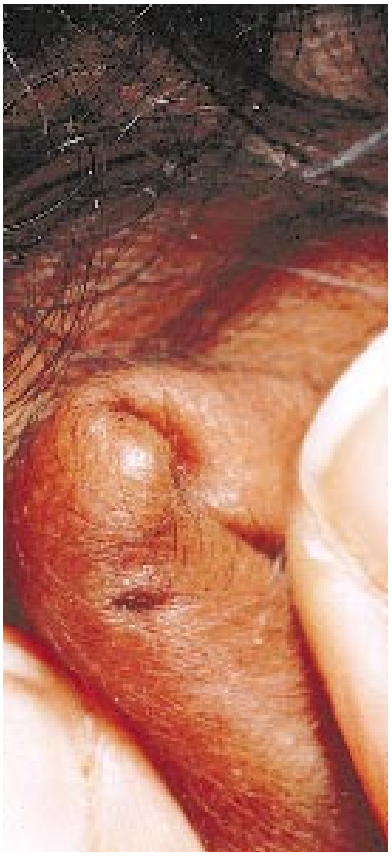

Figure 1.142. There were bilateral pits on the lobes of the ears in this otherwise normal infant.

1.143

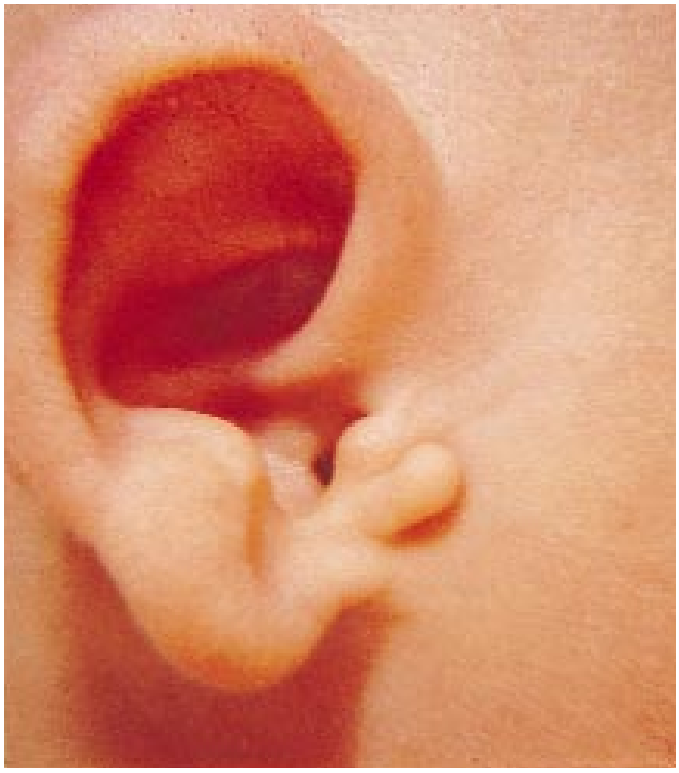

Figure 1.143. Preauricular skin tag in an otherwise normal infant. These skin tags often contain a core of cartilage and appear to represent accessory hillocks of His. Hillocks normally develop in the recess of the mandibular and hyoid arches and coalesce to form the auricle.

1.144

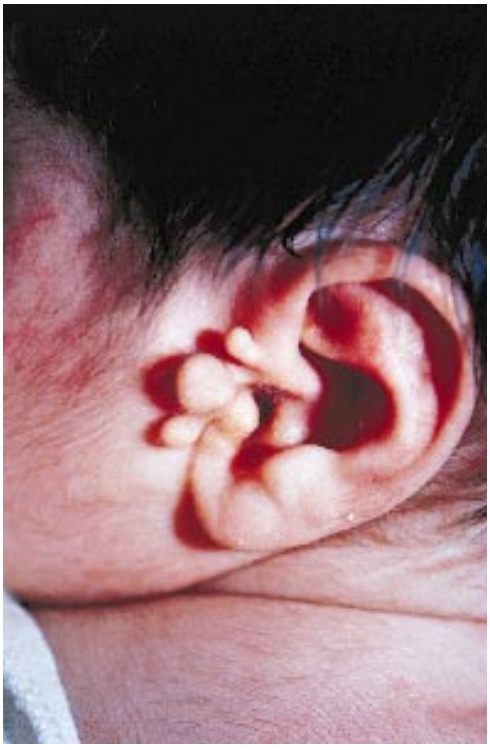

Figure 1.144. Multiple preauricular skin tags in an infant with a normal ear. Note that skin tags may be pedunculated.

1.145

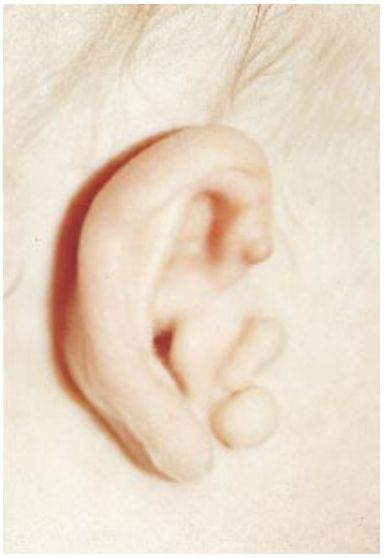

Figure 1.145. Preauricular skin tags in an infant with cupping of the ear.

1.146

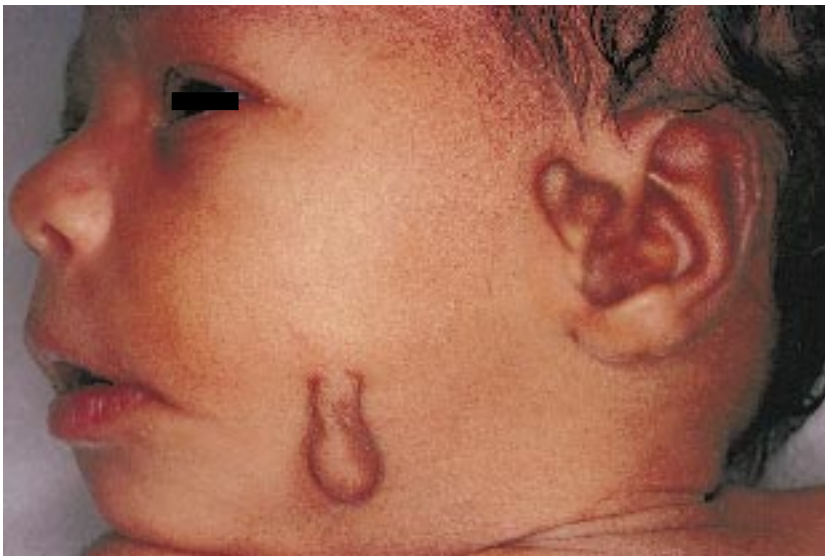

Figure 1.146. Preauricular skin tags and skin tags along a line connecting the oral commissure with the external auditory canal are seen in syndromes involving the first and second branchial arch, as in this infant with Goldenhar's syndrome.

1.147

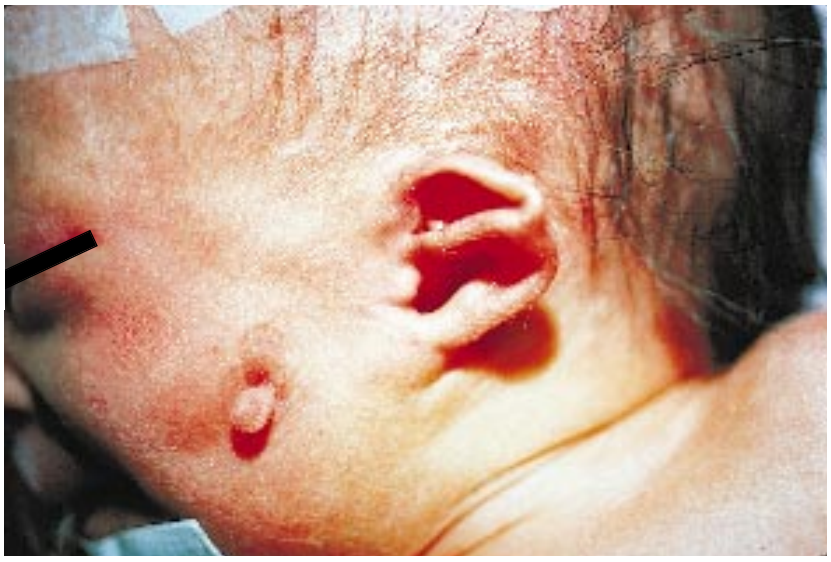

Figure 1.147. This infant exhibited abnormal ears with skin tags and a fistula. Abnormal ears, fistulae, and skin tags are seen more commonly in the first branchial arch syndrome as this infant with Treacher-Collins syndrome.

1.148

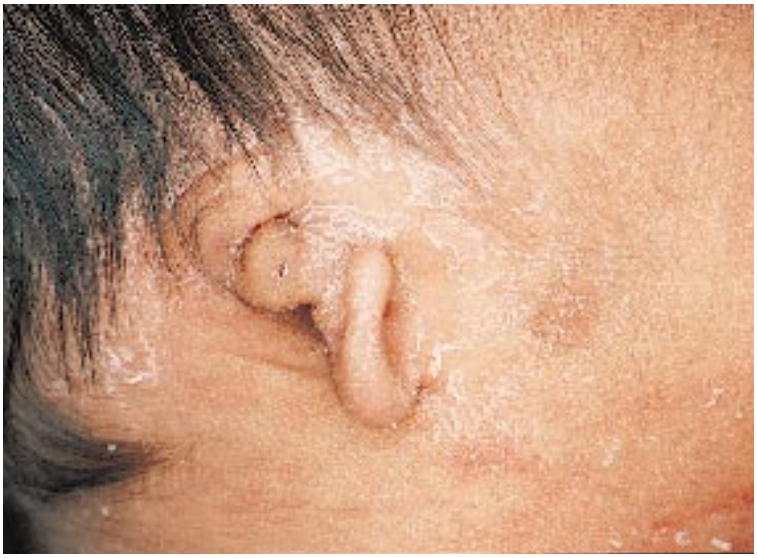

Figure 1.148. Microtia with atresia of the external auditory canal on the right side in an otherwise normal infant. Hypoplasia of the pinna or microtia ("small ear") is the most common isolated intrinsic malformation of the auricle. When microtia is unilateral, the right side is more commonly involved. The spectrum of this abnormality ranges from a small but structurally normal ear, through remnants of cartilage and skin surrounding a small external auditory canal, to total absence of auricular structures.

1.149

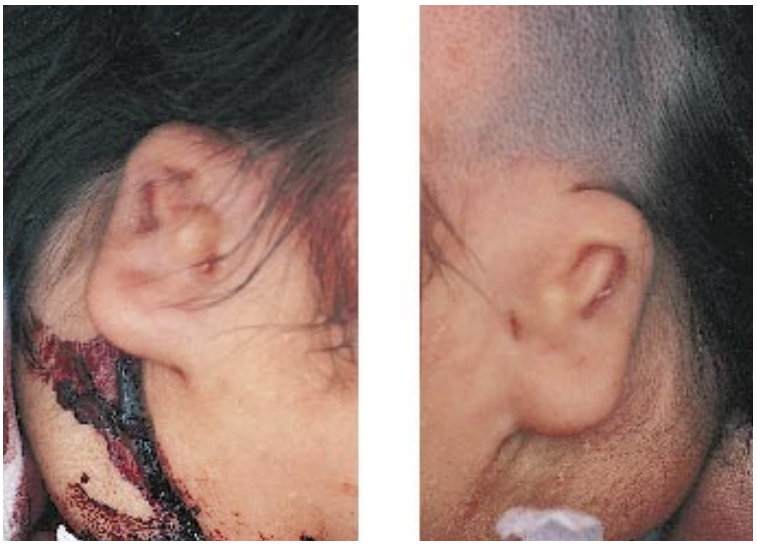

Figure 1.149. Bilateral microtia with atresia of the external auditory canals in an infant with Nager's acrofacial dysostosis syndrome. Varying degrees of microtia occur in syndromes involving the branchial arches such as Treacher-Collins, and Goldenhar's syndrome, and Nager's syndrome (acrofacial dysostosis).

1.150

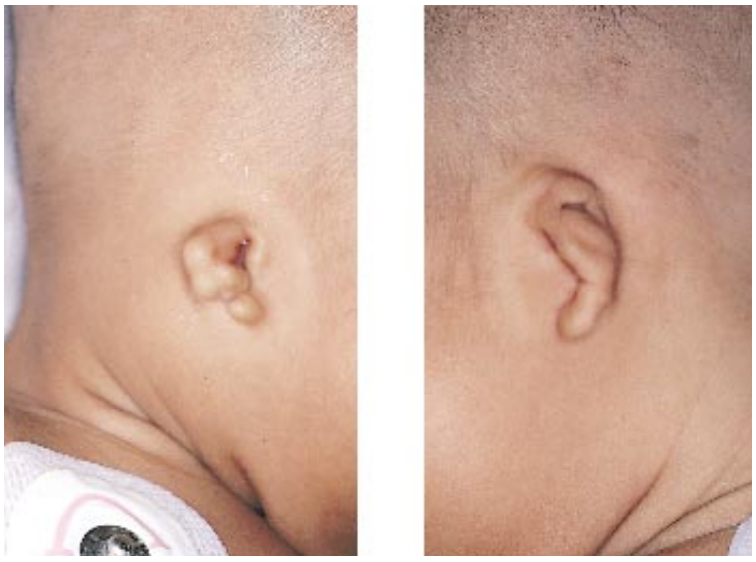

Figure 1.150. Bilateral microtia with absence of external auditory canals in the infant of a mother treated with retinoic acid during the first trimester of pregnancy.

1.151

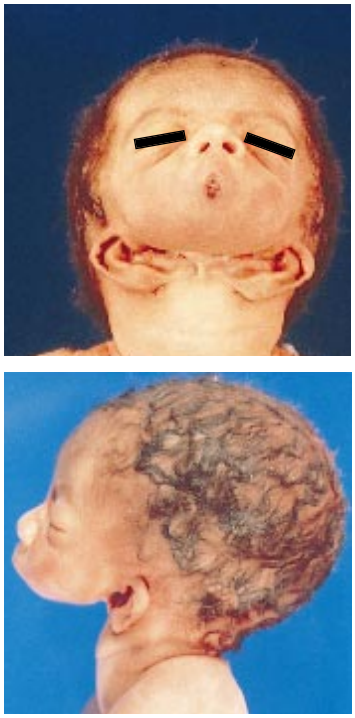

Figure 1.151. In this premature infant of 29 weeks' gestation and birthweight 1120 g there is a branchial arch embryopathy resulting in agnathia, microstomia, and small posteriorly positioned hypoplastic tongue. The ears are very low set and the lower lobes may be fused to the neck which was short and thin. Aural ascent does not occur due to the lack of development of the jaw, hence the low position of the ears. These infants typically have hypoplastic lungs. (C.Langston)

1.152

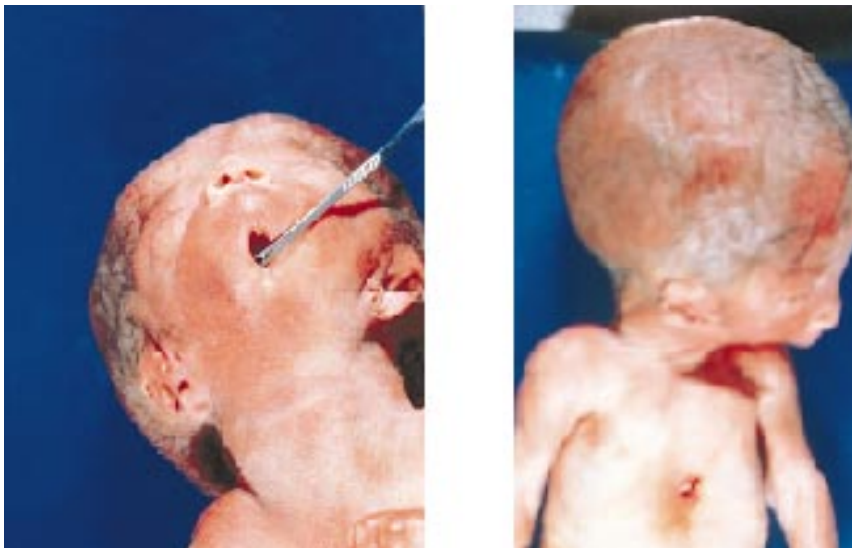

Figure 1.152. Another example of agnathia. Note the low-set ears and microstomia. Hydrocephalus and congenital heart disease are commonly present in branchial arch embryopathy. (C.Langston)

1.153

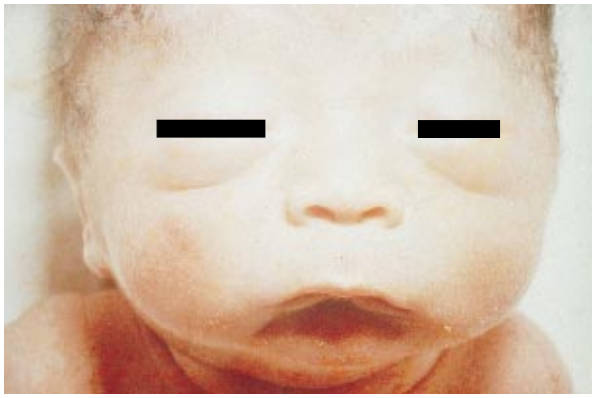

Figure 1.153. This infant with severe micrognathia had significant respiratory distress. Micrognathia is most commonly familial or idiopathic, but many syndromes are associated with this finding.

1.154

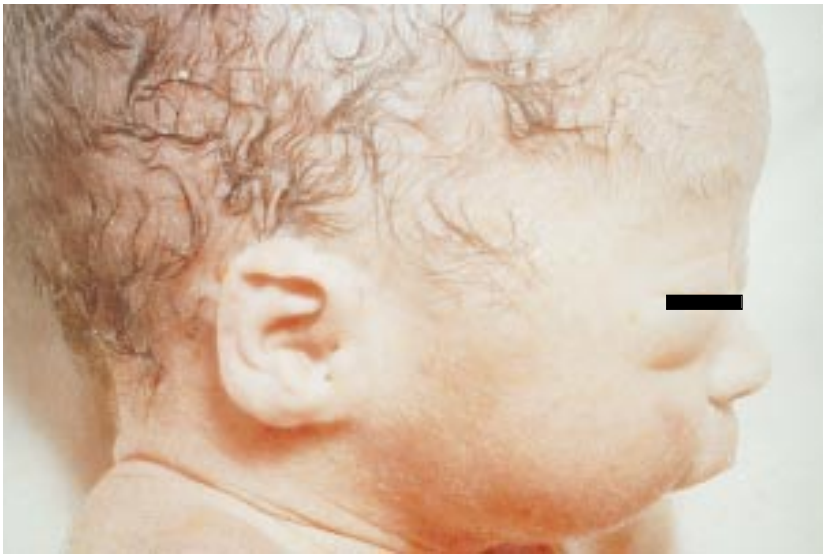

Figure 1.154. A lateral view of the same infant as in Figure 1.53 showing the marked micrognathia.

1.155

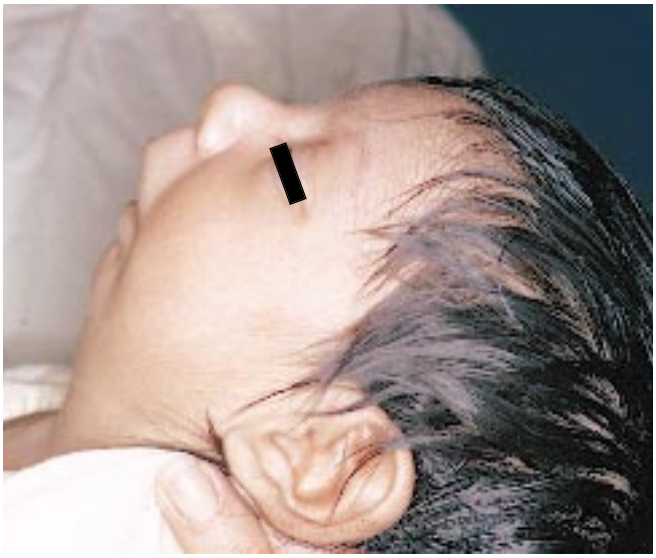

Figure 1.155. Severe micrognathia in an infant who had a small cleft palate (Robin's anomalad). This infant had respiratory distress and major problems with feeding.

1.156

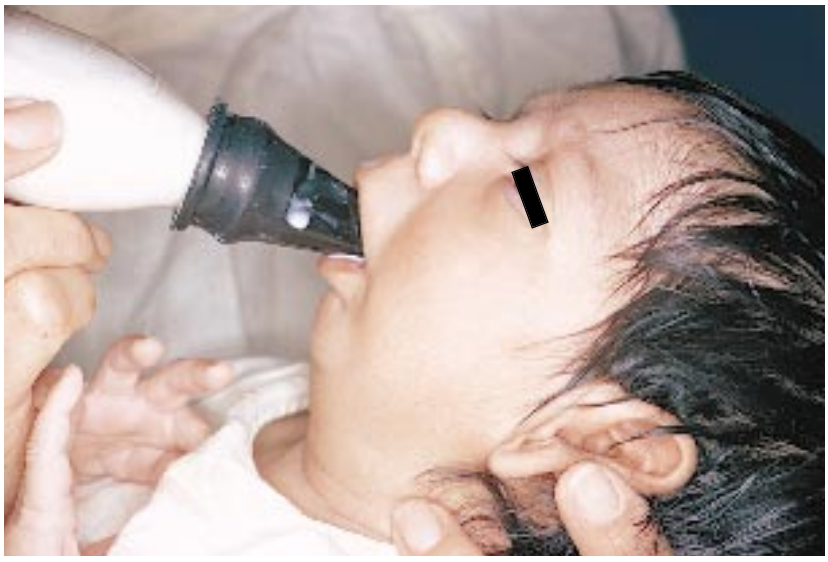

Figure 1.156. Feeding was accomplished in the same infant by the use of a lamb's nipple.

1.157

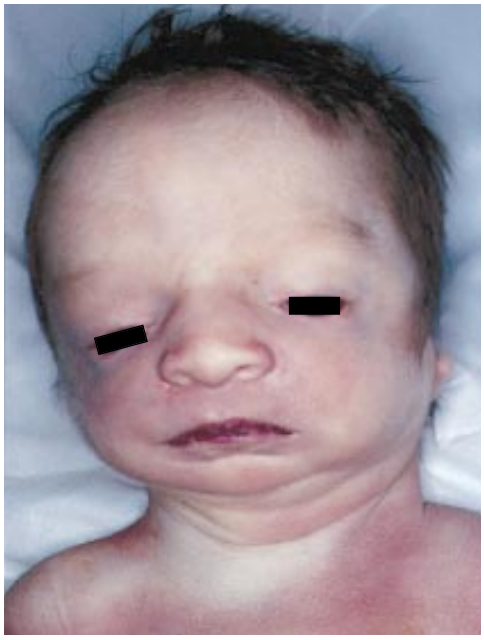

Figure 1.157. Marked micrognathia in an infant with Treacher-Collins syndrome (mandibulofacial dysostosis). In addition to the micrognathia, note the antimongoloid slant of the eyes, prominent nose, and malar hypoplasia.

1.158

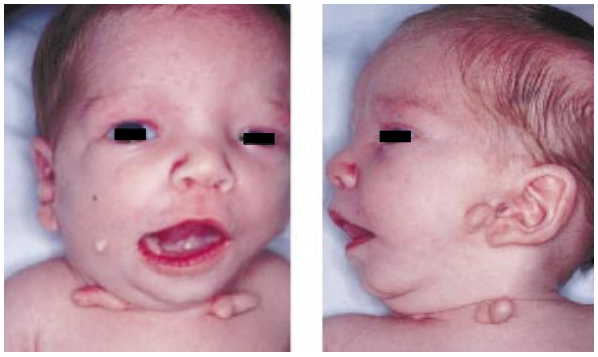

Figure 1.158. Micrognathia in an infant with Goldenhar's syndrome (hemifacial microsomia). In addition, note the preauricular skin tags, unilateral macrostomia, and skin tags due to the extra branchial arch anomalies.

1.159

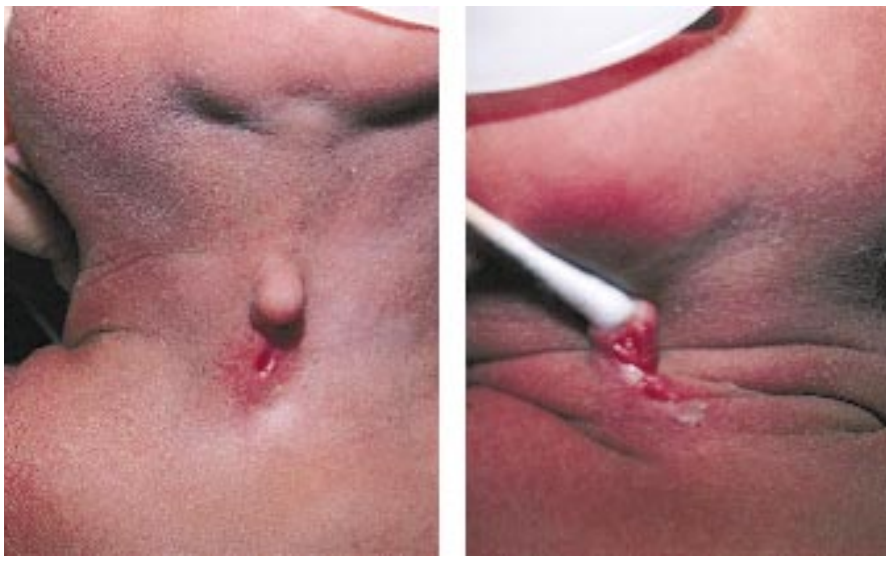

Figure 1.159. A congenital midline cervical cleft is a rare developmental anomaly. It represents failure of the branchial arches to fuse in the midline. It most commonly affects females, and presents at birth with a ventral midline defect of the skin of the neck. A reddened weeping strip of atrophic skin approximately 5 mm in width may occur at any level between the chin and sternal notch. Often there is a nipple-like projection at the upper end of the fissure and an associated sinus tract at the caudal end which may discharge mucoid material. This condition may be misinterpreted as a branchial cleft anomaly or thyroglossal duct cyst.

1.160

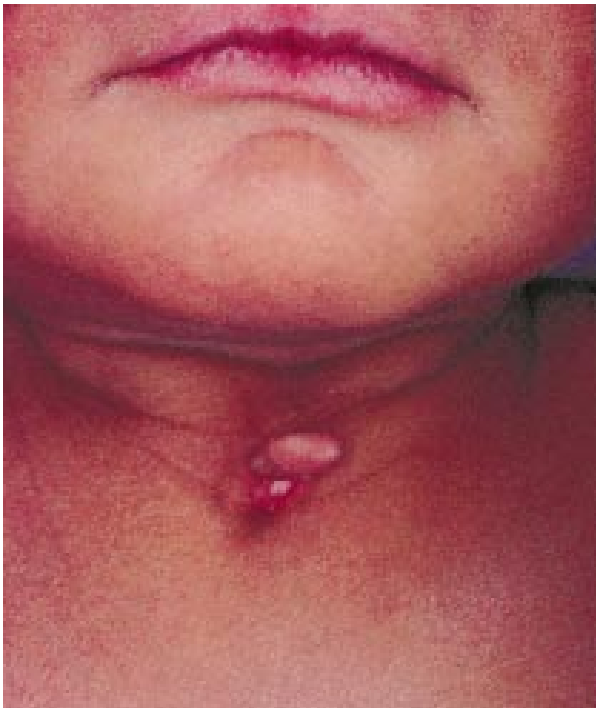

Figure 1.160. Another example of a congenital midline cervical cleft. Note the characteristic nipple-like projection, atrophic skin defect, and caudal fistulous tract. This may become a fibrous "cord" and result in a web-like contracture. This must be differentiated from a thyroglossal duct cyst/sinus which develops if the thyroglossal duct fails to close after the descent of the thyroid gland into the lower neck. It can occur anywhere on a line connecting the sternal notch and the base of the tongue.

1.161

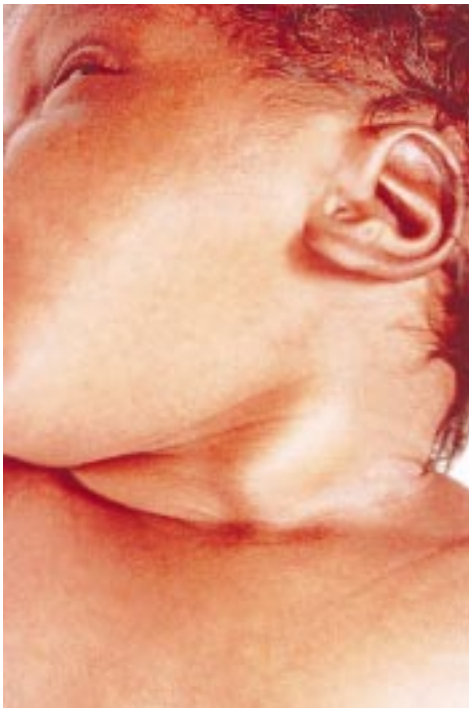

Figure 1.161. When delivery has involved excessive rotation or gross lateral rotation of the neck, a lump may appear in the sternomastoid muscle (sternomastoid tumor). This usually becomes apparent in the second week of life and commonly is situated in the lower half of the muscle. It may enlarge before resolving spontaneously, and may result in torticollis as a result of contraction of the sternomastoid muscle causing flexion of the head toward the side of the lesion. This condition must be differentiated from superior oblique palsy (IVth cranial nerve palsy) by an ophthalmologist.

1.162

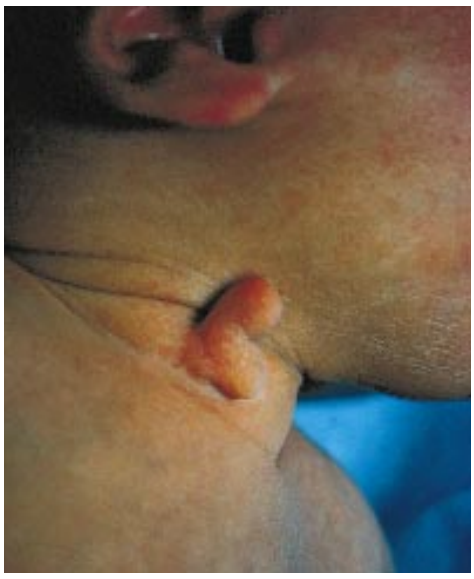

Figure 1.162. Abnormal development of the branchial clefts and arches may result in remnants, fistulae or cysts. Defects are usually unilateral and the external opening lies at the anterior edge of the sternocleidomastoid muscle, usually at the lower third. Secondary bacterial infection and cyst formation may occur. In this infant there is a branchial cleft remnant.

1.163

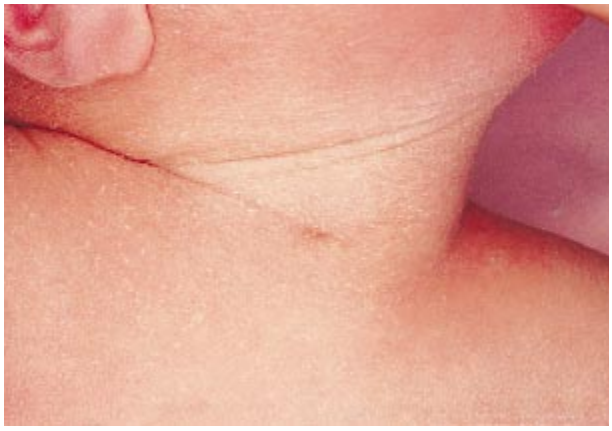

Figure 1.163. The subtle finding of a branchial sinus may be missed if examination of the infant is not thorough.

1.164

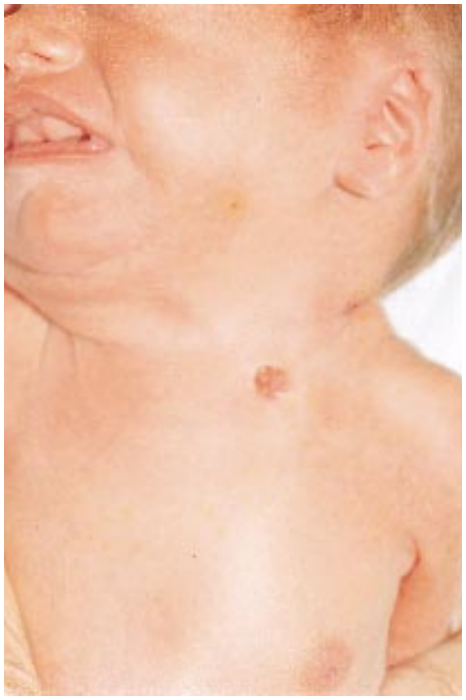

Figure 1.164. Branchial remnants tend to occur along the course of the sternomastoid muscle.

1.165

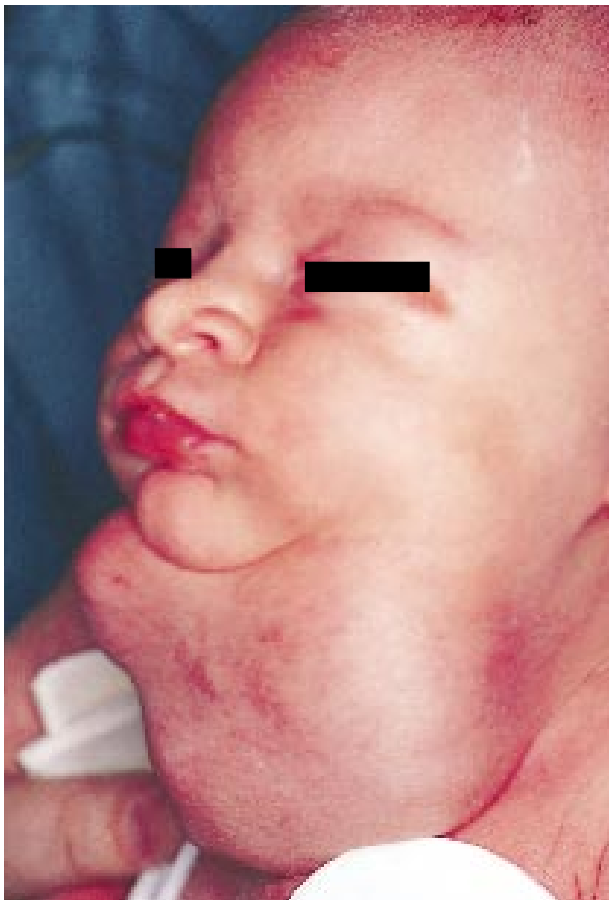

Figure 1.165. The large cystic hygroma (lymphangioma) presented in this infant as a large soft fluctuating mass. These are located most commonly in the neck and consist of proliferation of lymph vessels. Although not malignant, they may spread over the neck with extension into the mouth.

1.166

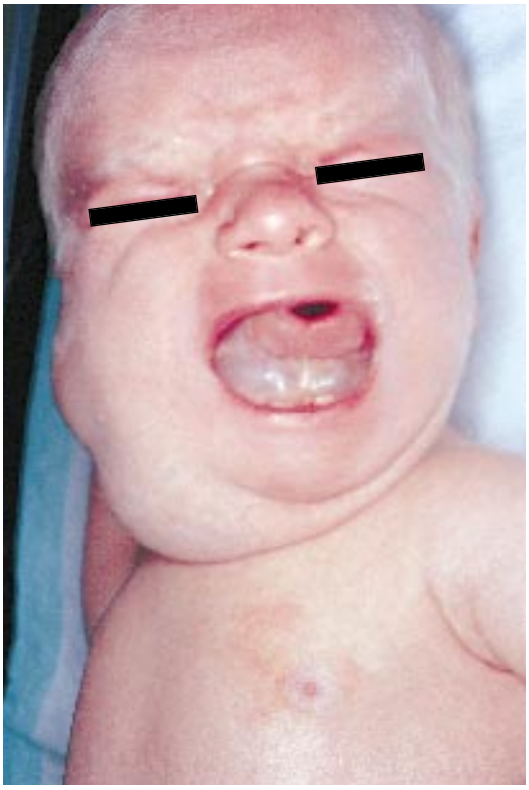

Figure 1.166. A large cystic hygroma involving the right side of the neck and face with extension into the mouth. The mass compromised respiration in this infant. Such masses in the neck should be differentiated from thyroglossal duct and cervical cysts.

1.167

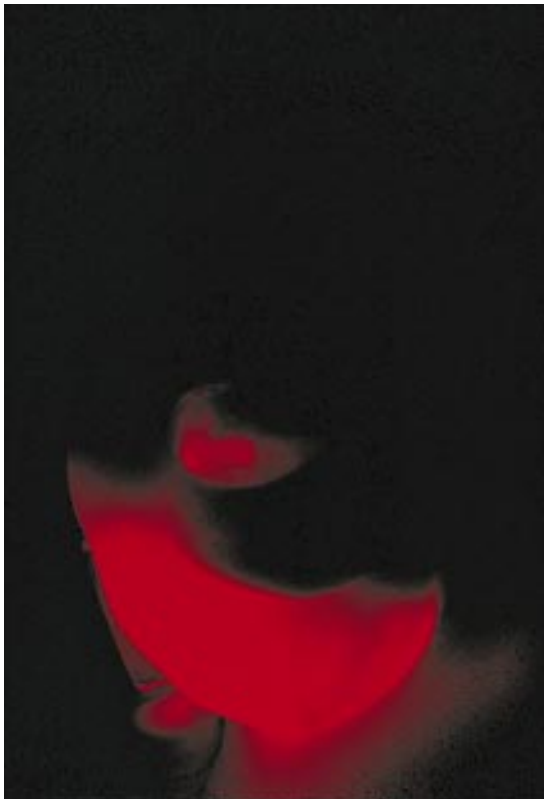

Figure 1.167. Transillumination of the cystic hygroma in the same infant.

1.168

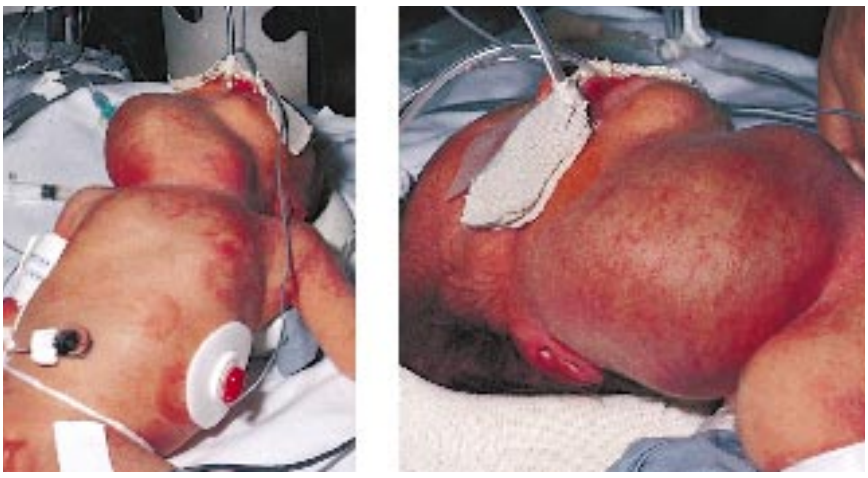

Figure 1.168. The large mass present at birth in the cervical area of this infant caused severe respiratory distress. It was a malignant teratoma of the neck.

1.169

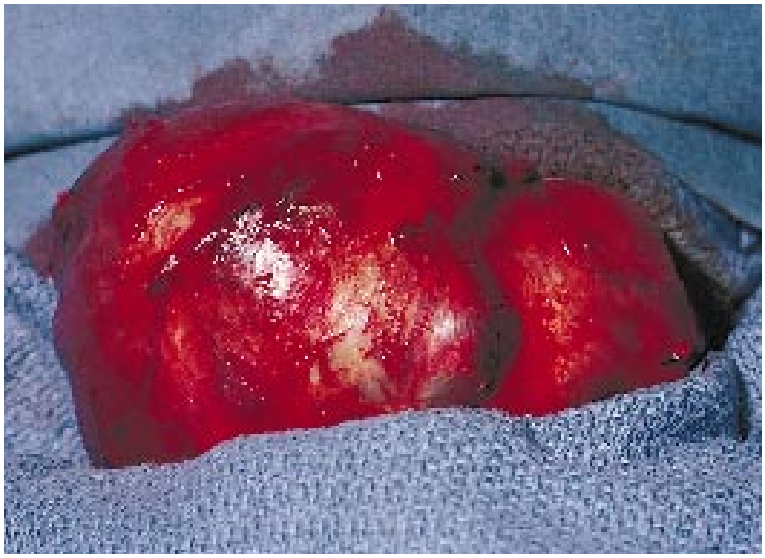

Figure 1.169. The surgical specimen of the mass of the same infant showed mixed yolk sac and embryonal remnants.

Chapter 2
Ophthalmology†

Blinding diseases can destroy useful vision unless rapidly diagnosed and treated. The initial routine examination of all infants should be carried out by the primary care physician, and should include direct ophthalmoscopy, and an orderly structural examination to include the eyebrows, lids, and lashes and lacrimal system, conjunctiva, sclera, cornea, iris (note pupils), anterior chamber, lens, vitreous, and fundus (especially optic nerve and macula). Look for symmetry of ocular structures and clarity of optical media (clear cornea, lens, vitreous). The red reflex should be bright and symmetrical. In all preterm infants ≤1250 g at birth, after an initial period of retinal development (from 4 to 6 weeks of life), an ophthalmologist trained to screen retinopathy of prematurity should initiate regular ophthalmologic examinations until inner retinal vascularization is complete, follow the progression and regression of retinopathy of prematurity (ROP), determine the need for surgical therapy for ROP, and follow the infant for the development of refractive errors, strabismus, amblyopia, etc. (all are increased in preterm infants). In any infant suspected of congenital intrauterine infections, genetic syndromes, family history of eye disease in parents or siblings, severe central nervous system abnormalities, maternal drug use or abuse, and obvious eye abnormalities or failure to obtain bilateral red reflexes, an ophthalmology consultation should be considered. The eyes are not completely developed anatomically or functionally at birth and are constantly changing during the neonatal period. It is important to recognize the normal findings during different stages of growth and understand what is abnormal.

†Photos and text for Chapter 2 provided by Helen A. Mintz-Hittner, M.D., Clinical Professor, Department of Ophthalmology and Visual Science, The University of Texas Medical School at Houston, and Clinical Professor, Department of Ophthalmology, Baylor College of Medicine, Houston, Texas.

OPHTHALMOLOGIC EXAMINATION OF THE NEWBORN

I. Examination of the Eyes should take place

A. During the initial routine examination (1st day of life) of all infants (by the pediatrician/neonatologist) to exclude obvious anomalies (must include bilateral red reflexes).

B. Following an initial period of stabilization (1st week of life) in all preterm infants ≤ 1250 grams at birth (by the pediatrician/neonatologist) to exclude obvious anomalies and to assess gestational age.

C. Following an initial period of retinal development (from 4 to 6 weeks of life) in all preterm infants ≤1250 grams at birth (by an ophthalmologist trained to screen retinopathy of prematurity [ROP]):

1. To initiate regular ophthalmologic examinations until inner retinal vascularization is complete (may not be to the ora serrata).

2. To follow the progression and regression of ROP.

3. To determine the need for surgical therapy, which is usually necessary from 32 to 42 weeks postconceptual age (gestational age + postnatal age), thus ROP occurs early in larger (higher gestational age) infants and later in smaller (lower gestational age) infants.

4. To follow for the development of refractive errors, strabismus, amblyopia, etc. (all of which are more frequent in preterm infants).

D. At any time when any of the following are suspected or proven (by an ophthalmologist):

1. congenital intrauterine infections;

2. genetic syndromes;

3. family history of eye disease in parents or siblings;

4. severe central nervous system abnormalities;

5. maternal drug use or abuse;

6. obvious eye abnormalities or failure to obtain bilateral red reflexes.

II. Examination Techniques and Normal Findings

A. The use of direct ophthalmoscopy and dilating drops (cyclopentolate 0.2% and phenylephrine 1%) is safe and effective without causing hypertension or bradycardia in all but the smallest and most unstable infants. Hold the eyelids open for a few seconds; blot away excess.

B. A functional examination — for visual acuity, visual field, motility, and refraction — is not part of the routine initial examination. Note that good fixation and following and consistently straight eyes may not be present until 6 months of age; however, if there is no visual interest, nystagmus, bilaterally dull red reflexes, asymmetrical red reflexes, or a consistently crossed eye, an examination by an ophthalmologist is recommended.

C. During an orderly structural examination, note obvious orbital abnormalities (overview) and then proceed from the anterior to the posterior parts of the eye: an external examination includes the eyebrows, lids, lashes, lacrimal system; an internal includes the conjunctiva, sclera, cornea, iris (note pupils), anterior chamber, lens, vitreous, fundus (especially optic nerve and macula). Look for symmetry of ocular structures and clarity of optical media (clear cornea, lens, vitreous). The red reflex should be bright and symmetrical.

D. Be aware of the *urgency* of ophthalmologic examinations:

1. To prevent progressive ocular damage (e.g., glaucoma, retinopathy of prematurity, etc.).

2. To prevent unilateral deprivation amblyopia due to any unilateral obstruction to the visual axis (lid tumor, ptosis, corneal clouding such as glaucoma, corneal injury such as forceps, cataract, vitreous hemorrhage, etc.). Immediately patch both eyes to prevent irreversible severe amblyopia from developing, and refer to an ophthalmologist as soon as the obstruction is recognized.

3. To prevent bilateral deprivation amblyopia due to any bilateral obstruction to the visual axes (especially cataracts). Cataract surgery and refractive correction must be completed by 6 weeks postnatal age (in a term infant) to obtain optimal visual results. Other bilateral obstructions (corneal and vitreal) are less amenable to surgical correction with optimal visual results; however, refer to an ophthalmologist as soon as the obstructions are recognized. Note: asymmetrical refractive errors can cause relative unilateral refractive amblyopia; bilateral large farsighted refractive errors can cause relative bilateral refractive amblyopia.

TRAUMA (Iatrogenic)

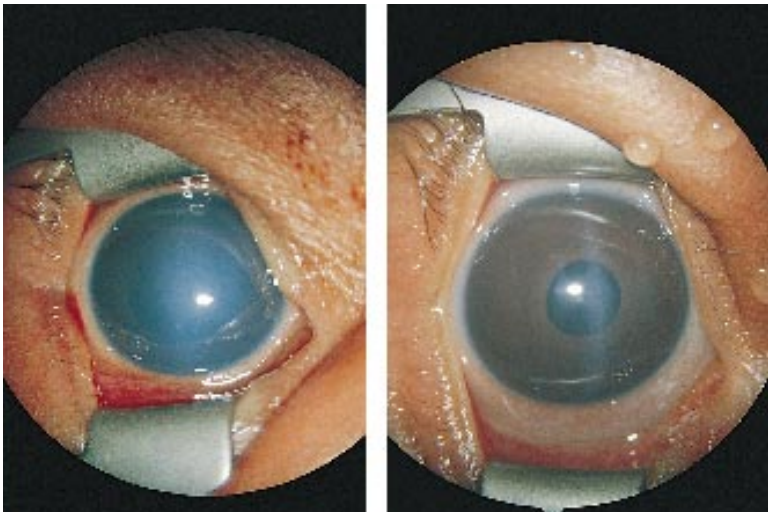

2.1

Figure 2.1. The ocular photograph on the left shows acute linear corneal edema which is transient but is usually associated with permanent corneal damage. The ocular photograph on the right shows the same eye, 2 weeks later, with breaks in Descemet's layer of the cornea which marks the axis of severe myopic astigmatism.

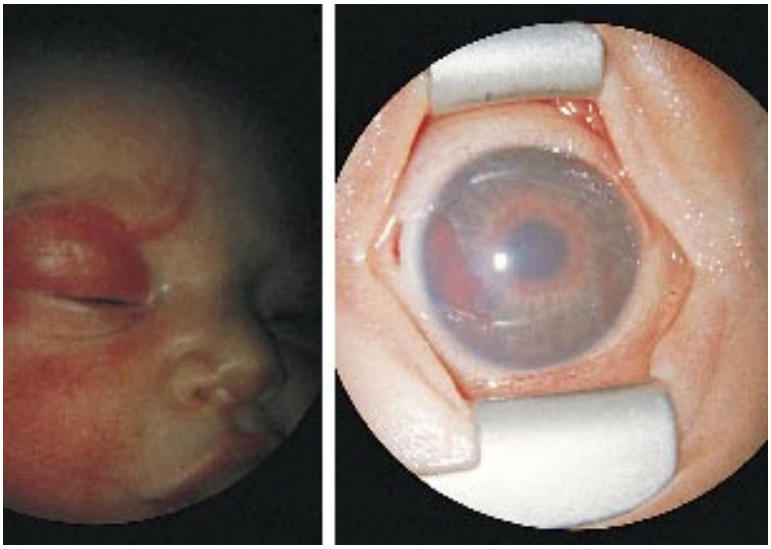

2.2

Figure 2.2. On the left is a mark on the face, directly over the eye, indicating the exact location that forceps were applied. On the right, the eyelids have been opened to reveal a partial hyphema caused by damage to the root of the iris, which resolved without any treatment or permanent ocular damage. The blood is in the anterior chamber of the eye, between the posterior corneal surface and the anterior iris surface. Blood in the anterior chamber of a neonate usually resolves rapidly without any treatment.

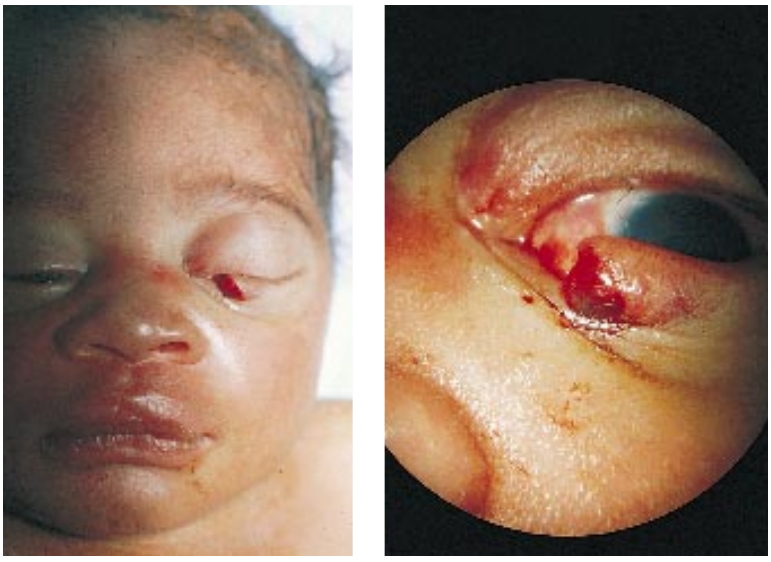

2.3

Figure 2.3. The mark on the face on the left indicates that forceps had slipped between the left eye and the nasal orbital wall. A close-up view of the same injury shows that there is a lid laceration involving the left lacrimal drainage system. Any laceration involving the lid margin should be repaired surgically as soon as possible in order to prevent permanent lid notching. When the nasal lid margin is involved, special attention must be given to repair the lacrimal system to prevent watering of the eye.

2.4

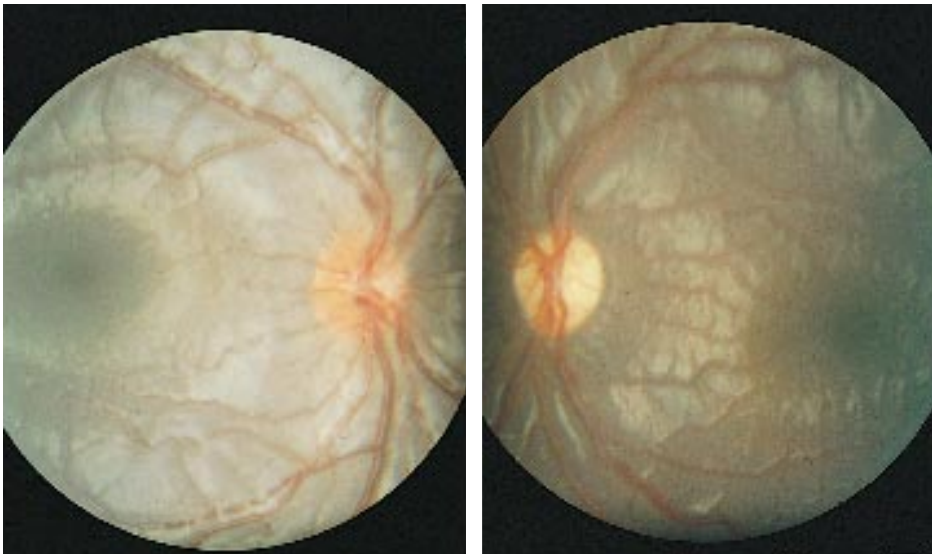

Figure 2.4. These figures are of the optic nerves of the infant shown in Figure 2.3, one year later. On the left is the normal right optic nerve; on the right is the left optic nerve which has developed complete optic nerve atrophy, related to stretching of the left optic nerve occurring when the forceps had slipped between the left eye and the nasal orbital wall. As a result, the eye is totally blind.

2.5

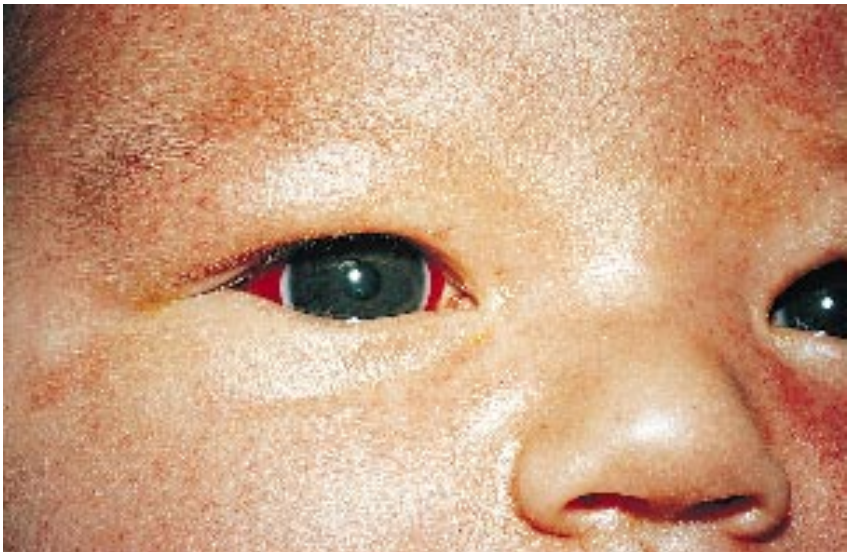

Figure 2.5. Subconjunctival hemorrhages are very common in the neonate immediately following birth. They resolve spontaneously without any consequences.

2.6

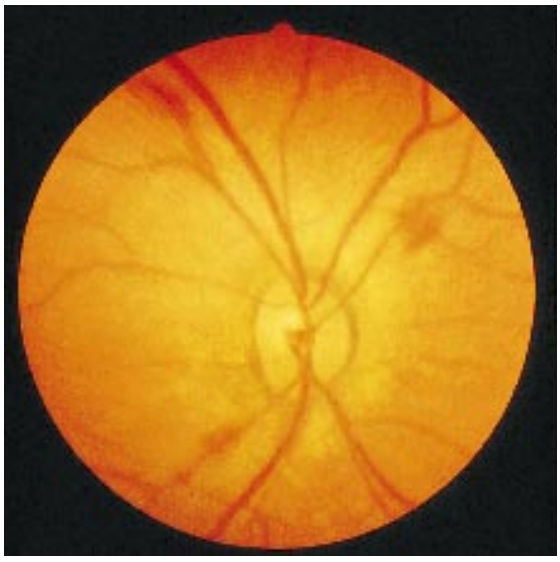

Figure 2.6. Retinal hemorrhages occur frequently in the neonate, especially following vaginal delivery. In some studies, the incidence of small retinal hemorrhages is as high as 25% irrespective of whether the delivery was spontaneous or required the application of forceps. These retinal hemorrhages resolve spontaneously without any consequences. In contrast, hemorrhages into the vitreous gel may prevent light from getting through to the retina for several days or even weeks and will cause a severe, irreversible deprivation amblyopia.

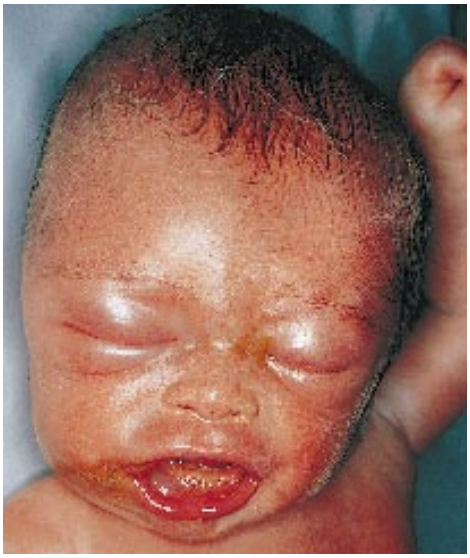

2.7

Figure 2.7. Chemical conjunctivitis in a premature infant resulting from the use of silver nitrate for Crede prophylaxis. Sometimes this is so severe that it prevents visualization of the eye on the initial examination in the nursery. This usually improves within 24 to 48 hours and an ocular examination should be performed at that time. For prophylaxis, at the present time, different antibiotic preparations have been suggested. However, because of resistant *Neisseria* gonococcus strains, many centers still use silver nitrate.

INFECTION (Acquired)

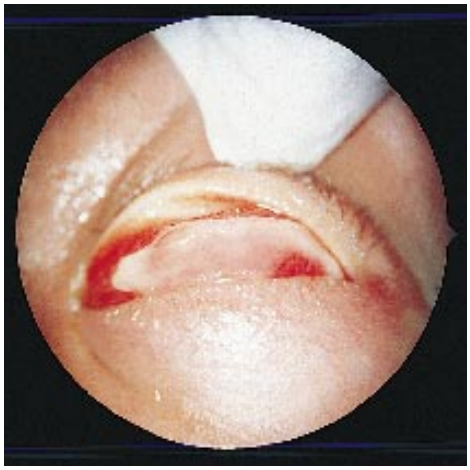

2.8

Figure 2.8. Trachoma inclusion conjunctivitis (TRIC or chlamydial conjunctivitis) usually does not become clinically apparent before the 6th day of life. This shows a dense white membrane which developed over a period of a week. TRIC is one of the few infections which cause the formation of conjunctival membranes, shown on the conjunctival surface of the upper eyelid of this eye. Tetracycline and erythromycin have been used for Crede prophylaxis in some nurseries because of the increasing incidence of chlamydial infection.

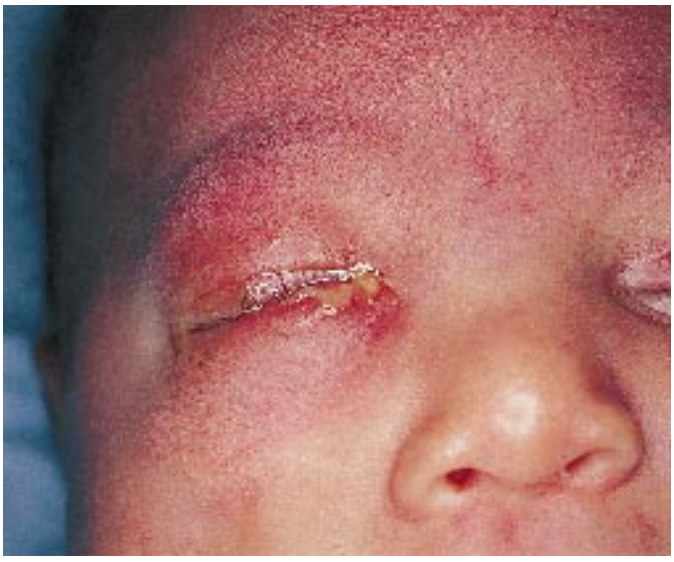

2.9

Figure 2.9. *Escherichia coli* conjunctivitis is present in this right eye. The most common conjunctivitis in the neonate in the first 24 hours of life is a chemical conjunctivitis. If the conjunctivitis is due to an infection, the most common cause is *Staphylococcus aureus*, but many other organisms may be responsible. Culture and sensitivity will suggest the appropriate antibiotic therapy.

2.10

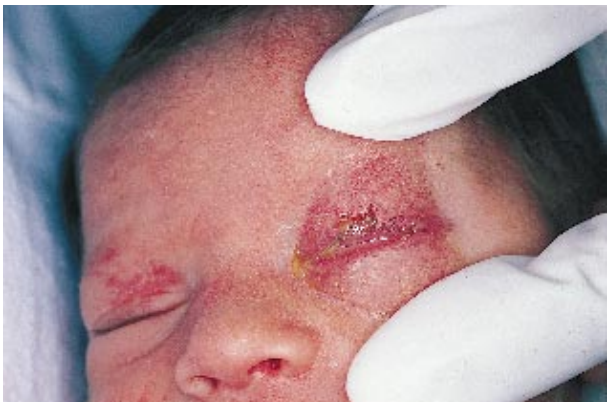

Figure 2.10. *Neisseria gonorrhoeae*: Gonococcal conjunctivitis, which became clinically apparent in this infant by the 2nd day of life, developed a purulent drainage quickly. *Neisseria* is one of the few organisms which attack the intact corneal epithelium. Because of this ability to cause corneal ulceration with perforation and subsequent endophthalmitis, *Neisseria* was once the most common cause of blindness in infants in this country.

2.11

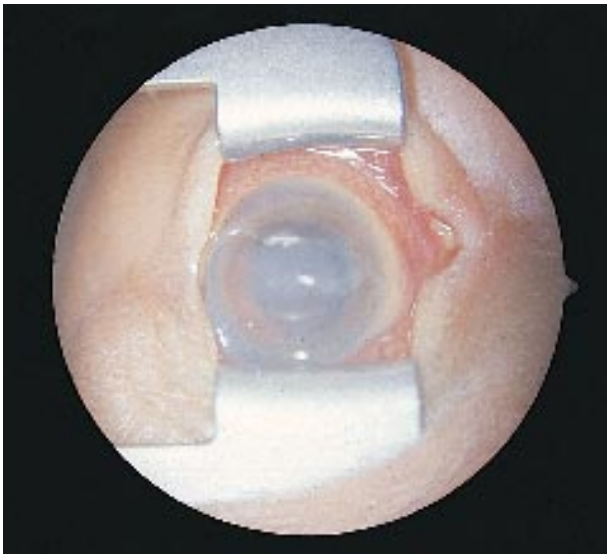

Figure 2.11. *Pseudomonas aeruginosa*: Corneal ulcer with perforation in a preterm infant. *Pseudomonas* is one of the few organisms which attack the intact corneal epithelium. Because of this ability, corneal ulceration with perforation and subsequent endophthalmitis may occur in preterm infants. Any preterm infant who is chemically paralysed while on mechanical ventilation may develop corneal exposure with subsequent corneal ulcer. Thus, it is imperative to use a lubricating ophthalmic ointment or to tape the eyes shut in this clinical setting.

2.12

Figure 2.12. *Candida albicans*: Retinitis is seen as small white infiltrates ("cotton-patches") scattered in the retina. They reflect the high blood flow through the choroidal vascular system of the eye and resolve slowly with treatment for systemic candidiasis.

INFECTION (Congenital intrauterine: TORCH diseases: Toxoplasmosis, Other, Rubella virus, Cytomegalovirus, Herpes simplex virus)

2.13

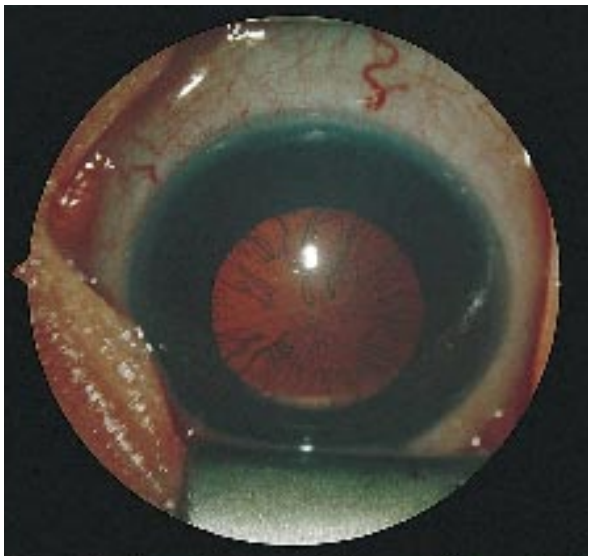

Figure 2.13. TORCH disease must be considered with persistent tunica vasculosa lentis in any small-for-gestational-age infant. This is a grade 3 tunica vasculosa lentis in an infant with congenital rubella who was 35 weeks gestational age and weighed 860 g at birth.

2.14

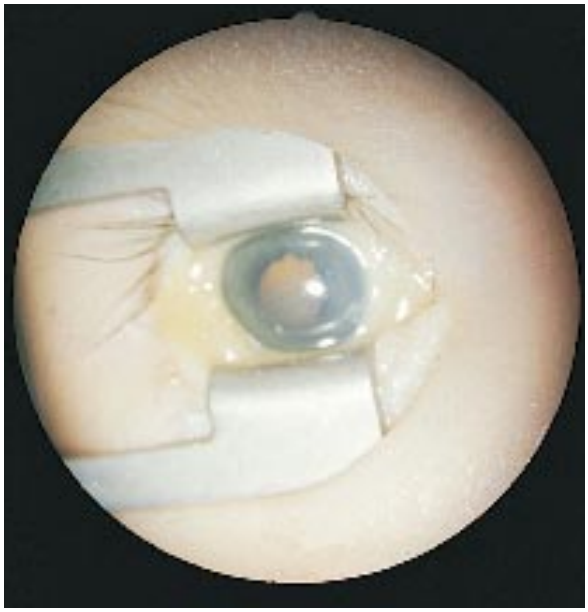

Figure 2.14. TORCH diseases must be considered with unilateral or bilateral microphthalmia in any small-for-gestational-age infant. This is a microphthalmic eye in an infant with congenital toxoplasmosis who weighed 2500 g at birth and was 39 weeks gestational age.

2.15

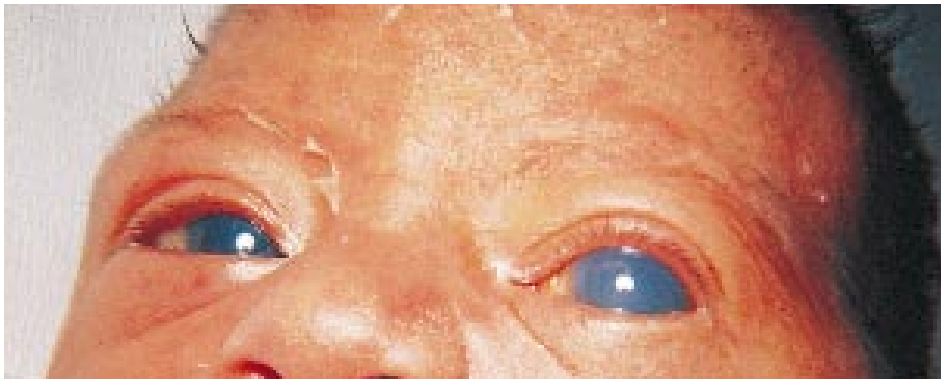

Figure 2.15. Rubella glaucoma is an uncommon ocular finding in infants with congenital rubella. Glaucoma occurs in less than 10% of infants with congenital rubella and usually is transient. It is probably related to inflammation.

2.16

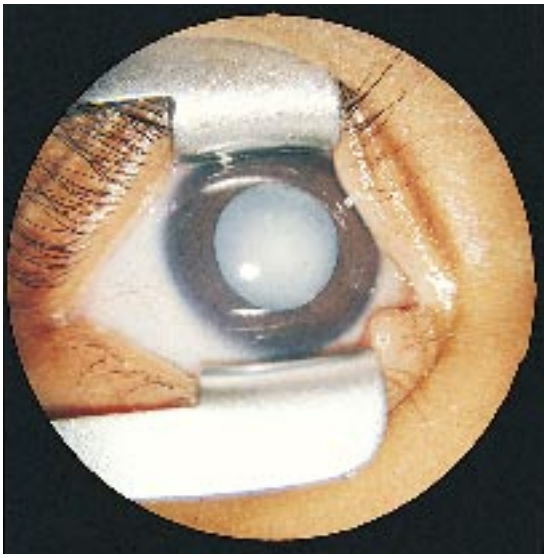

Figure 2.16. Rubella cataract is the most common ocular finding in infants with congenital rubella and occurs in up to 75% of these infants. Classically, the cataract is nuclear, and the virus can be isolated from the lens for years following birth.

2.17

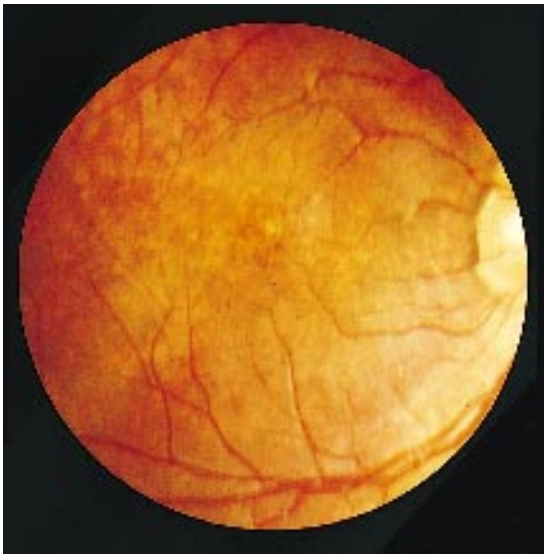

Figure 2.17. Rubella retinitis appears as a salt and pepper retinitis classically and reflects damage to the retinal pigment epithelium. It can be present without any decrease in visual acuity.

2.18

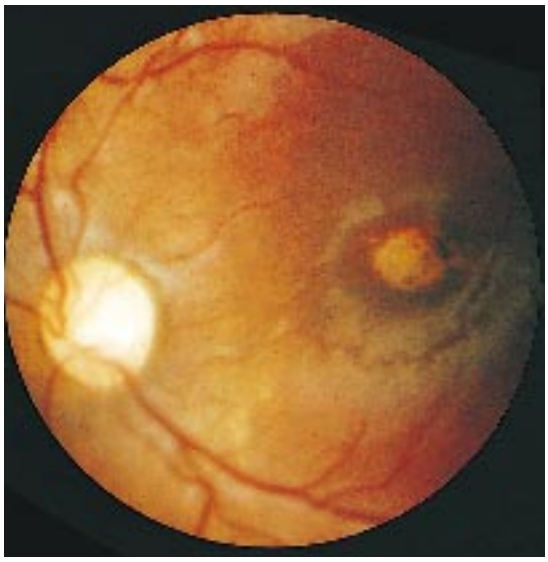

Figure 2.18. Cytomegalovirus may cause a small macular chorioretinal scar. This is the most typical lesion in cytomegalovirus infection.

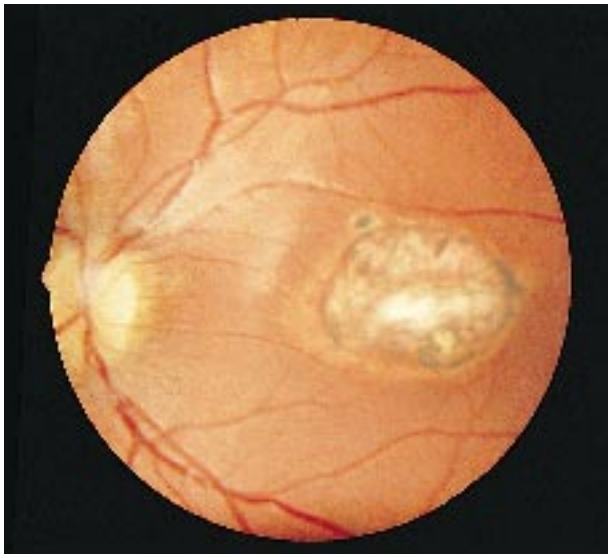

2.19

Figure 2.19. Toxoplasmosis may cause a large macular chorioretinal scar. This is the most typical lesion of toxoplasmosis infection, but it is indistinguishable clinically from a large macular chorioretinal scar of cytomegalovirus infection.

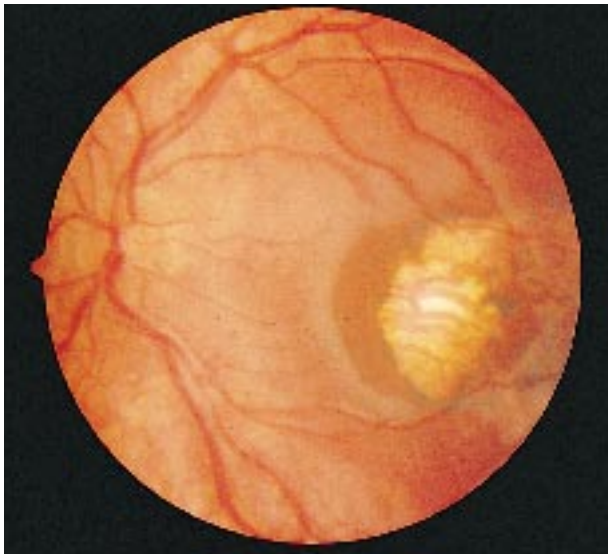

2.20

Figure 2.20. Cytomegalovirus was the cause of this large macular chorioretinal scar. It closely resembles the scar of toxoplasmosis shown in Figure 2.19.

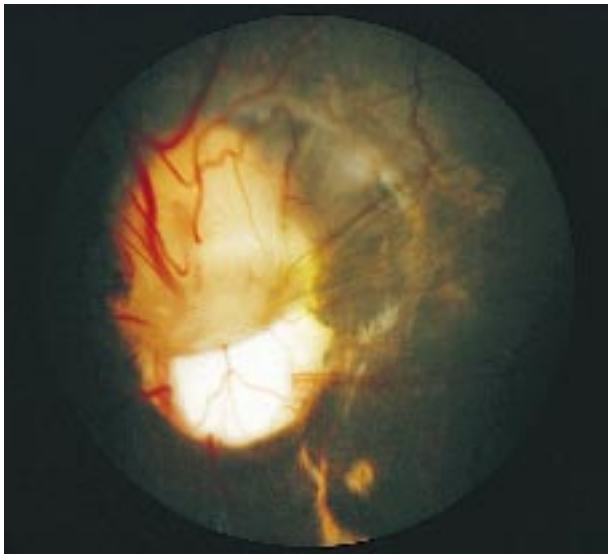

2.21

Figure 2.21. Cytomegalovirus may cause a coloboma of the optic nerve. This failure of the fetal fissure to fuse posteriorly may occur in infants with cytomegalovirus infection. When there is ocular involvement in cytomegalovirus infection, there is usually damage to the central nervous system.

2.22

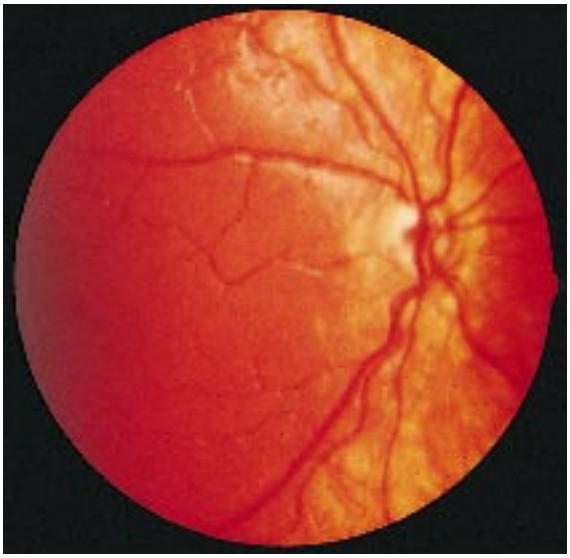

Figure 2.22. Cytomegalovirus may cause hypoplasia of the optic nerve. This lack of development of the optic nerve in infants with cytomegalovirus infection may be associated with severe damage to the central nervous system.

2.23

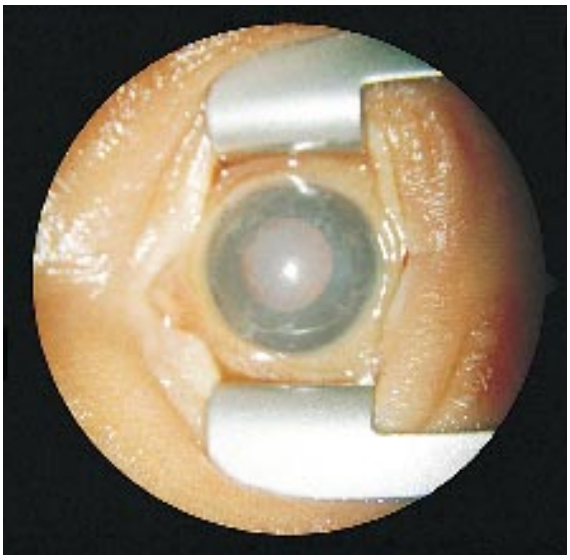

Figure 2.23. Herpes simplex infection can be devastating not only to the eye but to the central nervous system. Occasionally, a superficial herpetic corneal ulcer with edema, as shown in this figure, can allow rapid diagnosis of herpetic infection with the opportunity to institute systemic therapy immediately.

2.24

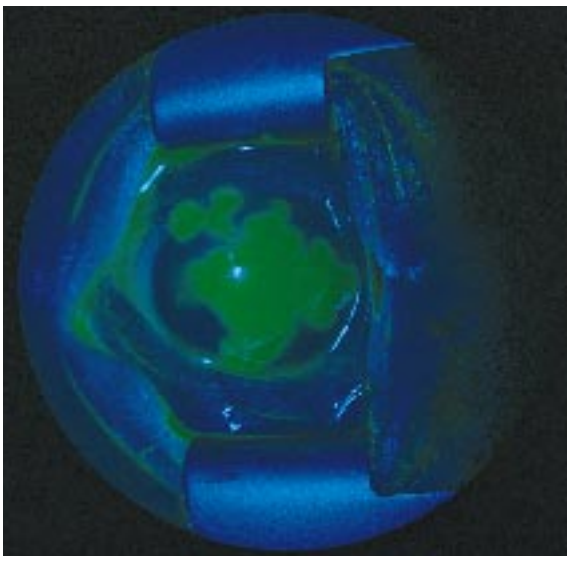

Figure 2.24. This herpes simplex corneal ulcer with dendrites, shown unstained Figure 2.23, is stained with fluorescein and viewed with a cobalt blue filter. Such a corneal lesion allows early diagnosis. If therapy is begun immediately, herpes simplex infection does not necessarily correlate with severe central nervous system damage.

2.25

Figure 2.25. Herpes simplex can cause a necrotizing chorioretinitis. It usually appears within the first few days following birth as macular or peripheral retinal edema.

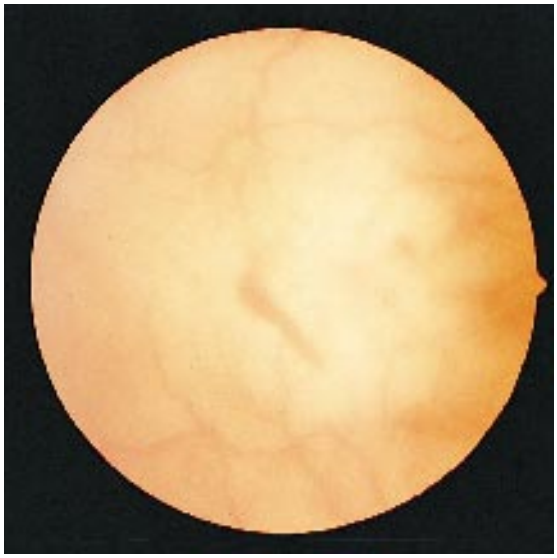

2.26

Figure 2.26. Herpes simplex necrotizing chorioretinitis usually progresses rapidly and usually correlates with severe central nervous system necrosis. This is the same eye as in Figure 2.25, 4 days later.

LACRIMAL ABNORMALITIES

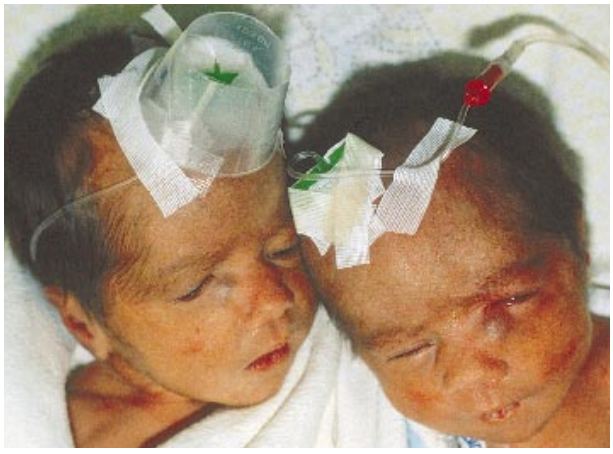

2.27

Figure 2.27. A dacryocystocele may occur as an autosomal dominant in families as exemplified by these twins. The lacrimal sac is blocked at both ends and a sterile swelling appears as a purplish swelling adjacent to the base of the nose. Simple lacrimal probing allows for a swift resolution of this problem; however, if there is anything atypical about the location or the appearance of the swelling, an ultrasound of the brain should be obtained to exclude an encephalocele.

2.28

Figure 2.28. If a lacrimal cyst becomes infected, the skin overlying the cyst becomes edematous and erythematous. Because septicemia, meningitis, and/or cavernous sinus thrombosis may occur, systemic antibiotics are indicated. Following a short period of antibiotics, probing of the lacrimal system should be performed.

LIDS

2.29

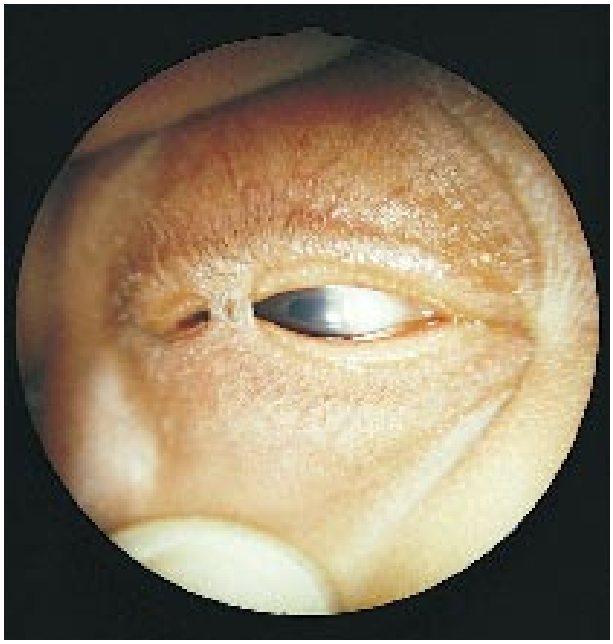

Figure 2.29. Ankyloblepharon filiforme adnatum is shown in this figure with fusion of the upper and lower eyelids by small filiform attachments which can be cut with scissors. Blepharophimosis is a narrow palpebral fissure which occurs as a congenital anomaly and should be included in the differential diagnosis of ankyloblepharon filiforme adnatum.

2.30

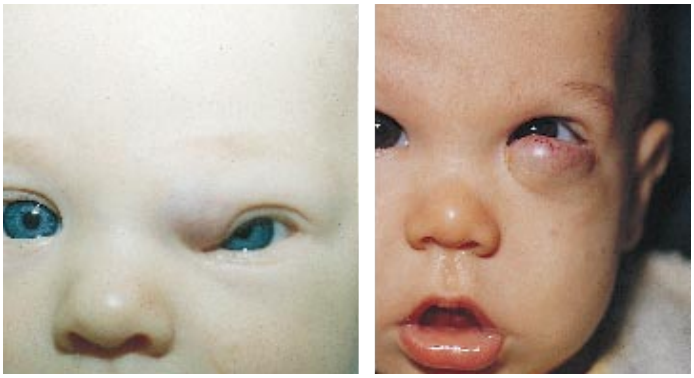

Figure 2.30. Capillary hemangiomas of the lids most frequently arise nasally from either the superior or the inferior palpebral fissure. They are poorly defined soft swellings of the eyelid with purple (red-blue) discoloration of the skin. They require treatment when rapid growth threatens the visual axis which can lead to irreversible deprivation amblyopia.

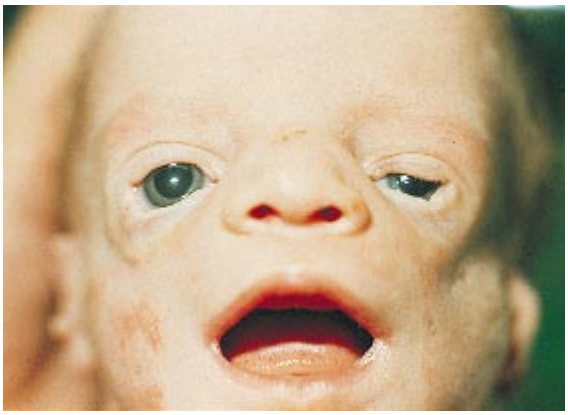

2.31

Figure 2.31. Treacher-Collins syndrome is characterized by malformations of the structures formed from the first branchial arch, groove, and pouch. Mandibulofacial dysostosis with antimongoloid slanting of the palpebral fissure and coloboma of the lower temporal lid is inherited as an autosomal dominant (5q11) disorder.

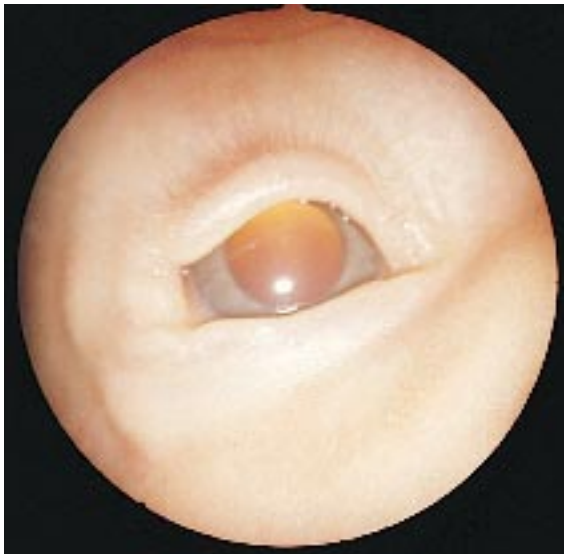

2.32

Figure 2.32. The coloboma of the lid in the Treacher-Collins syndrome involves the lateral third of the lower lid and may not affect the lid margin. Other lower lid anomalies such as absent lacrimal punctae and irregular lower lid lashes may also be present.

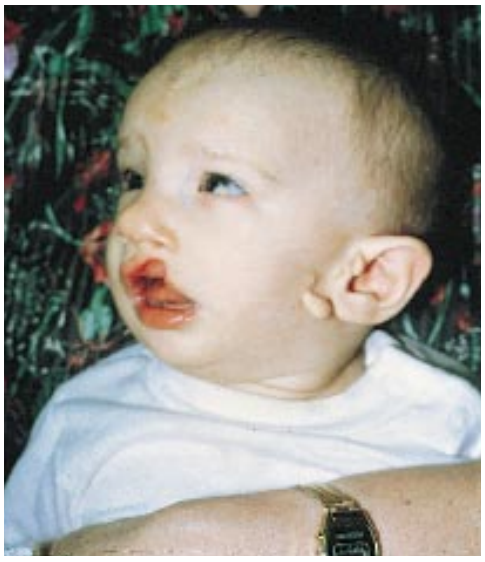

2.33

Figure 2.33. The most common findings of Goldenhar's syndrome, which is characterized by hemifacial macrosomia, are colobomas of the upper lids, solid epibulbar dermoids located at the inferotemporal border of the cornea, and solid lipodermoids located in the superotemporal sulcus near the lacrimal gland. Oculoauriculovertebral dysplasia is sporadic and the basic defect is unknown.

2.34

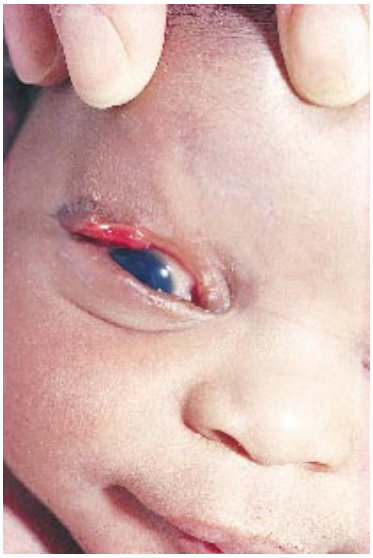

Figure 2.34. The coloboma of the lid in Goldenhar's syndrome involves the middle third of the upper lid which does affect the lid margin.

2.35

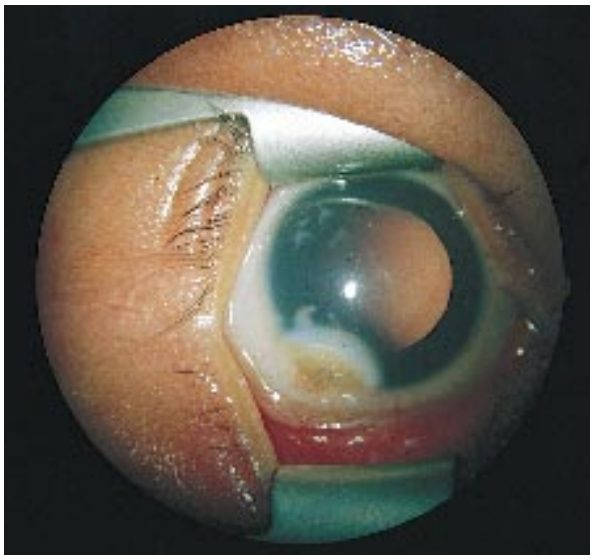

Figure 2.35. This typical dermoid of the Goldenhar's syndrome occurs as a solid mass of the conjunctiva at the inferotemporal border of the cornea. Flattening of the cornea occurs in the meridian of the dermoid, causing an associated astigmatism and occasionally a secondary amblyopia.

2.36

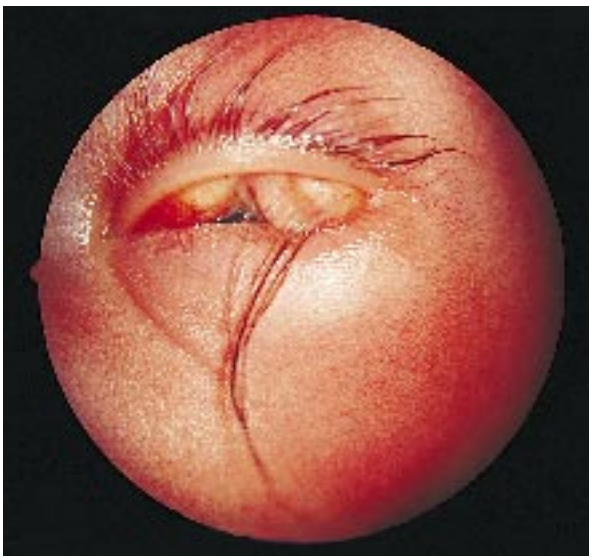

Figure 2.36. This complex choristoma located in the superotemporal sulcus of the left eye with the upper lid everted demonstrates the long lashes which may be present. This is different from the lipodermoid noted in the same position in some patients with Goldenhar's syndrome.

2.37

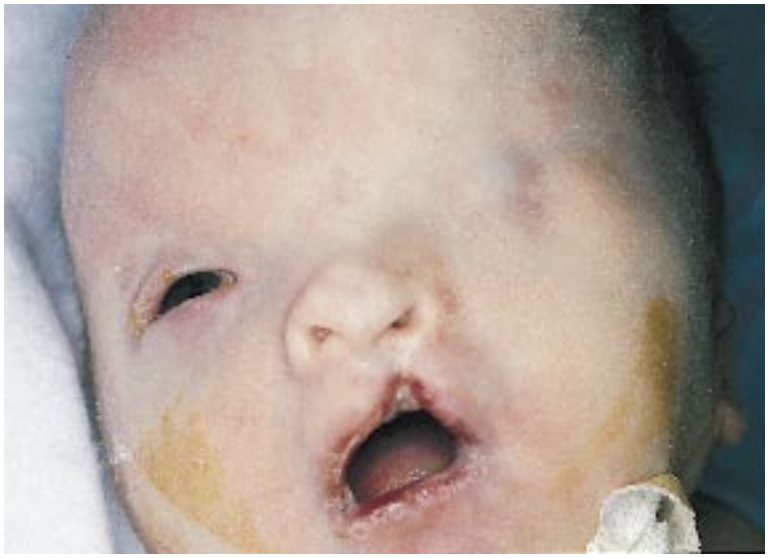

Figure 2.37. Fraser's syndrome is an autosomal recessive disorder which occurs when the maturation of the lids is interrupted and the lid folds fail to develop. This infant shows complete cryptophthalmos by the left lid (surface ectoderm) with complete coverage of the corneal epithelium.

2.38

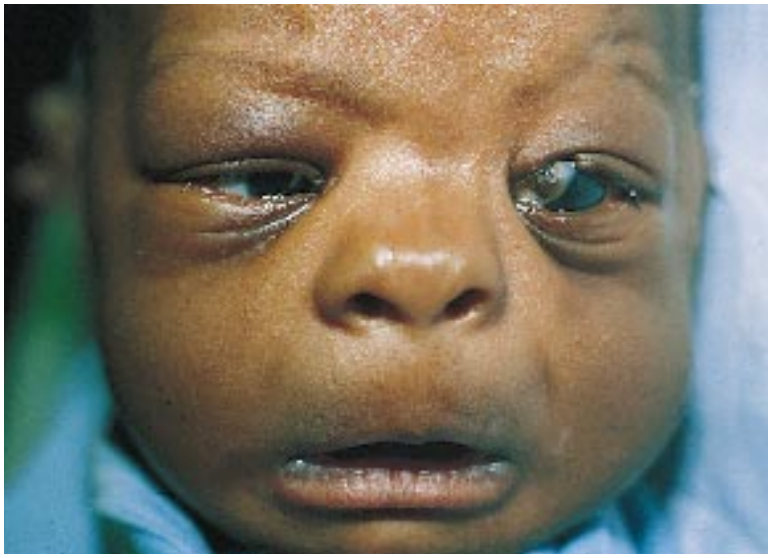

Figure 2.38. This figure demonstrates Fraser's syndrome with partial cryptophthalmos. There is a continuation of the left superonasal lid (surface ectoderm) with the corneal epithelium.

2.39

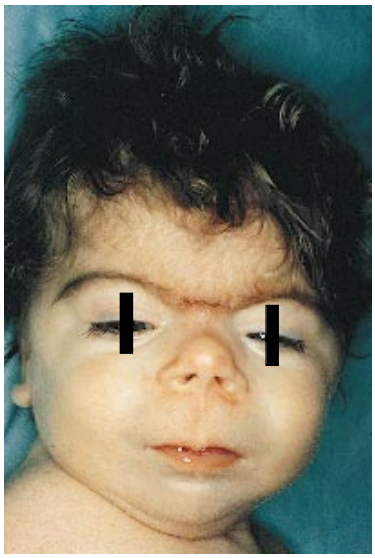

Figure 2.39. The typical confluent eyebrows, long curly eyelashes, and telecanthus associated with the Cornelia de Lange syndrome are present in this infant. Telecanthus is the lateral displacement of the inner canthi such that the medial portion of the eye is partially obscured, giving rise to the impression of strabismus and hypertelorism. In hypertelorism the eyes are widely spaced. Because a low nasal bridge may give rise to the impression of widely spaced eyes, the distance between the two eyes should always be measured.

2.40

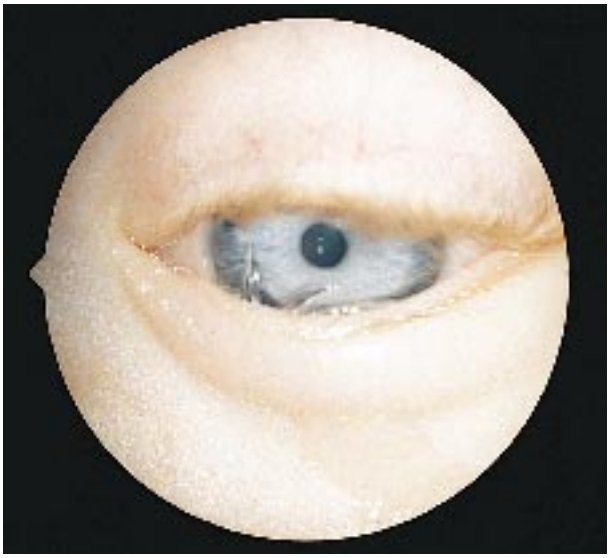

Figure 2.40. Congenital entropion is shown in this patient with epiblepharon allowing the inturning of the lower nasal lid such that the lashes irritate the cornea.

2.41

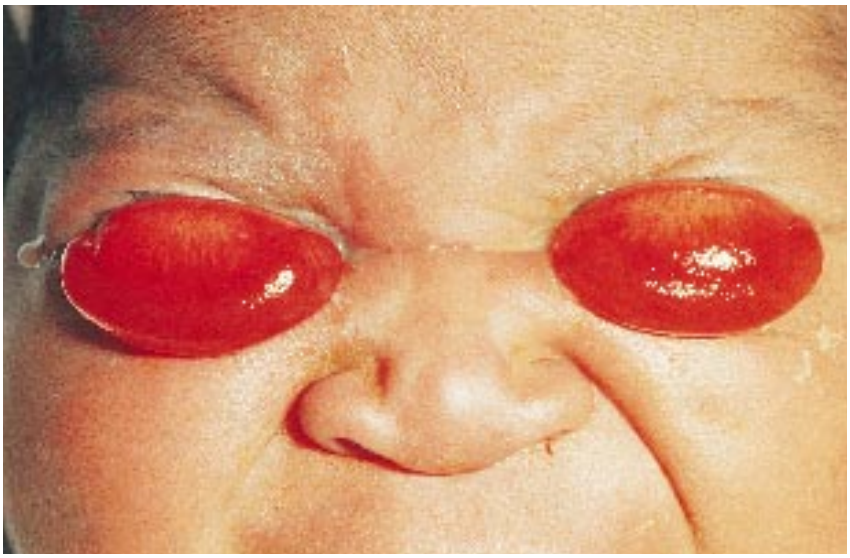

Figure 2.41. Congenital ectropion occurs as a result of intrauterine prolapse of the conjunctiva. This may require temporary taping or suturing of the lid margins. In the absence of microphthalmos, buphthalmos, or eyelid defects, primary eyelid eversion is rare and follows a benign course. The tarsal conjunctiva is chemotic, hyperemic, and protrudes outward. The lid returns to normal a few days following application of ophthalmic ointment and moist sterile gauze dressings.

2.42

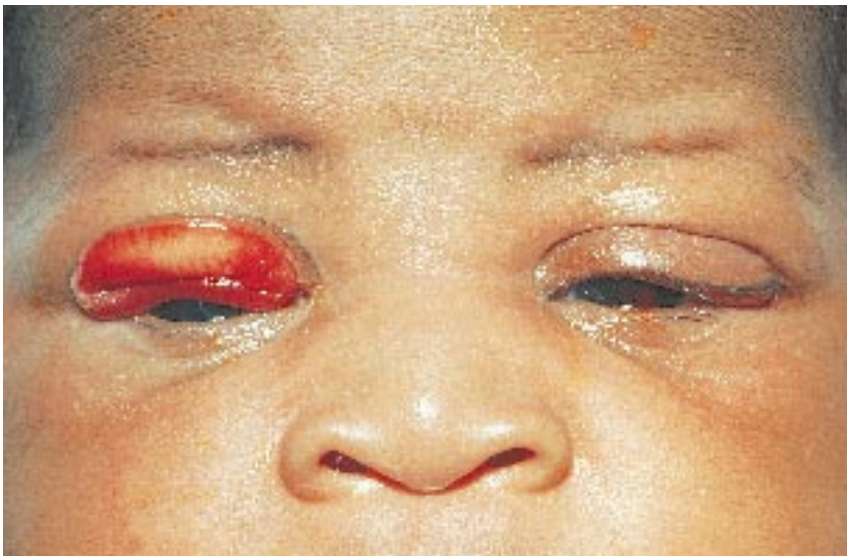

Figure 2.42. The same patient showing a residual right upper lid ectropion after five days of bilateral pressure patches. If this occurs as a unilateral condition, it is essential to tape both eyes closed to prevent deprivation amblyopia.

2.43

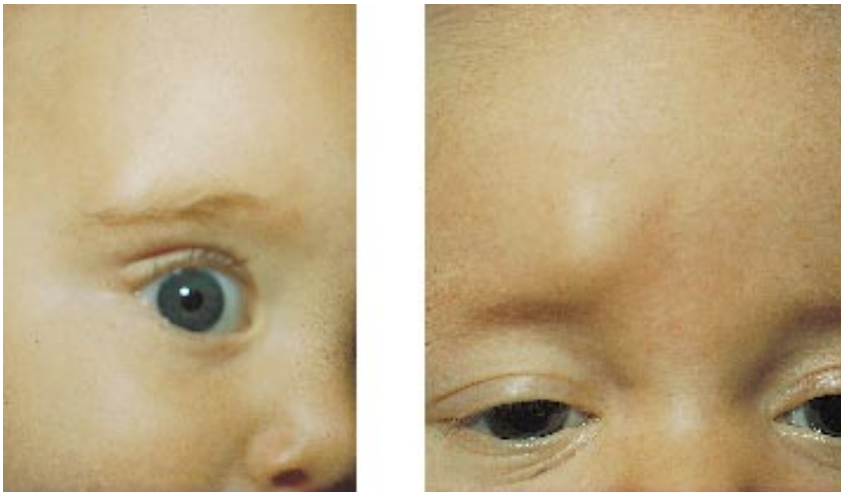

Figure 2.43. Dermoid cysts occur when surface ectodermal elements are sequestered along the closure lines of the fetal bony sutures. These cystic dermoids demonstrate the superotemporal and the superonasal locations.

2.44

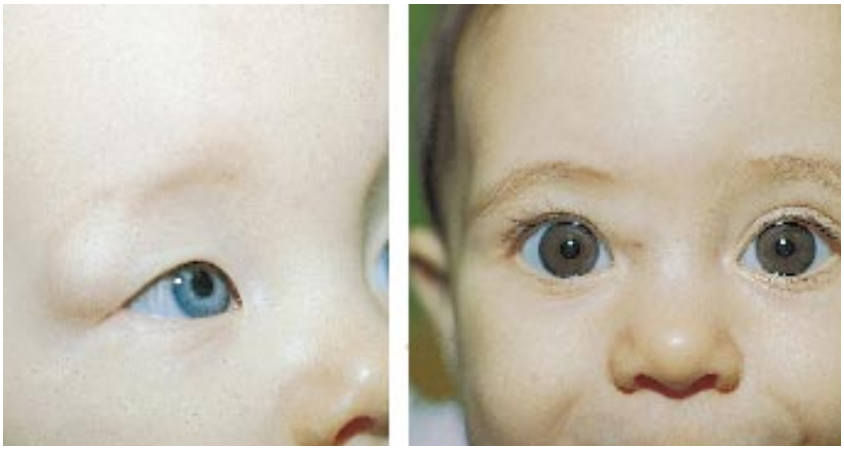

Figure 2.44. These cystic dermoids demonstrate the inferotemporal and the inferonasal locations. They are lined by keratinized squamous epithelial cells and contain hair follicles and sebaceous glands.

2.45

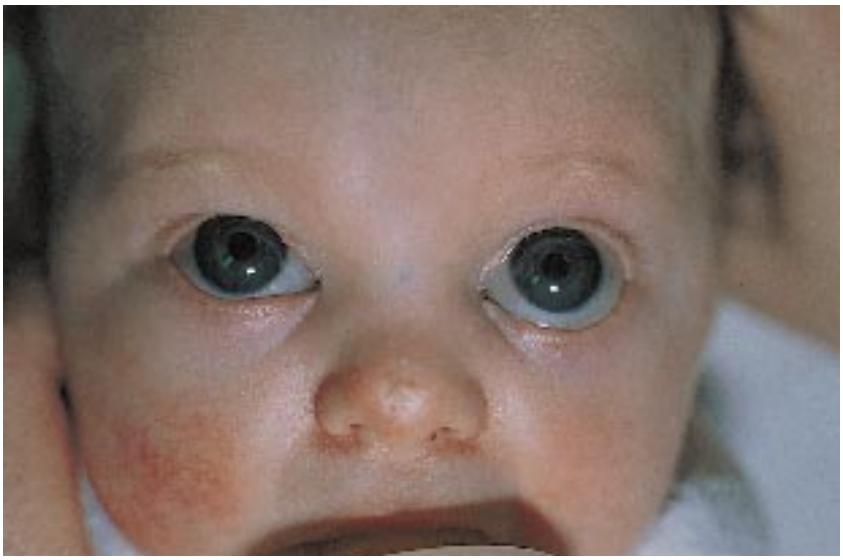

Figure 2.45. Exophthalmos and lid retraction occur infrequently. This patient demonstrates the typical lid signs of neonatal hyperthyroidism. Children with craniofacial anomalies and shallow orbits also may demonstrate severe exophthalmos and lid retraction.

2.46

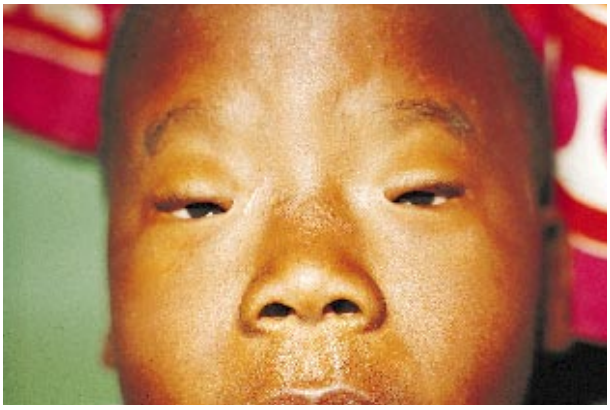

Figure 2.46. This patient demonstrates bilateral blepharoptosis, blepharophimosis, and epicanthus inversus with normal globes and normal vision which occurs as an autosomal dominant. This is distinct from bilateral anophthalmia, microphthalmia, or nanophthalmia where the globes are not present or small with absent or impaired vision. The epicanthus is a crescentic fold of skin running vertically between the lids over the inner canthus. It can be most prominent in the upper eyelid (epicanthus tarsalis); most prominent in the lower eyelid (epicanthus inversus); or equally distributed between the upper and lower eyelids (epicanthus palpebralis).

OCULAR SIZE

2.47

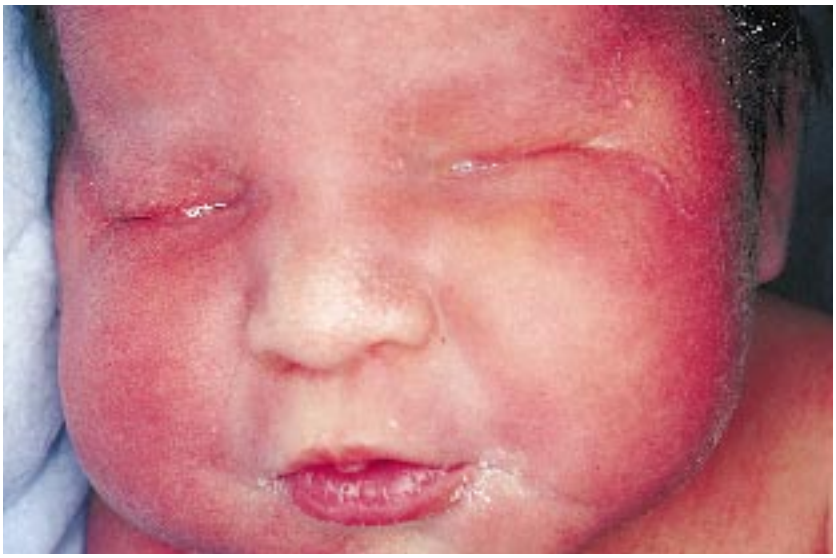

Figure 2.47. At term birth, the normal ocular sagittal length is 17.5 mm, and the normal corneal diameter is 10 mm. This is a term infant with very severe bilateral microphthalmia. The globes are virtually absent and the infant is totally blind. This may occur unilaterally or bilaterally and is often associated with other anomalies of the central nervous system.

2.48

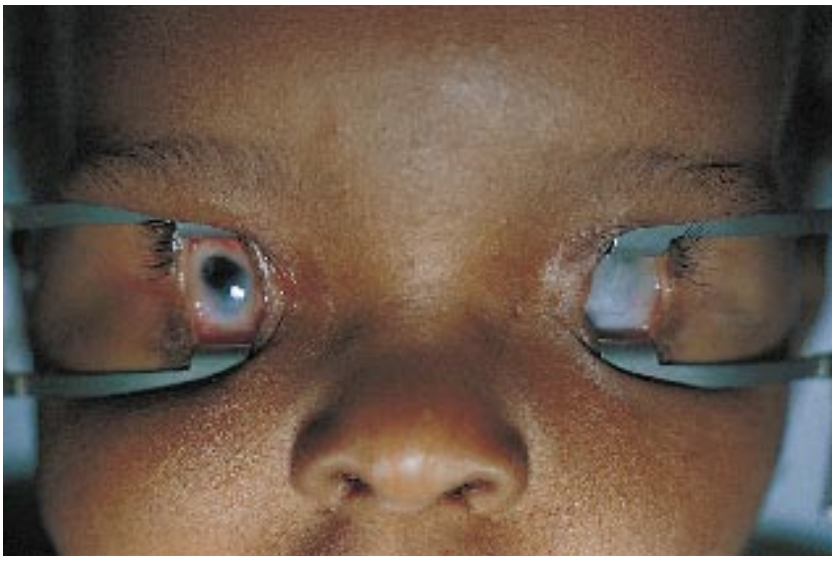

Figure 2.48. This is another term infant with severe bilateral microphthalmia. The globes are small, and vision is extremely poor. There are several forms of microphthalmia including those associated with congenital infection, chromosomal abnormalities, and the CHARGE syndrome.

2.49

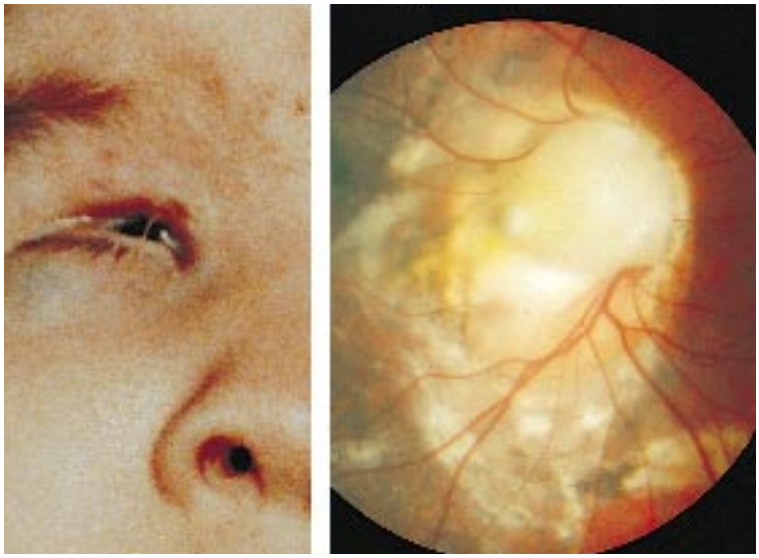

Figure 2.49. Colobomatous microphthalmia may be inherited as an autosomal dominant disorder with extremely variable expressivity. On the left is severe microphthalmia presenting as a cystic eye. On the right is a coloboma of the optic nerve with continuous coloboma of the choroid and retina which was present in another member of the same family.

2.50

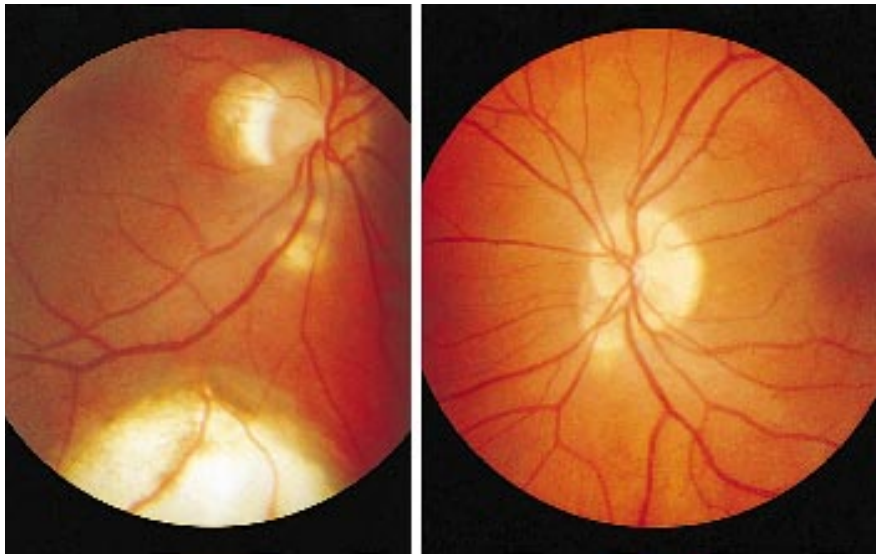

Figure 2.50. On the left is a minimal coloboma of the optic nerve with peripheral coloboma of the choroid and retina in another member of the same family. On the right is a very minimal coloboma of the choroid and retina adjacent to the normal optic nerve in a member of the same family who was totally unaware that she carried the gene for autosomal dominant colobomatous microphthalmia.

ANTERIOR SEGMENT
(Cornea, iris, and trabecular meshwork [glaucoma])

2.51

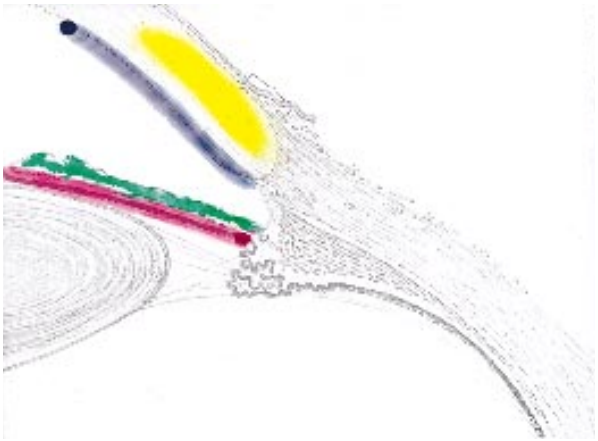

Figure 2.51. When the structures of the anterior segment are subdivided according to their embryonic layer of origin, various patterns emerge. In this figure, the neuroectoderm, consisting of the anterior rim of optic cup, iris pigment epithelium and pupillary musculature is shown in red; the 1st neural crest mesenchymal wave (corneal endothelium and trabecular meshwork) is shown in black; the 2nd neural crest mesenchymal wave (corneal stroma) is shown in yellow; and the 3rd neural crest mesenchymal wave (iris stroma) is shown in green.

2.52

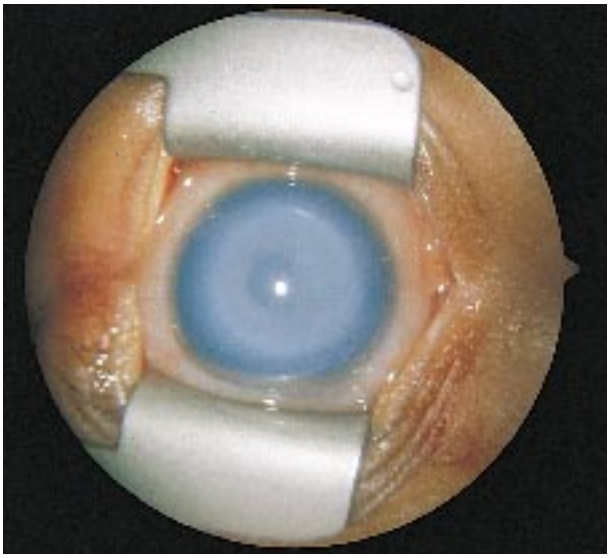

Figure 2.52. Peters anomaly is shown in this figure. Corneal clouding is marked because corneal endothelium is abnormal, and glaucoma is common because the trabecular meshwork may be altered. This photograph demonstrates severe corneal clouding which would justify a penetrating corneal transplant in at least one eye of a bilaterally affected infant even though the prognosis for a successful corneal transplant in infants is poor.

2.53

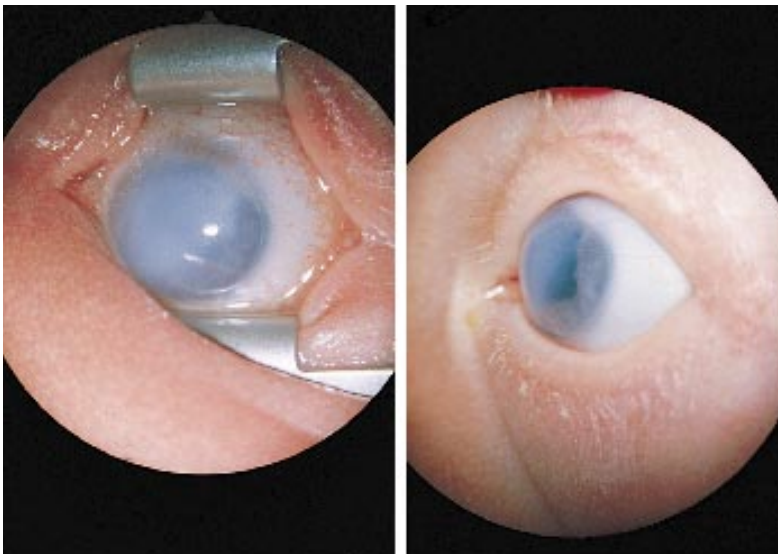

Figure 2.53. Anterior segment mesenchymal dysgenesis in one member of an autosomal dominant (4q28-31) family with variable expressivity is shown in this figure. On the left is an eye with a large area of severe corneal clouding. On the right, the same eye demonstrates the adhesions of the iris to the corneal endothelium.

2.54

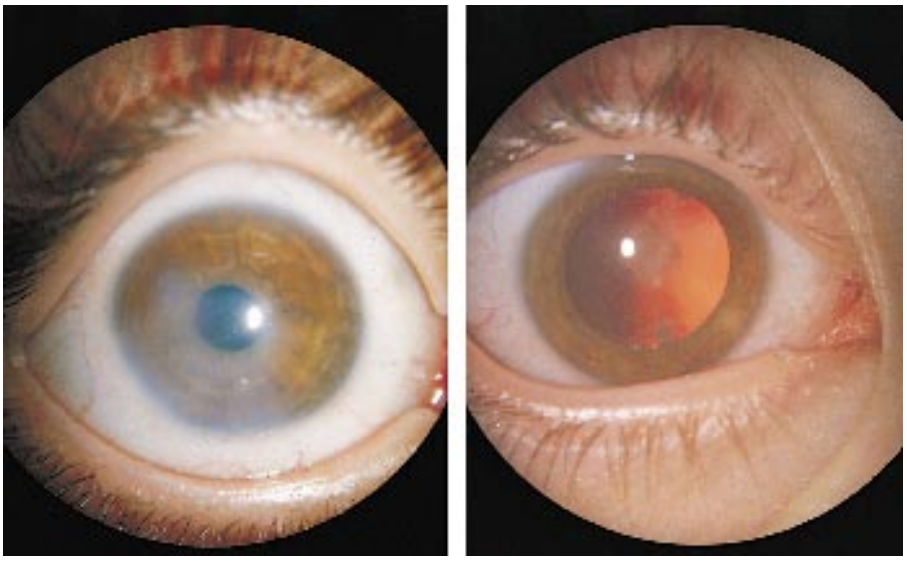

Figure 2.54. This figure shows anterior segment mesenchymal dysgenesis in members of the same family as in Figure 2.53. On the left is a smaller area of moderate corneal clouding, and on the right is a tiny area of minimal corneal opacity and a central cataract.

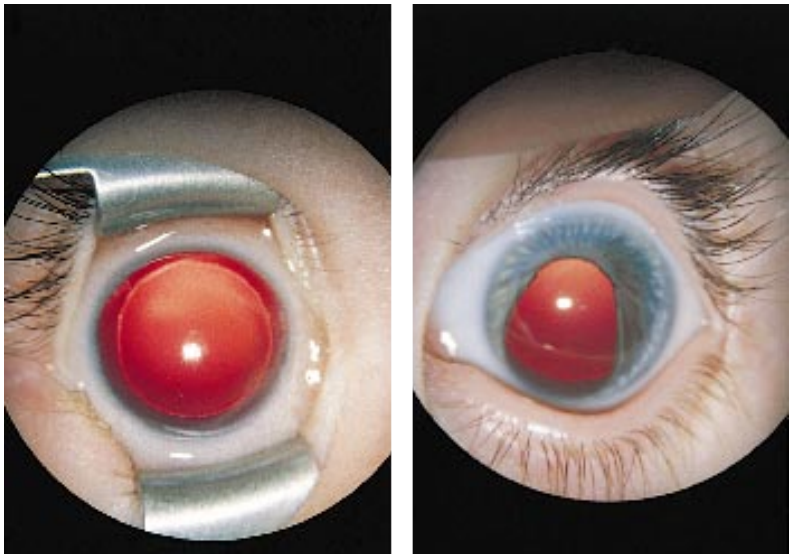

2.55

Figure 2.55. Aniridia in members of an autosomal dominant (11p13; PAX6) family with variable expressivity is shown in this figure. Neuroectodermal layers of the iris are abnormal. On the left is an eye with complete aniridia. On the right is an eye with an atypical (i.e., any location except inferonasal) iris coloboma.

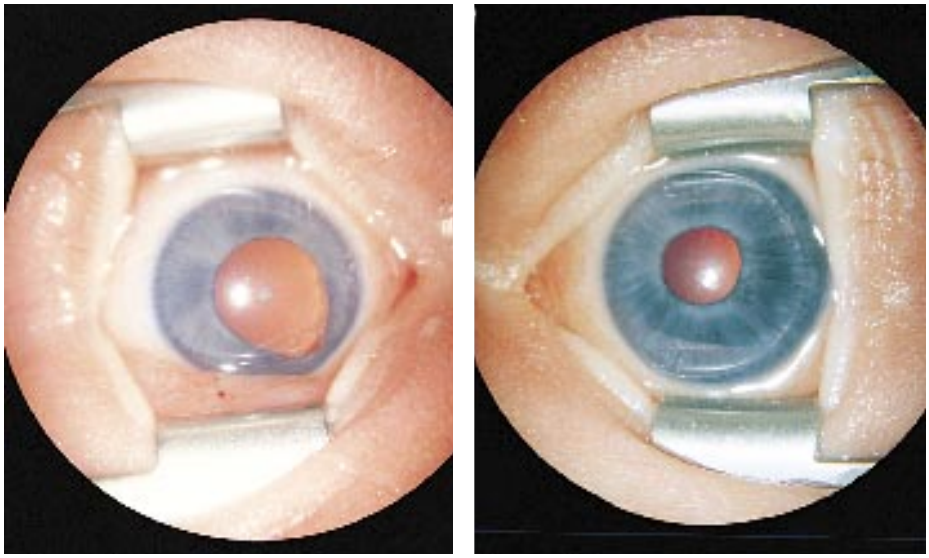

2.56

Figure 2.56. This figure shows aniridia in members of the same family, as in Figure 2.55. On the left is a typical (inferonasal location) iris coloboma. On the right is an eye with an eccentric round pupil with iris thinning and no iris collarette.

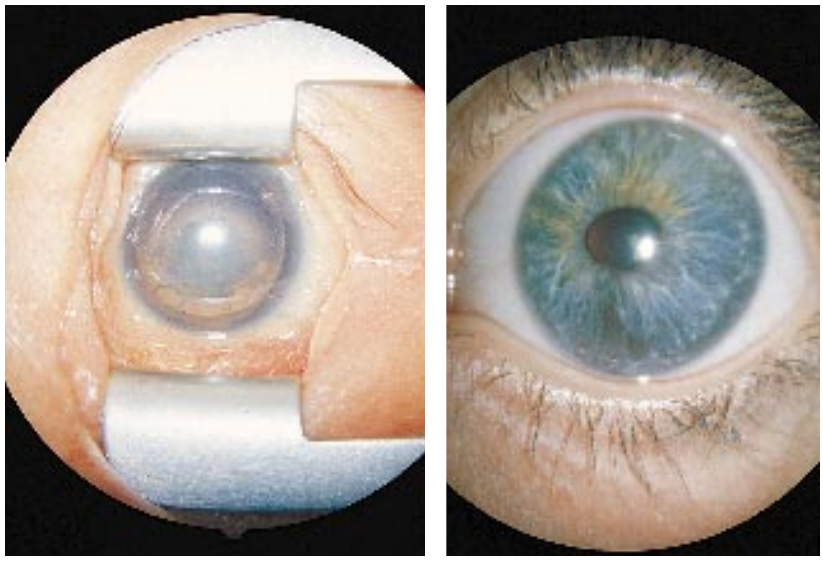

2.57

Figure 2.57. Aniridia also occurs as a deletion syndrome (del 11p13) known as the WAGR syndrome (*W*ilms' tumor, *A*niridia, *G*enitourinary anomalies, and mental *R*etardation). On the left is a nearly complete aniridia with minimal iris remnants and a dense cataract. On the right is a very minimal aniridia with an eccentric round pupil with iris thinning and no iris collarette.

2.58

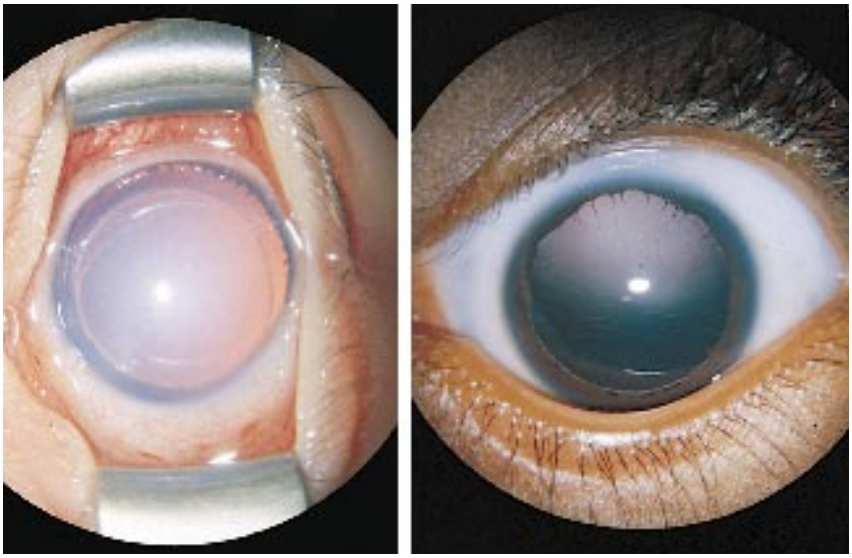

Figure 2.58. Aniridia with cerebellar malformation is an autosomal recessive disorder which seems to be associated with little variability in expression. On the left is a rather complete aniridia with corneal clouding due to glaucoma. On the right is another virtually complete aniridia with minimal iris remnants.

2.59

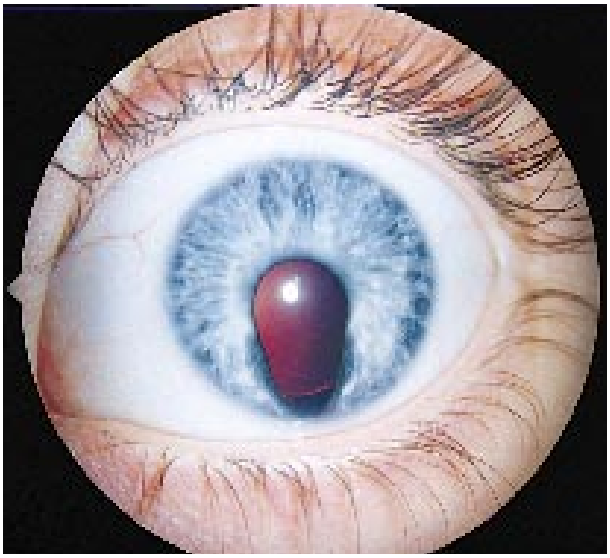

Figure 2.59. This figure shows a typical (inferonasal) isolated iris coloboma related to a failure of fusion of the optic cup at its most anterior extent. All iris structures are intact except in the inferonasal position.

2.60

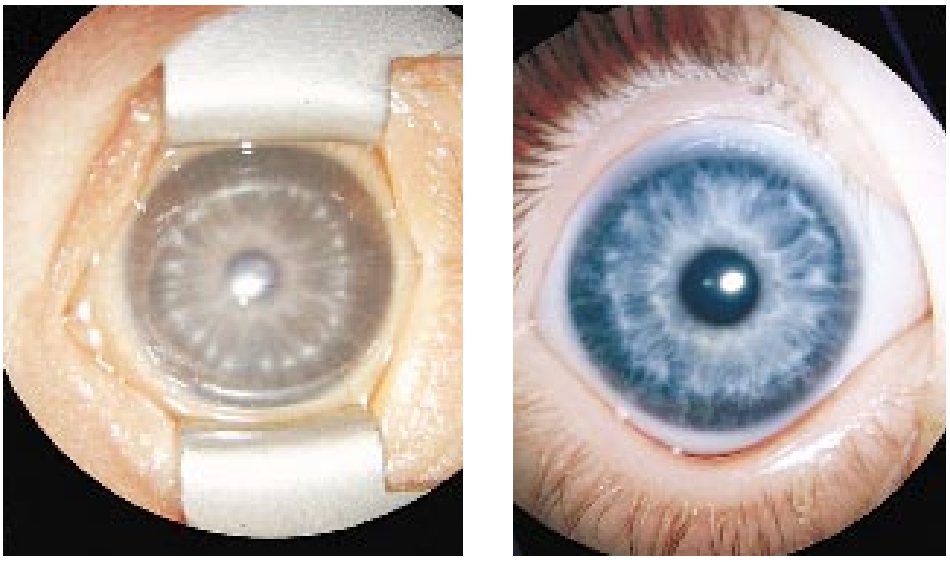

Figure 2.60. This figure demonstrates Brushfield's spots in an infant with brown irides which are pathognomonic for Down syndrome. In contrast, Brushfield's spots in an infant with blue irides is a nonspecific finding of many blue irides.

2.61

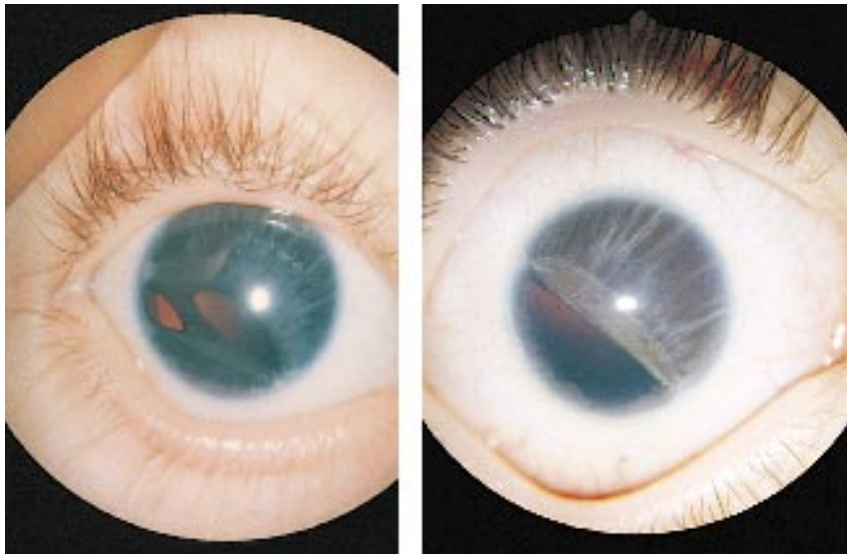

Figure 2.61. Rieger's syndrome is an autosomal dominant (4q23-q27) disorder with abnormal irides, associated with an abnormal umbilicus and malformed teeth. Abnormal iris stroma is present, and glaucoma is common. Families may exhibit variable expressivity. On the left is an eye with polycoria, dyscoria, and correctopia present at birth. On the right is the same eye several years later demonstrating early glaucoma due to progressive obliteration of the chamber angle by adhesions of the iris to an anterior Schwalbe's line.

2.62

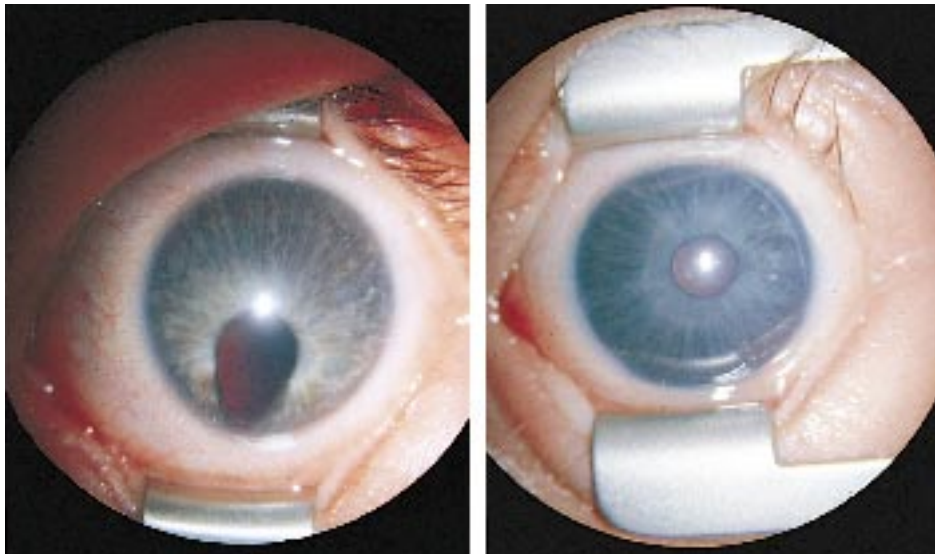

Figure 2.62. This figure demonstrates less severe anomalies of the anterior segment. On the left is an eye with dyscoria and correctopia which was present at birth resembling an iris coloboma due to a small iris adhesion to an anterior Schwalbe's line. On the right is an eye with a central pupil, which is fortuitous since glaucoma is less likely to occur in eyes with central pupils.

2.63

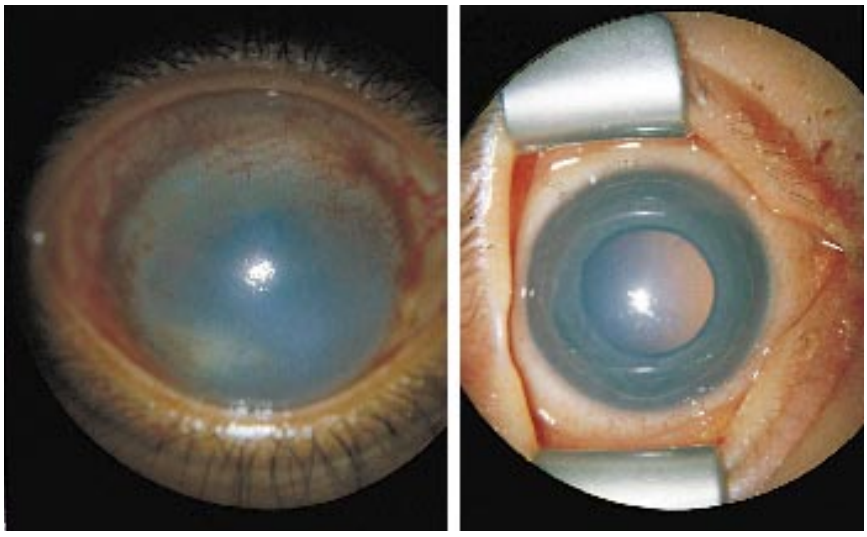

Figure 2.63. This figure shows members of a family with autosomal dominant pseudo-Rieger's syndrome which has been associated with an abnormal pituitary or an empty sella in some affected family members. An abnormal iris stroma is present and glaucoma is common. Families may exhibit variable expressivity. On the left is an eye with end stage glaucoma with secondary corneal clouding. On the right is an eye with early glaucoma with abnormal adhesions of the iris to an anterior Schwalbe's line extending 360 degrees.

2.64

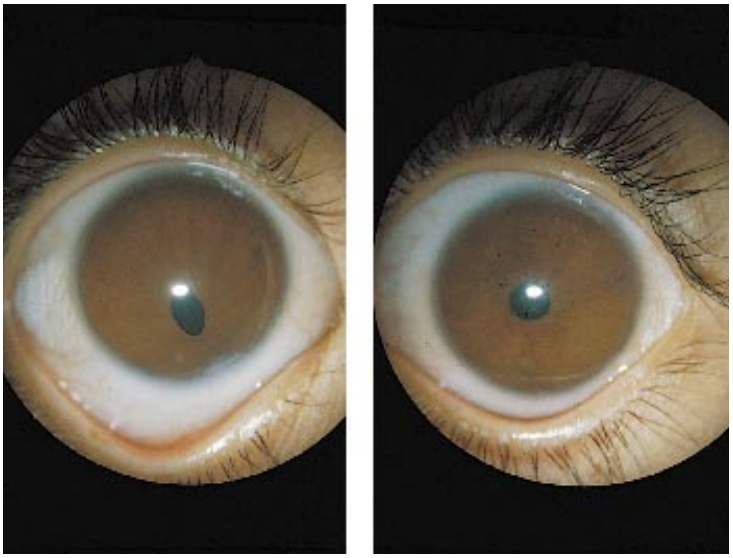

Figure 2.64. Anterior segments in members of the same family with pseudo-Rieger's syndrome are shown as in Figure 2.63. On the left is an eye with an eccentric pupil resembling an iris coloboma due to a small iris adhesion to an anterior Schwalbe's line. On the right is an eye with a central pupil which does not have an associated glaucoma.

2.65

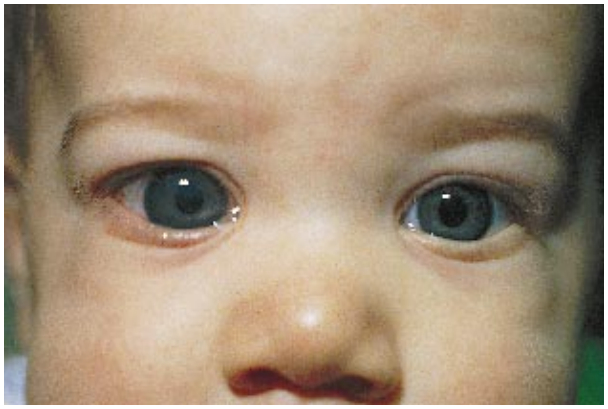

Figure 2.65. This infant demonstrates the asymmetrical eye size seen with unilateral glaucoma which is an autosomal recessive disorder. Megalocornea (a constant enlarged corneal diameter present at birth) must be considered in patients with bilateral glaucoma (a corneal enlargment which is progressive up to age 2 years). In megalocornea, the intraocular pressure is not increased. Glaucoma usually presents with excessive tearing, photophobia, and corneal clouding.

2.66

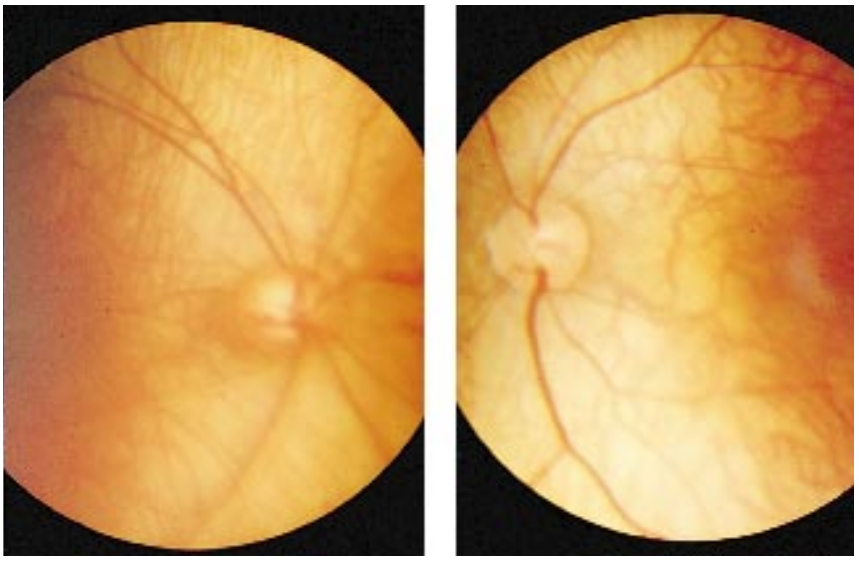

Figure 2.66. These photographs are of the optic nerves of the infant shown in Figure 2.65. The optic nerves reveal asymmetrical cupping reflecting the increased intraocular pressure in the right eye (figure left) and the normal intraocular pressure in the left eye (figure right).

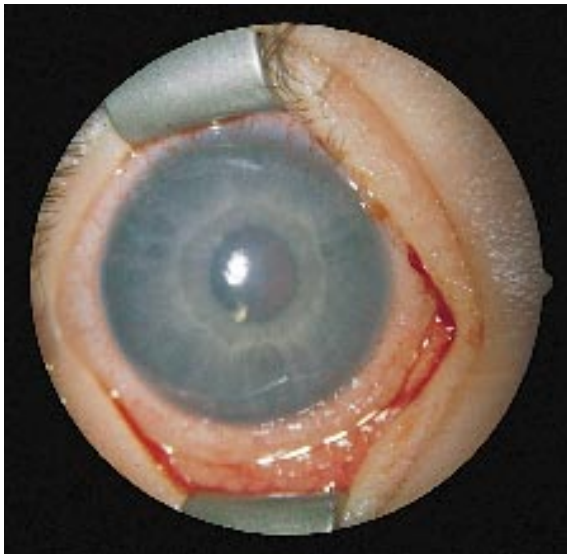

2.67

Figure 2.67. The affected eye of the same infant as in Figure 2.66 demonstrates the corneal enlargement and clouding secondary to corneal edema.

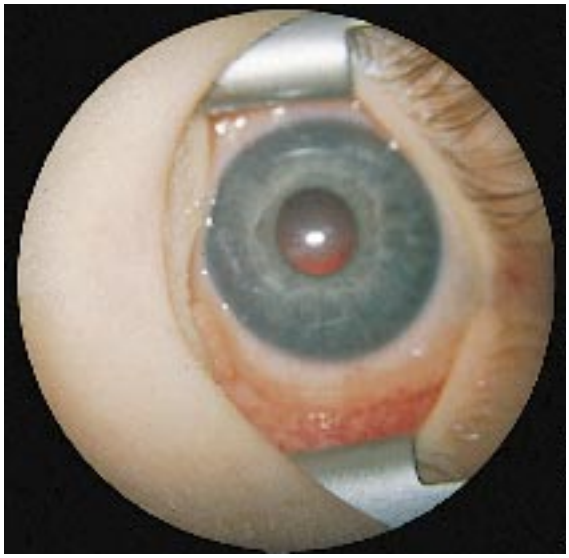

2.68

Figure 2.68. This figure is of the unaffected eye of the same infant. The asymmetry is extremely important in detecting glaucoma in early cases.

2.69

Figure 2.69. This infant has neurofibromatosis which is an autosomal dominant (Type 1, 17q11.2; Type 2, 22q11.2-q13) disorder. The asymmetrical eye size demonstrated is due to glaucoma. The thickening of the right upper temporal lid is a plexiform neuroma which is pathognomonic for neurofibromatosis.

2.70

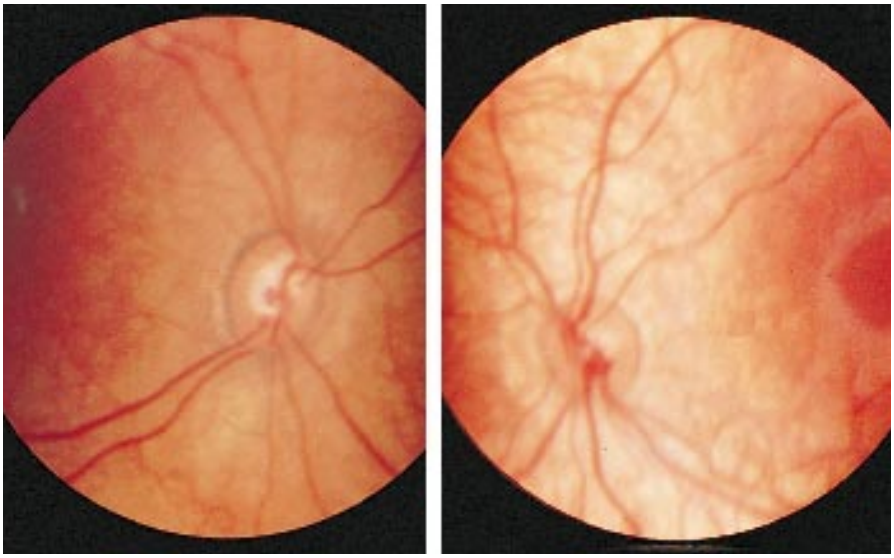

Figure 2.70. These photographs are of the optic nerves of the patient in Figure 2.69. The optic nerves reveal asymmetrical cupping, reflecting the increased intraocular pressure in the right eye (on the left) and the normal intraocular pressure in the left eye (on the right).

2.71

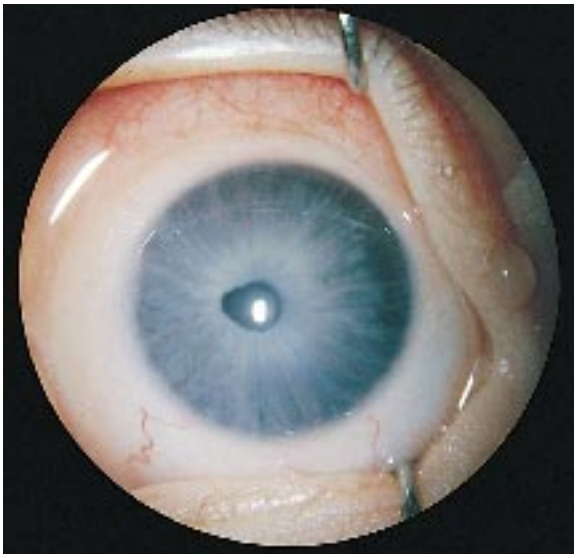

Figure 2.71. The affected eye of the same infant exhibits minimal corneal enlargement, clouding secondary to corneal edema, and ectropion uvea with displacement of the pupil temporally.

2.72

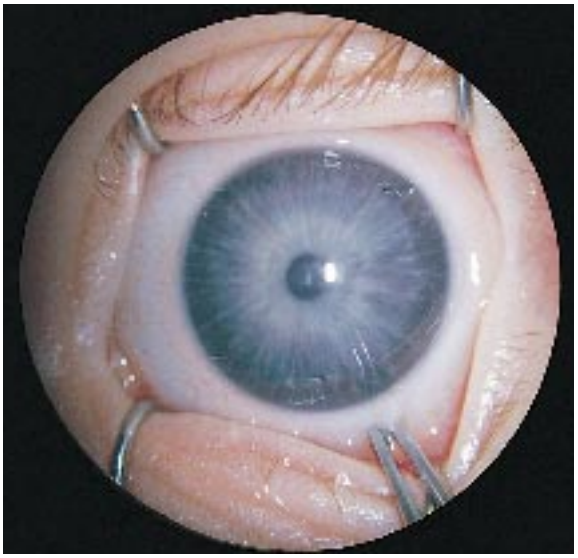

Figure 2.72. This photograph is of the unaffected eye of the same infant showing a clear cornea and central pupil. Again, the asymmetry is very important in diagnosing this glaucoma early.

2.73

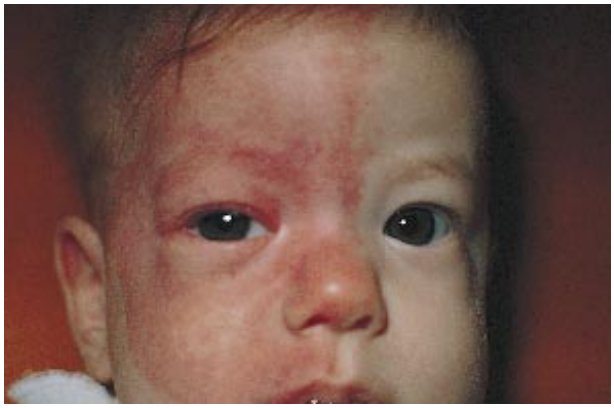

Figure 2.73. This infant has Sturge-Weber syndrome with glaucoma. The unilateral facial hemangioma is pathognomonic for Sturge-Weber syndrome, and the involvement of the upper lid and conjunctiva is associated with choroidal hemangiomas and secondary glaucoma.

2.74

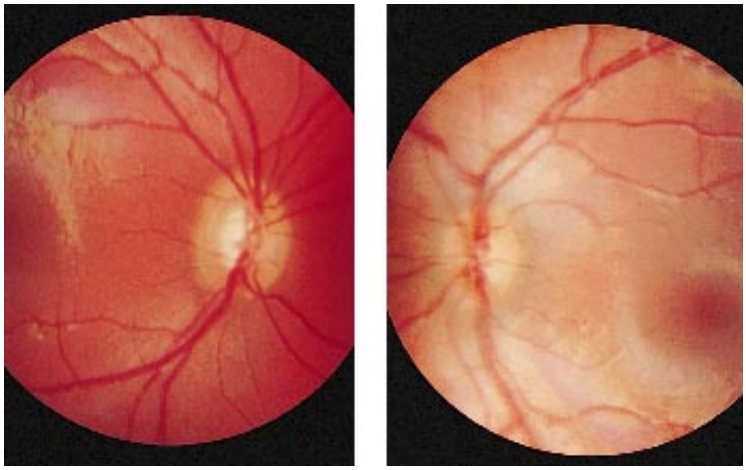

Figure 2.74. The photographs of the optic nerves in the same infant as shown in Figure 2.73 demonstrate the asymmetrical cupping reflecting the increased intraocular pressure in the right eye (on the left) and the normal intraocular pressure in the left eye (on the right).

2.75

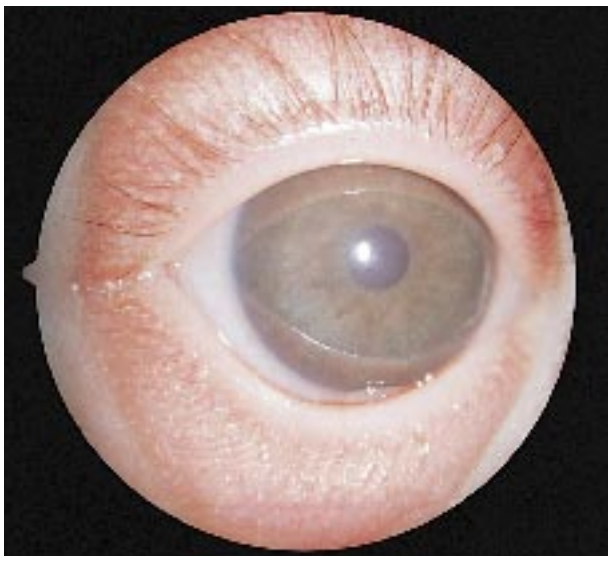

Figure 2.75. The affected eye of the same patient demonstrates minimal corneal enlargement, clouding secondary to corneal edema, and erythema of the conjunctiva reflecting the presence of a choroidal hemangioma.

2.76

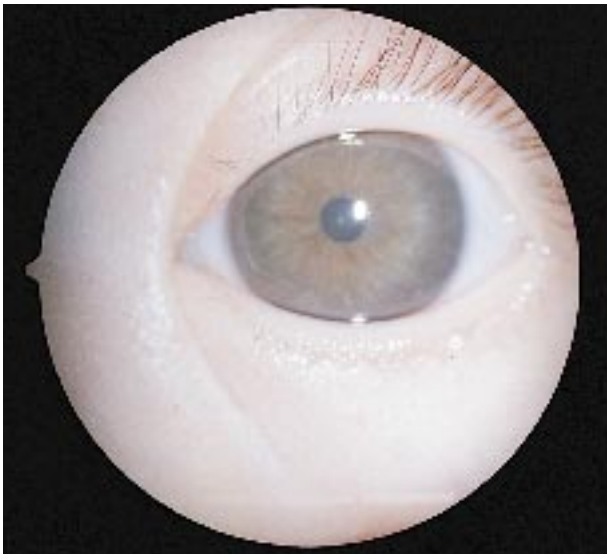

Figure 2.76. Note the clear white conjunctiva in the unaffected eye of the same infant as in Figures 2.73-2.75.

2.77

Figure 2.77. This patient demonstrates heterochromia of the irides which is occasionally seen in tuberous sclerosis, an autosomal dominant (9q33-34; 16p13) disorder. Sector iris pigmentation is also seen in tuberous sclerosis due to abnormal neural crest migration of melanocytes into the iris stroma.

2.78

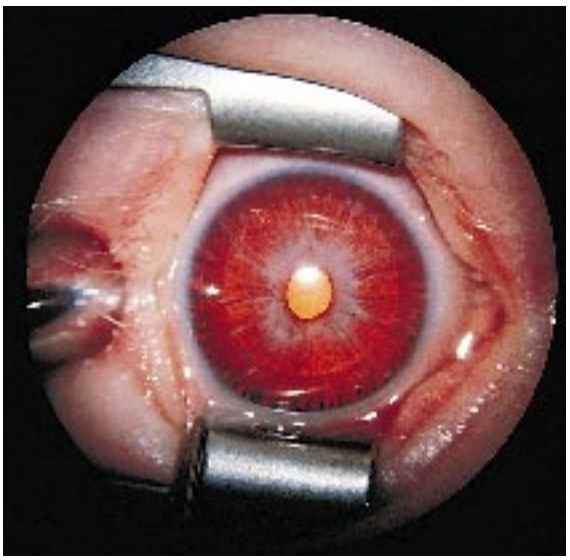

Figure 2.78. Oculocutaneous albinism is complete albinism with a lack of pigmentation in the eye and skin and is inherited as an autosomal recessive (tyrosinase deficiency; 11q14-q21) disorder. The iris pigment epithelium contains no melanin, and the iris has no color. Thus, the iris has a pink color, and the hair is totally white. This form of albinism is distinct from ocular or incomplete albinism with a partial lack of pigment in the eye and skin which is inherited as an X-linked recessive (Xp22.3) disorder. The iris pigment epithelium contains less melanin, and the iris has a light color. Thus, the iris is usually blue, and the hair is blond.

LENS

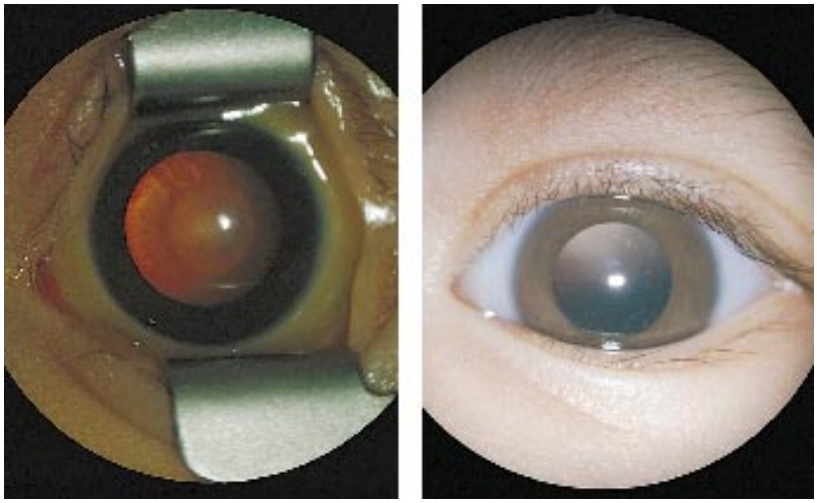

2.79

Figure 2.79. The cataract shown on the left is a classical "oil drop" cataract present at birth in an infant with galactosemia which is an autosomal recessive (galactokinase deficiency; 9p13) disorder. On the right, the same eye is shown several years later with the cataract almost completely gone after years of good dietary control.

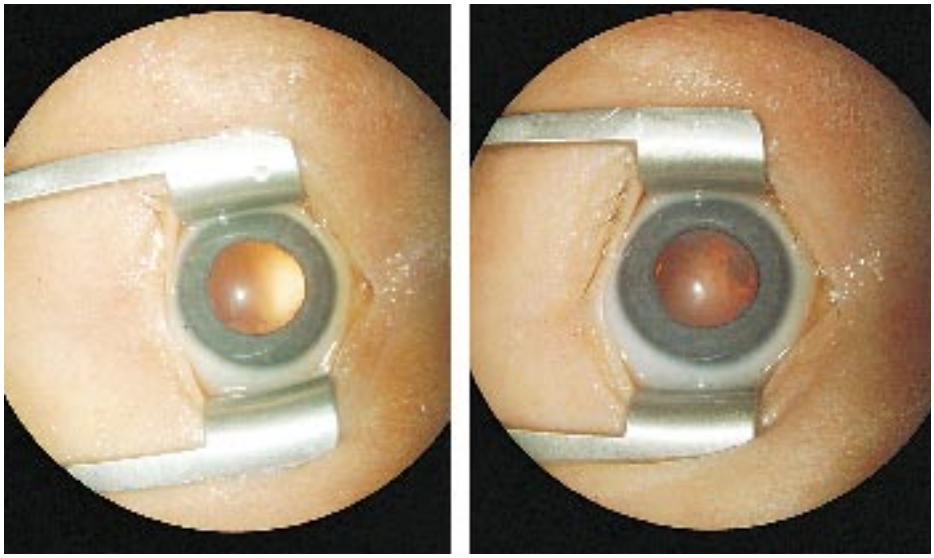

2.80

Figure 2.80. The Hallermann-Streiff syndrome is an autosomal dominant syndrome which is associated with hypotrichosis, mandibular hypoplasia, beaked nose, and endocephaly. The figure on the left demonstrates an early cataract in a child with the Hallermann-Streiff syndrome. The figure on the right is of the same eye a few weeks later showing progression to a dense cataract requiring surgery.

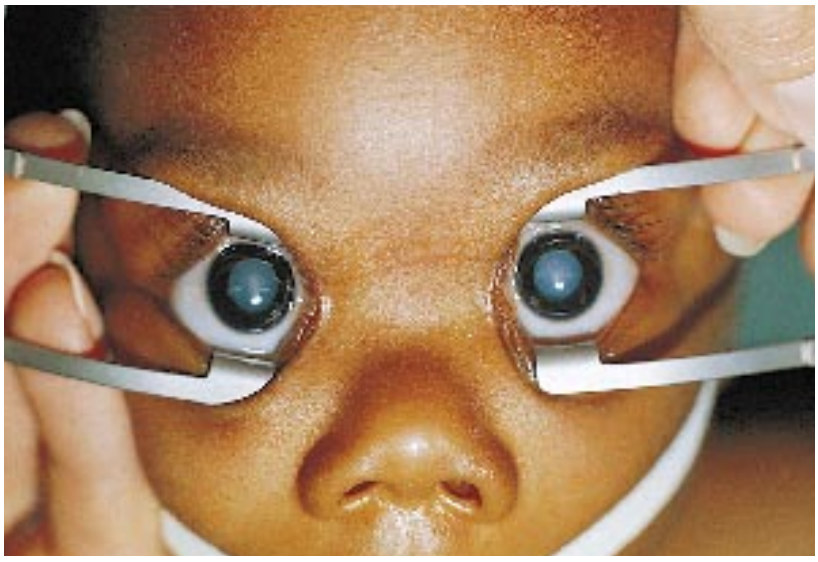

2.81

Figure 2.81. Dense bilateral cataracts represent an "ocular emergency" since immediate referral can result in normal vision (20/20) and stereoacuity. This perfect result cannot be obtained if surgery with optical correction has not been completed by the age of 6 weeks following birth.

2.82

Figure 2.82. This is the same patient shown in Figure 2.81 following bilateral removal of cataracts and immediate fitting with aphakic contact lenses. The infant developed perfect vision and binocular fusion.

2.83

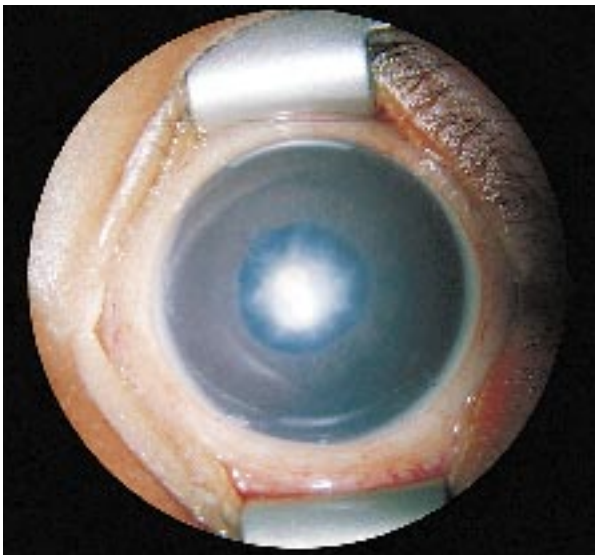

Figure 2.83. Cataracts are present in Lowe syndrome (oculocerebrorenal syndrome) which is an X-linked recessive disorder (Xq25). In this syndrome, glaucoma is also frequently present.

2.84

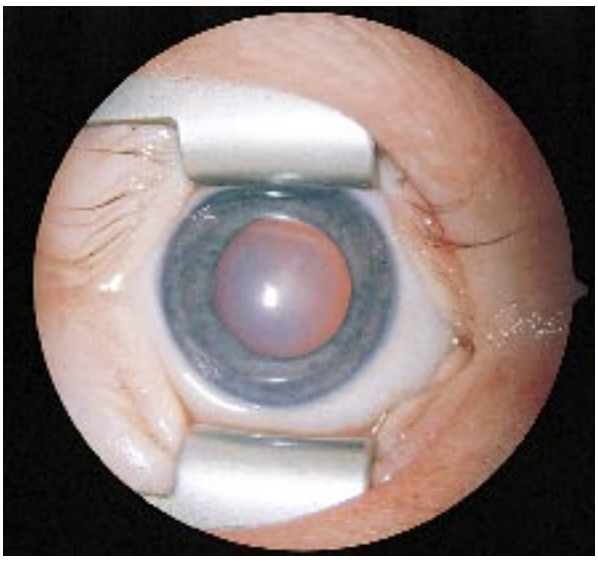

Figure 2.84. In the rhizomelic chondrodysplasia punctata syndrome, an autosomal recessive disorder, cataracts are frequently present.

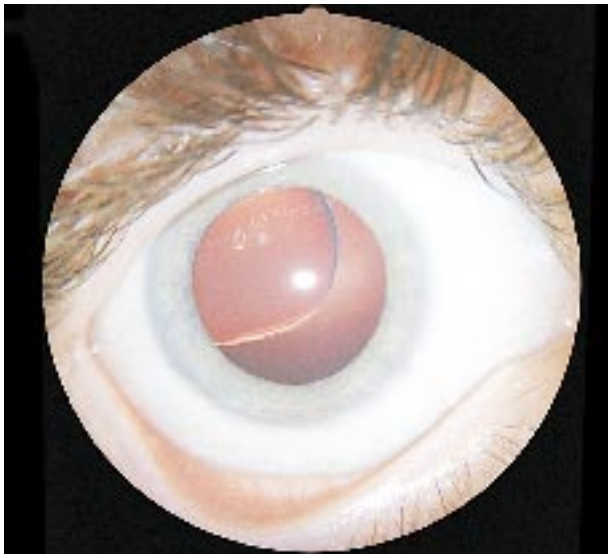

2.85

Figure 2.85. The lens is dislocated superotemporally in the infant with Marfan syndrome which is an autosomal dominant (15q15-21) disorder.

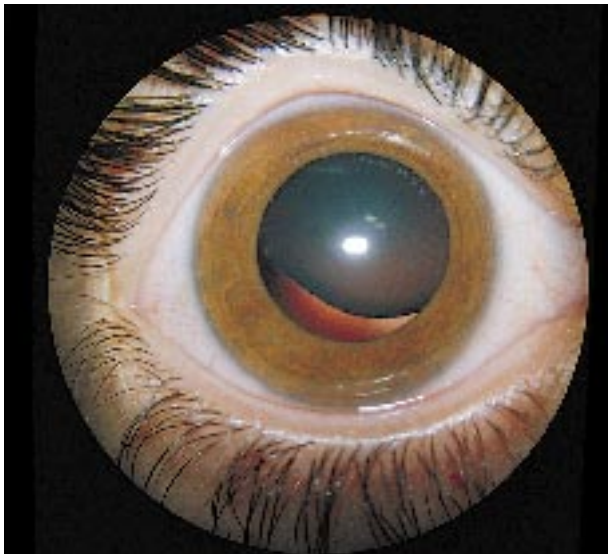

2.86

Figure 2.86. Homocystinuria is an autosomal recessive (cystathionine ß-synthetase deficiency; 21q22) disorder which is associated with lenses usually dislocated inferiorly. Patients are tall, have osteoporosis, arachnodactyly, and mental retardation.

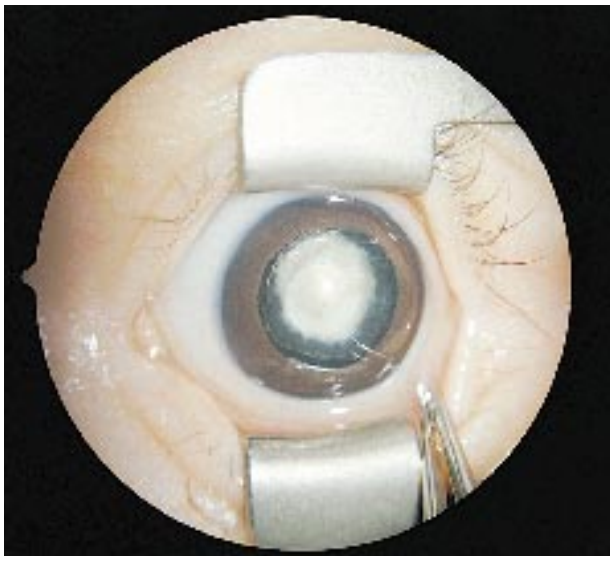

2.87

RETINA-VITREOUS

Figure 2.87. Persistent hyperplastic primary vitreous (PHPV) results from a failure of the embryonic hyaloid artery system to involute. In this eye, the persistence is primarily anterior with formation of a large cataract.

2.88

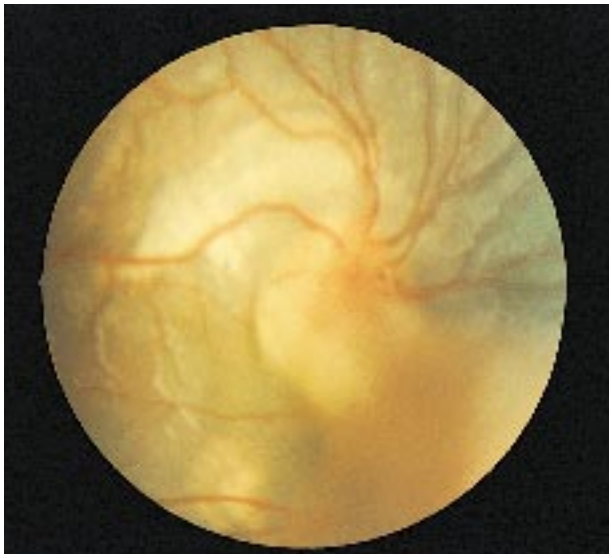

Figure 2.88. In this eye, the PHPV is primarily posterior with the presence of a large stalk to the optic nerve.

2.89

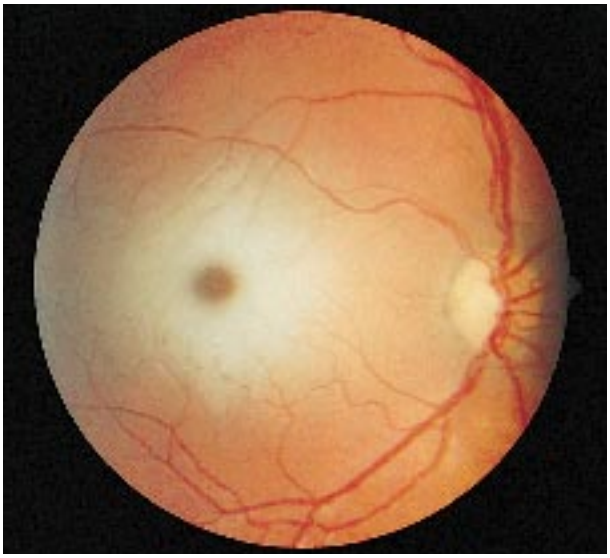

Figure 2.89. Tay-Sachs disease (GM_2 gangliosidosis Type I) is an autosomal recessive (12q22-25) disorder which develops a macular cherry-red spot due to deposition of abnormal lipid in the ganglion cell layer of the inner retina surrounding the normal macula.

2.90

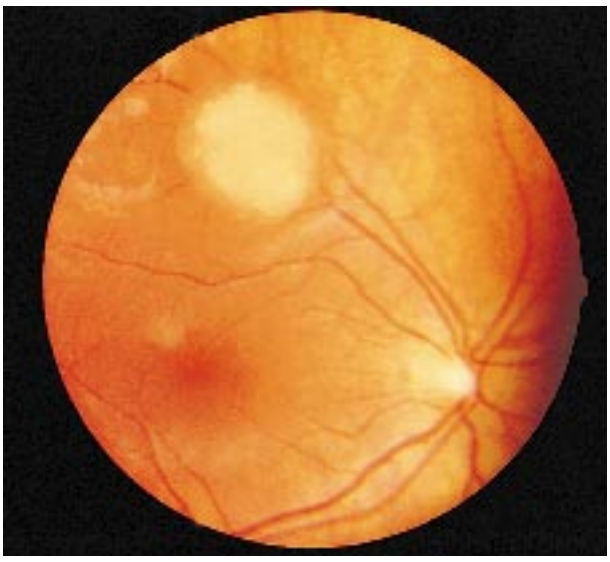

Figure 2.90. Tuberous sclerosis is an autosomal dominant (9q33-34, 16p13) disorder of neural crest origin. This figure shows a retinal astrocytic hamartoma.

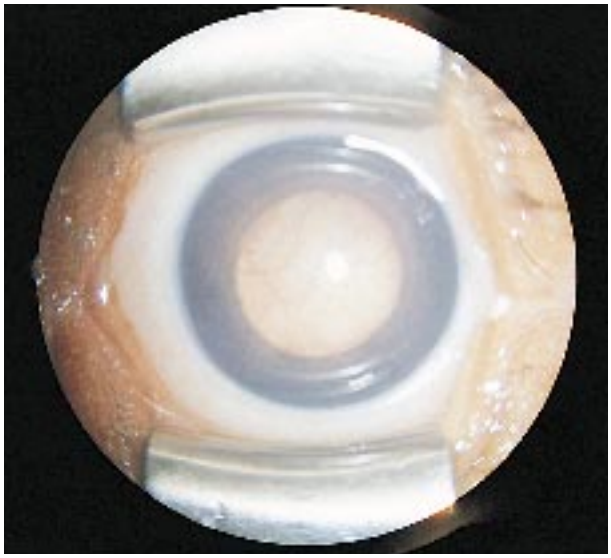

2.91

Figure 2.91. Retinoblastoma is an autosomal dominant (13q14) disorder which usually occurs without mental retardation or other systemic malformations. This is a left eye with a large tumor treated by enucleation. The differential diagnosis includes all causes of leukocoria (white pupil) including congenital cataracts, persistent hyperplastic primary vitreous, cicatricial retinopathy of prematurity, and the entities in the differential diagnosis of cicatricial retinopathy of prematurity.

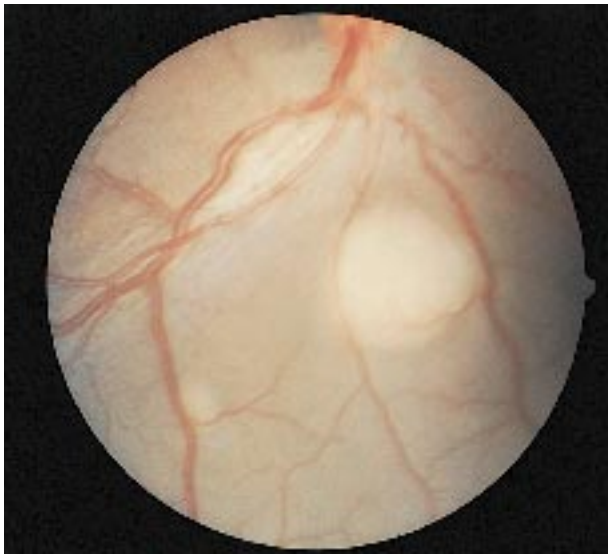

2.92

Figure 2.92. The right eye of the same patient as shown in Figure 2.91. These small tumors were treated with phototherapy.

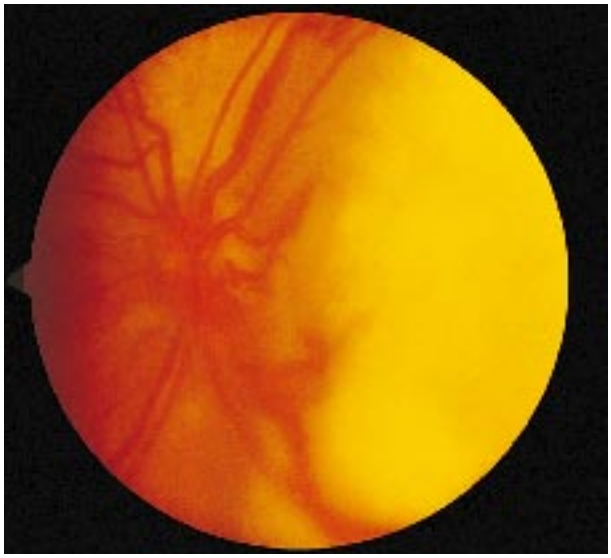

2.93

Figure 2.93. Retinoblastoma also occurs as a deletion syndrome (del 13q14) with mental retardation and other systemic malformations. This is a left eye with a large tumor treated by enucleation.

2.94

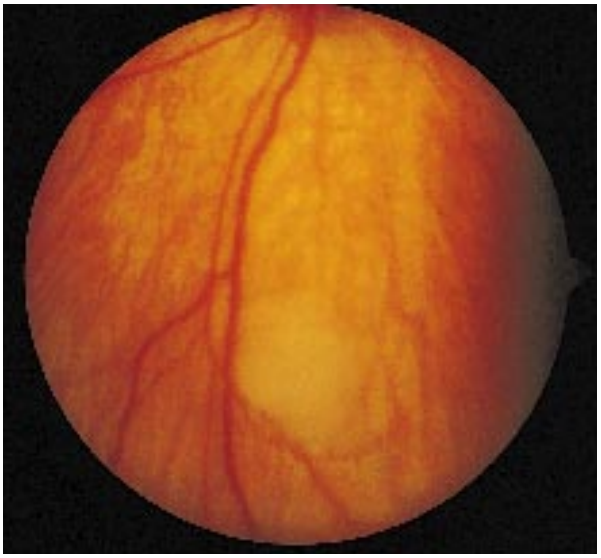

Figure 2.94. This is the right eye of the patient shown in Figure 2.93. This small tumor was treated by cryotherapy. Currently, episcleral plaque radiotherapy and carboplatin chemotherapy are used to treat small ocular tumors, especially when preservation of useful vision is possible.

RETINOPATHY OF PREMATURITY

Active Retinopathy of Prematurity

There are three parameters to the classification system known as the International Classification of Active Retinopathy of Prematurity (ICROP): location of the disease (zone), extent of the disease (clock hours), and severity of abnormal vascular response (stage). Screening for active retinopathy of prematurity should begin after 4 weeks but before 6 weeks following birth. The critical time for screening is from 32 to 42 weeks postconceptual age. Follow-up examinations vary depending on the clinical findings.

2.95

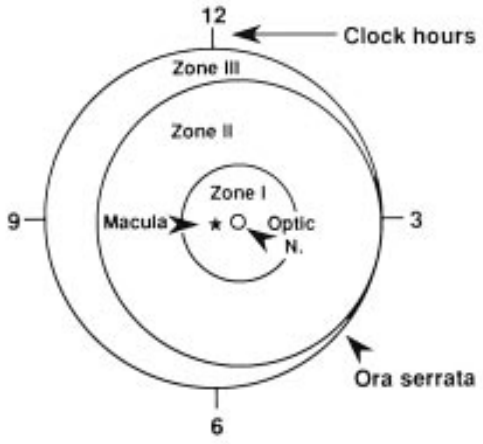

Figure 2.95. The location (zone) and extent (clock hours) of the disease must be drawn on a form similar to this.

2.96

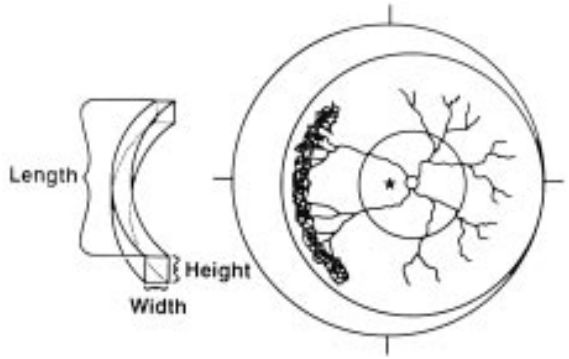

Figure 2.96. The volume (stage) of abnormal vascular response (ridge with or without extravascular fibrovascular proliferation) must be indicated for each clock hour. The location of this volume and vascular engorgement of the posterior inner retinal vessels determine when surgical intervention must be initiated.

2.97

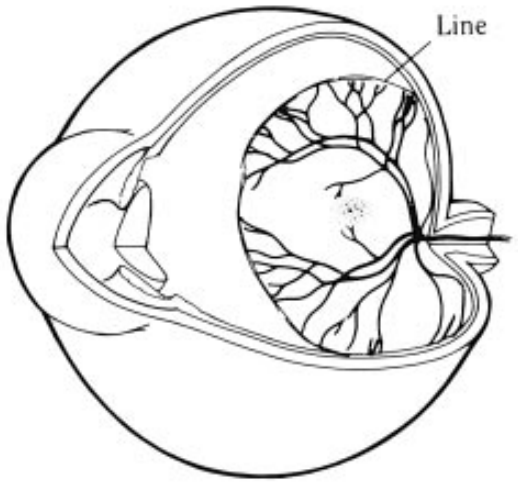

Figure 2.97. This figure depicts active retinopathy of prematurity: stage 1 (demarcation line).

2.98

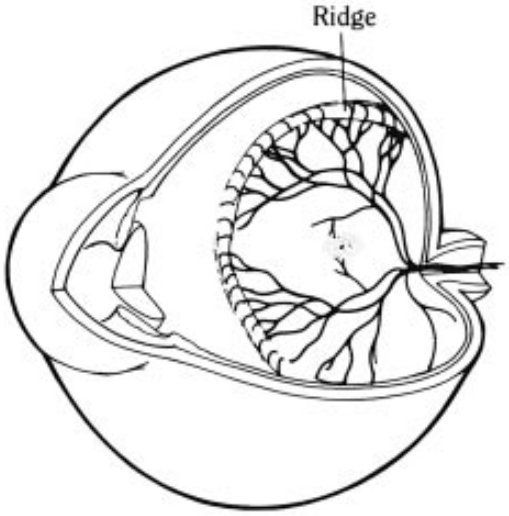

Figure 2.98. This figure depicts active retinopathy of prematurity: stage 2 (ridge).

2.99

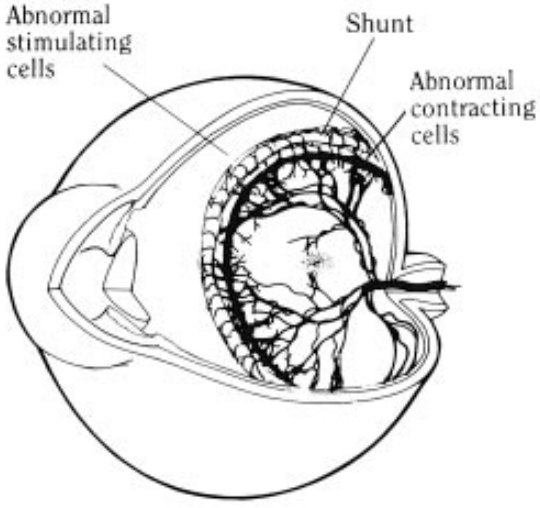

Figure 2.99. This figure depicts active retinopathy of prematurity: stage 3 (ridge with extraretinal fibrovascular proliferation).

2.100

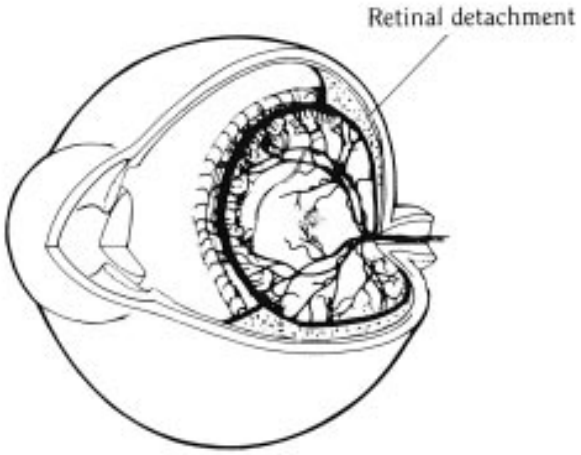

Figure 2.100. This figure depicts active retinopathy of prematurity: stage 4a (partial retinal detachment not involving the macula). More severe forms of retinal detachment (not shown) are stage 4b (partial retinal detachment involving the macula) and stage 5 (total retinal detachment).

2.101

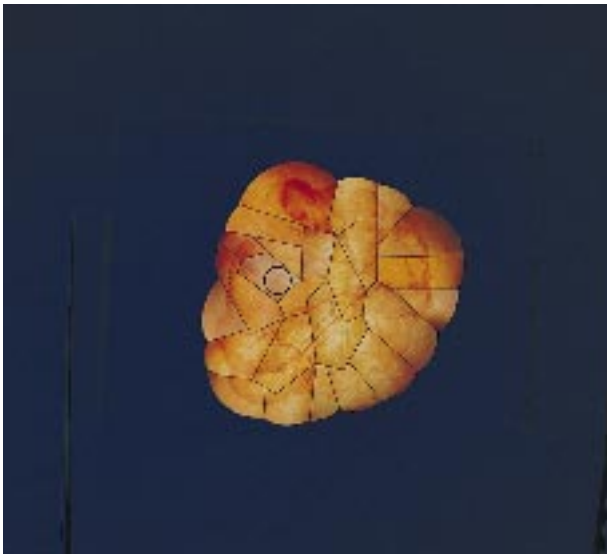

Figure 2.101. In this retinal montage there is zone I retinopathy of prematurity (stage 3 with plus disease). The same magnification is used in all four of the ROP montages.

2.102

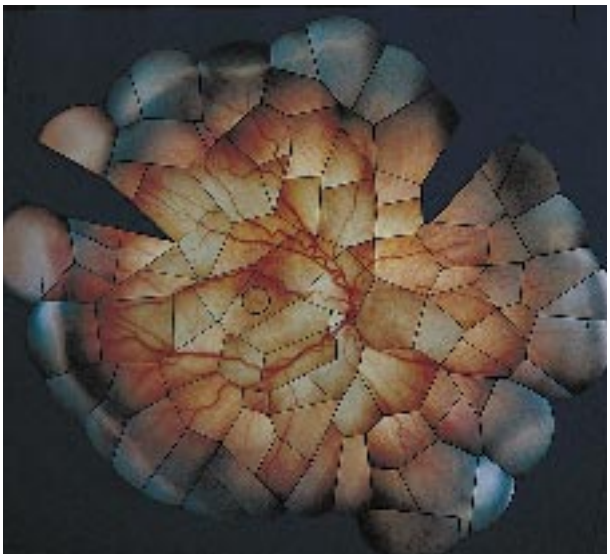

Figure 2.102. A retinal montage which shows zone II retinopathy of prematurity (stage 4a with plus disease).

2.103

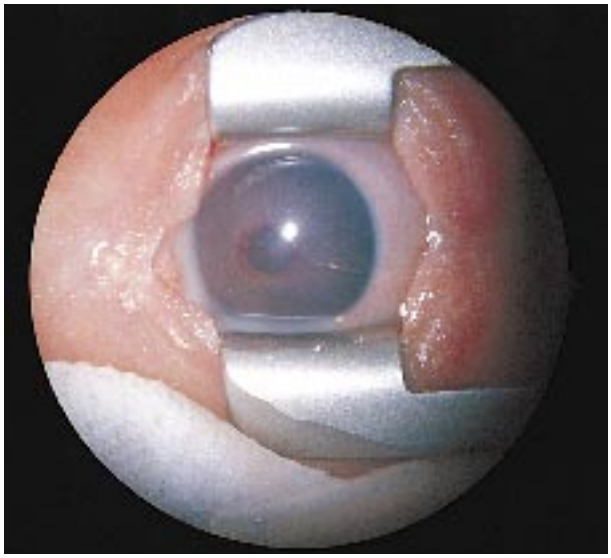

Figure 2.103. In this photograph note the vessels of the iris collarette which are engorged, making dilatation of the pupil difficult.

2.104

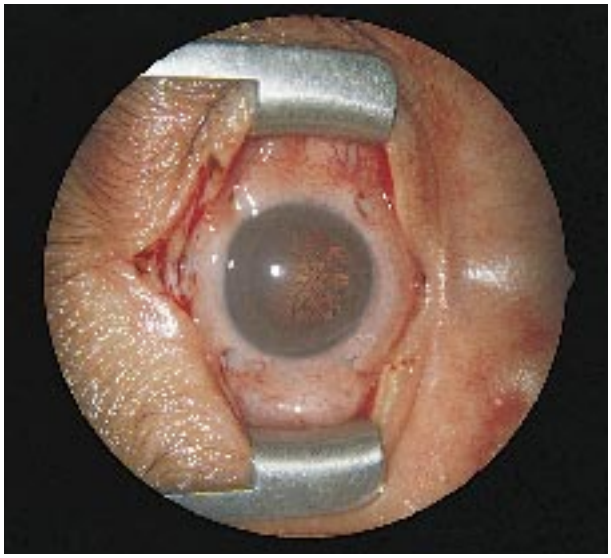

Figure 2.104. A persistent and engorged tunica vasculosa lentis occurs in those infants who are very immature and develop severe active retinopathy of prematurity.

Cicatricial (Spontaneous Regression) Retinopathy of Prematurity

The anatomical macular outcome which correlates with final visual acuity is measured by two parameters: macular ectopia and vessel traction.

2.105

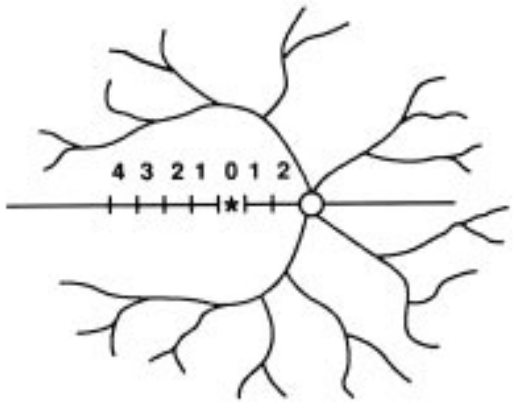

Figure 2.105. This is the grading system for macular ectopia. The normal macular position is between 2 and 3 disc diameters from the temporal margin of the optic disc. The numbering system is shown.

2.106

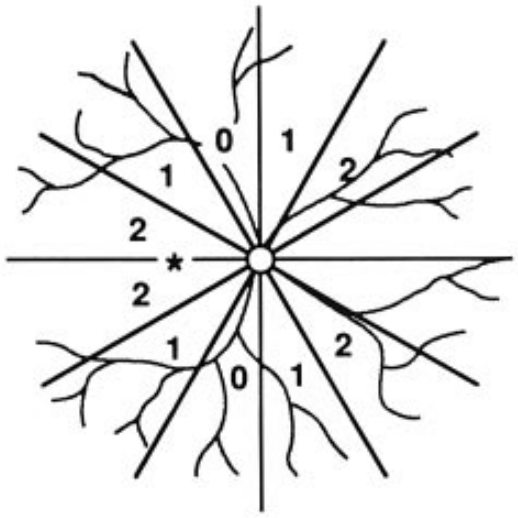

Figure 2.106. In the grading system for vessel traction, the normal position of retinal vessels for the first two disc diameters is between the vertical meridian and the 30 sectors temporal to the vertical meridian. The numbering system is shown.

2.107

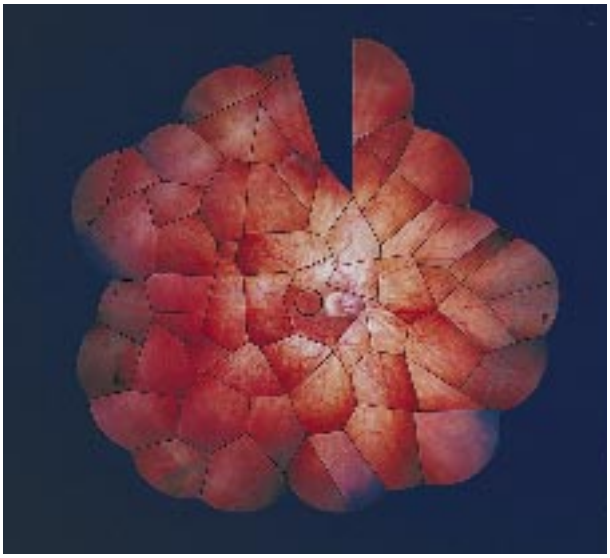

Figure 2.107. This retinal montage shows nasal dragging of the macula with macular ectopia of 2 and vessel traction of 1. Vision is 20/400.

2.108

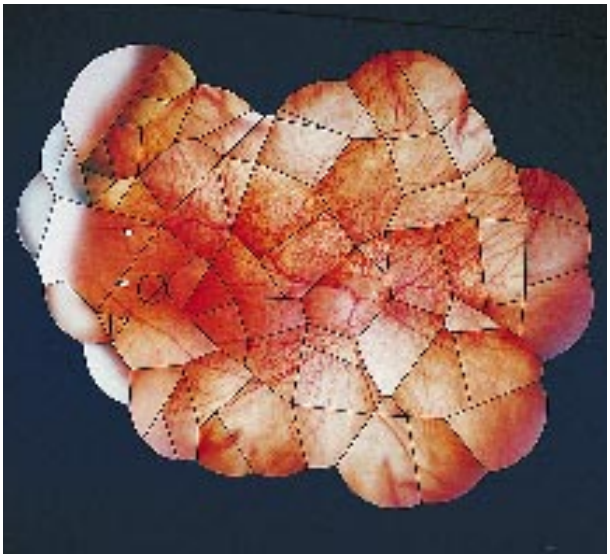

Figure 2.108. In this retinal montage note the temporal dragging of the macula with macular ectopia of 4 and vessel traction of 2. Vision is 20/400.

2.109

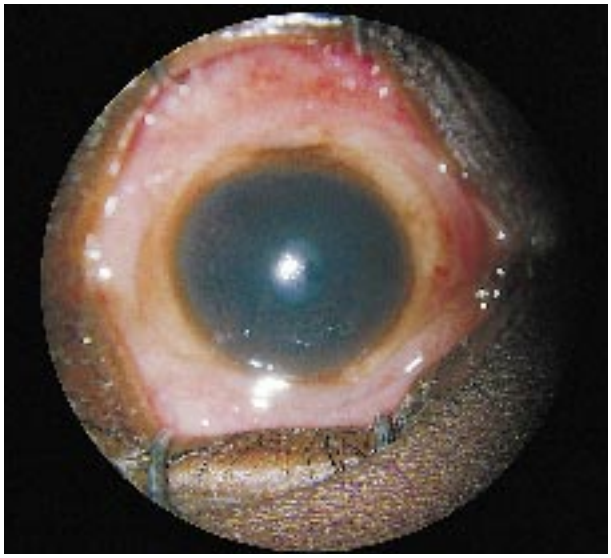

Figure 2.109. An angle closure glaucoma is a common complication of very severe ROP. Conjuctival erythema, corneal clouding, a nondilatable pupil, and a flat anterior chamber are present.

2.110

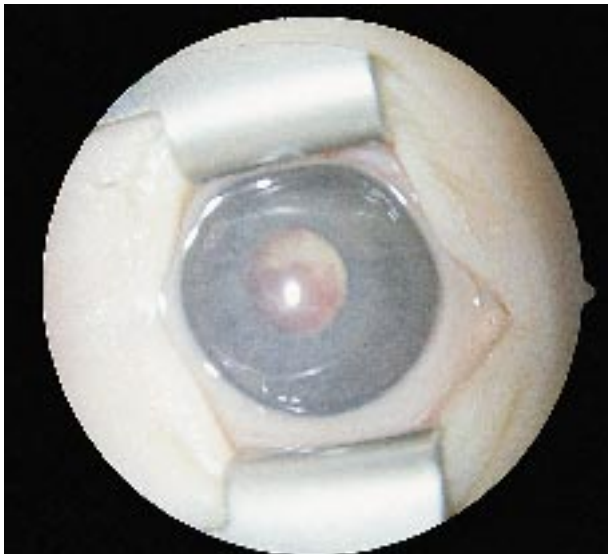

Figure 2.110. In complete retinal detachment there is a fibrovascular mass behind the lens which provided the original name for retinopathy of prematurity: "RLF" or retrolental (behind the lens) fibroplasia (fibrovascular mass).

Differential Diagnosis for Retinopathy of Prematurity

A. Abnormal neuroectodermal migration or differentiation of the retina (from inner to outer layers) can be associated with abnormal migration or differentiation of the central nervous system as in the following examples.

2.111

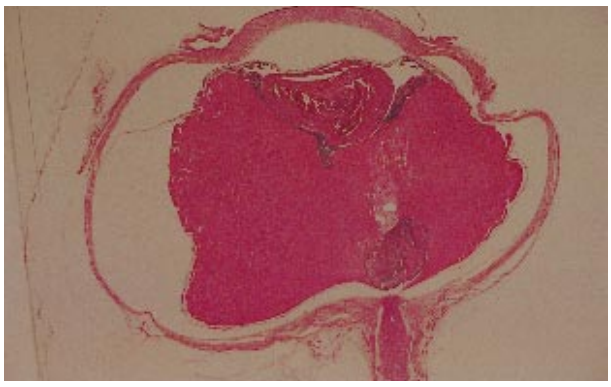

Figure 2.111. Walker-Warburg syndrome is an autosomal recessive disorder with absence of the normal cascade of retinal differentiation reflected in abnormal development of all retinal layers. Remnant retina is "retrolental" (behind the lens) and lissencephaly is present in the central nervous system.

2.112

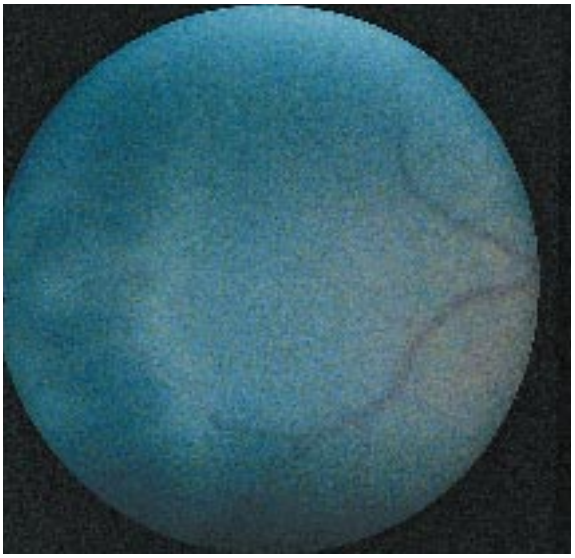

Figure 2.112. The Dandy-Walker deformity with a posterior encephalocele is another autosomal recessive disorder which demonstrates the absence of the normal cascade of retinal differentiation in the retinal periphery.

2.113

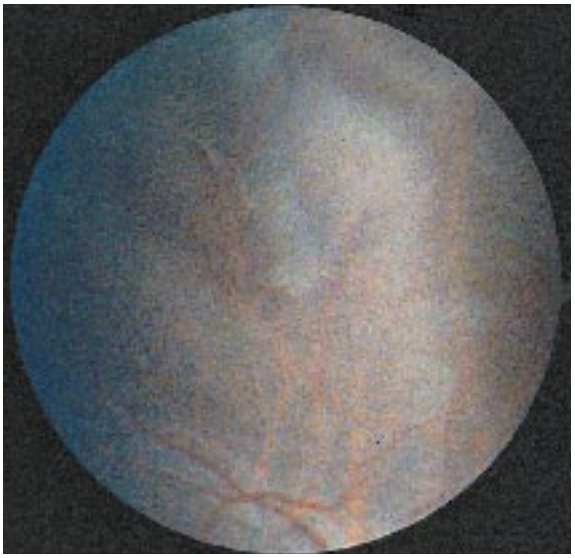

Figure 2.113. Stickler syndrome is an autosomal dominant (12q13) disorder which may be diagnosed in the newborn period by recognizing the association between the Robin's anomalad of cleft palate, small mandible, and backward displacement of the tongue. A progressive arthropathy can be identified radiographically. The Kniest syndrome may be an autosomal recessive disorder of the same gene. Abnormal thinning of the peripheral retina which precedes giant retinal tears is seen in these retinas.

2.114

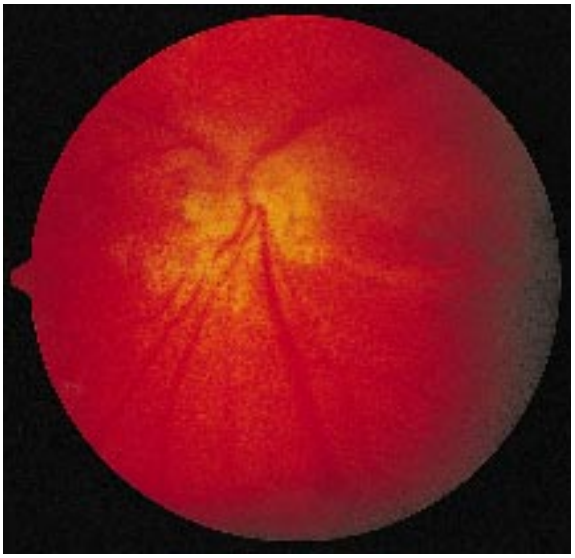

Figure 2.114. Juvenile retinoschisis is an X-linked recessive (Xp22) disorder which can present with peripheral and/or foveal involvement. Clinically this is seen as vitreous veils and strands with retinal detachment peripherally and/or a star-shaped or spoke-like configuration in the fovea. Splitting of the nerve fiber layer in the inner retina is present pathologically.

2.115

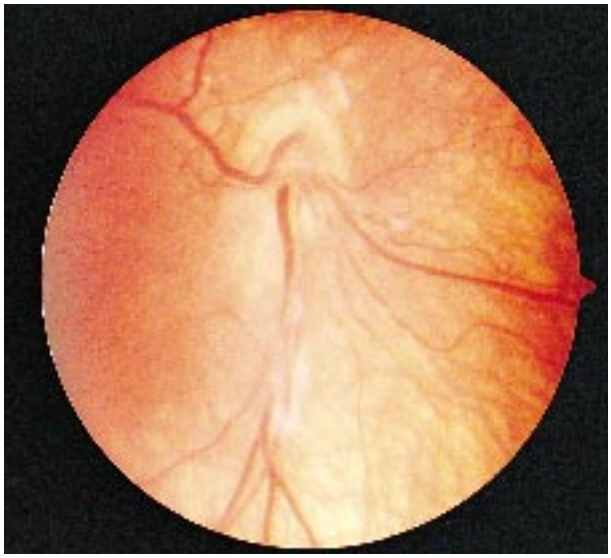

Figure 2.115. Incontinentia pigmenti is an X-linked dominant (Xq27-28) disorder (i.e., limited to females). There is abnormal melanin within the retinal pigment epithelium and abnormal vascularization of the peripheral retina. Skin, skeletal and central nervous systems are also affected in this disorder.

B. Abnormal formation of inner retinal vessels can occur due to genetic abnormality and can be associated with abnormal vascularization of other organ systems as in the following examples.

2.116

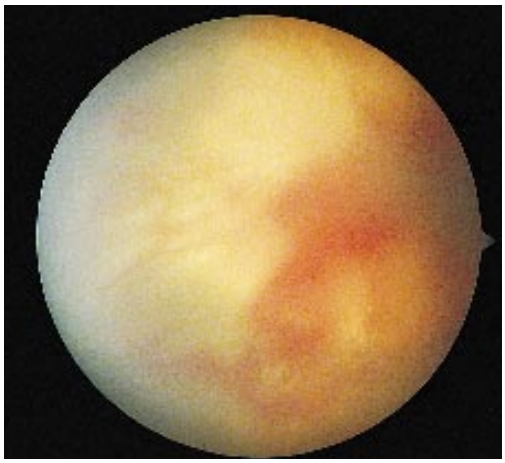

Figure 2.116. Norrie syndrome is an X-linked recessive (Xp11.3) disorder which has been classically described as congenital blindness in all patients with a dysplastic retina histologically. Hearing loss and mental retardation have been associated progressive findings. Currently, this classic definition has been revised to include other phenotypes of the Norrie disease gene.

2.117

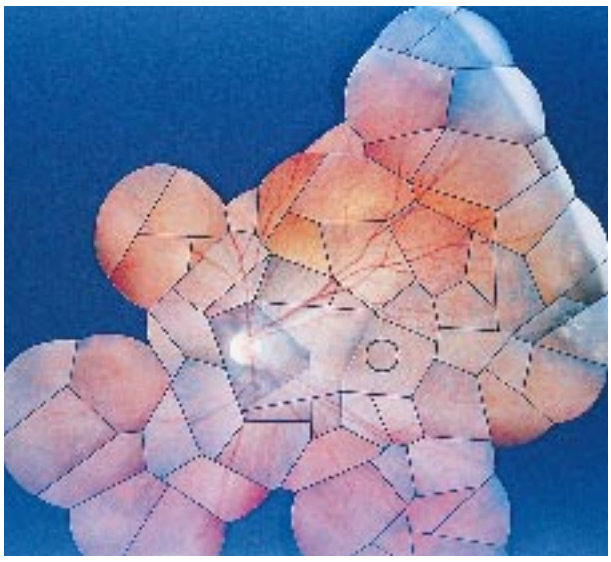

Figure 2.117. Exudative vitreoretinopathy can be a phenotype of the Norrie disease gene (Xp11.3) in term infants with ocular involvement only. Clinically, there is a progressive peripheral retinal neovascularization resembling cicatricial Grade II to IV RLF with macular ectopia as shown in this montage. An autosomal dominant (11q13) exudative vitreoretinopathy may be clinically indistinguishable.

2.118

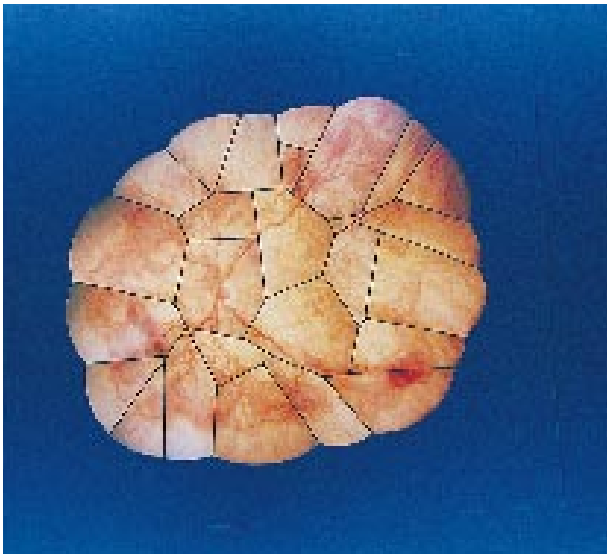

Figure 2.118. Preterm infants can present with a phenotype of the Norrie disease gene that involves all of the systems vascularized by the dorsal embryonic aortic arches (aorta, thymus, ear, brain, and eye). Clinically, there is an acute peripheral retinal neovascularization resembling active Stage III ROP as shown in this montage.

C. Abnormal formation of inner retinal vessels can occur in response to an intrauterine insult and can be associated with gross CNS changes as in the following examples.

2.119

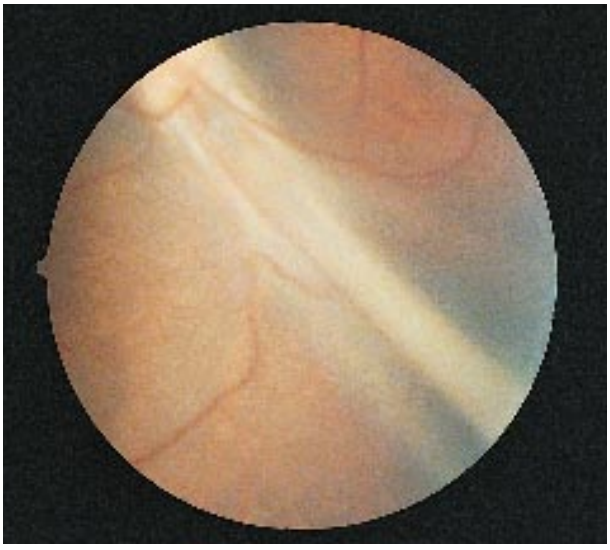

Figure 2.119. The retina of an Asian infant who presented with an anterior encephalocele. Anterior encephaloceles and this retinal picture are more common in Asians and Africans because of their thin ethmoidal structures.

2.120

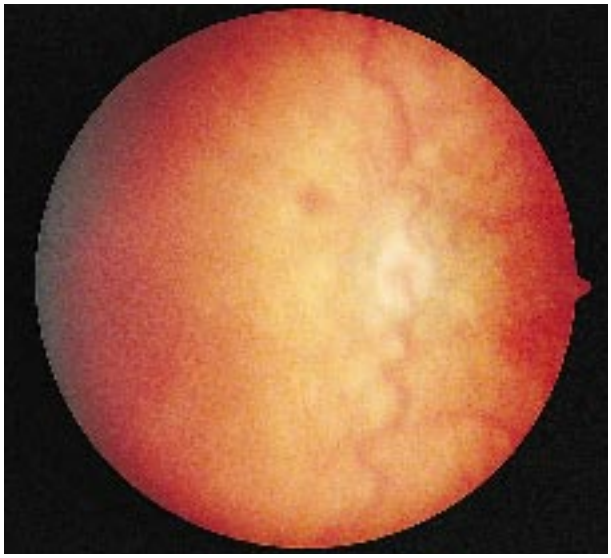

Figure 2.120. This is the retina of an infant who suffered an intrauterine infarction of both middle cerebral arteries. Similar intrauterine stresses can be associated with retinal pictures virtually indistinguishable from ROP.

OPTIC NERVE

2.121

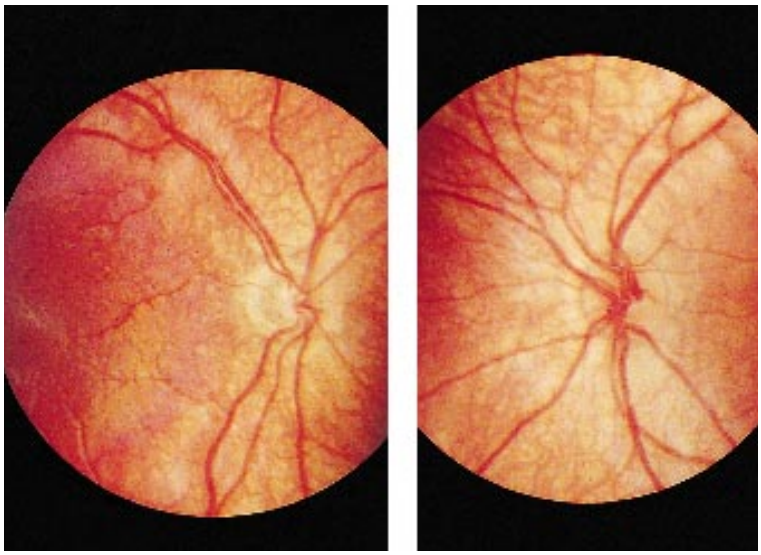

Figure 2.121. Note the hypoplastic optic nerve on the left and a normal optic nerve in the fellow eye on the right. Optic nerve hypoplasia may occur unilaterally or bilaterally, both sporadically, as part of de Mosier syndrome with absence of corpus callosum, and as part of autosomal recessive optic nerve hypoplasia. It may be necessary to evaluate the endocrine status of the infant (growth hormone and thyroid hormone are most commonly decreased).

2.122

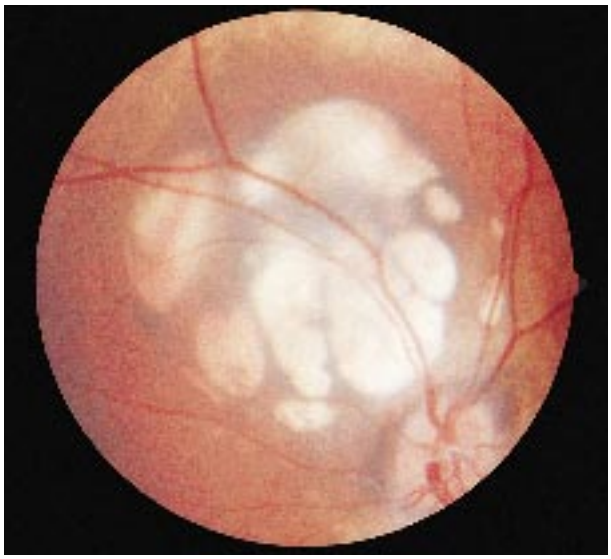

Figure 2.122. Aicardi's syndrome presents with characteristic chorioretinal "lacunar" lesions. The syndrome is an X-linked dominant (Xp22) disorder (limited to females). Optic nerve colobomas can occur. The CT scan shows agenesis of the corpus callosum and affected patients have severe mental retardation and infantile massive spasms.

2.123

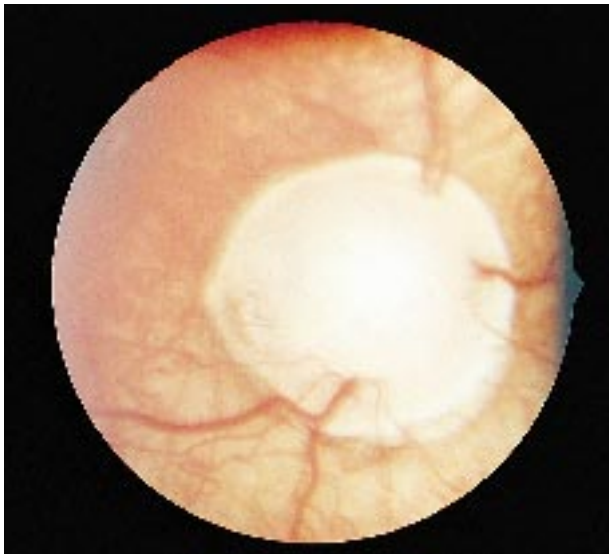

Figure 2.123. Optic nerve coloboma (without microphthalmia) may occur as an autosomal dominant or sporadically. It is appropriate to examine other family members, especially any with a history of "glaucoma," because of variable expressivity.

2.124

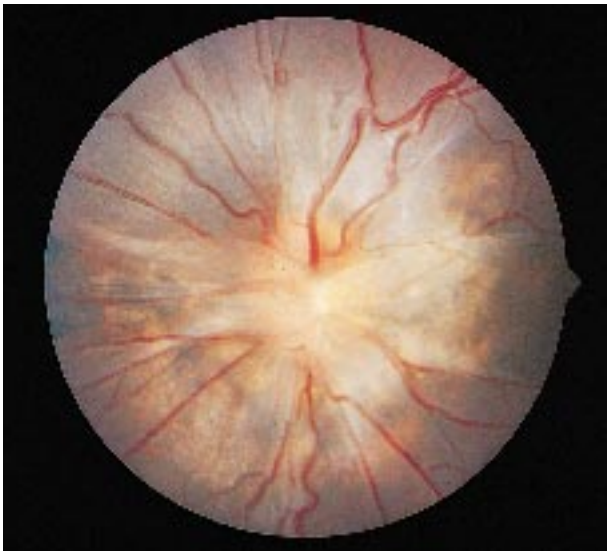

Figure 2.124. Morning glory optic nerve anomaly is characterized by an enlarged and excavated disc. Note the symmetry of the fundus excavation with respect to the disc which suggests an anomalous funnel-shaped enlargement of the distal optic stalk at its junction with the primitive optic vesicle as the primary embryological defect. Vision is always poor and there may be associated defects such as the transsphenoidal form of basal encephalocele.

Chapter 3
The Central Nervous System

Central nervous system disorders are among the three major causes of mortality in neonates. All of the conditions that affect the infant's brain do so in part because this system is developing at a rapid rate. The neurologic examination of the newborn must thus be interpreted in the context of the child's brain maturation (gestational age) and level of alertness. The examination should be brief so as to avoid hypoxemia and fluctuations in arterial blood pressure. Head circumference is a useful measure of intracranial volume, and longitudinal measurements in particular provide important information. Observation of movement and symmetry can contribute significantly to the evaluation while minimizing the effects of handling, especially in the sick neonate. These observations should include any available assessment of the fetus in the intrauterine environment. Examination of the following cranial nerves is possible: 1 (olfaction); 2 (optic fundi); 3 (pupils); 3, 4, 6 (extraarticular movements, facial sensation and masticatory power); 7 (facial motility); 5, 7, 9, 10, 12 (sucking and swallowing); 11 (sternocleidomastoid function); and 12 (tongue function). Reliable assessment of cranial nerves 2 (vision) and 8 (audition) may require testing of auditory or visual evoked responses. Motor examination should include an assessment of tone and posture, motility and strength, and tendon and plantar reflexes. Primary neonatal reflexes including Moro's reflex, palmar grasp, and tonic neck response should also be considered. Although a sensory examination is possible, it is usually very limited and can be noxious. Because of the limitations of the neurologic exam and the complex support required by the sick neonate, frequently additional, usually non-invasive, neurodiagnostics will be required. These can include brain imaging (ultrasonography, computed tomography, magnetic resonance imaging, brain scan), neurophysiologic techniques (electroencephalogram, nerve conduction, electromyography), and cerebrospinal fluid examination.

3.1

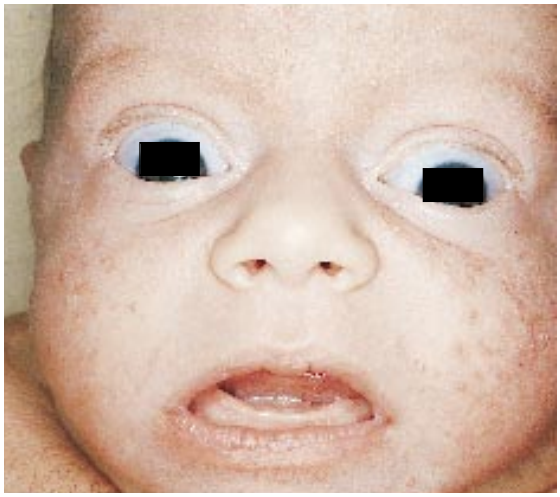

Figure 3.1. "Setting sun" sign in a normal newborn infant. The setting sun sign means that conjugate upward deviation is decreased. The upper eyelids are retracted and the irides are partly covered by the lower eyelid giving the appearance of a sunset. This is rarely observed as an isolated finding in an otherwise normal newborn infant. It may be normal if it is transient, but if it persists, it must be investigated. Note associated neonatal acne in this infant.

3.2

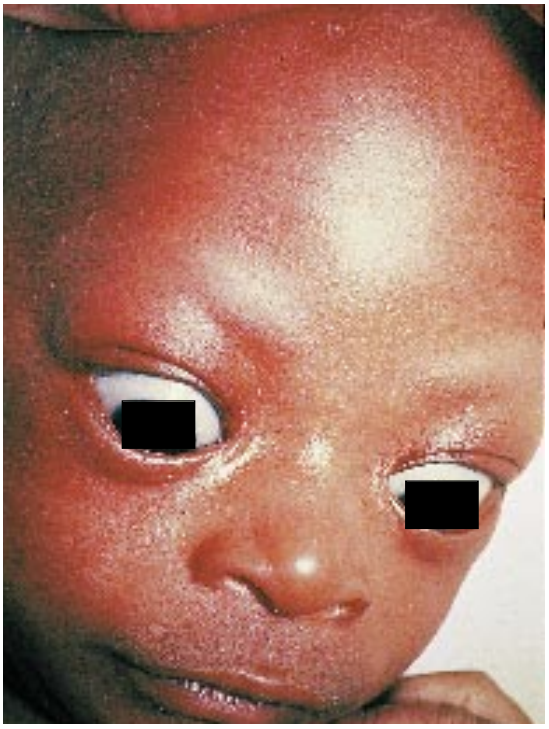

Figure 3.2. Persistent "setting sun" sign in an abnormal newborn infant. The setting sun sign is usually due to a lesion in the region of the quadrigeminal plate of the midbrain and signifies increased intracranial pressure. Increased intracranial pressure may result from hydrocephalus or subdural hematoma. It can occur in parenchymal or midbrain lesions, especially kernicterus.

3.3

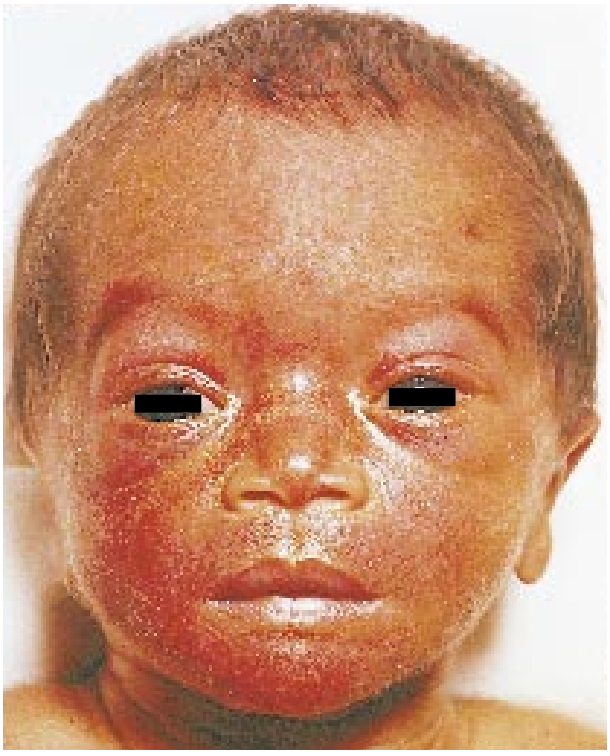

Figure 3.3. This premature infant with wide open eyes and a hyperalert expression continued to have an increased state of arousal, which is abnormal in the first hours of life. CT scan demonstrated a tentorial tear with hemorrhage. Hyperalert states may be the result of intracranial pathology or may be related to maternal drug ingestion. Infants with severe intracranial irritation may also have an anxious expression and furrowed brows.

3.4

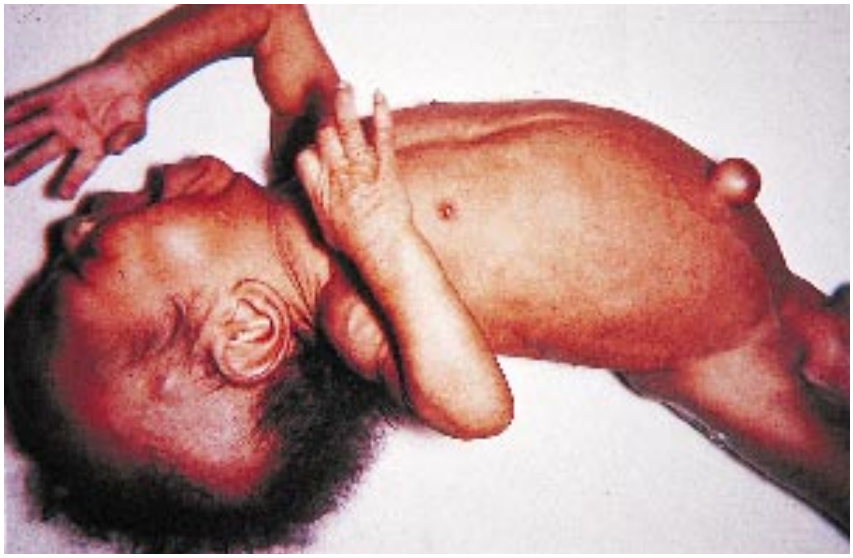

Figure 3.4. Opisthotonic posturing in an infant with congenital rubella encephalitis. Severe cortical irritation or damage may produce marked hypertonicity of the spinal muscles. The neck is hyperextended and the spine is arched. Note the flexed arms, fisted hands, and extended legs. Contractures may occur if the child remains in an opisthotonic posture.

3.5

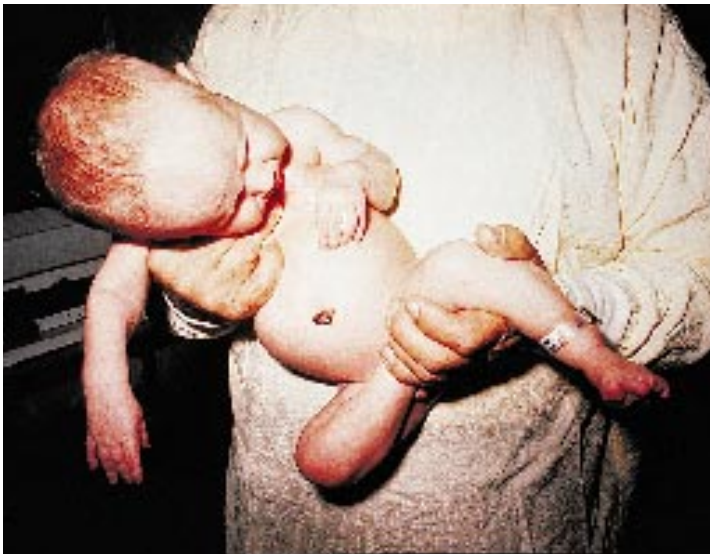

Figure 3.5. Marked hypotonia in a term infant with Lowe syndrome. Note that the infant hangs limply when supported in a prone position.

3.6

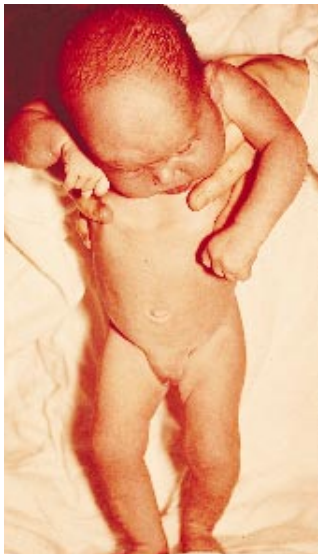

Figure 3.6. Extreme hypotonia in a term infant who appears to slip through the hands of her examiner when held upright under the arms. Most term newborns can maintain the head in the same plane as the trunk when lifted by the arms or ventrally suspended. Extreme head lag is a sign of hypotonia that can be seen in infants with Down syndrome, prematurity, or brain damage.

3.7

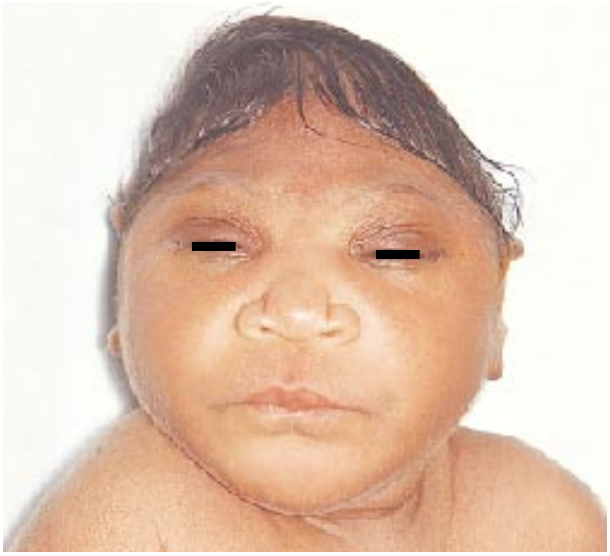

Figure 3.7. Microcephaly in a term infant with congenital rubella. Microcephaly may be idiopathic or acquired as a result of intracranial pathology. It may also result from serious perinatal brain injury in which case the FOC (fronto-occipital circumference) may be normal at birth, but then fail to increase as the brain fails to grow after birth. Severe physical and mental retardation may follow. This infant had an FOC of 30 cm and closed fontanelles.

3.8

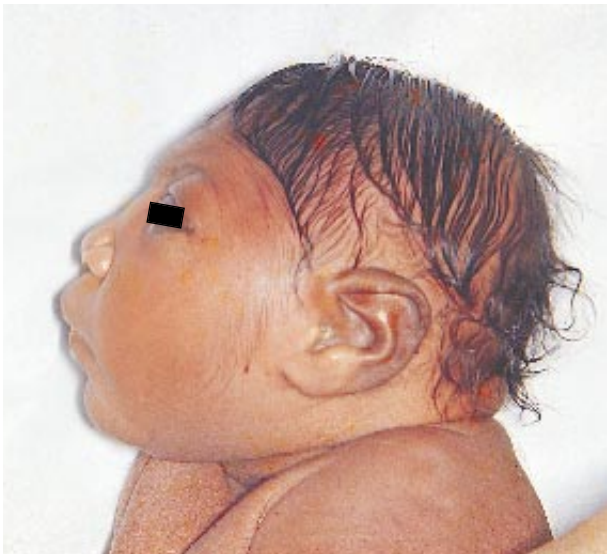

Figure 3.8. Lateral view of the same infant with microcephaly. Microcephaly occurs with intrauterine infections (rubella, cytomegalovirus, toxoplasmosis), chromosomal abnormalities (cri du chat syndrome, trisomy 13), and toxic drug effects (fetal alcohol syndrome, fetal aminopterin syndrome).

3.9

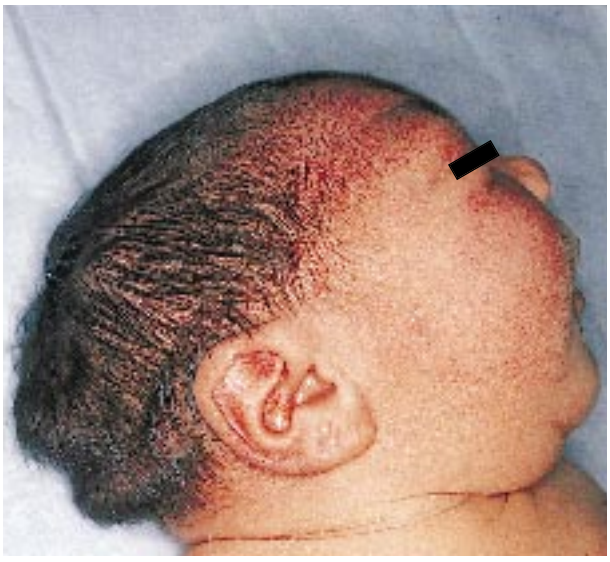

Figure 3.9. Infant with severe microcephaly of unknown etiology. One must consider heredity, infection, or irradiation.

3.10

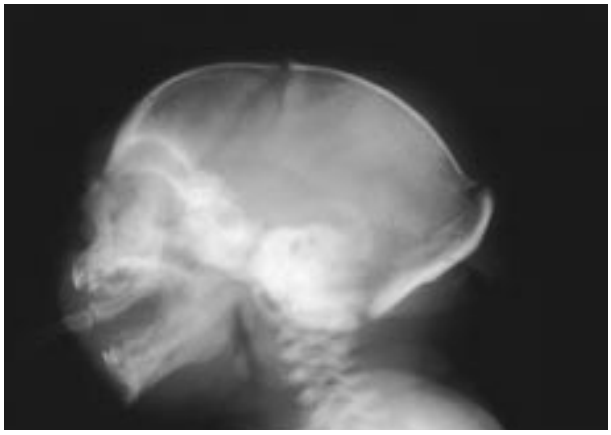

Figure 3.10. Lateral skull radiograph of the same infant. Note the severe microcephaly. The normal ratio of cranial vault to bony facial structures is 4:1.

3.11

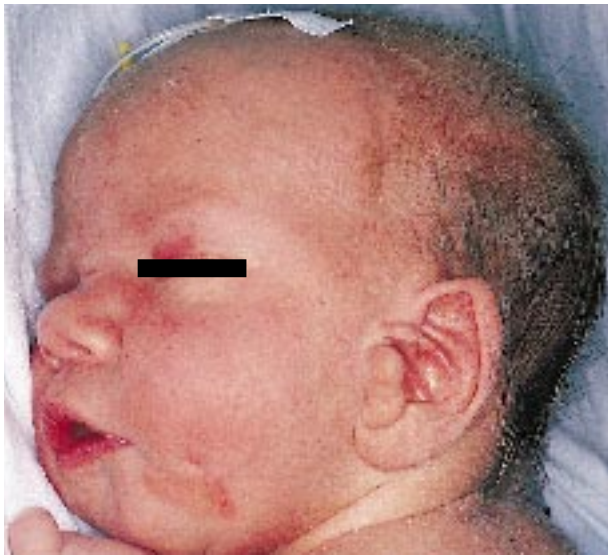

Figure 3.11. Macrocephalic head with a fronto-occipital circumference of 39 cm in a hypotonic infant with a left cheek skin pit, ear tags, and Goldenhar's syndrome. This infant had an increased head circumference at birth, a fontanelle of normal size, and cranial sutures that are not widened. The face appears relatively normal in size.

3.12

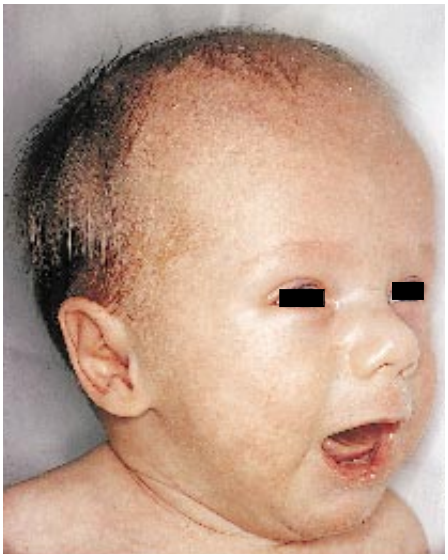

Figure 3.12. This term infant had macrocephaly, a prominent brow, and distended scalp veins. Transillumination was positive with the lack of underlying brain tissue being consistent with hydranencephaly.

3.13

Figure 3.13. Transillumination of the head of the same infant with hydranencephaly shown in Figure 3.12. This results from failure of the development of the cerebrum with resulting gross dilatation of the ventricles. Note the "jack-o-lantern" appearance of the eyes and an area of opacity in the transilluminated head. Infants with hydranencephaly may have isolated nubbins of brain tissue. This condition has an extremely poor prognosis.

3.14

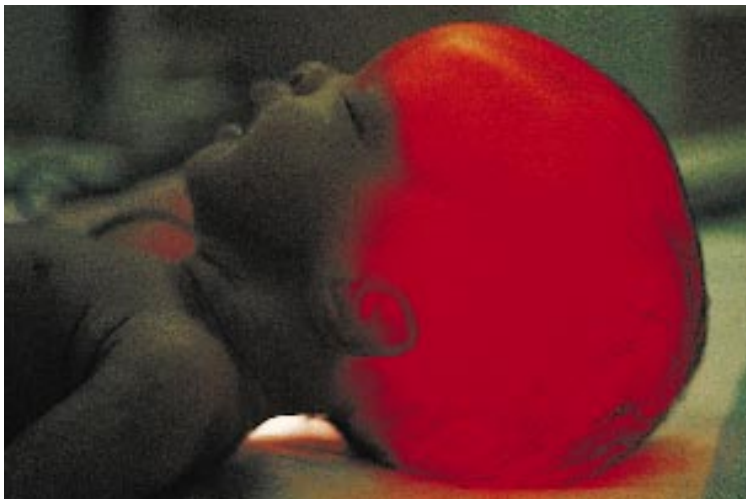

Figure 3.14. Transillumination of the lateral view of the head of another infant with hydranencephaly. Note the large head size compared with that of the face. Typically infants with hydranencephaly present with heads that are macrocephalic. Infants with hydrocephalus will also have transillumination of the skull, but this would become readily apparent only if there was massive enlargement of the head.

3.15

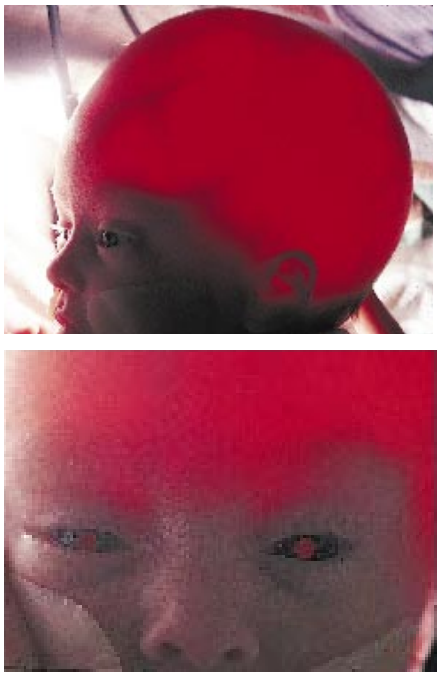

Figure 3.15. Lateral and anterior-posterior views of the head of an infant with hydranencephaly. Note the large head, some prominence of scalp veins, the "jack-o-lantern" appearance of the eyes, and the total lack of brain tissue.

3.16

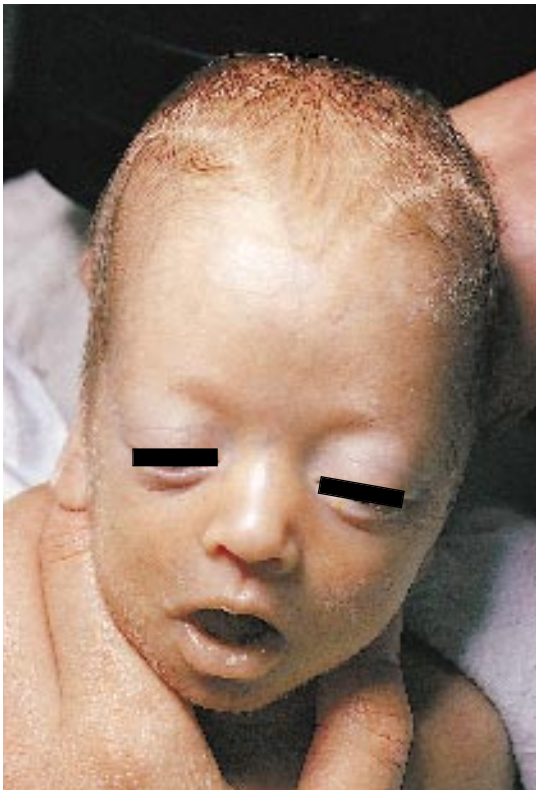

Figure 3.16. Clinical appearance of an infant with hydranencephaly. Note the prominent scalp veins and brow. There is macrocephaly and a large open anterior fontanelle associated with poor mineralization of the skull.

3.17

Figure 3.17. Transillumination of the head of the same infant with hydranencephaly. Note the "jack-o-lantern" appearance of the eyes indicating the lack of neural tissue behind the globe.

3.18

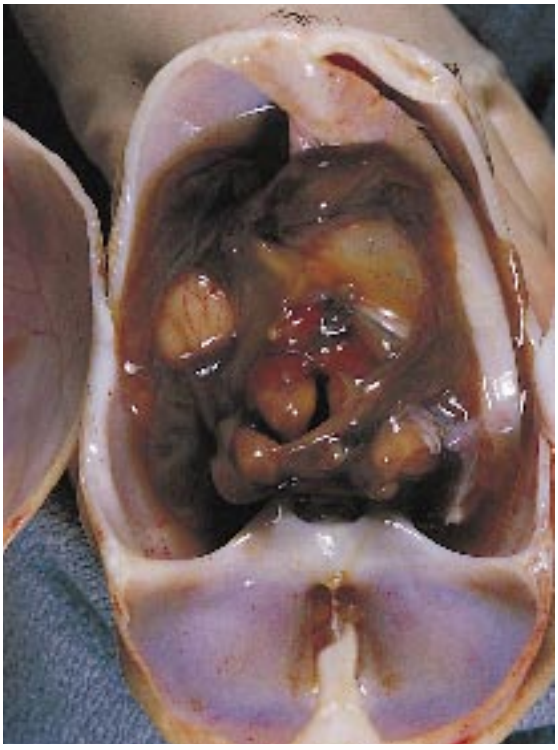

Figure 3.18. Autopsy view of the skull of the same infant with hydranencephaly. Note the empty cranial vault with lack of development of the cerebrum.

3.19

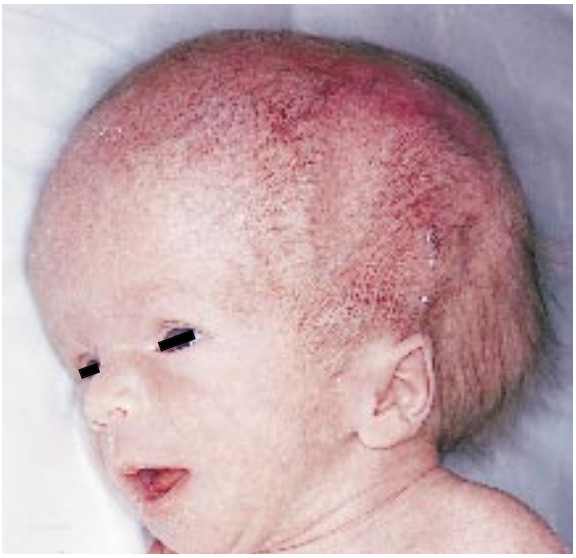

Figure 3.19. Lateral view of the head of an infant with macrocephaly due to a large porencephalic cyst.

3.20

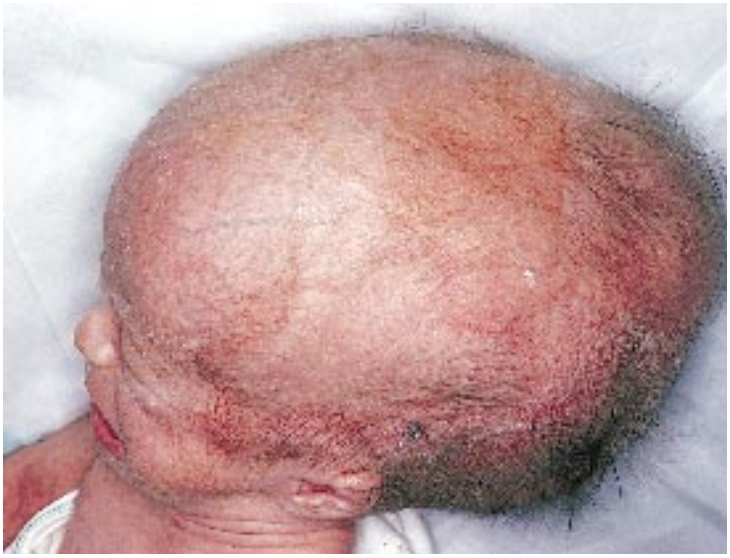

Figure 3.20. Another view of the head of the same infant showing the marked distortion of the posterior occiput and the engorged scalp veins.

3.21

Figure 3.21. Transillumination of the skull of the same infant. The fluid-filled lobulated space-occupying cyst results in marked distortion of the cranial vault.

3.22

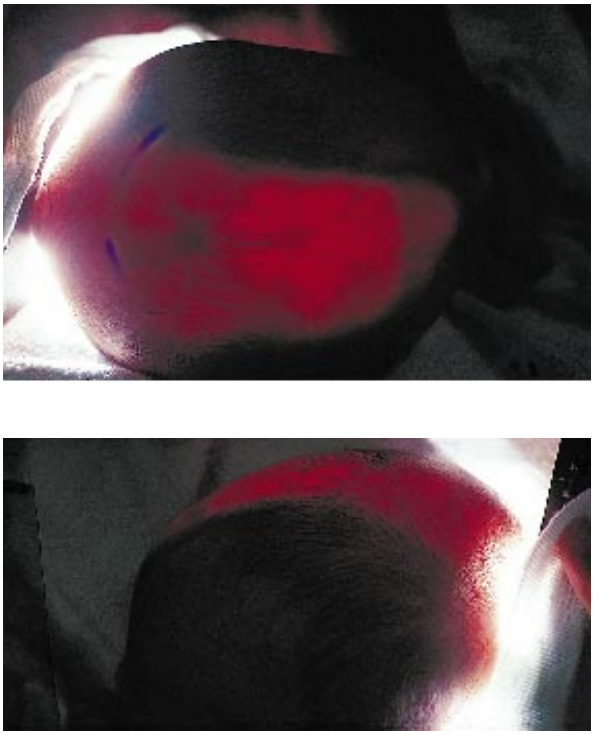

Figure 3.22. Transillumination of the skull of another infant with a smaller porencephalic cyst with the presence of some normal neural tissue.

3.23

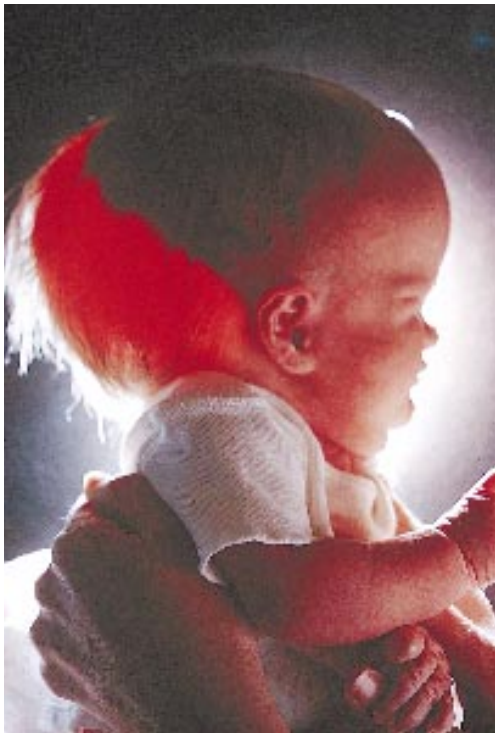

Figure 3.23. Transillumination of the skull of an infant with a Dandy-Walker malformation. Note the bulging occiput and enlargement of the head, and a large posterior fossa cyst.

3.24

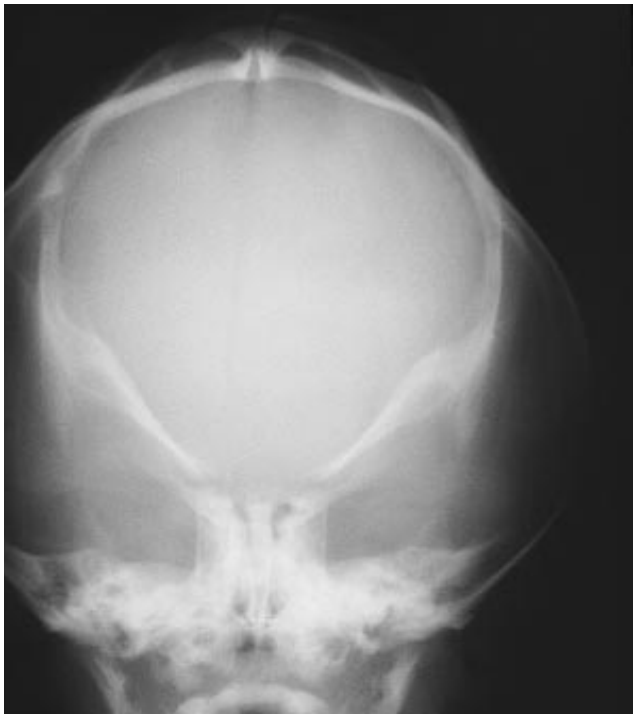

Figure 3.24. Cranial ultrasound study of an infant with an increased fronto-occipital circumference. Scanning section reveals large posterior fossa with hydrocephalus as the result of a Dandy-Walker malformation. This ultrasound marking is referred to as the "Chinese lantern" sign.

3.25

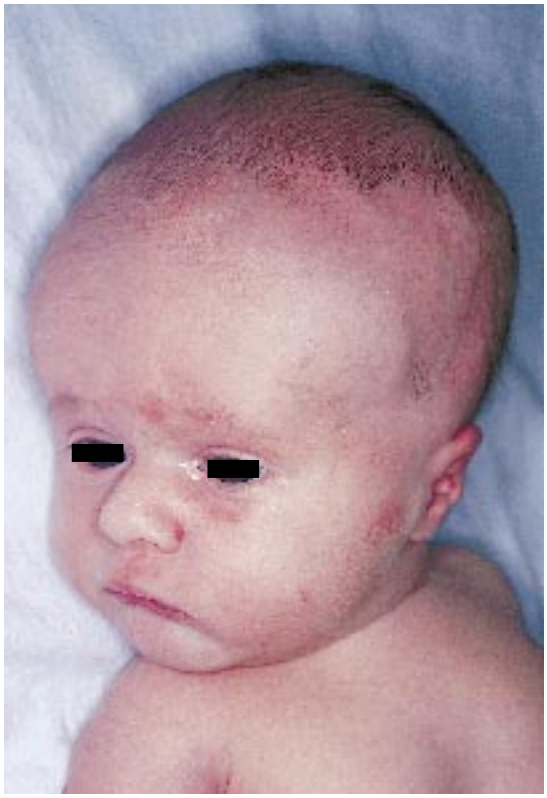

Figure 3.25. A premature infant (birth weight 1250 g) now aged two months with "pseudohydrocephalus." These infants have rapidly growing heads as a result of normal catch-up growth. Frontal bossing with prominent temporoparietal bulging suggests a diagnosis of hydrocephalus which can easily be excluded by a cranial ultrasound examination.

3.26

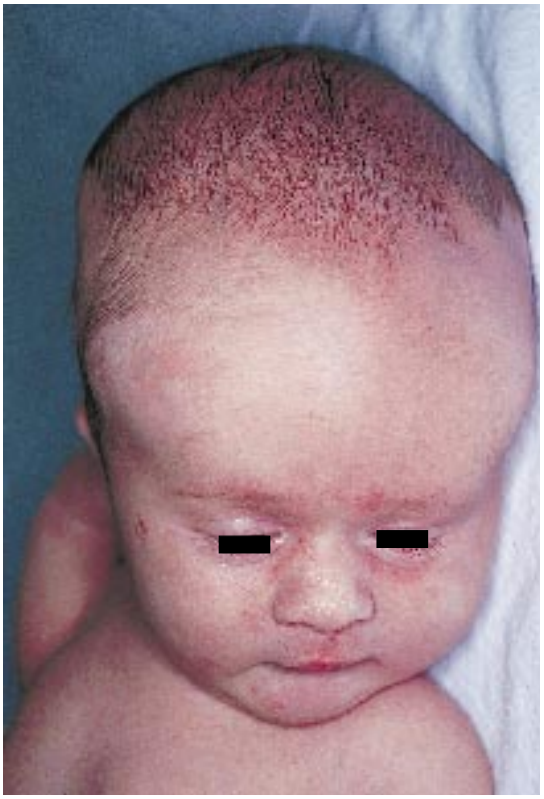

Figure 3.26. Superior view of the same infant with apparent hydrocephalus (pseudohydrocephalus of prematurity).

3.27

Figure 3.27. The same premature infant had some increased transillumination of the cranial vault. This was not pathologic but was the result of poor mineralization with transient increased skull lucency.

3.28

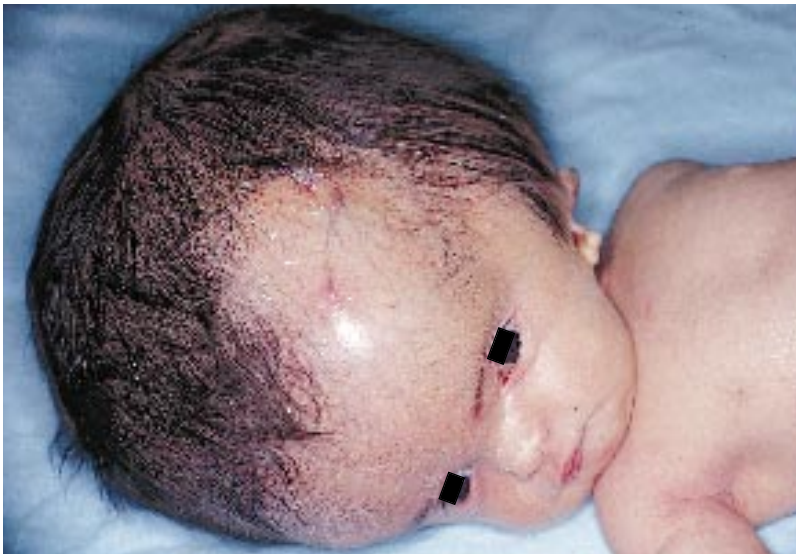

Figure 3.28. This term infant shows massive head enlargement as the result of congenital hydrocephalus. This results from overproduction or obstruction of the circulation of the cerebrospinal fluid. It can be inherited as an X-linked recessive trait in a male infant as the result of aqueductal stenosis. Other underlying brain defects may be present.

3.29

Figure 3.29. Congenital hydrocephalus in a term male infant with respiratory failure. Note the common association of the adducted thumbs, seen in the X-linked variant, and the prominent scalp veins. The birth weight of this infant was 3800 g, the length 53 cm, and the fronto-occipital circumference 52.5 cm.

3.30

Figure 3.30. Transillumination of the skull of the same infant with congenital hydrocephalus. Note the very prominent scalp veins which probably reflect the marked increase in intracranial pressure.

3.31

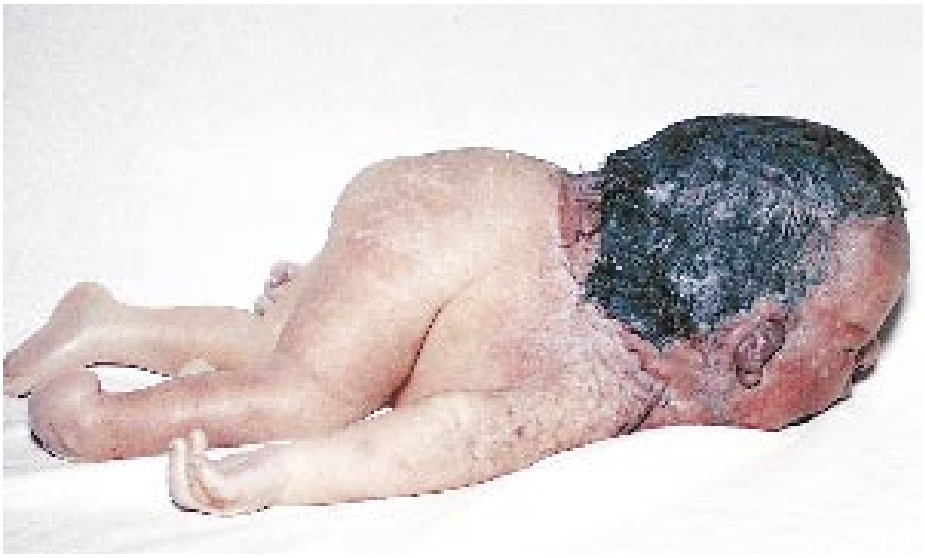

Figure 3.31. Iniencephaly is the most severe form of a closed neural tube defect. It results in enlargement of the foramen magnum and fusion of the posterior occiput with the cervicothoracic spine. It is incompatible with survival.

3.32

Figure 3.32. Radiograph of the same infant with iniencephaly. Note absence of the laminal and spinal processes of the cervical, dorsal, and sometimes lumbar vertebrae. The vertebrae are reduced in number and are irregularly fused.

3.33

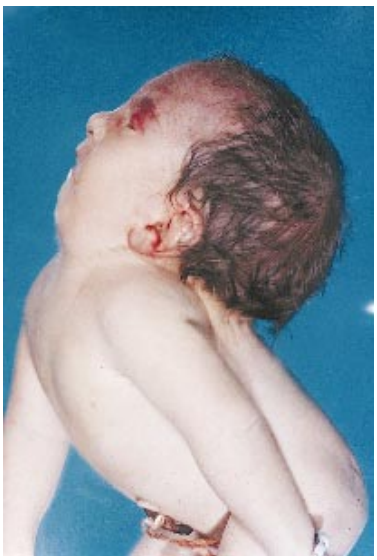

Figure 3.33. Another infant with iniencephaly showing the lack of a neck due to the fusion of the posterior occiput with the cervicothoracic spine.

3.34

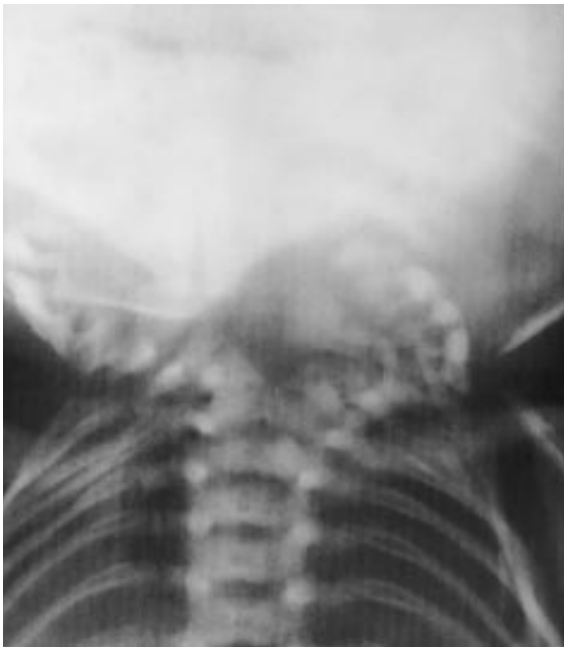

Figure 3.34. Radiograph of the same infant with iniencephaly. Note the schistasis of the cervical vertebrae.

3.35

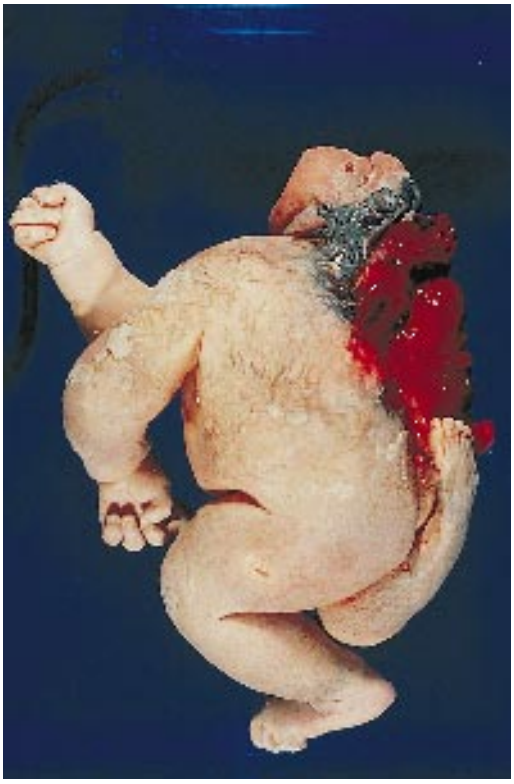

Figure 3.35. Craniorachischisis represents the most severe form of an open neural tube defect. Note that the defect in this infant is open from the anterior to the posterior neural pore.

3.36

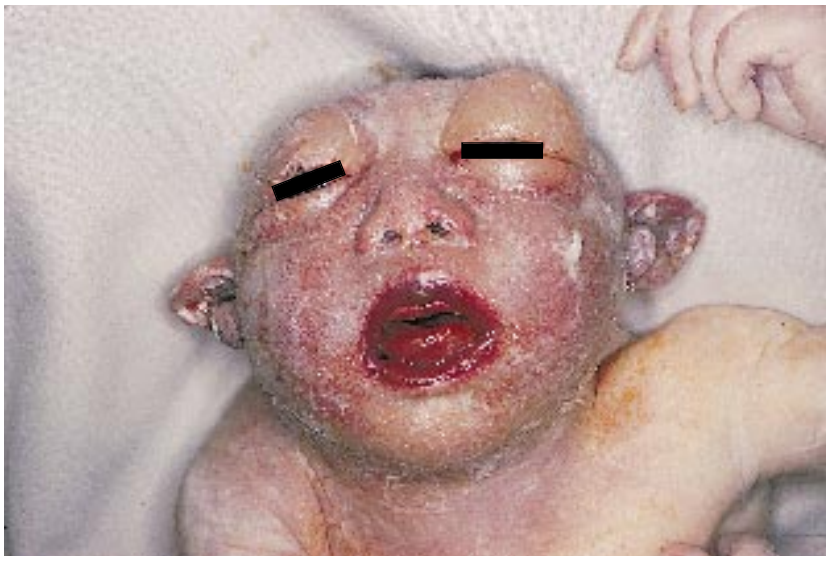

Figure 3.36. Anencephaly is a developmental defect in the brain with an open cranium resulting from failure of the anterior neural tube to close. It is a major open neural tube defect in which there is absence of skull bones, cranial vault, and incomplete development of the brain. Malformation of other organs may occur such as adrenal hypoplasia and genitourinary abnormalities. Anencephaly in this term infant left an exposed fibrotic degenerating ill-defined mass of neural tissue. Most of these infants are stillborn and the remainder die in the immediate neonatal period.

3.37

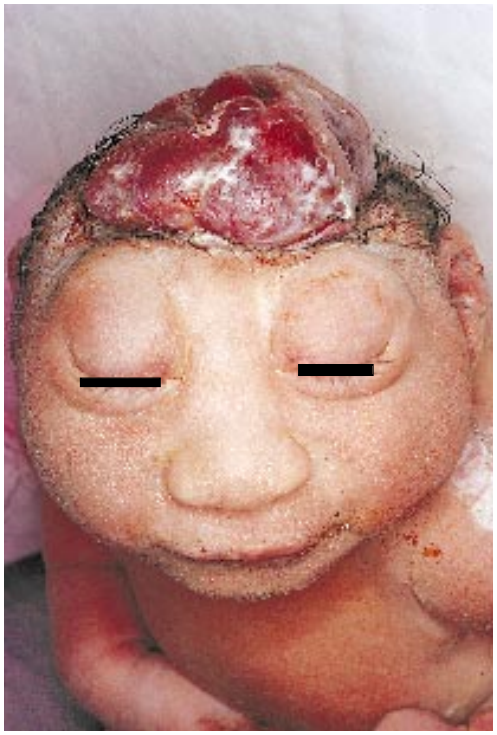

Figure 3.37. Another infant with anencephaly. Anencephaly is more common in females.

3.38

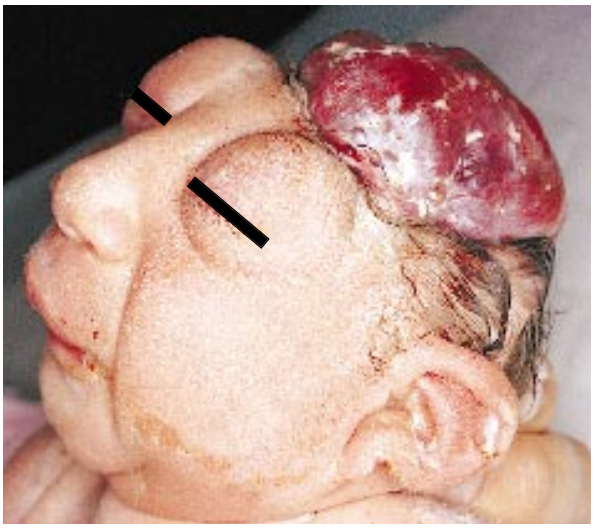

Figure 3.38. The lateral view of the same infant with anencephaly.

3.39

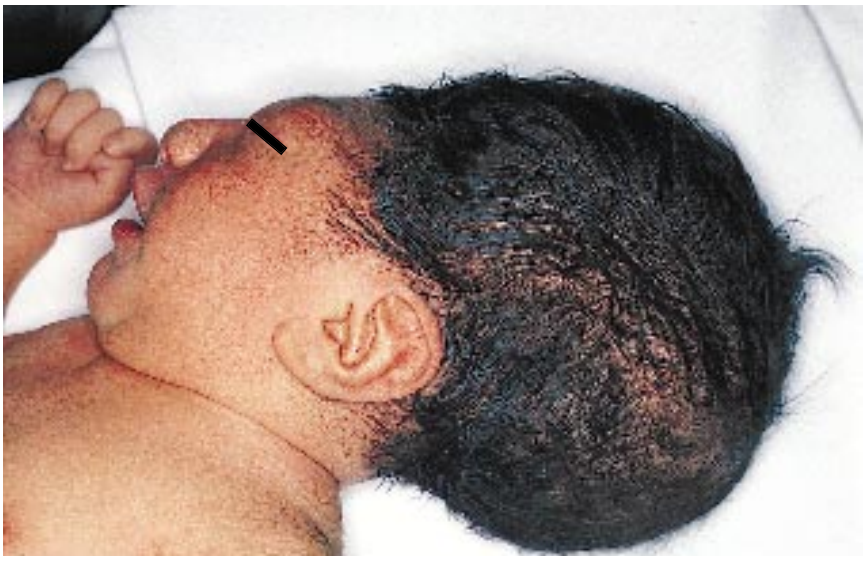

Figure 3.39. Encephaloceles may occur at any midline point in the skull and result from failure of the neuroectodermal axis to develop normally. This results in bony defects of the skull with protrusion of the meninges which may contain neural tissue. They are most common in the occipital area. The prognosis is better if the rest of the skull is normal and there is no herniation of neural tissue.

3.40

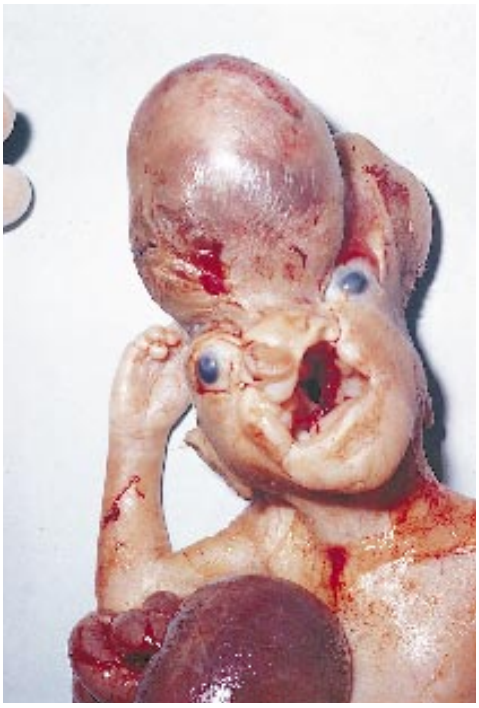

Figure 3.40. Encephaloceles occur at any midline point in the skull. The exception is the occurrence of an asymmetric encephalocele that occurs with a severe amniotic band disruption sequence. This infant with disruption shows the large asymmetric encephalocele and the involvement of the mouth, nose, eyes, and head.

3.41

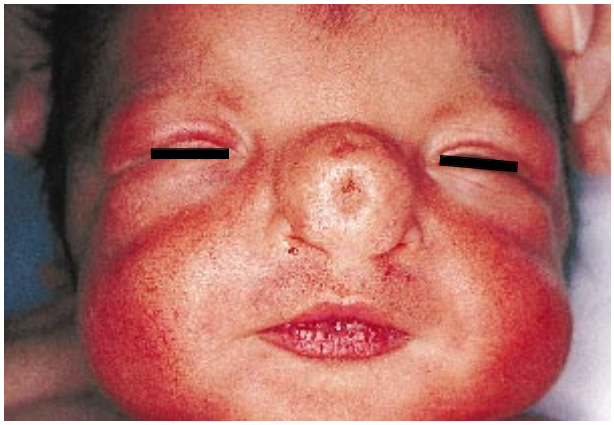

Figure 3.41. Abnormal facial and nasal appearance of an infant with an anterior encephalocele. This infant has a severe midline nasal schistasis. The external airways were obstructed. The CT scan demonstrated a communicating encephalocele. At surgery, an ethmoid encephalocele was removed.

3.42

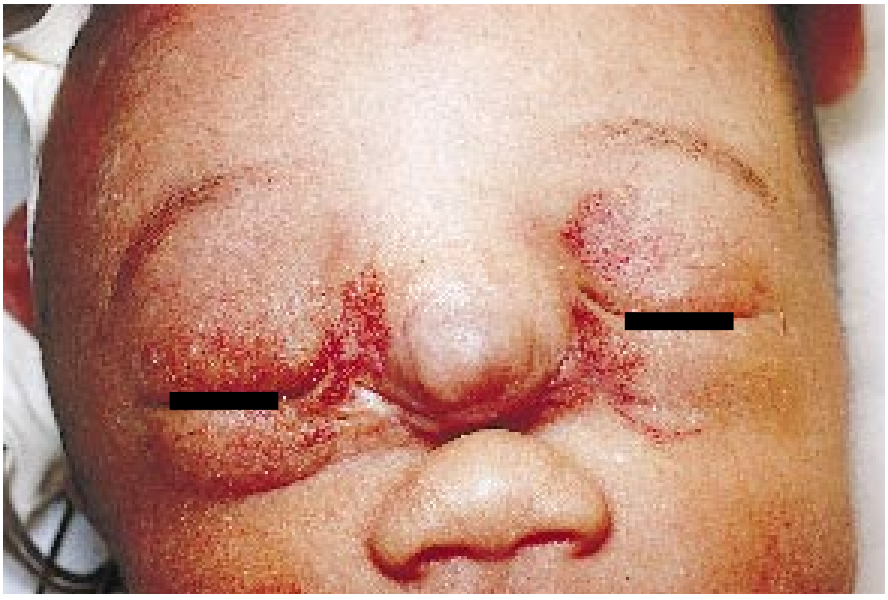

Figure 3.42. The soft tissue mass in this infant proved to be an anterior encephalocele.

3.43

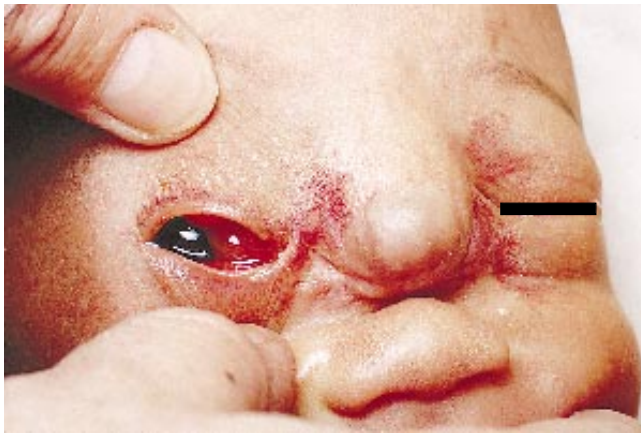

Figure 3.43. Retraction of eyelids of the same infant reveals that the soft tissue mass occupies the nasal aspect of the orbit with distortion of the globe.

3.44

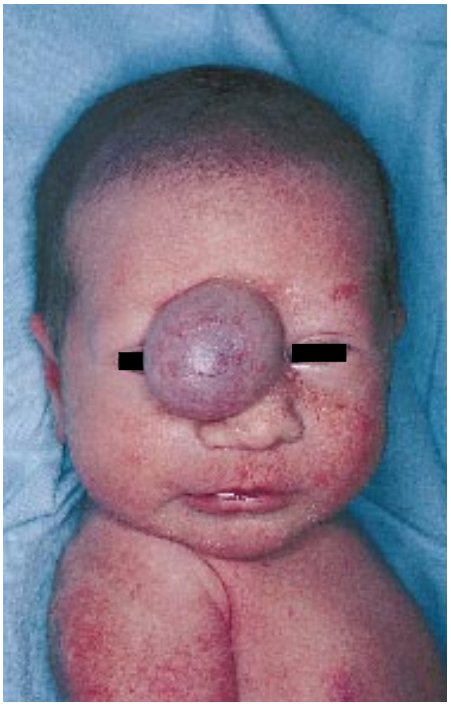

Figure 3.44. A term infant with an anterior encephalocele. In the Western hemisphere and Europe, the majority of encephaloceles are posterior, whereas in the Far East (India, Sri Lanka, Africa, etc.), the majority of encephaloceles are anterior.

3.45

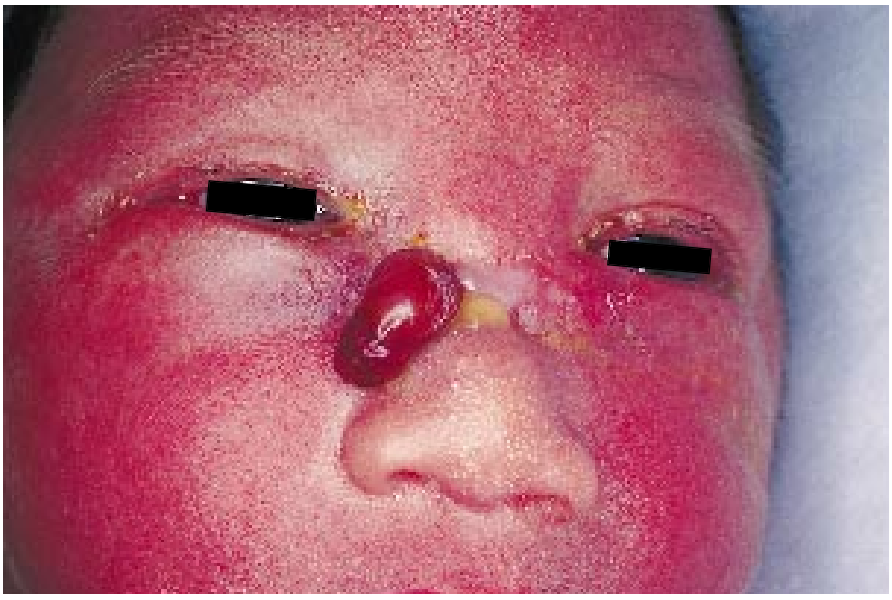

Figure 3.45. In this infant with an anterior encephalocele, the fluid draining from the mass was positive for glucose confirming the origin of the fluid as CSF (cerebrospinal fluid).

3.46

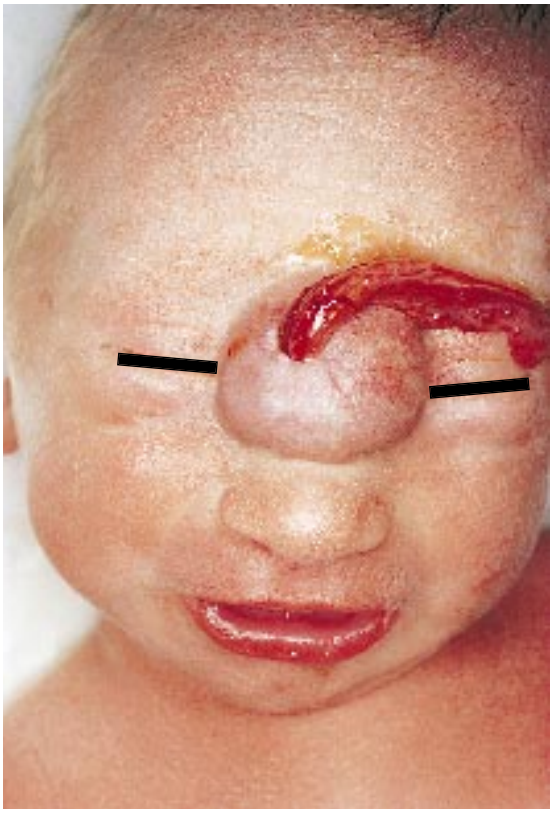

Figure 3.46. This anterior encephalocele presented as a soft tissue midline mass which caused nasal obstruction and respiratory distress.

3.47

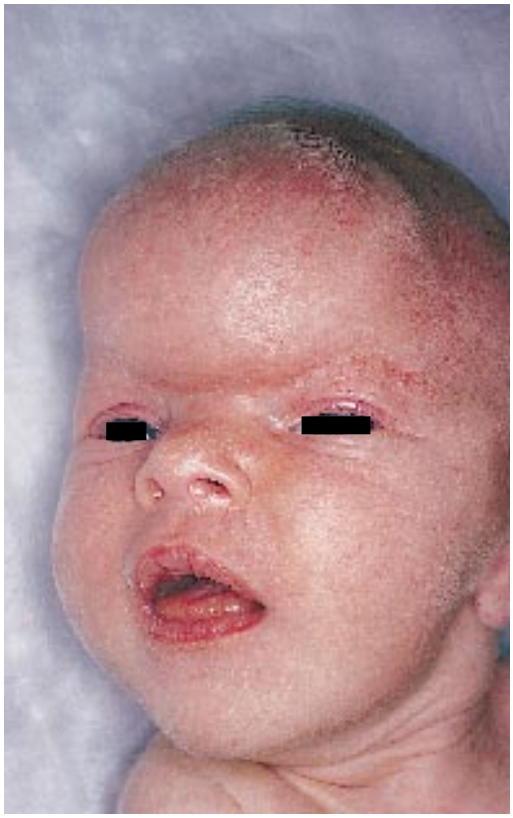

Figure 3.47. The abnormal brow appearance in this term infant is the result of a frontal encephalocele.

3.48

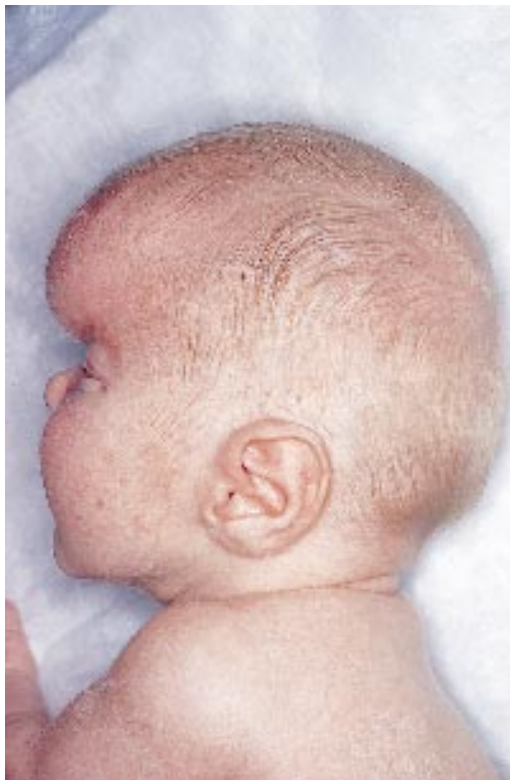

Figure 3.48. Lateral view of the same infant with a frontal encephalocele.

3.49

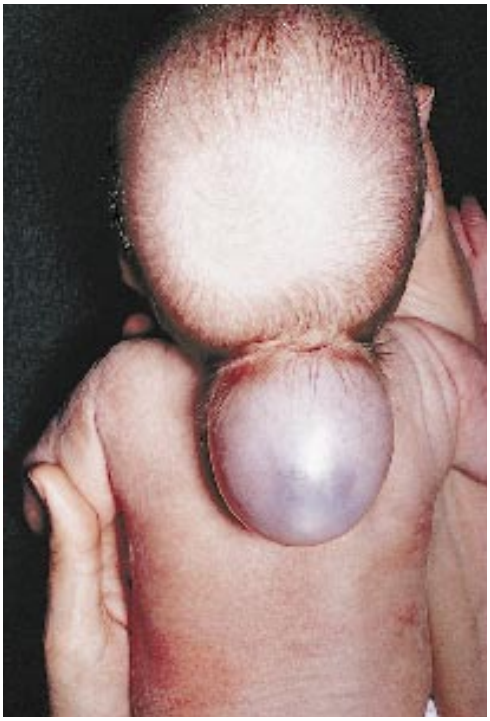

Figure 3.49. A posterior encephalocele in an infant may be difficult to distinguish from a cervical meningocele. It is both a posterior encephalocele and cervical myelomeningocele when there is involvement of both the bony skull and spine. Cervical myelomeningoceles are usually not associated with other neurologic abnormalities.

3.50

Figure 3.50. Inferior view with transillumination of the posterior structure in an occipital encephalocele. In a cranial encephalocele there is a herniation of meninges through a skull defect.

3.51

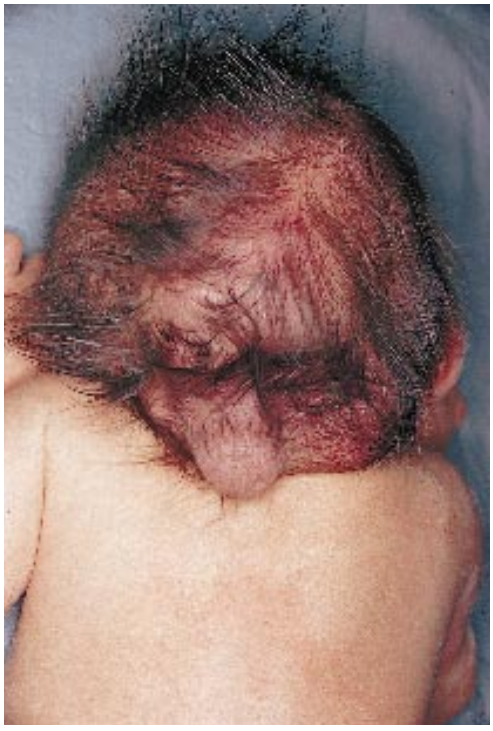

Figure 3.51. Infant with a posterior small occipital encephalocele. Occipital encephalocele present as a protruding soft tissue mass from the base of the skull.

3.52

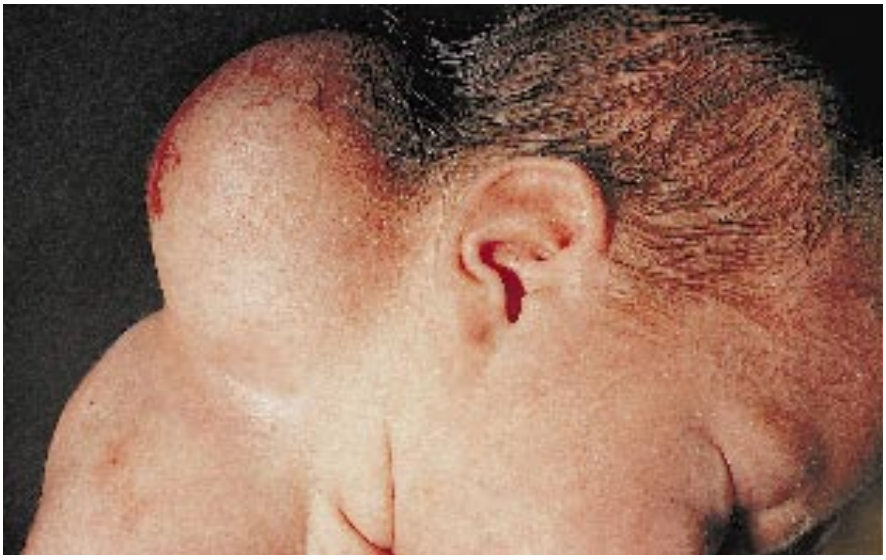

Figure 3.52. Posterior encephaloceles may be distinguished from associated cervical spine abnormalities by MRI.

3.53

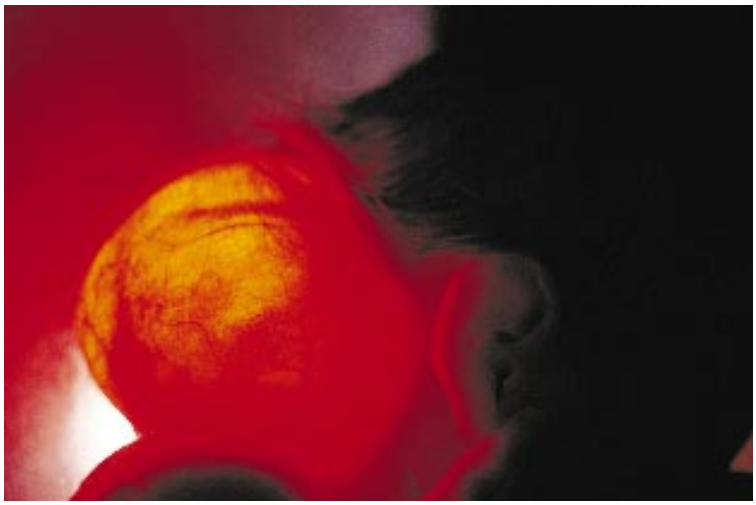

Figure 3.53. Transillumination of the posterior encephalocele in the same infant.

3.54

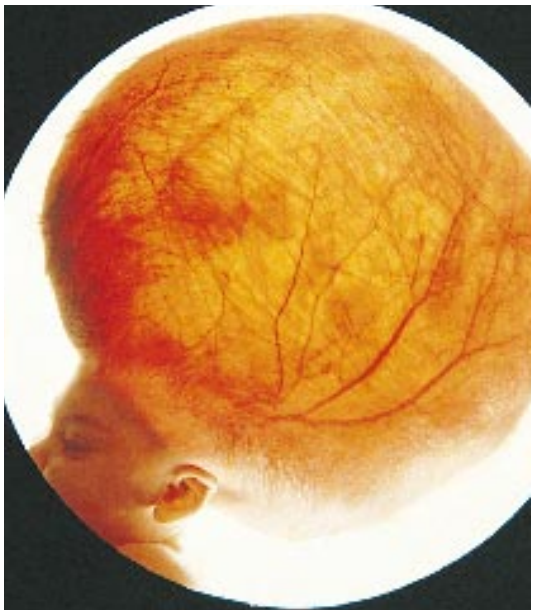

Figure 3.54. In this massive occipital encephalocele note the lack of neurologic tissue.

3.55

Figure 3.55. Rupture of a large posterior encephalocele with protrusion of neural components. This results in a poor prognosis.

3.56

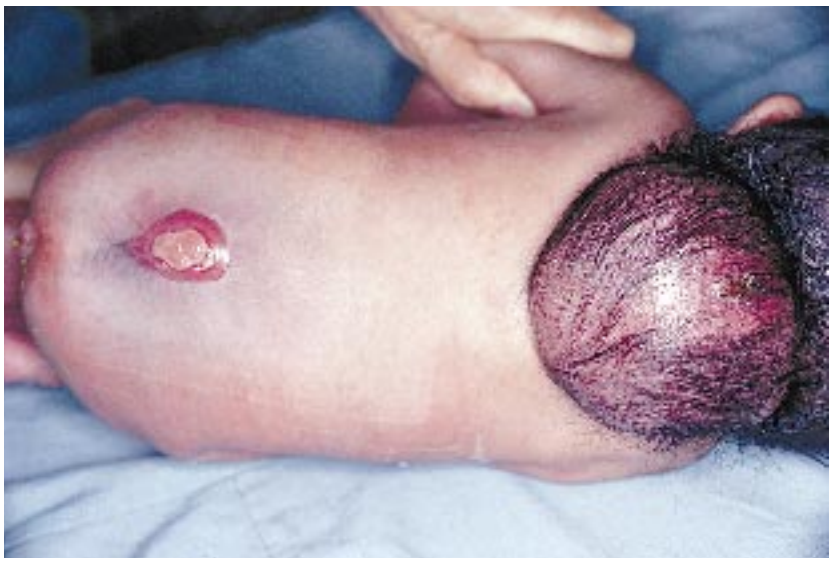

Figure 3.56. Infant with both a posterior encephalocele and a lumbar myelomeningocele. The lumbar area is the most common site for myelomeningoceles.

3.57

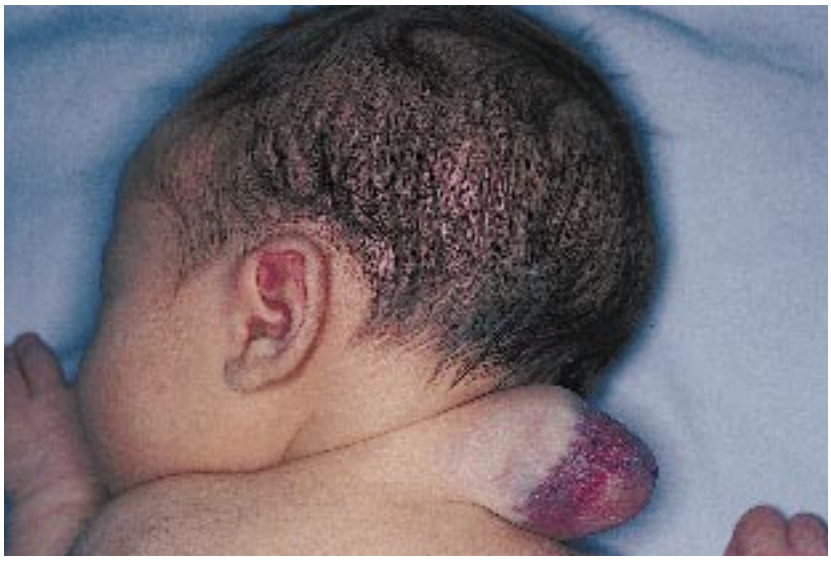

Figure 3.57. A cervical meningocele may be difficult to differentiate from an occipital encephalocele. Further study in this infant showed that this was a cervical meningocele.

3.58

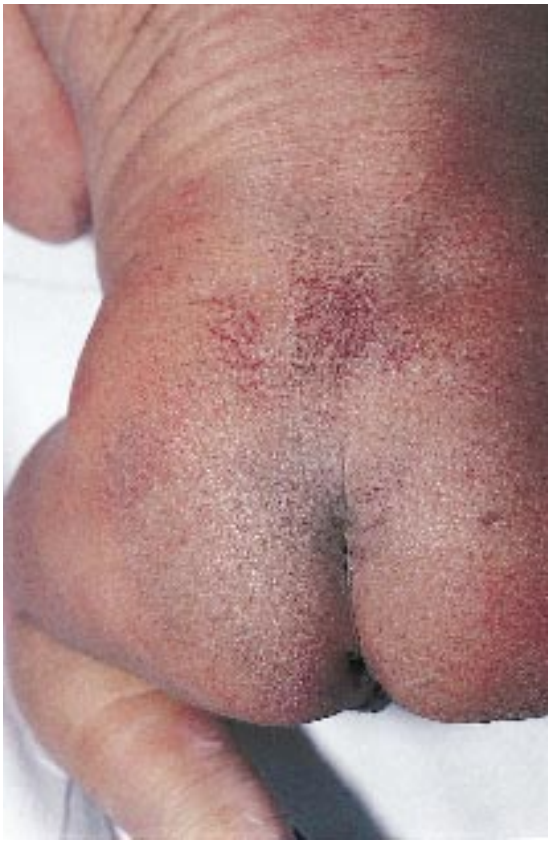

Figure 3.58. A midline hair tuft in the lumbosacral area. This infant had a tethered cord on MRI study. Hair tufts, skin tags, sinuses, and abnormal pigmentation that occur in the midline along the length of the spinal column should always alert one to the possibility of an associated underlying neurologic abnormality. With a tethered cord the neural tissue is firmly attached at its caudal end, being bound by a stout connective tissue band to the interior of the bony canal. With growth, the spinal canal normally grows more rapidly than the spinal cord resulting in traction on the cord. This may gradually pull the lower end of the brainstem down into the foramen magnum like a cork into a bottle. This is the Arnold-Chiari malformation.

3.59

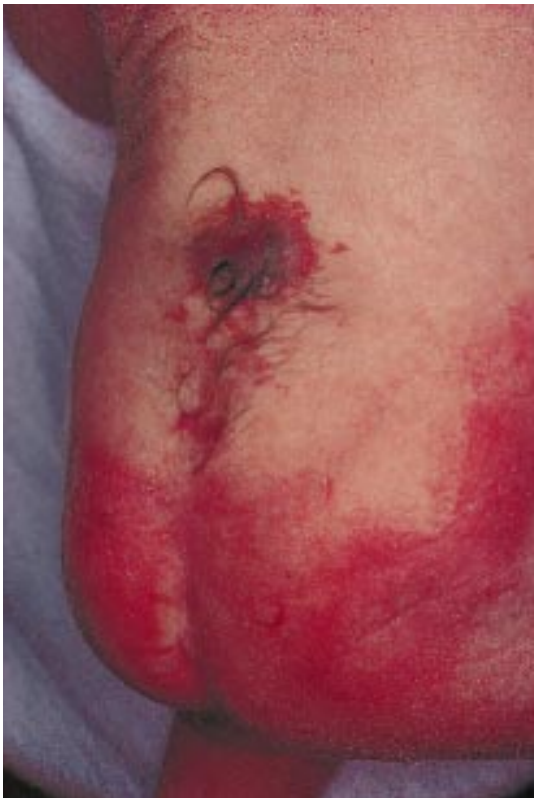

Figure 3.59. A midline tuft of hair with a pigmented nevus in the lumbosacral area. This should alert one to the possibility of an associated underlying neurologic abnormality.

3.60

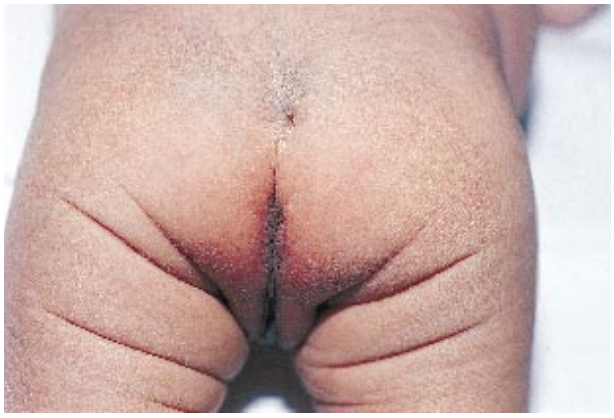

Figure 3.60. Midline pilonidal dimples or sinuses are common deformities. They represent the point of attachment of the distal end of the neural tube to the coccyx. If there is a deep dimple, an MRI should be performed to exclude a neural tube defect. The MRI was normal in this infant.

3.61

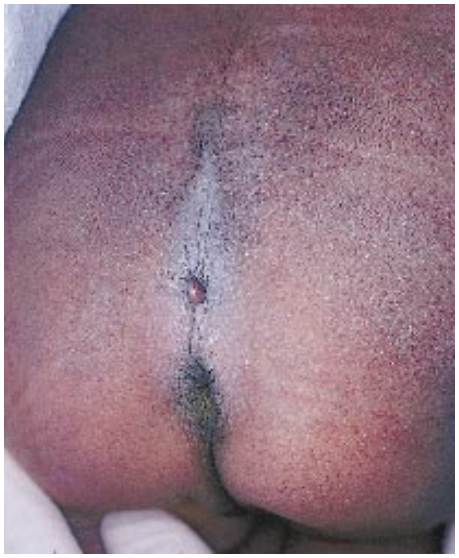

Figure 3.61. This infant had a midline small skin tag with depigmentation of the skin in the lumbosacral region. The MRI revealed a tethered cord.

3.62

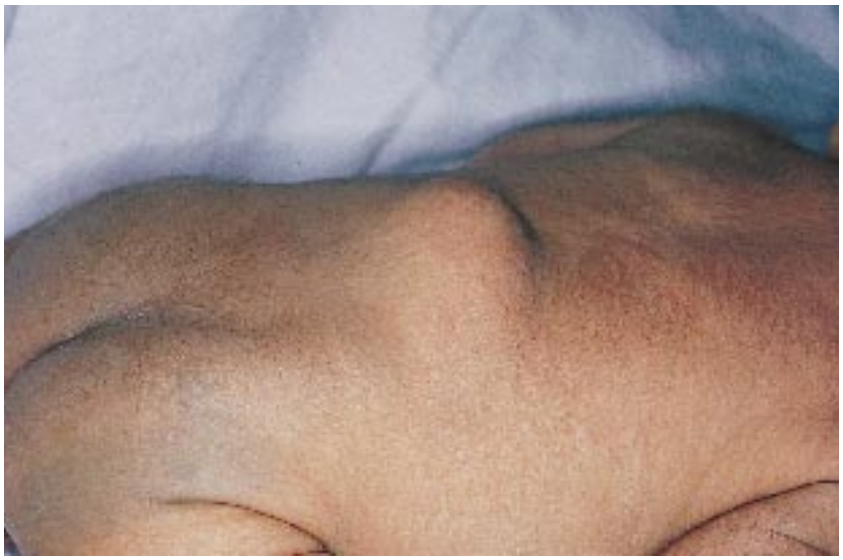

Figure 3.62. This infant has a lumbar meningocele which is an example of a closed neural tube defect. The neural tube closes by infolding from the coccyx to the nasion and defects of fusion can occur anywhere along this axis. Meningoceles occur when the membranes surrounding the spinal cord bulge outward through a dorsal defect in the bony spinal canal. The resulting mass may be tense or fluctuant and is covered by intact skin.

3.63

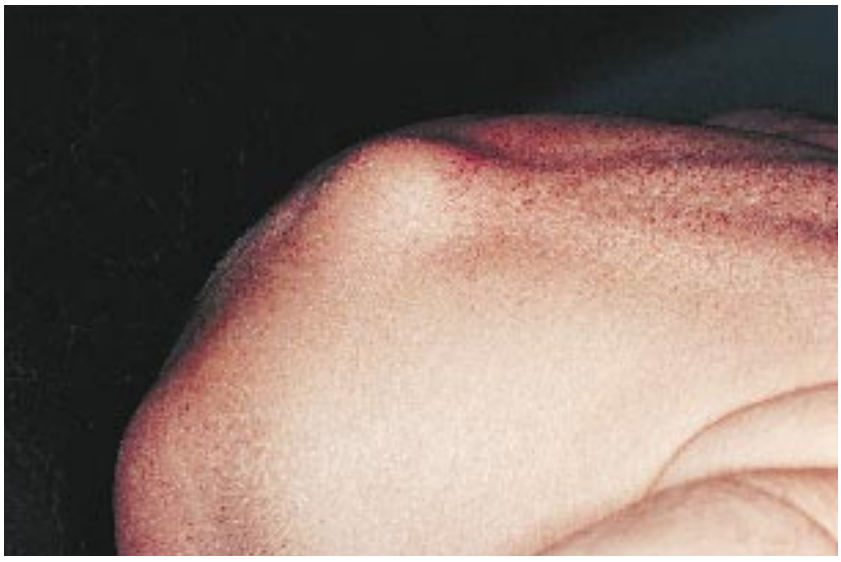

Figure 3.63. A lumbosacral meningocele is present in this infant. The lumbosacral area is the most common location for both meningoceles and myelomeningoceles. Infants with meningoceles and myelomeningoceles may have an Arnold-Chiari malformation and a high percentage develop hydrocephalus. The quality of life is influenced by the site of the neurologic lesion.

3.64

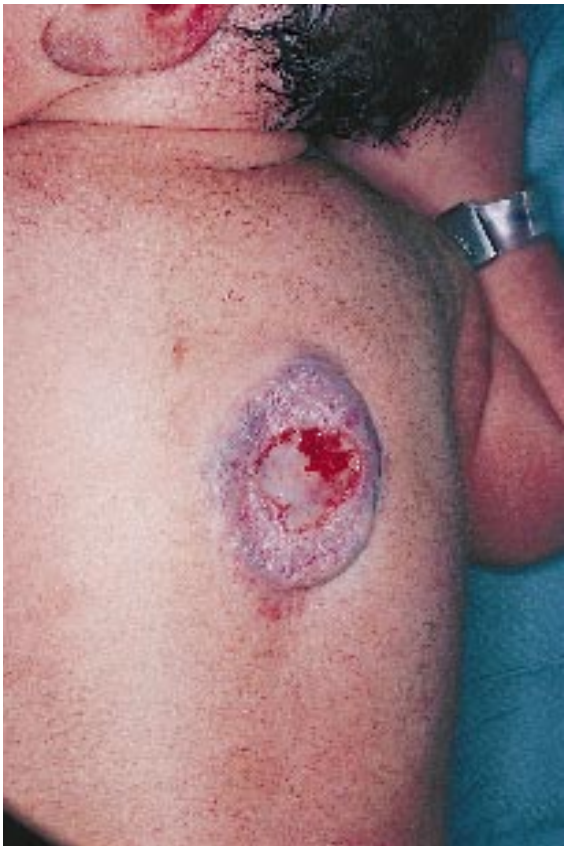

Figure 3.64. This infant has a thoracic myelomeningocele which presents as an open midline defect. Although myelomeningoceles occur most commonly at the lumbosacral level, they may affect the neural tube at any level. The posterior elements covering the spinal canal fail to form, but in this type of defect the cystic mass that bulges out posteriorly contains neural tissue and the surface of the meninges is exposed to the exterior with no skin covering. Large lesions may incorporate a large segment of the spinal cord itself.

3.65

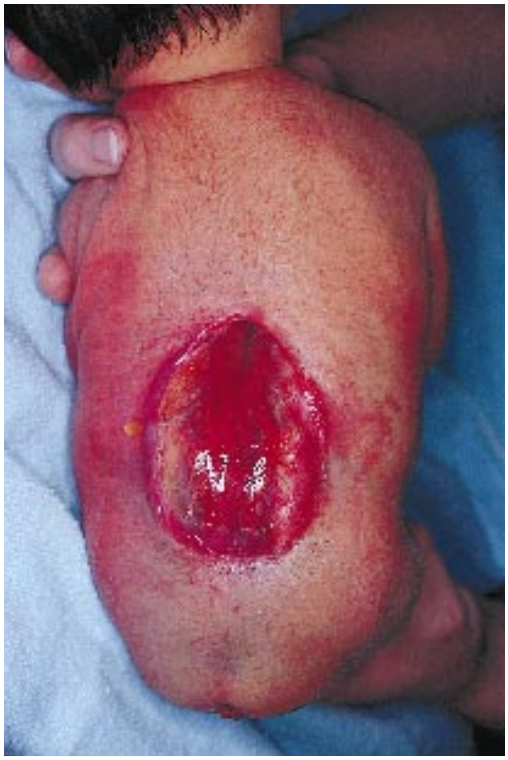

Figure 3.65. Thoracolumbosacral myelomeningocele with exposure of the central spinal canal. Note the leaking of cerebrospinal fluid. The meningeal sac often ruptures before birth or during delivery, thus exposing the neural tissue to direct injury or the risk of infection. Loss of neurologic function distal to the lesion is the rule. There may be absence of control of the urinary and anal sphincters, bladder paralysis, and variable degrees of sensory and motor deficit to the lower limbs.

3.66

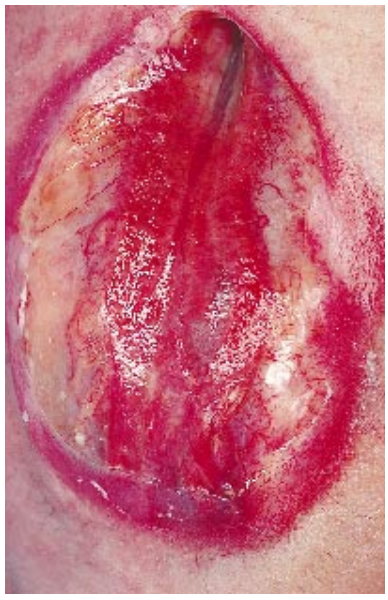

Figure 3.66. A close-up view of the thoracolumbosacral myelomeningocele with the exposed central canal visible.

3.67

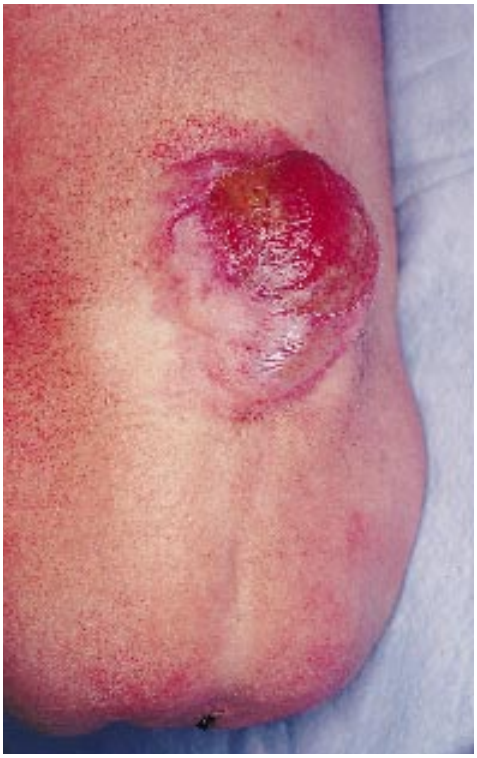

Figure 3.67. In this infant with a lumbosacral myelomeningocele note that with this low level of involvement, there was no anal wink, the hips were flexed, and there were bilateral clubfeet. Clubfeet and rocker-bottom feet are commonly associated with myelomeningoceles.

3.68

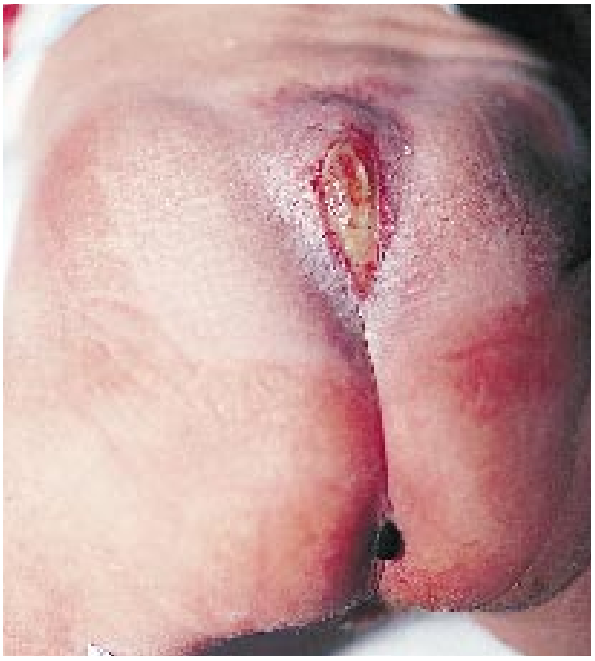

Figure 3.68. In this infant with a lumbosacral meningocele note that the sac is closed and that there is an overlying hair tuft. Trivial abnormalities such as nevi, sinuses, and hair tufts may indicate an underlying central nervous system abnormality.

3.69

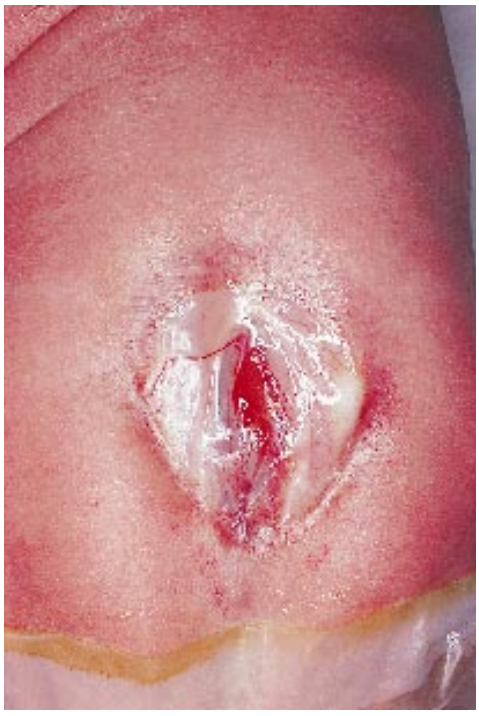

Figure 3.69. An infant with rachischisis or myelomeningocele. In contrast to encephaloceles, myelomeningoceles represent failure of closure of the posterior neuropore. There is usually lack of fusion of the vertebral arches with broadened vertebrae and dorsal protrusion of the neural tissue in an enclosed sac with a thin membrane that can easily rupture. Secondary hydrocephalus is a common association.

3.70

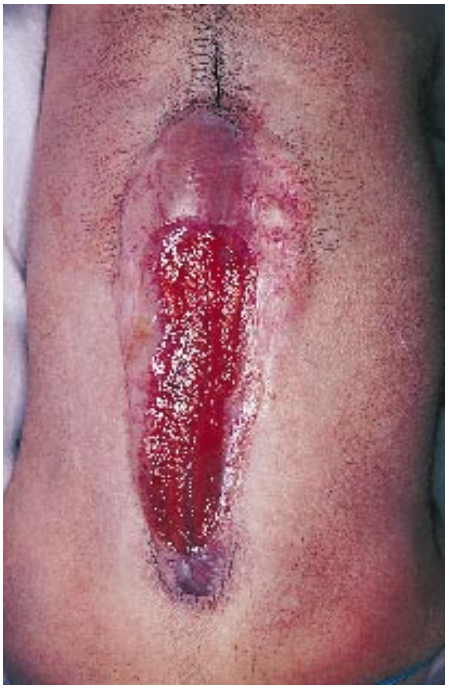

Figure 3.70. Thoracolumbar myelomeningocele in another infant. Diastematomyelia (congenital medial cleft of the spinal cord) is usually associated with spina bifida occulta. There may be tufts of hair (hypertrichosis) in the area of the mid to lower thoracic spinal column. The condition is diagnosed by MRI.

3.71

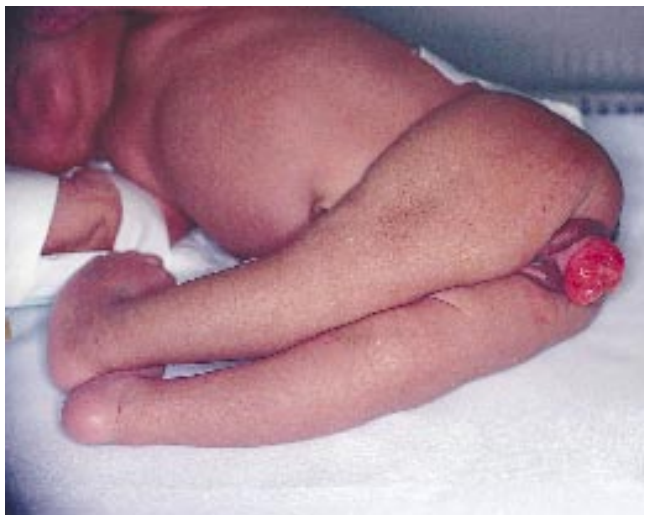

Figure 3.71. In infants with a myelomeningocele there may be associated abnormal posture. Note the severely deformed lower limbs from lack of movement in utero resulting in genu recurvatum, and the rocker-bottom feet. This infant also shows procidentia (prolapse of the uterus with protrusion of the cervix). Procidentia is a very uncommon finding in the neonate but, if present, is invariably associated with a neural tube defect.

3.72

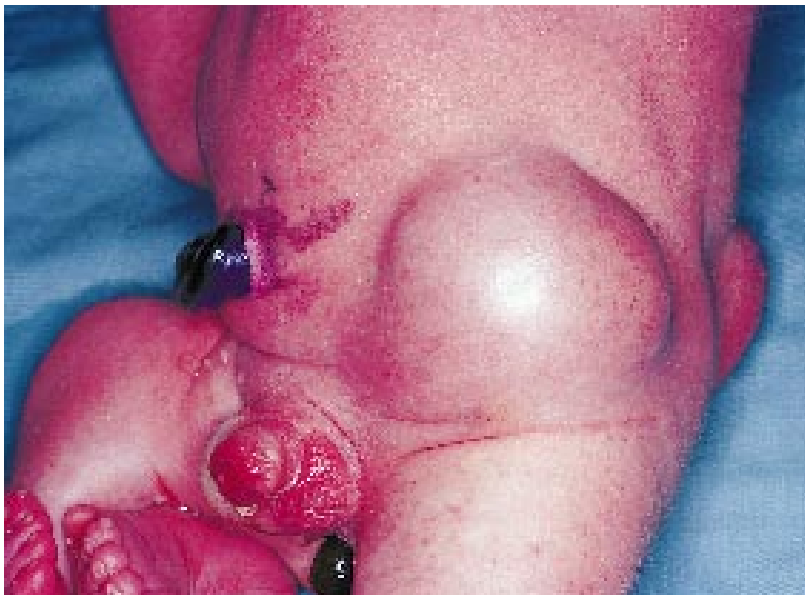

Figure 3.72. Lumbar myelomeningocele and anterior abdominal wall hernia.

3.73

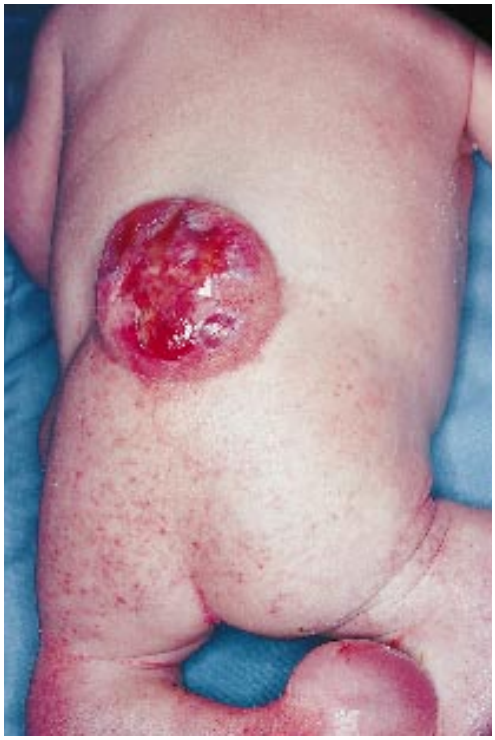

Figure 3.73. Posterior view of the same infant as in Figure 3.72 showing the lumbar myelomeningocele.

3.74

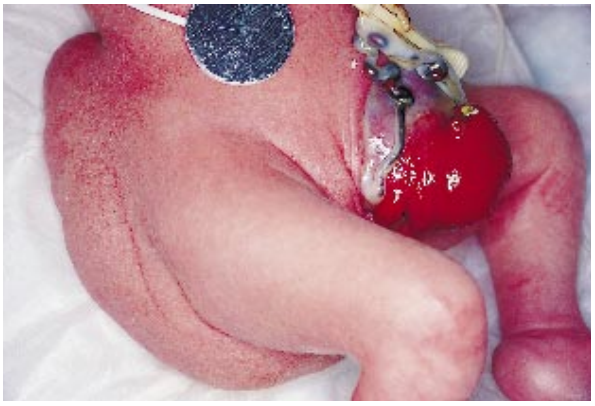

Figure 3.74. A 31-week gestation premature infant with a cloacal exstrophy sequence (exstrophy of the cloaca, imperforate anus, ambiguous genitalia, and myelocystocele). There is a myelocystocele (hydromyelia; syringomyelocele) extending from T7 to the sacrum, and the infant also had an associated Arnold-Chiari malformation.

Myelocystoceles are due to dilatation of the central canal (hydromyelia) and to protrusion over the surface of the posterior aspect of the much expanded spinal cord which may be covered by meninges and skin. In such cases, the cavity is cranially and caudally directly connected with the central canal. The spinal nerves do not traverse the cavity (as they do in the common myelomeningocele) but course around it.

3.75

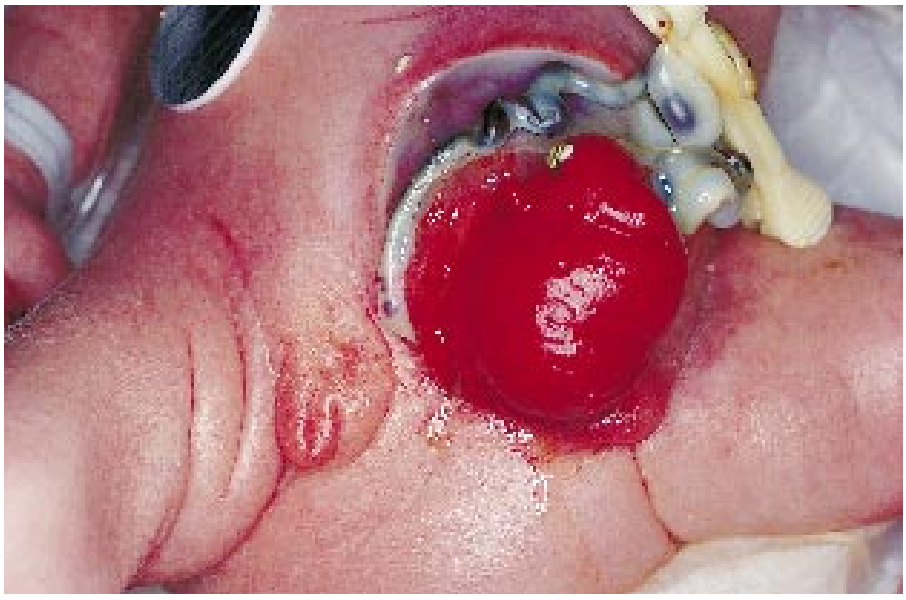

Figure 3.75. A close-up view of the exstrophy of the cloaca. Note the ureteral openings.

3.76

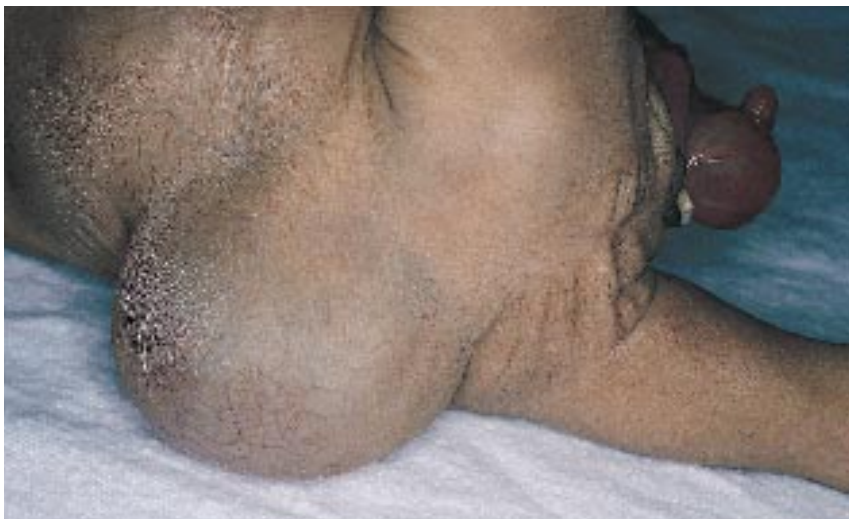

Figure 3.76. Another infant with the cloacal exstrophy sequence. Associated anomalies include imperforate anus, ambiguous genitalia, cloacal exstrophy, and lumbosacral myelocele.

3.77

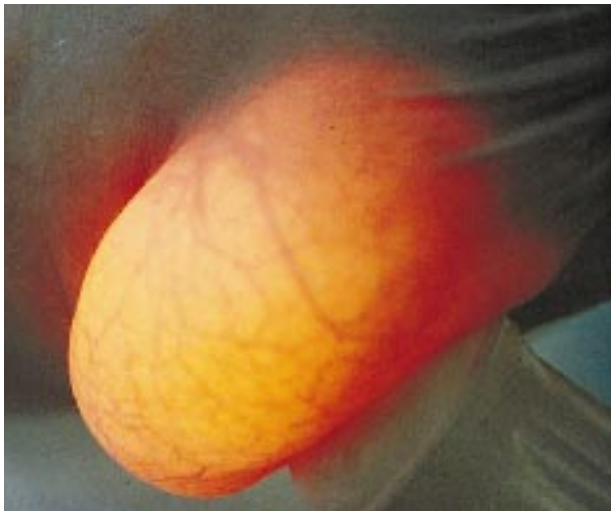

Figure 3.77. Transillumination of the lumbosacral mass of the same infant shows the myelocystocele.

3.78

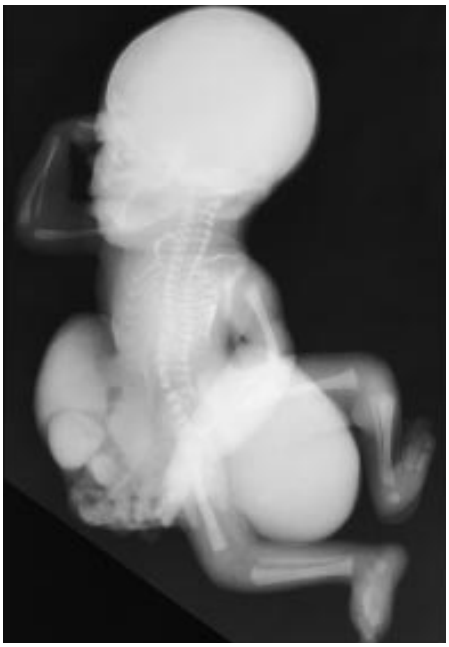

Figure 3.78. Radiograph of another infant with the cloacal exstrophy sequence. Note the large myelocystocele, omphalocele, and cloacal exstrophy.

3.79

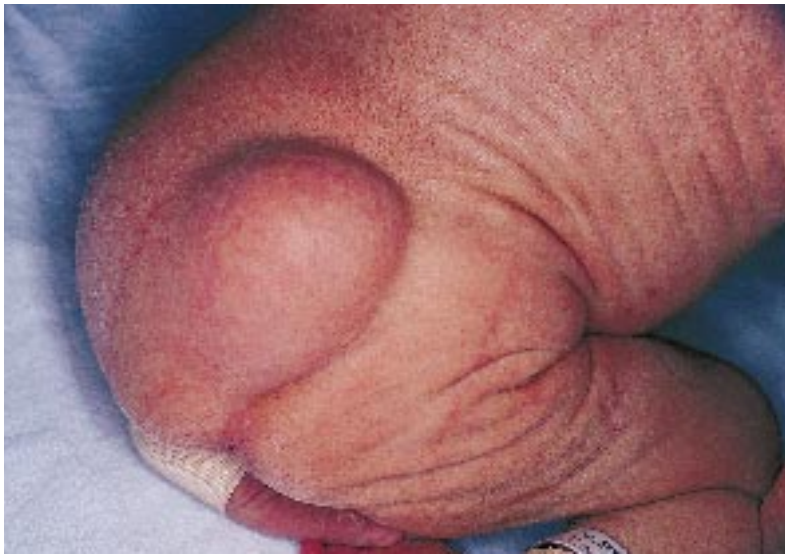

Figure 3.79. This lipomeningocele is a simple meningocele with infiltration of fibrous and fatty tissue continuous with a subcutaneous lipoma. The lipoma may even extend into the spinal canal. Because of the presence of the lipoma, as seen in this infant, the meningocele is not midline. There was an underlying tethered cord as demonstrated by MRI.

3.80

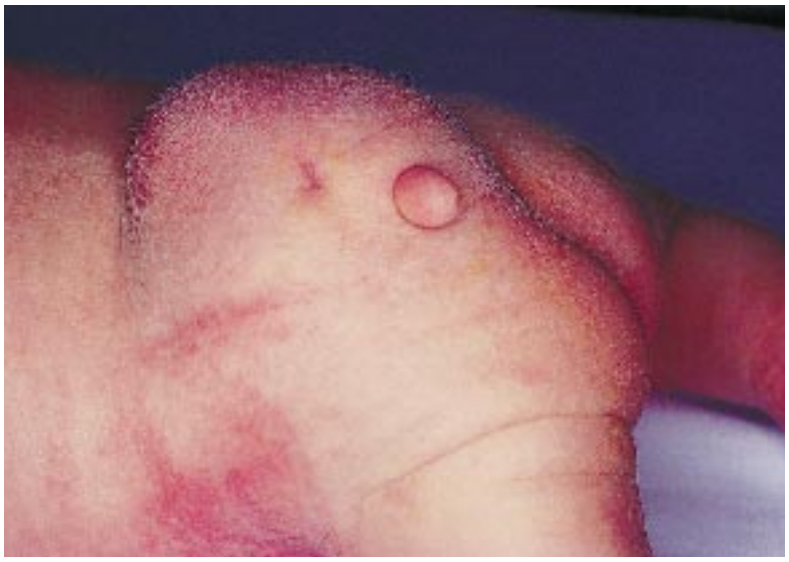

Figure 3.80. Note the associated protrusion of a skin tag in another variant of a lipomeningocele. In infants with lipomeningoceles, skin tags may be present, there may be some skin discoloration due to the presence of the lipoma, and the lesions are usually not midline because of the presence of the lipoma. Lipomeningoceles are relatively rare defects.

3.81

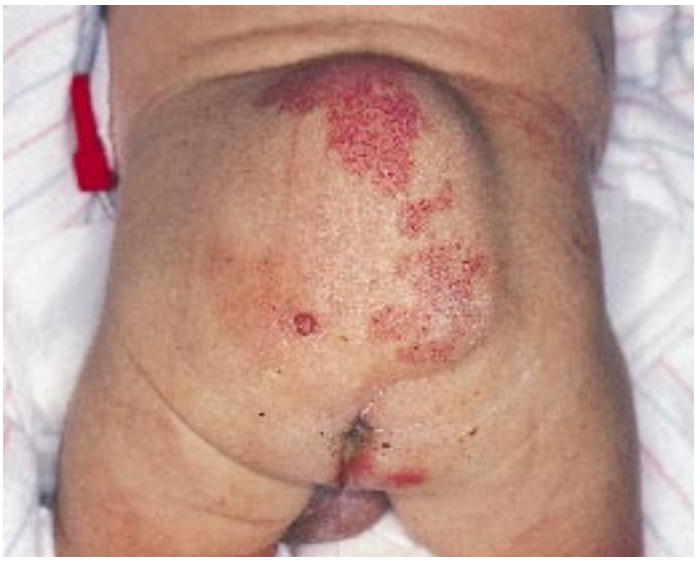

Figure 3.81. In this infant with a lipomeningocele with a tethered cord, note the associated skin discoloration with a small skin tag.

3.82

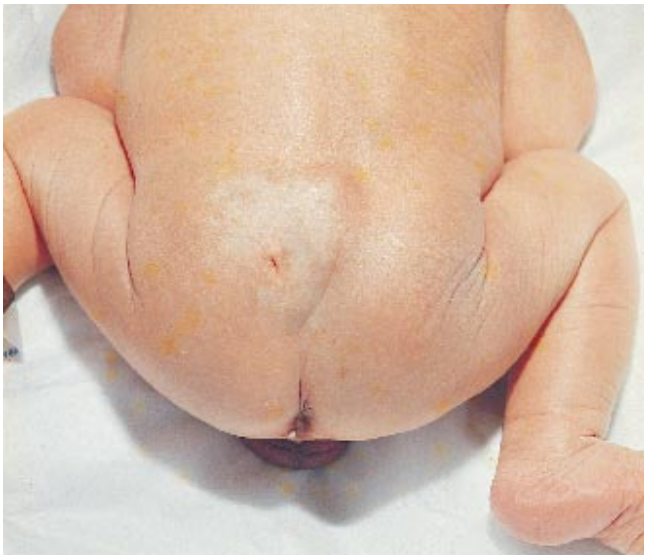

Figure 3.82. A lipomeningocele with an associated sinus tract is present in this infant.

3.83

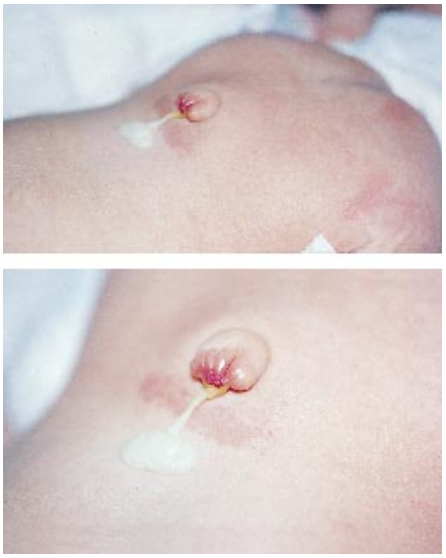

Figure 3.83. Infant with a large dermal sinus tract associated with cord tethering and spinal dysraphism. On MRI there was a tethered cord and spina bifida both above and below the lesion.

3.84

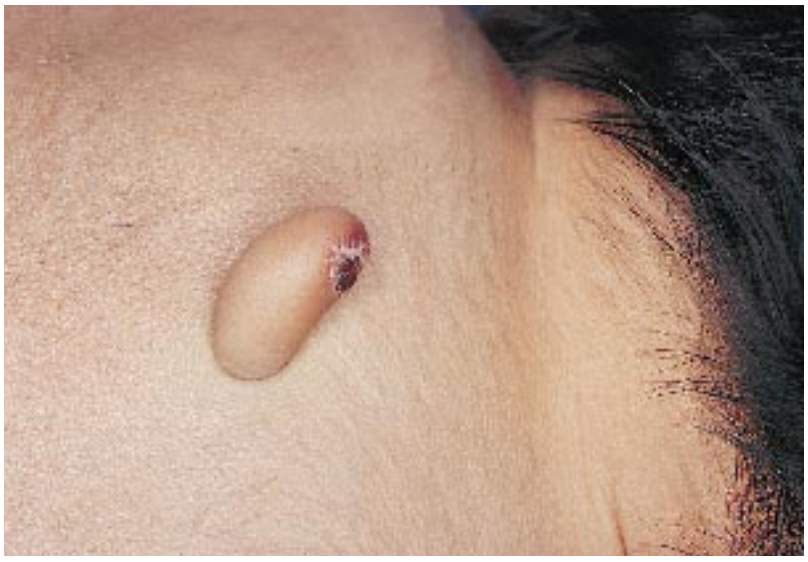

Figure 3.84. Small "finger-like" dermal tag extending from the midline of the back at the T4 level. Underlying the skin tag there was bony dysraphism with a small band of soft tissue extending toward the spinal cord. There were multiple rib anomalies with fusion of several upper thoracic ribs. MRI showed a spina bifida of the upper thoracic spine and tethering of the spinal cord distally.

3.85

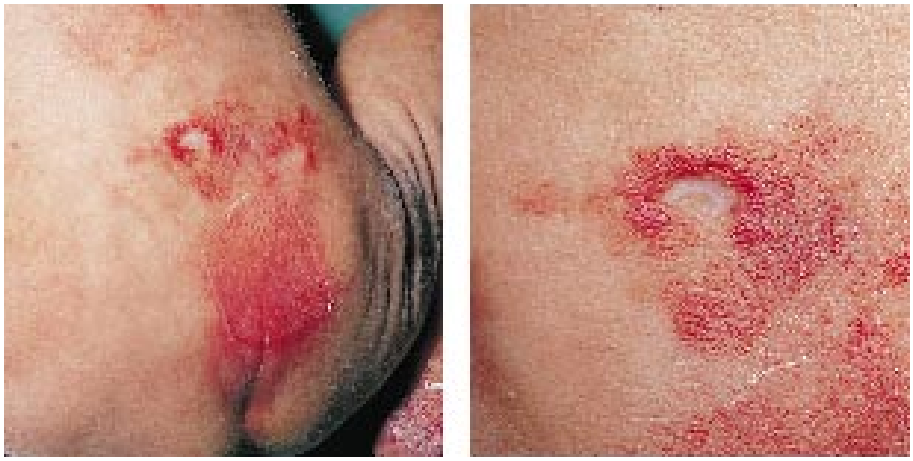

Figure 3.85. On the left is a photograph of a large midline skin defect representing a large dermal sinus. Right is a close-up of the dermal sinus.

3.86

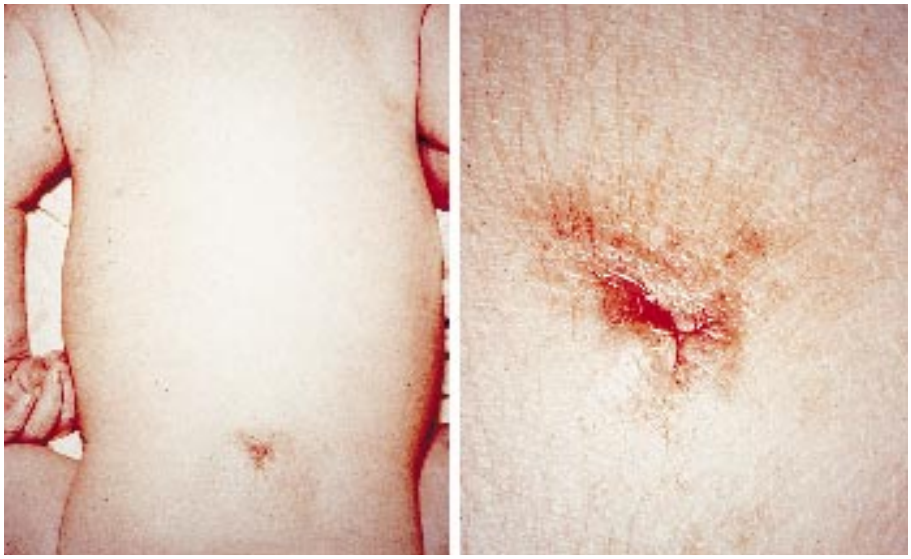

Figure 3.86. Left, photograph of another variant of a dermal sinus. Right, close-up of the same sinus. Dermal sinuses occur midline anywhere along the spinal cord and warrant examination of the central nervous system.

3.87

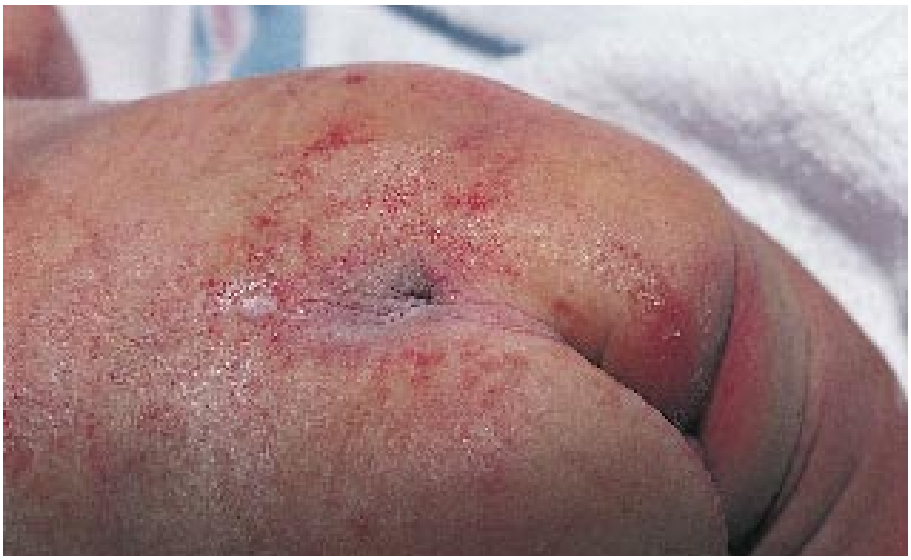

Figure 3.87. Midline skin defect with an inferior deep pilonidal dimple. MRI of the spinal column revealed a tethered spinal cord. A pilonidal sinus may connect with the underlying distal end of the spinal canal. This should be suspected when the bottom of a midline pit over the sacrum cannot be seen, if there is any fluid emerging from the depths of such a pit, or when the pit contains hairs.

3.88

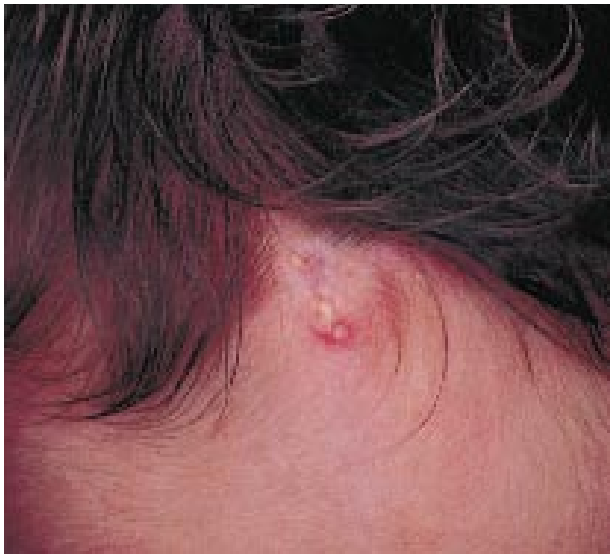

Figure 3.88. Midline skin defect at the inferior aspect of the hairline of an infant with an associated dermal sinus tract. This infant had an associated lateral nasal cleft.

3.89

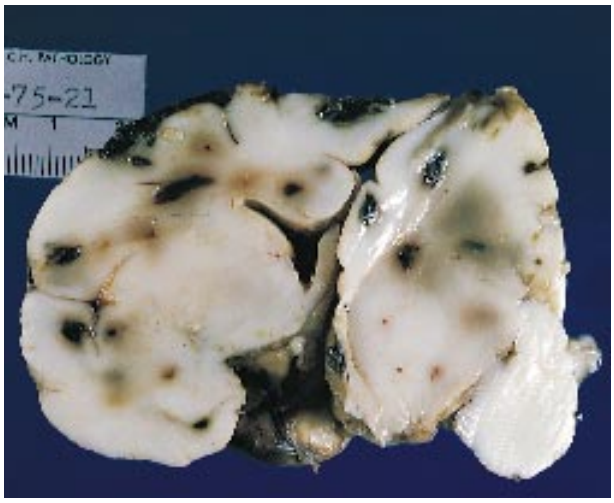

Figure 3.89. Anoxic encephalomalacia and hemorrhages in an autopsy specimen of a brain. Note the multiple areas of hemorrhage in the brain of this term infant.

3.90

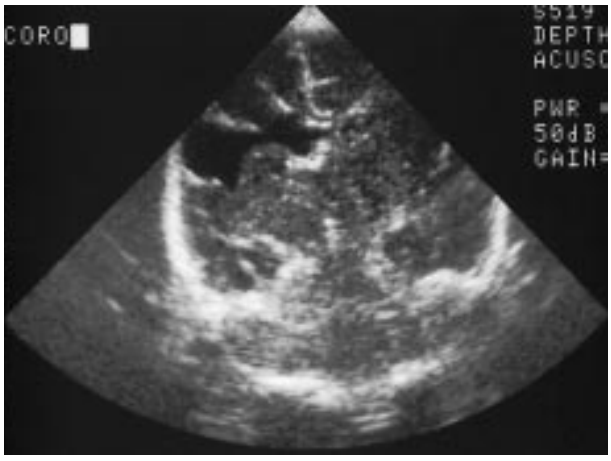

Figure 3.90. Head ultrasound examination of an infant with schizencephaly. This is the most severe of the cortical malformations as the result of abnormal migration occurring no later than the 2nd month of gestation. There is complete agenesis of a portion of the cerebral wall leaving bilateral schisms or clefts.

3.91

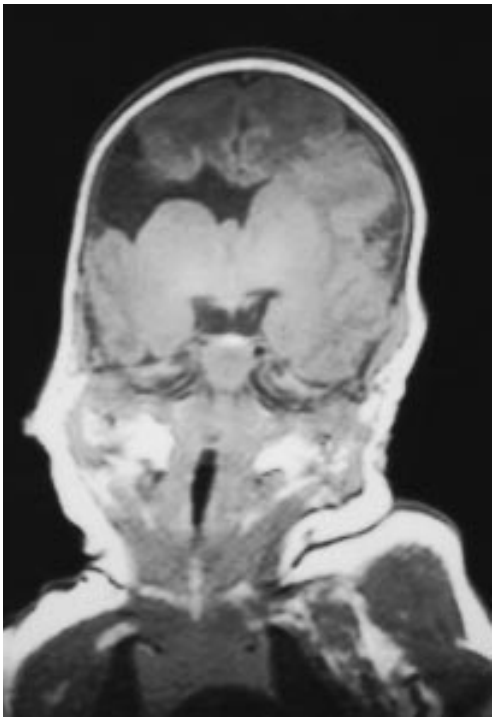

Figure 3.91. Clefts or "lips" demonstrated in the right hemisphere in the MRI of the head of an infant with schizencephaly. The lips of the clefts may become widely separated and massive dilation of the ventricles may occur. This can result in a striking degree of transillumination of the skull with an incorrect diagnosis of hydranencephaly. Infants who survive have severe seizures with marked spasticity (sometimes preceded by hypotonia), and severe retardation.

3.92

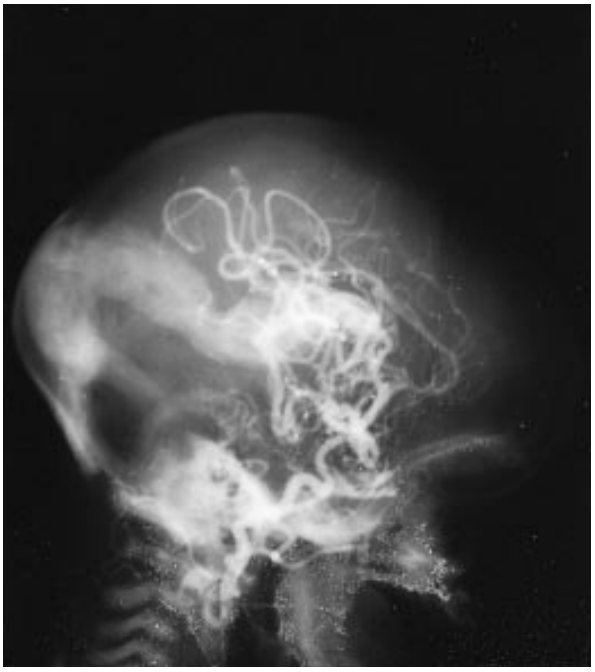

Figure 3.92. Angiogram of an infant who presented with severe congestive heart failure. Note the large arteriovenous malformation of the great vein of Galen. These malformations have been diagnosed both pre- and postnatally with the use of ultrasonography, CT scan, or MRI.

3.93

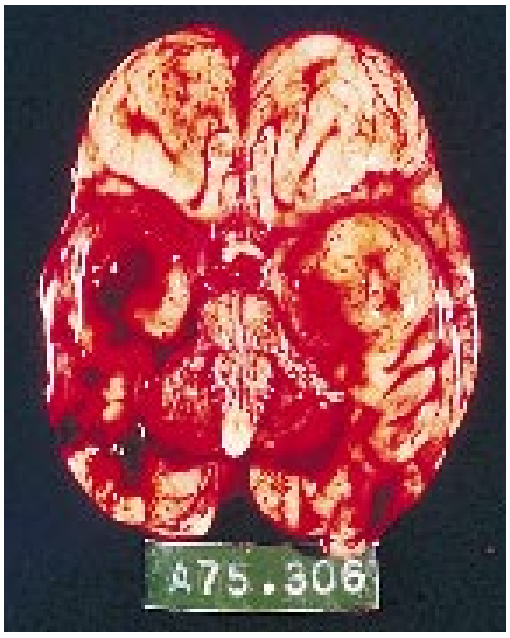

Figure 3.93. Autopsy specimen of the brain of a premature infant who suffered from a large subarachnoid hemorrhage. Note the bleeding especially around the temporal lobes.

3.94

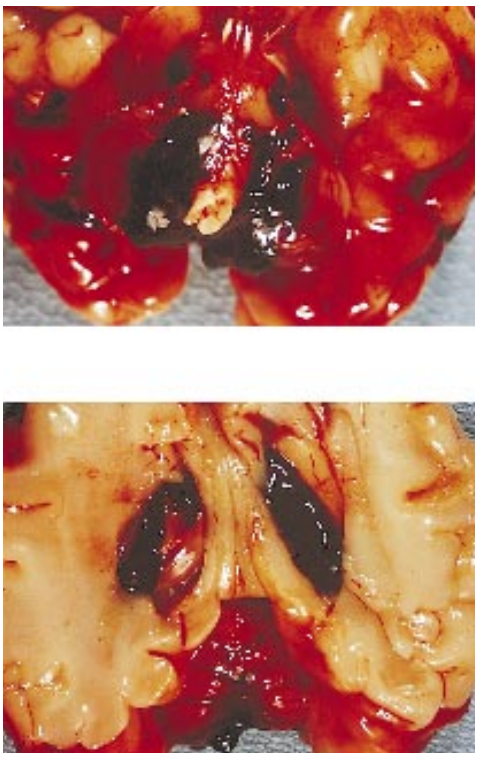

Figure 3.94. Autopsy specimens of the brains of two infants showing massive hemorrhage. Top, hemorrhages at the base of the brain. Bottom, massive bilateral intraventricular hemorrhages.

3.95

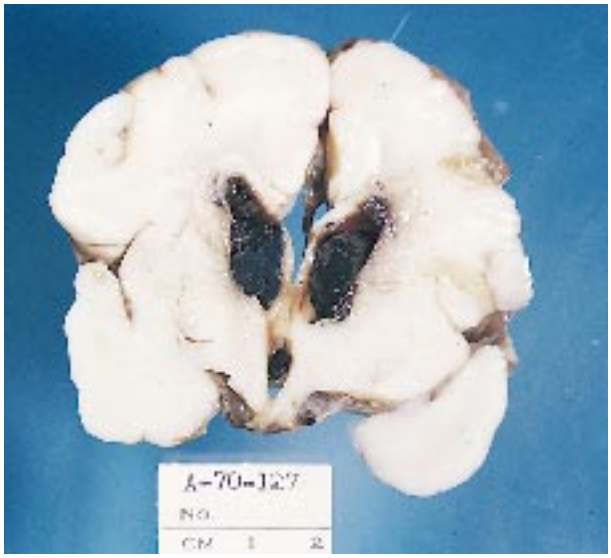

Figure 3.95. Autopsy coronal views of the brain with bilateral intraventricular hemorrhage. Note the lack of convolutions and convexities in this immature brain. The ventricles are enlarged as a result of massive bleeding.

3.96

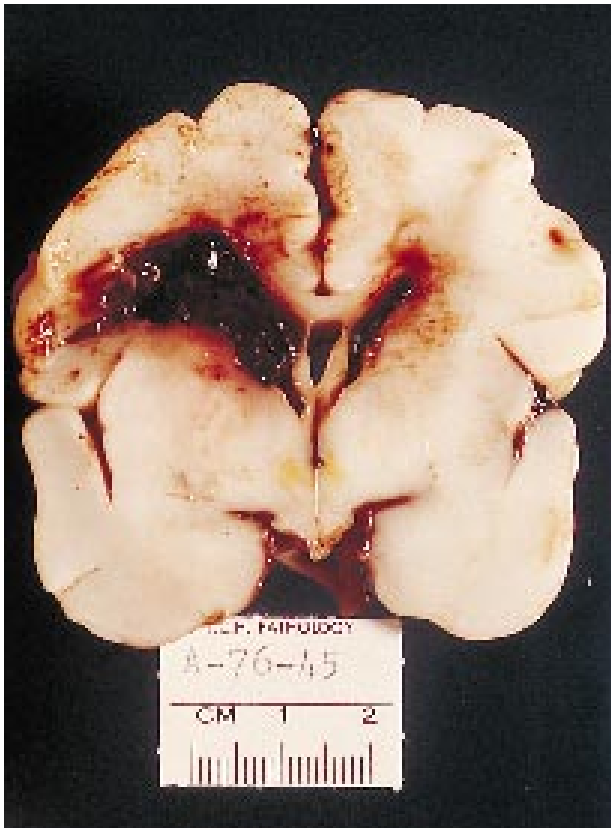

Figure 3.96. Autopsy specimen of a brain with bilateral intraventricular hemorrhage. Note the marked extension of the hemorrhage into the right cerebrum. This constitutes a grade IV intraventricular hemorrhage.

3.97

Figure 3.97. Autopsy specimens of casts of blood from a large intraventricular hemorrhage. Top, cast of the lateral ventricle; bottom, cast of the fourth ventricle.

3.98

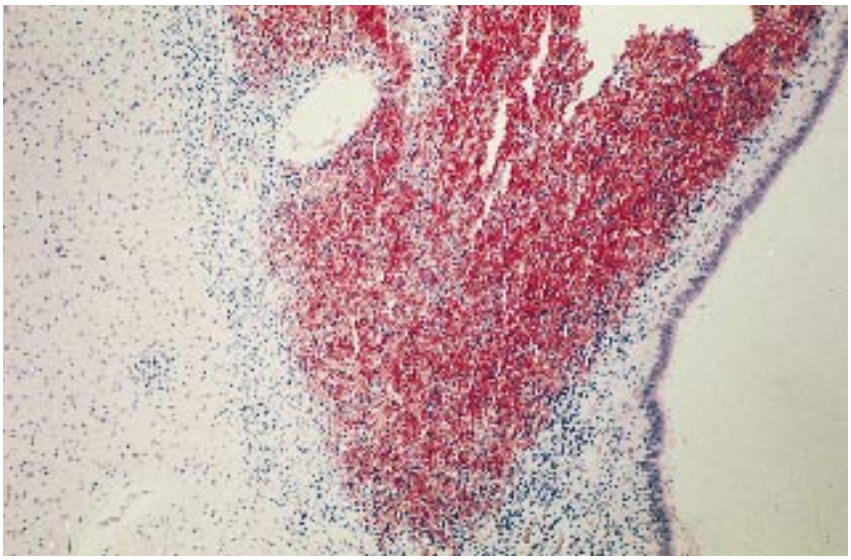

Figure 3.98. Histology of a section from the brain of a premature infant with a subependymal hemorrhage. Note, on the right, the lack of congestion/blood in the adjacent ventricle. This indicates that the subependymal hemorrhage has not broken through into the ventricle.

3.99

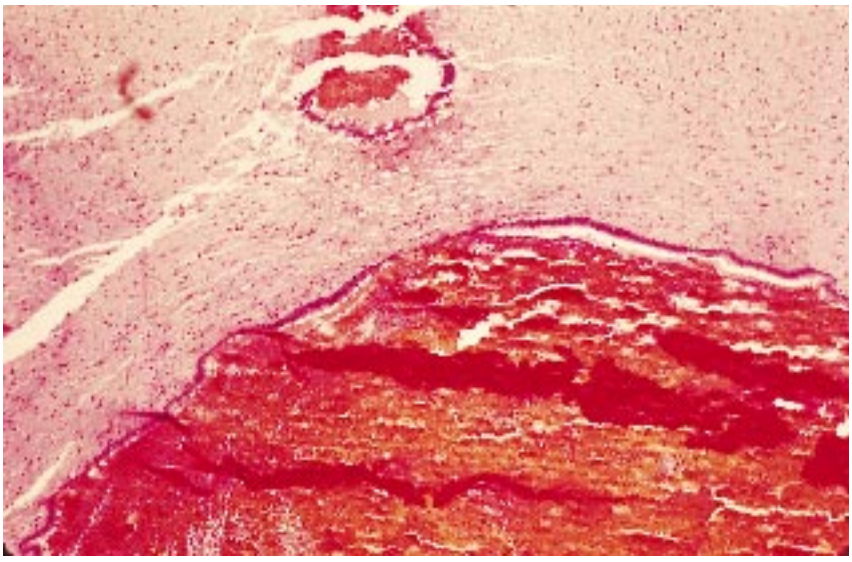

Figure 3.99. In contrast, this histology represents a section from the brain of a premature infant who has had an intraventricular hemorrhage. Note that the congestion/blood has broken through into the ventricle which is filled with blood.

Classification for periventricular-intraventricular hemorrhage (PVH-IVH):

Grade I. Subependymal hemorrhage.
Grade II. Hemorrhage into the ventricles.
Grade III. Hemorrhage into the ventricles with dilatation of the ventricles.
Grade IV. Hemorrhage into the ventricles with dilatation of the ventricles and extension into the parenchyma.

3.100

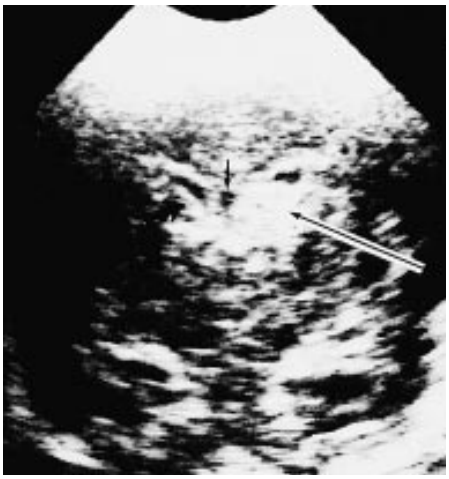

Figure 3.100. A coronal ultrasound scan through the brain of a premature infant with a grade I PVH-IVH. There is a large left-sided subependymal hemorrhage (large arrow) with a less echogenic area on the right. Note the midline septum pellucidum (small superior arrow). (Figures 3.100–3.103 are from Langston C, Wolfson R. JAMA 1983; 250:3213 and are reprinted with the permission of the American Medical Association. Copyright 1983, American Medical Association.)

3.101

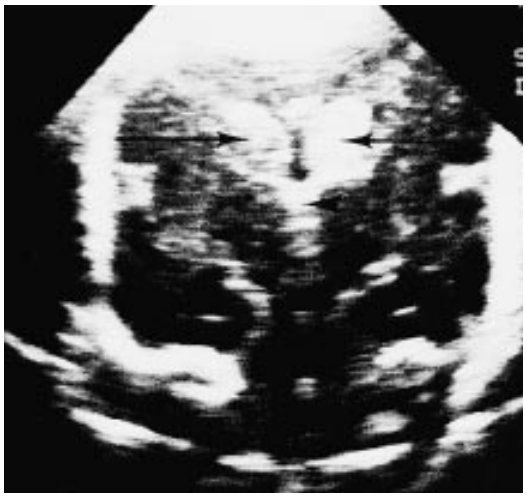

Figure 3.101. A coronal ultrasound scan shows echogenic blood in the mildly dilated lateral ventricles (arrows) and in the 3rd ventricle (arrowhead).

3.102

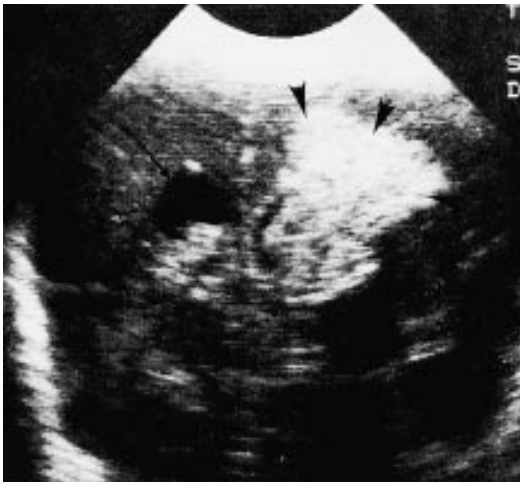

Figure 3.102. This coronal ultrasound scan shows extension of blood into the parenchyma of the brain (arrow heads). Note the large dilated right lateral ventricle (arrows).

3.103

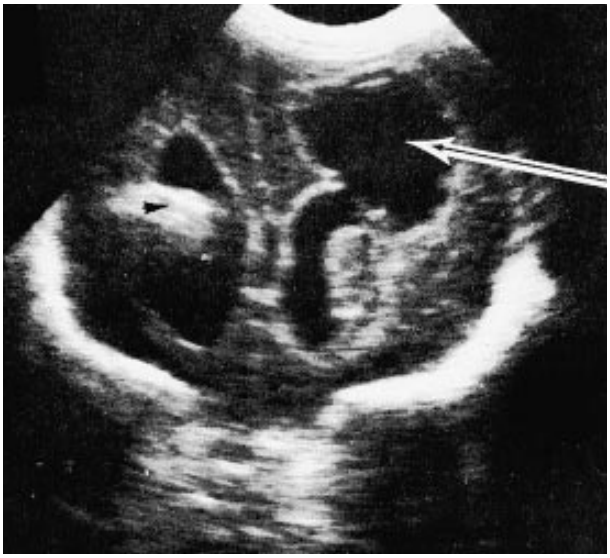

Figure 3.103. This coronal ultrasound scan shows conversion of intraparenchymal bleeding to a large area of porencephaly (arrow). The echogenic shunt tube is placed in the dilated right lateral ventricle (arrowhead).

3.104

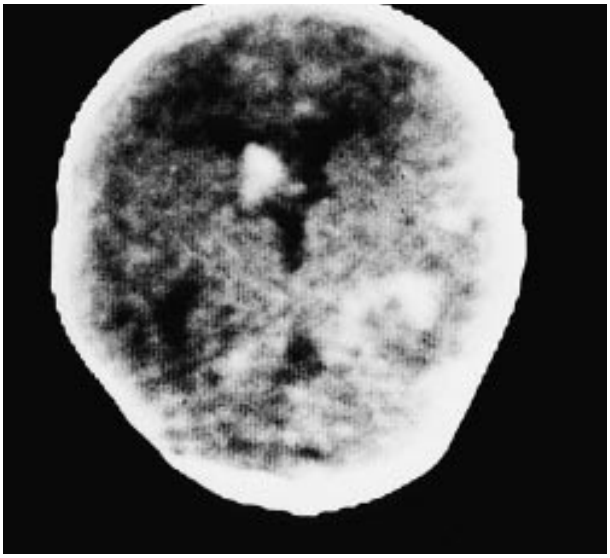

Figure 3.104. A CT scan of an infant with a grade II PVH-IVH. There is blood within the lateral ventricles without ventricular dilatation.

3.105

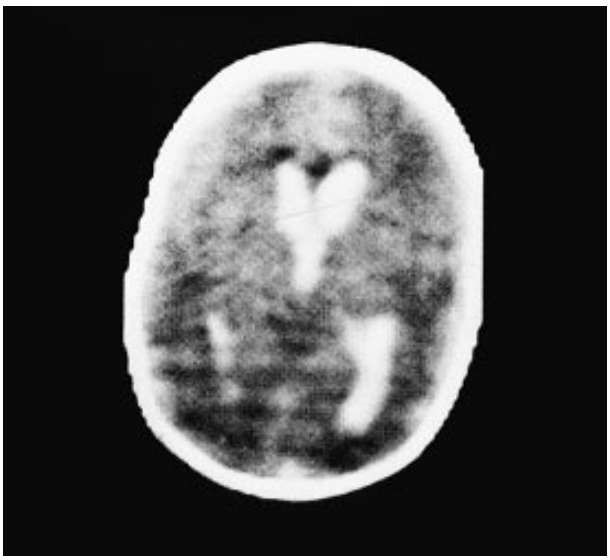

Figure 3.105. A CT scan of an infant with a grade III PVH-IVH. There is blood within the dilated lateral ventricles.

3.106

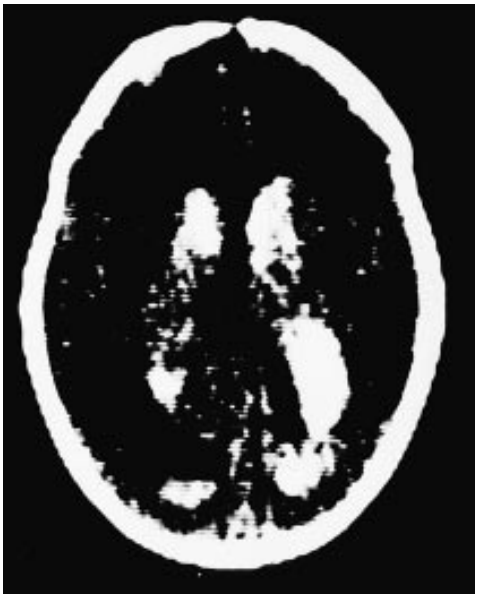

Figure 3.106. A CT scan of an infant with a grade IV PVH-IVH. Note the blood within the lateral ventricles and extension into the cerebral parenchyma.

3.107

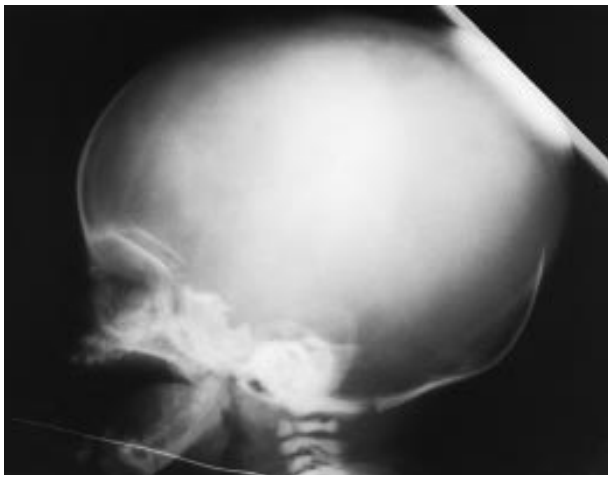

Figure 3.107. This term infant presented with marked increase in head size (fronto-occipital circumference 41 cm). A lateral skull radiograph showed the enlarged head and an increased density over the parietal area.

3.108

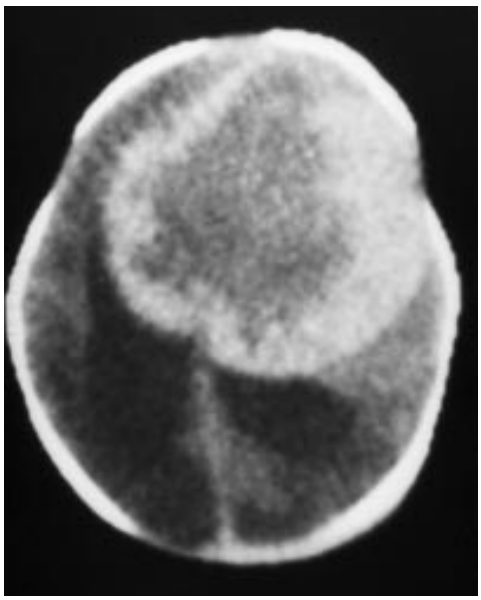

Figure 3.108. A CT scan of the same infant showed a large brain tumor. The infant died at the age of 2 days and autopsy diagnosis was glioblastoma multiforme. There was hydrocephalus and a massive brain tumor with diffuse encephalomalacia and marked distortion of the brain.

The presentation of congenital brain tumors includes:

1) Stillborn with megalencephaly, with tumor replacing nearly all of the brain.
2) Liveborn with dystocia secondary to hydrocephalus.
3) Normal at birth but with abrupt cranial enlargement within a few days.

3.109

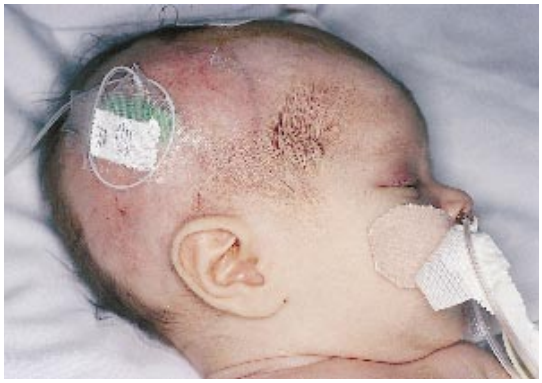

Figure 3.109. This term infant, born by spontaneous vaginal delivery, developed seizures on the first day of life and was treated with phenobarbital. The EEG showed decreased activity of the left temporal region. The fronto-occipital circumference increased rapidly in the first few days of life from 38.5 cm at birth to 41 cm at 10 days of age. Note the enlargement of the head and the illusion of low-set rotated ears.

3.110

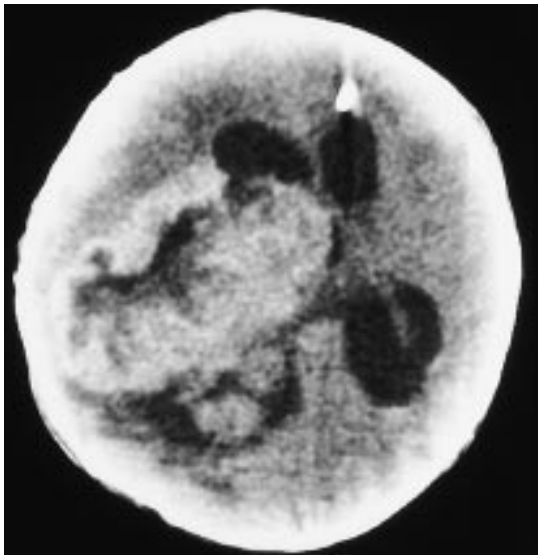

Figure 3.110. A CT scan of the same infant revealed a large choroid plexus tumor. These tumors are usually associated with hydrocephalus. Hydrocephalus may occur as a result of an increased production of CSF or may be due to obstruction of the flow of CSF. A rapid increase in the size of the tumor or hydrocephalus may be associated with hemorrhage and necrosis in the tumor as occurred in this infant.

3.111

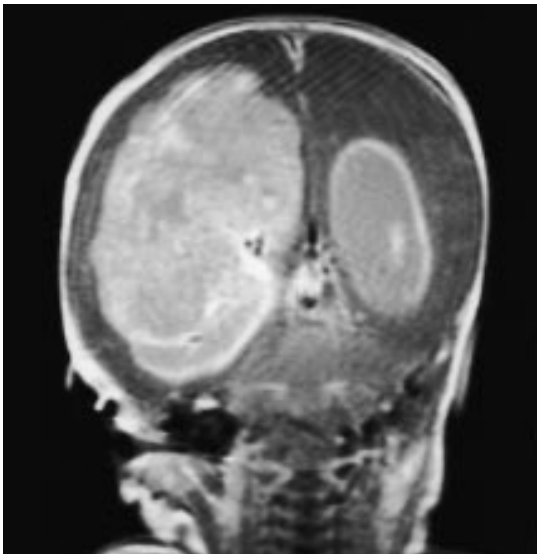

Figure 3.111. MRI of the same infant on the 9th day of life revealed a large mass on the right side extending to the midline with ventricular dilatation and hydrocephalus. The infant died at 31 days of age.

3.112

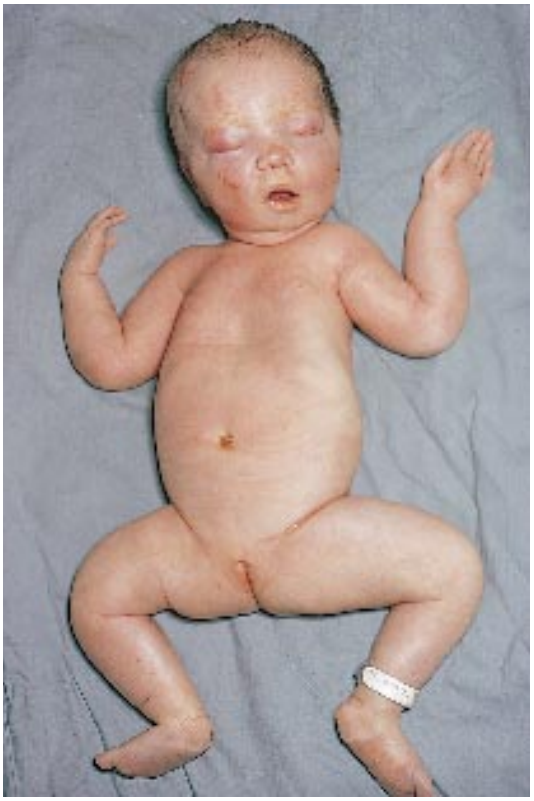

Figure 3.112. There was marked lack of fetal movement, vaginal delivery was difficult, and there was a fracture of the left humerus and of the right femur present at birth in this floppy term infant. Note the "frog leg" position with marked hypotonia, areflexia, and paradoxical respiration. The diagnosis was amyotonia congenita.

3.113

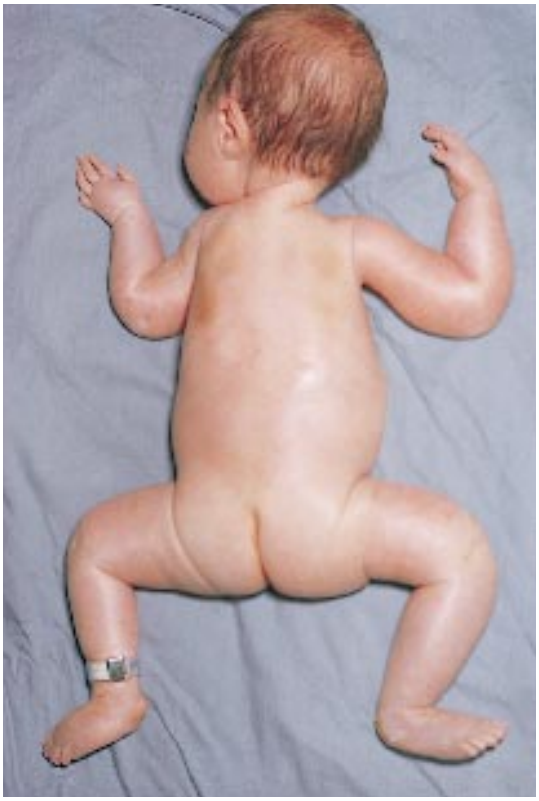

Figure 3.113. Posterior view of the same infant. Note again the hypotonia and the "frog leg" position with swelling of the left arm and the right leg. This swelling is the result of fractures at the time of birth.

3.114

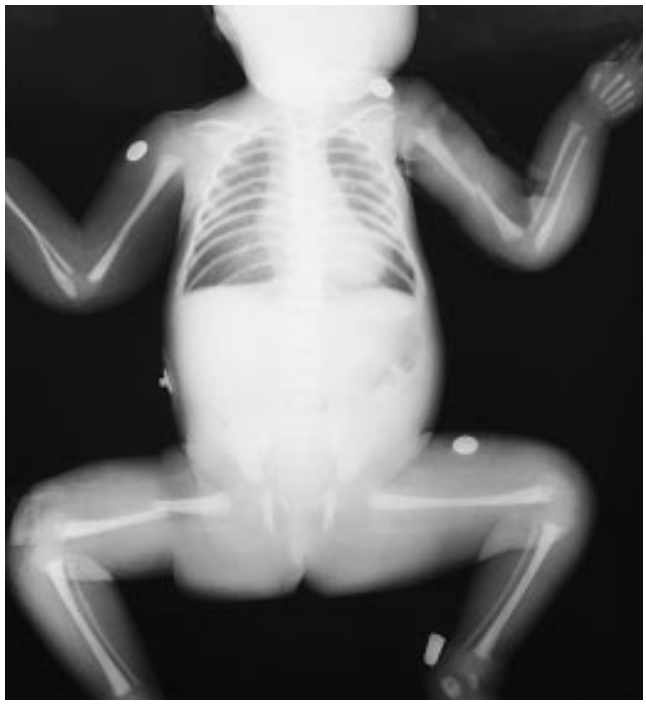

Figure 3.114. Radiograph of the same infant. Note the very thin bones, lack of muscle tissue, and fracture of the left humerus and right femur.

3.115

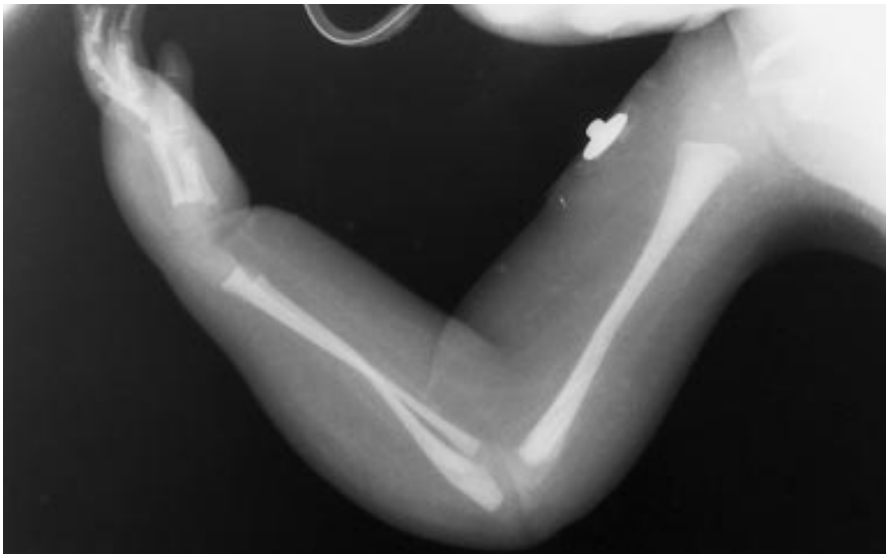

Figure 3.115. Radiograph of the right arm of the same infant shown in Figure 3.112-3.114. Note the marked thinning of the bones and lack of muscle mass. This poor development of bone and muscle results from lack of fetal movement.

3.116

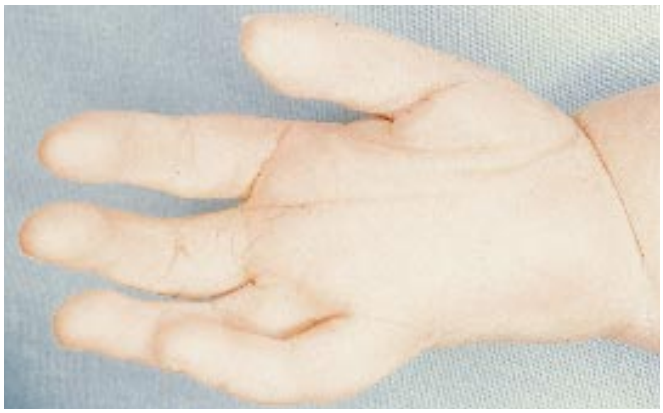

Figure 3.116. Right hand of the same infant with amyotonia congenita. Note the lack of finger creases and the abnormal appearance of the hand due to lack of intrauterine fetal movement. Finger creases normally develop at 11 to 12 weeks gestational age.

3.117

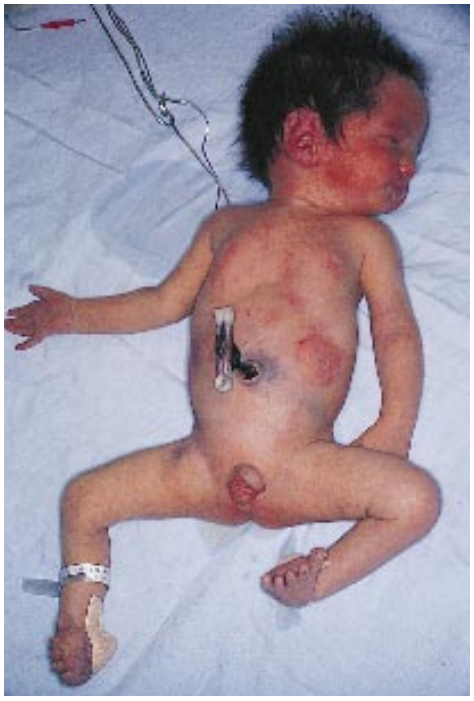

Figure 3.117. In this male infant with myotonic dystrophy, note the marked hypotonia, cryptorchidism, and clubfoot.

3.118

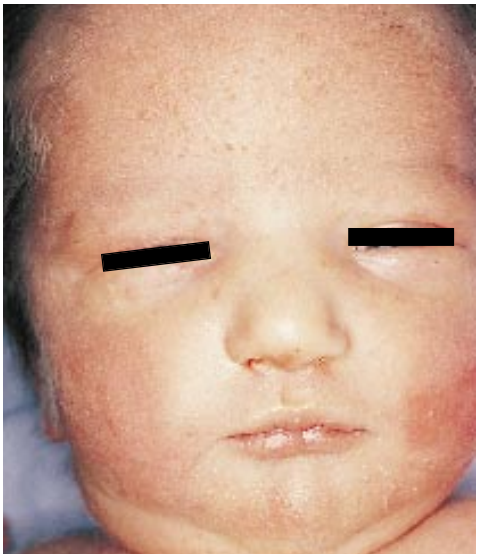

Figure 3.118. The face of the same infant as shown in Figure 3.117 shows the typical lack of expression and the bilateral ptosis seen in myotonic dystrophy. This should be differentiated from neonatal myasthenia gravis.

About 10 to 15% of infants of myasthenic mothers are affected and signs present in the baby at or shortly after birth. The clinical picture of neonatal myasthenia gravis is dominated by general hypotonia, there being symmetrical involvement of the face, trunk and limbs. In severe cases there is lack of facial expression and difficulty in sucking and swallowing. Prognosis is good, with improvement within a week; the infant may be symptomatic as long as 6 weeks.

3.119

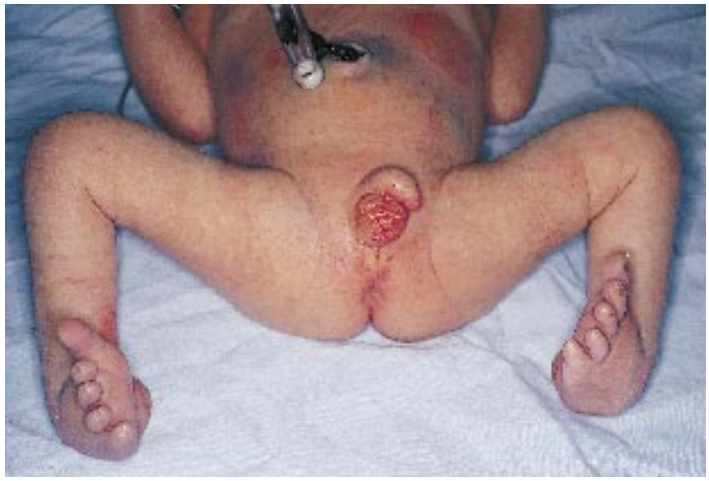

Figure 3.119. Cryptorchidism and clubfoot in the same infant with myotonic dystrophy.

3.120

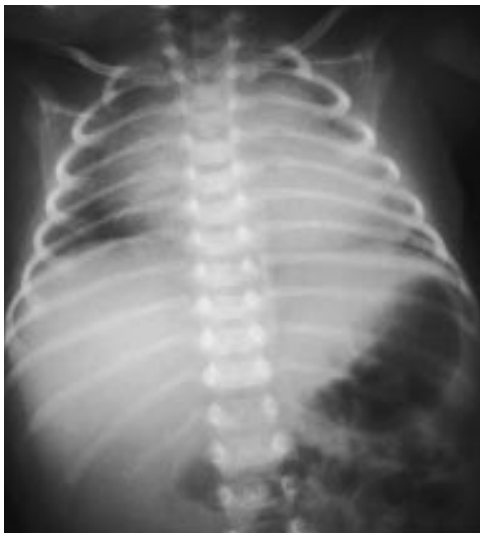

Figure 3.120. Radiograph of thorax of a hypotonic infant with the fetal akinesia syndrome. Note the thin, gracile, downslanting ribs, long thin clavicles, and splayed chest. The poor inspiration is due to poor muscle effort because of the hypotonia.

Index